EFFECTS OF ANTIRETROVIRAL DRUGS ON THE TRANSLOCATION STATUS OF HUMAN IMMUNODEFICIENCY VIRUS TYPE 1 REVERSE TRANSCRIPTASE

Bruno Marchand

Department of Microbiology & Immunology

McGill University, Montreal

January, 2007

A thesis submitted to McGill University in partial fulfilment of the requirements of the degree of Doctor of Philosophy

ABSTRACT

The reverse transcriptase of the Human Immunodeficiency Virus type 1 (HIV-1) is responsible for transcribing the viral single-stranded RNA genome into double-stranded DNA. Due to its vital role in the viral life cycle, it is often targeted in the treatment of HIV-1 infected patients. Inhibitors that block the reverse transcriptase enzyme were shown to interfere with nucleotide incorporation. At the end of a nucleotide incorporation cycle, the newly incorporated substrate is still located in the nucleotide binding site. In order to continue the elongation of the DNA chain, the enzyme has to move by one nucleotide relative to the nucleic acid template to free the nucleotide binding site. This movement is referred to as translocation. Translocation is extremely rapid and is therefore kinetically invisible.

In order to study the mechanism of translocation, I developed site-specific footprinting assays with a resolution of a single nucleotide, which allowed us to detect the precise positioning of the reverse transcriptase on a DNA template. Using these techniques, in combination with kinetic analysis as well as other enzymatic assays, I studied the translocational status of the reverse transcriptase in various conditions, and concluded that this enzyme translocates according to a "Brownian ratchet model". In this model, the enzyme oscillates between pre- and post-translocated positions and the nucleotide substrate traps the post-translocational state.

I identified important factors that affect the translocational equilibrium: the sequence of the nucleic acid template, the nature of the nucleotide at the 3' end of the primer, the

presence of mismatches in the double-stranded nucleic acid substrate, the presence of nucleotides, the presence of inhibitors, the nature of these inhibitors, the presence of drug resistance conferring mutations and the temperature are parameters that have all been shown to modify the translocational equilibrium of the reverse transcriptase. Most importantly, we found that the translocational status of the reverse transcriptase had a direct effect on the efficacy of certain inhibitors. Thus, our results have not only important implications with regards to the mechanism of reverse transcriptase translocation, but also shed light on mechanisms of drug action and drug resistance.

RÉSUMÉ

La transcriptase inverse du Virus d'Immunodéficience Humaine de type 1 (VIH-1) est responsable de la transcription du génome viral composé d'ARN simple brin en ADN double brin. Étant donné son rôle vital dans le cycle viral, cet enzyme est une cible de choix pour le traitement des patients infectés par le VIH-1. Les inhibiteurs qui bloquent la transcriptase inverse affectent régulièrement l'incorporation des nucléotides. Après l'incorporation d'un nucléotide, ce dernier est toujours situé dans le site de liaison des nucléotides. Afin de libérer ce site, la transcriptase inverse doit se déplacer d'un nucléotide par rapport à la matrice d'acide nucléique, déplacement que nous appelons la translocation. Celle-ci est un mouvement très rapide qui est cinétiquement invisible.

Afin d'étudier le mécanisme de translocation, j'ai dévelopé des tests d'empreinte moléculaire ayant une résolution d'un seul nucléotide nous permettant de détecter la position précise de l'enzyme sur une matrice d'ADN. En utilisant ces tests, en combinaison avec des analyses cinétiques et autres expériences enzymatiques, j'ai étudié le statut translocationel de la transcriptase inverse, et nous en sommes venus à la conclusion que cet enzyme se déplace selon un modèle dans lequel un mouvement Brownien est responsable du déplacement de l'enzyme. Celui-ci est stabilisé par la liaison d'un nucléotide dans le stade post-translocationel.

J'ai identifié des facteurs importants influençant la translocation : la séquence de la matrice d'acide nucléique, la nature du nucléotide à l'extrémité 3' de l'amorce, la présence d'erreurs d'association dans le substrat d'acide nucléique double brin, la

présence de nucléotides, la présence d'inhibiteurs, la nature de ces inhibiteurs, la présence de mutations conférant une résistance aux médicaments et la température ont tous été démontrés comme modifiant l'équilibre de translocation de la transcriptase inverse. Par dessus tout, nous avons découvert que la translocation avait un effet direct sur l'éfficacité de certain médicaments. Nos résultats ont non seulement des implications importante en ce qui concerne le mécanisme de translocation, mais nous éclairent également sur les mécanismes d'action des médicaments et de résistance à ceux-ci.

PREFACE

This thesis was written in accordance with McGill University's "Guideline for Thesis Preparation". The format of this thesis conforms to the "Manuscript-based thesis" option which states:

"Candidates have the option of including, as part of the thesis, the text of one or more papers submitted, or to be submitted, for publication, or the clearly-duplicated text (not the reprints) of one or more published papers. These texts must conform to the "Guidelines for Thesis Preparation" with respect to font size, line spacing and margin sizes and must be bound together as an integral part of the thesis."

Manuscripts included in this thesis:

Marchand, B., K.L. White, J.K. Ly, N.A. Margot, R. Wang, M. McDermott, M.D. Miller and M. Götte, 2006. Effects of the Translocation Status of HIV-1 Reverse Transcriptase on the Efficiency of Excision of Tenofovir. Antimicrob Agents Chemother. Submitted

Marchand, B., E.P. Tchesnokov and M. Götte, 2007. The Pyrophosphate Analogue Foscarnet Traps the Pre-Translocational State of HIV-1 Reverse Transcriptase in a Brownian Ratchet Model of Polymerase Translocation. J. Biol. Chem. **282** (5) : 3337-46.

Marchand B. and M. Götte. 2004. Impact of the Translocational Equilibrium of HIV-1 Reverse Transcriptase on the Efficiency of Mismatch Extension and the Excision of Mispaired Nucleotides. Int. J. Biochem. Cell Biol. **36** : 1823-35

Marchand B. and M. Götte. 2003. Site-Specific Footprinting Reveals Differences in the Translocation Status of HIV-1 Reverse Transcriptase: Implications for Polymerase Translocation and Drug Resistance. J.Biol.Chem. **278** (37):35362-72

The contribution of co-authors to published or submitted articles appears in the section "CONTRIBUTIONS OF AUTHORS". The journal of submission and information from published articles can be found on the title page of the concerned chapters.

Other manuscripts not included in this thesis, but to which a significant contribution was made by the candidate, are listed as follows:

Frankel, F.A., **B. Marchand**, D. Turner, M. Götte, and M.A. Wainberg. 2005. Impaired Rescue of Chain-Terminated DNA Synthesis Associated with the L74V Mutation in Human Immunodeficiency Virus Type 1 Reverse Transcriptase. Antimicrob Agents Chemother **49:**2657-64.

Roldan, A., R.S. Russel, **B. Marchand**, M. Götte, C.Liang, and M.A. Wainberg. 2004. *In Vitro* Identification and Characterization of an Early Complex Linking HIV-1 Genomic RNA Recognition and $Pr55^{Gag}$ Multimerization. J Biol Chem. **279**:39886-94.

Diallo, K., **B. Marchand**, X. Wei, L. Cellai, M. Götte, and M.A. Wainberg. 2003. Diminished RNA Primer Usage Associated with the L74V and M184V Mutations in the Reverse Transcriptase of Human Immunodeficiency Virus Type 1 Provides a Possible Mechanism for Diminished Viral Replication Capacity. J Virol. **77**:8621-32.

Girouard, M., K. Diallo, **B. Marchand**, S. McCormick, and M. Götte. 2003. Mutations E44D and V118I in the Reverse Transcriptase of HIV-1 Play Distinct Mechanistic Roles in Dual Resistance to AZT and 3TC. J Biol Chem. **278**:34403-10.

McLellan, N., X. Wei, **B. Marchand**, M.A. Wainberg, and M. Götte. 2002. Non-Radioactive Detection of Retroviral-Associated RNase H Activity in a Microplate-Based, High-Throughput Format. Biotechniques. **33**:424-9.

ACKNOWLEDGEMENTS

I would first like to thank my supervisor, Matthias Götte, without whom none of this would have been possible. I would like to thank him for the scientific and technical guidance that he has given me throughout the years.

I would also especially like to thank Xin Wei (Sam), Nathan McLellan and Karidia Diallo for the assistance that they have given me in my earlier days in Matthias' lab.

I would like to thank the current and former members of Matthias' lab for their friendship and their support: Mélanie Girouard, Claudia D'Abramo, Stephen Barry, Egor Tchesnokov, Aneeta Mistry, Rose Chen, Jérome Deval, Meoin Hagege, Maryam Ehteshami, Dimitry Coutsinos, Brian Scarth, Greg Beilhartz, Konstantin Ivanov, Megan Powdrill, Jordan Gagnon, Colin Vasquez, and most importantly, Suzanne McCormick, without whom I would have spent twice as long in Matthias' lab.

I would also like to thank Greg Beilhartz for proofreading this manuscript, and Brian Scarth for creative consulting in titeling.

J'aimerais finalement remercier mes parents et mes frères qui m'ont toujours supporté sans conditions.

CONTRIBUTIONS OF AUTHORS

In the manuscripts entitled "Site-specific footprinting reveals differences in the translocation status of HIV-1 reverse transcriptase" and "Impact of the translocational equilibrium of HIV-1 reverse transcriptase on the efficiency of mismatch extension and the excision of mispaired nucleotides", B. Marchand conducted the totality of the experiments presented.

The manuscript entitled "Effects of the translocation status of HIV-1 reverse transcriptase on the efficiency of excision of tenofovir" was writen in collaboration with K.L. White. K.L. White has been responsible for the virological results (fig. 3.2) as well as the determination of K_i and K_i/K_m values for tenofovir-DP, ddATP, AZA-TP and AZT-TP (table 3.1). B. Marchand has been responsible for the rescue of chain-terminated DNA synhtesis assays (fig. 3.3), the determination of the kinetic constants for chain-terminator removal (table 3.3), the site-specific footprints (fig. 3.4 and table 3.2) and the gel mobility shift assays (fig. 3.5).

The work load for the manuscript entitled "The pyrophosphate analogue foscarnet traps the pre-translocational state of HIV-1 reverse transcriptase in a Brownian ratchet model of polymerase translocation" was shared with E.P. Tchesnokov. E.P. Tchesnokov was responsible for the determination of the kinetic constants during nucleotide incorporation in the absence and presence of foscarnet (fig. 4.4 and table 4.1). B. Marchand was responsible for the primer extension assays (fig. 4.1), the site-specific footprints (fig. 4.2 and 4.5) and the gel mobility shift assays (fig. 4.3).

TABLE OF CONTENTS

LIST OF FIGURES AND TABLES

CHAPTER 1

INTRODUCTION

Retroviruses posses a single-stranded RNA genome. However, the provirus, found in infected cells, is composed of double-stranded DNA (238, 239). An enzyme, either of cellular or viral origin, must be responsible for the transcription of the viral RNA genome to the proviral DNA genome. A factor was identified in retroviral virions possessing an RNA-dependent DNA-polymerase activity (6, 240), an activity never observed before. This novel enzyme was named reverse transcriptase (RT). It was later found that a DNA-dependent DNA-polymerase was also present in retroviral virions (52, 204, 226). Evidence that the 2 activities shared a common active site started to accumulate (43, 44, 101) and it was concluded that a single enzyme was responsible for both activities. A third activity that was inseparable from the reverse transcriptase was described as a nuclease activity with the properties of a ribonuclease H (RNase H) (7, 107, 165), which degrades the RNA portion of RNA-DNA hybrids. The finding of this latter activity leaves us with an enzyme capable of using the viral RNA genome as a template to form an RNA-DNA hybrid, degrading the RNA portion of this hybrid, and producing a double-stranded DNA copy of the viral genome.

The human immunodeficiency virus type 1 (HIV-1) is a retrovirus that was identified as the causative agent of the acquired immune deficiency syndrome (AIDS) (11, 53). The HIV-1 genome has been sequenced and was shown to have the main genes characteristic of retroviruses; *gag*, *pol* and *env*, along with other open-reading frames (189, 210, 249). The reverse transcriptase is encoded in the *pol* gene in retroviruses. Two proteins of 66 and 51 kDa, identified as p66 and p51, were isolated from the virus and were shown to have reverse transcriptase activity (37, 132). The 2 proteins were recognized by the same monoclonal antibody and the sequencing of their N-terminus showed an identical

sequence related to the predicted sequence of a portion of the *pol* gene (37). The p66 protein is expected to be 560 amino acids long and correspond to amino acids 156 to 715 of the *pol* gene product (132). It was later shown that p51, being 440 residues in length, arises from proteolytic cleavage of p66 by the retroviral protease, which is also encoded in the *pol* gene (48). It was also demonstrated that the most active form of the HIV-1 reverse transcriptase enzyme was a heterodimer of p66 and p51 (167). Although both subunits share the same sequence, evidence shows that only p66 possess an active site for polymerase activity (84, 128).

1.1 Structure of the reverse transcriptase

Sequence alignment studies demonstrated homologies between retroviral RTs and non-retroviral enzymes (99). It was observed that the N-terminus of retroviral RTs, including the enzymes from the human T-cell leukemia virus type I (HTLV-I), the bovine leukemia virus (BLV), the Rous sarcoma virus (RSV), the murine Moloney leukemia virus (Mo-MLV) and HIV-1, show high homology to non-retroviral polymerases, including for example the α subunit of *E. coli* DNA-dependent RNA polymerase. This homology includes a segment shown to be present in a number of non–retroviral polymerases; the YXDD motif (X = M in HIV-1). This sector is composed of 2 aspartic acid residues (185 and 186 in HIV-1) surrounded by a set of non-polar amino acids (102).

The C-terminal of retroviral RTs was found to be homologous to the sequence of *E. coli* ribonuclease H (RNase H) enzyme. The RT from Mo-MLV is 30% identical to the *E. coli* RNase H.

Between the 2 functional segments, a region that is less conserved between retroviral RTs was observed. This region was believed to be a connection fragment between the 2 conserved enzymatic sites.

The accuracy of this alignment was later confirmed by a mutagenesis study of Mo-MLV reverse transcriptase (236). Mutations introduced in the N-terminal 2 third of the enzyme disrupted the polymerase activity of RT, while mutations introduced in the C-terminal third of the protein disrupted the RNase H activity. Furthermore, constructs containing only the N-terminal 2 thirds of RT or only the C-terminal third were prepared. The N-terminal constructs retained the RNA-dependent polymerase activity of RT, while losing the RNase H activity. On the other hand, the C-terminal constructs retained the RNase H activity but not the polymerase activity. This showed without any doubts that the polymerase activity of RT is located near the N-terminal, while the RNase H activity is located near the C-terminal of the retroviral enzyme.

Mutagenesis studies identified important functional regions of the HIV-1 reverse transcriptase (125). In the region of amino acids 180 to 190 of RT, 3 mutations significantly reduced the activity of the enzyme. The mutation of amino acid 185 from D to H completely disrupted the activity of RT. This was expected as the Asp doublet at 185 and 186 is a very conserved region of retroviral and non retroviral polymerases (99, 102). The mutations Y to S at residue 183 and G to R at 190 also resulted in reduced enzymatic activity. Tyr 183, being well conserved in retroviral reverse transcriptases, seems to be an important residue for polymerase activity. Gly 190 however, is not as

conserved and it is believed that a change in hydrophobicity caused by the G to R mutation may be responsible for the decrease in polymerase activity. Another Asp residue was found to be crucial in polymerase activity. A mutation of the residue 110 from D to E also disrupts the polymerase activity of RT completely. Three amino acid changes conferred resistance to the active metabolite of the nucleoside analogue zidovudine (AZT). The mutations D113G, A114S and W266S all rendered the enzyme less sensitive to zidovudine-triphosphate (AZT-TP) (125). This suggests that these 3 amino acids play a role in the nucleotide substrate binding. In addition, mutations D113G and A114S also conferred resistance to the pyrophosphate analogue foscarnet, implying that these 2 residues would play an additional role in pyrophosphate exchange.

Crystal structures of the HIV-1 reverse transcriptase have been obtained either unliganded (87, 207), or bound to a double-stranded DNA substrate (38, 95), an RNA:DNA substrate (216), or a double-stranded DNA substrate including an incoming deoxynucleotide (88).

The first structure of the HIV-1 reverse transcriptase to be resolved was of the reverse transcriptase liganded to the inhibitor nevirapine (114). The polymerase domain of this enzyme has a shape reminiscent of a right hand, which forms a cleft that was also observed on the structure of another crystallized DNA polymerase; the klenow fragment of the *E. coli* DNA polymerase I (172). Due to its resemblance to a right hand, the subdomains of the polymerase domain were named: fingers, palm and thumb. Another subdomain lying between the polymerase domain and the RNase H domain was named connection subdomain (114). The palm subdomain, which contains the catalytic Asp triad (D110, D185 and D186), contacts all 3 other subdomains of the polymerase domain.

Hydrogen bonding can be observed between the palm, the thumb and the connection subdomains. The p51 subunit, having the same sequence as the polymerase domain of p66, has a strikingly different structural organization than p66. p51 doesn't have the cleft observed in p66, and the catalytic Asp triad is buried in the protein, explaining the lack of activity of this subunit in the heterodimer (84, 128). The subdomains observed in the p66 polymerase domain can be seen in p51, but their spacial arrangement differs largely from the p66 subunit. A groove passing from the RNase H active site through the connection subdomain and to the polymerase active site in the palm subdomain can be observed on this enzyme. It strongly suggests that a nucleic acid primer:template binds in this groove to contact the 2 active sites.

In the unliganded enzyme, the thumb moves toward the fingers (87, 207), closing the cleft observed in the nevirapine liganded enzyme. This suggests a certain flexibility of the thumb subdomain (see Fig. 1.1 for an identification of the subdomains in the unliganded enzyme).

The structure of RT liganded to double-stranded DNA or an RNA:DNA hybrid suggest that the cleft observed in the nevirapine bound enzyme is open (38, 95, 216). The nucleic acid substrate occupies the space left by the outward movement of the thumb (Fig. 1.2A). The nucleic acid substrate contacts the enzyme at multiple positions between the polymerase and the RNase H domains. The distance between these 2 domains is 60Å, and in terms of nucleotides, it is 17 base-pairs for double-stranded DNA (38, 95) and 18

Fig.1.1 Crystal structure of the reverse transcriptase. The subdomains of the polymerase domain are identified as follows; red: fingers, blue: palm, yellow: thumb and green: connection. The RNase H domain is shown in orange, and the p51 subunit is white. Important motifs are labelled in the color of their respective subdomain. α helices are labelled using letters while β sheets are labelled with numbers.

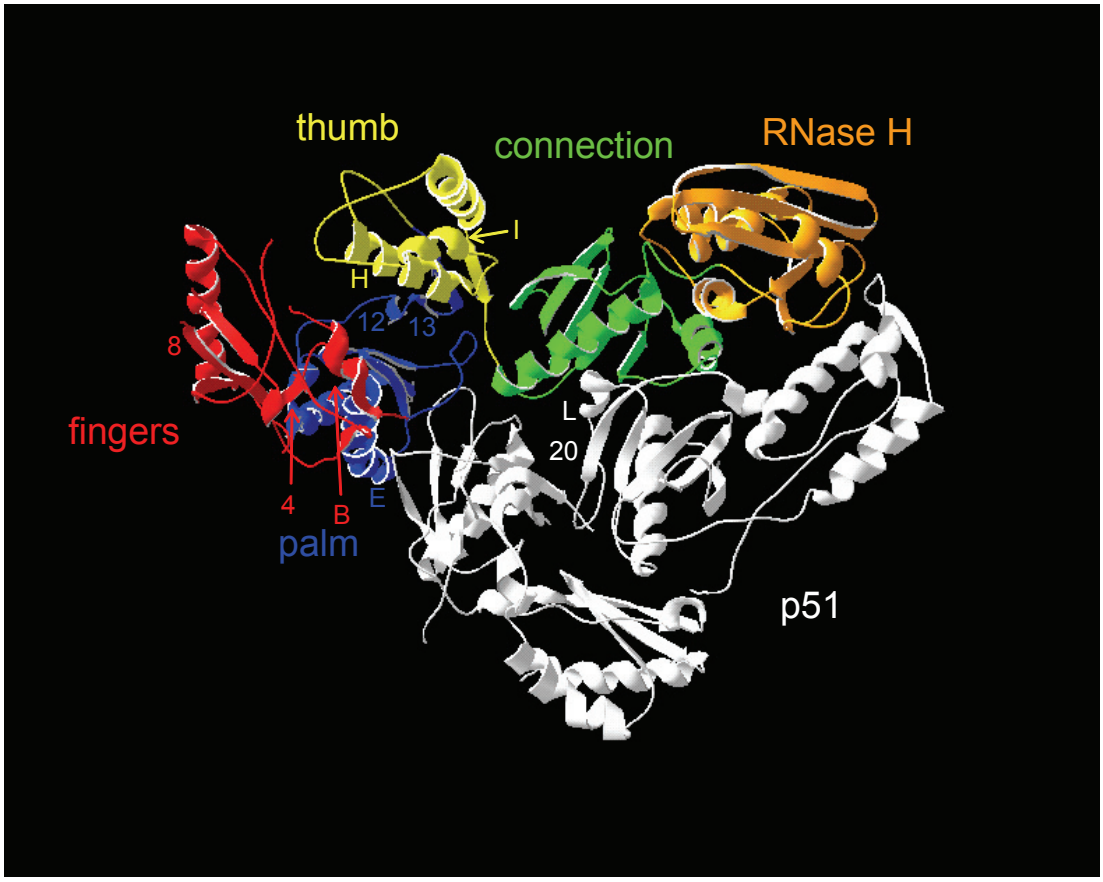
thumb
connection
RNase H
I
H
12
13
8
fingers
4
B
E
palm
L
20
p51

Fig.1.2 Structure of the binary and ternary complexes of the reverse transcriptase. The structure in A shows the polymerase domain of the reverse transcriptase bound to a DNA:DNA substrate. The enzyme is shown in blue while the DNA primer is colored in red and the DNA template in yellow. The subdomains are identified. In B, the polymerase domain is shown with a DNA:DNA substrate as well as a bound nucleotide. The same color code applies as in A, and the bound nucleotide is highlighted.

A

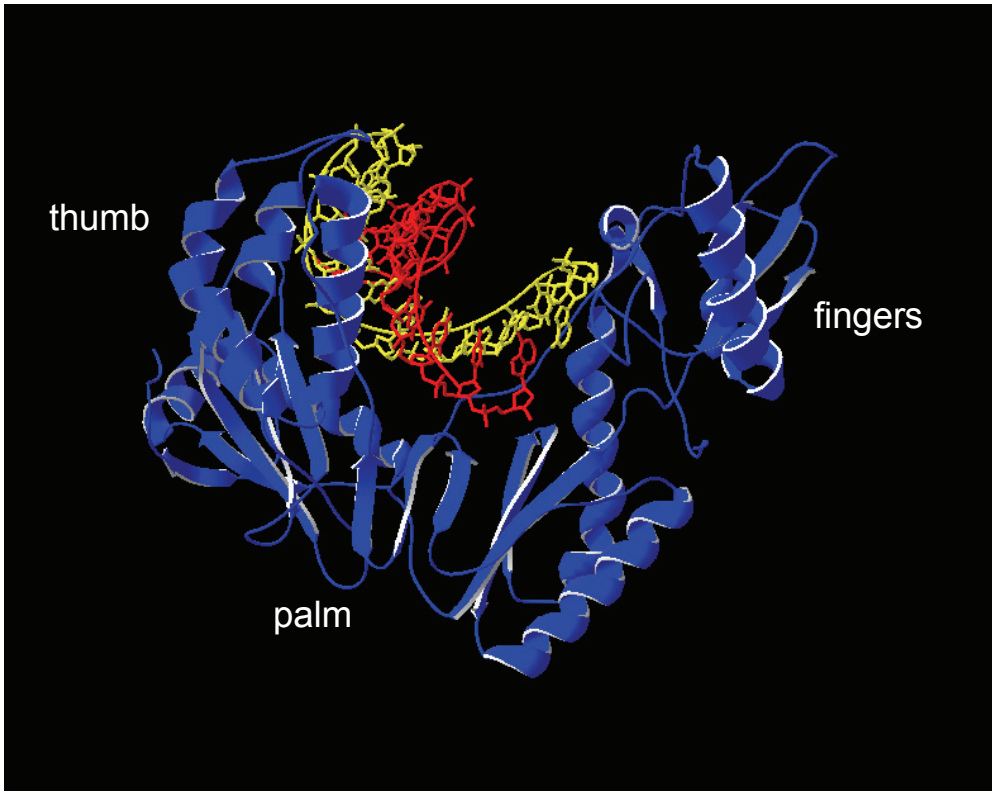

B

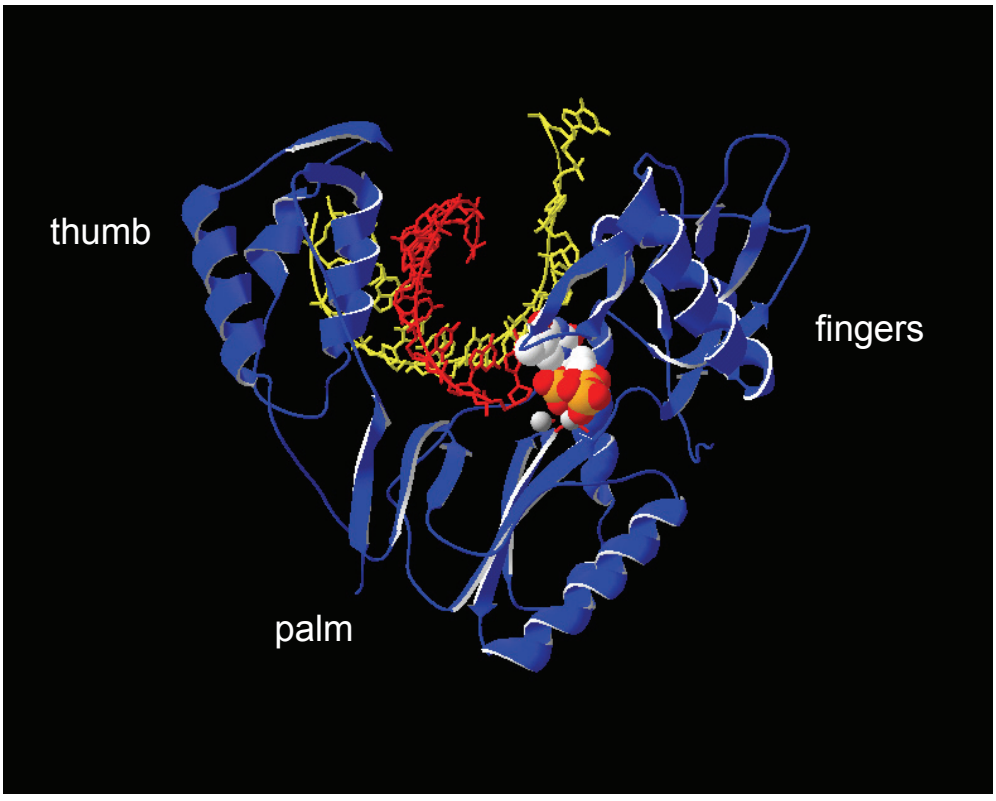

for an RNA:DNA hybrid (216). This difference between nucleic acid substrates agrees with published biochemical studies (63). The interactions between the protein and the nucleic acid involve mostly the sugar-phosphate backbone of the nucleic acid. The "floor" of the primer-template binding cleft is formed mainly by the connection subdomains of p66 and p51 and by the thumb of p51. However, few contacts are observed between this "floor" and the nucleic acid substrate. In p51, helix αL, which contacts the primer strand, and strand β20, which contacts the template strand, are the only contacts between p51 and the nucleic acid substrate. Both of these structures are located in the p51 connection subdomain.

In the polymerase domain, the 3' end of the primer is close to the catalytic Asp triad and is appropriately positioned for the nucleophilic attack of the α-phosphate of an incoming nucleotide. Residue D185 forms a hydrogen bond with the 3'-OH group of the ultimate nucleotide of the primer. The side-chains of Y183 and M184 (part of the YMDD motif) also have interactions with the ribose of the nucleotide at the 3' end of the primer (38). The β12 and β13 strands, located in the palm subdomain, form the "primer grip". These 2 β-strands are in close proximity to the phosphate joining the penultimate nucleotide to the nucleotide at the 3' end of the primer. The "template grip" is formed of strand β4 and helix αB of the finger subdomain, the β8-αE connecting loop and the β5a strand of the palm.

The thumb subdomain also contacts the nucleic acid substrate. The helix αH contacts the sugar-phosphate backbone of the primer strand, while the αI helix contacts the sugar-phosphate backbone of the template strand.

Interactions between the double-stranded DNA and the enzyme can also be observed in the RNase H domain. However, it can be seen that the DNA:DNA substrate is not in a favourable position for cleavage by RNase H. This can be expected since DNA:DNA is not a substrate for RNase H. In the RNA:DNA liganded structure, many interactions can be seen between the nucleic acid substrate and the enzyme. A region named "RNase H primer grip" contacts the DNA primer and include residues K395 and E396 of p51, G359, A360 and H361 of the p61 connection subdomain and T473, N474, Q475, K476, Y501 and I505 of the RNase H domain. The residues that contact the RNA template are K390 of p51 and R448, N474, Q475, Q500 and H539 of p66.

After the unliganded enzymes and nucleic acid bound enzymes, another structure shows RT liganded with a double-stranded DNA substrate and an incoming dTTP. The primer was chain-terminated with a 2'3'-dideoxynucleotide-monophosphate (ddNMP) in order to avoid incorporation of the incoming nucleotide. This structure shows similar domain and subdomain arrangements as well as interactions between the enzyme and the nucleic acid substrate as the previously discussed structures. One main difference is the inward movement of the tips of the fingers towards the palm subdomain, closing the cleft previously observed in nucleic acid bound structures, forming a binding pocket for the incoming nucleotide (Fig. 1.2B). This nucleotide base pairs with its complementary nucleotide on the template and stacks on one side with the ultimate nucleotide of the primer and on the other side with the side chains of R72 and Q151. The triphosphate moiety of the nucleotide interacts with K65, R72, the main chains of residues 113 and 114, and 2 Mg^{2+} ions. Residues 65 and 72 come in contact with the incoming dNTP as a

result of the closure of the fingers. As mentioned above, 2 divalent Mg ions interact with the incoming dNTP. One of them interacts with each of the 3 phosphates of the dNTP, as well as with the side chains of the catalytically active D110 and D185. The other ion interacts with the α-phosphate of the dNTP, all 3 catalytically active Asp (110, 185 and 186) and seems like it would interact with the missing 3'-OH of the primer.

The 3'-OH of the incoming nucleotide projects into a small pocket formed by residues D113, Y115, F116 and Q151, as well as the main chains of residues 113 and 115. This pocket is sufficiently large to accept 2 or 3 water molecules.

The side chain of Y115 has important interaction with the 2' position of the incoming dNTP. It would seem that this residue regulates the selection of 2' deoxynucleotides versus ribonucleotides. This observation was later confirmed by mutational analysis of residue 115. The substitution of Tyr115 by Val, Ala or Gly leads to a 10^3 to 10^5-fold increase in the ability of the reverse transcriptase to incorporate ribonucleotide rather than deoxyribonucleotide (22).

1.2 Function of the reverse transcriptase

As stated earlier, the role of the reverse transcriptase is to copy the viral RNA genome into double stranded DNA. In order to do so, the polymerase must go through many nucleotide incorporation cycles. To better understand the mechanisms of reverse transcriptase, Kati et al. (103) undertook a detailed kinetic study of the nucleotide incorporation activity of the reverse transcriptase.

First, single nucleotide incorporation on a DNA:DNA substrate was measured using steady state and pre-steady state kinetic assays. Under steady state conditions, in which the nucleic acid substrate is in excess over the enzyme, a catalytic rate (k_{cat}) of $0.18s^{-1}$ was measured. Under pre-steady state conditions, in which the nucleic acid substrate was only in slight excess over the enzyme, two elongation phases were observed; a first burst of incorporation, followed by a linear phase. The catalytic rate of the burst was measured at $20s^{-1}$, while the rate of linear phase was only $0.17s^{-1}$, which corresponds to the rate measured under steady state conditions. It was hypothesised from this observation that the rate limiting step must occur after nucleotide incorporation. In a single nucleotide incorporation assay, the enzyme must dissociate from the DNA substrate in order to bind another substrate and incorporate another dNTP. Therefore, the dissociation rate (k_{off}) of the reverse transcriptase from the DNA:DNA substrate was measured in order to identify the rate limiting step. The rate of dissociation measured was $0.17s^{-1}$, corresponding precisely to the rate limiting step in the single nucleotide incorporation assay. When an RNA:DNA template:primer substrate was used in the same pre-steady state conditions, a slightly faster burst of $66s^{-1}$ was observed and a slower linear phase of $0.06s^{-1}$ was measured.

K_d values for nucleic acid substrate binding were measured for both DNA:DNA and RNA:DNA substrates. The values measured were very close for the 2 substrates; 4.7 and 5nM for the DNA:DNA and RNA:DNA substrates respectively. These values are comparable to other studies using poly(rA)/oligo(dT) (90), poly(dA)/oligo(dT) (193) or random sequence synthetic oligonucleotides (192) as substrates. Competition assays also

showed that the 2 substrates compete with each other for binding to reverse transcriptase and therefore bind to the same active site.

K_d values for dNTP binding to the E•DNA complex were then measured using again DNA:DNA and RNA:DNA as nucleic acid substrate. Using a DNA:DNA substrate, dATP had a measured K_d of 4μM, but in the presence of an RNA:DNA substrate, the K_d measured was 14μM. These values are significantly higher than K_m values measured from steady state kinetic assays, which can be as low as 0.05μM (115, 194).

After the single nucleotide incorporation experiments, processive elongation was analyzed. The rate of dNTP incorporation on a DNA:DNA substrate observed was $20s^{-1}$, which corresponds to the rate of the burst measured in pre-steady state conditions in single nucleotide incorporation assays. The rate observed with an RNA:DNA substrate was correspondingly higher, as observed earlier. The dissociation rate of the nucleic acid substrate from the enzyme was significantly higher than that measured earlier; approximately $2.3s^{-1}$, as opposed to $0.17s^{-1}$ in single nucleotide incorporation events.

In order to reconcile these observations, the k_{off} for the nucleic acid substrate was measured in the presence of dNTPs in 2 different assays. First, an assay using an enzyme trap (unlabelled DNA:DNA substrate) was used to determine the stability of the reverse transcriptase on its nucleic acid substrate. Nucleotide analogues dATPαS and ddATP were used due to their slower rate of incorporation, allowing more dissociation before nucleotide incorporation occurs. When the results of the assay in the absence and in the presence of trap were compared, dissociation constant of $1.9s^{-1}$ and $0.7s^{-1}$ were measured

for dATPαS and ddATP respectively, suggesting a faster rate of dissociation of the E•DNA•dNTP complex compared to the E•DNA complex.

Steady state measurements of the incorporation of ddATP were also conducted in the presence and in the absence of the next templated nucleotide, dCTP. Due to the lack of a 3'-OH group, dCTP cannot be incorporated, therefore the dissociation constant can be measured just before the nucleotide is incorporated to the DNA primer. The k_{cat} obtained in the absence of dCTP was $0.18s^{-1}$, comparable to earlier observations in single nucleotide incorporation assays. In the presence of dCTP, the k_{cat} was significantly lower; $0.019s^{-1}$, suggesting a tighter binding of the enzyme to its nucleic acid substrate in the presence of the next templated nucleotide.

The discrepancy between the last two measurements, showing on one side that the enzyme is less stable after dNTP binding and that its stability is increased by the presence of the next dNTP on the other side, suggest two conformations of the E•DNA•dNTP complex. A first complex occurs when the dNTP binds to the E•DNA complex, and seems to destabilize the enzyme from its nucleic acid substrate, then a second complex occurs, in which the E•DNA•dNTP complex is stabilized. This model agrees with a rate limiting conformational change observed in other polymerases (118, 177, 260). It has been proposed by Huang *et al*. that the closure of the fingers observed in the structure of the ternary complex corresponds to this rate limiting step (88).

It was determined that divalent metal ions, most particularly Mg^{2+} are required for the polymerization activity of the reverse transcriptase (83). Two Mg^{2+} ions can also be

observed in the ternary structure of the reverse transcriptase complexed with a double-stranded DNA substrate as well as an incoming dTTP (88). Using these observations, as well as the structure of other polymerases (40, 110, 181), a model for phosphodiester bond formation between the incoming nucleotide and the 3' end of the primer was proposed (228). In this model, two metal ions are present at the active site of the enzyme as well as the 3' end of the primer and the incoming nucleotide. Metal ion A, which contacts the 3'-OH of the 3' end nucleotide of the primer, the side chain of D110, D185 and D186 on the reverse transcriptase, as well as the α-phosphate of the incoming nucleotide, lowers the affinity of the 3'-OH of the primer for the hydrogen, facilitating the $3'\text{-}O^-$ attack on the α-phosphate of the incoming nucleotide. Metal ion B, which contacts a non-bridging oxygen from each of the phosphates of the incoming nucleotide, as well as the side chains of D110 and D185 on the enzyme, assists in the release of the pyrophosphate created as a product of the reaction. Both metal ions stabilize the structure and the charge of the transition state.

Using the data mentioned above, it is possible to identify most of the steps of a nucleotide incorporation cycle (Fig. 1.3). First, the enzyme must associate with the nucleic acid substrate and locate a free 3' end. Once the enzyme is correctly positioned on the substrate, nucleotide binding can occur. Nucleotide binding should be favoured due to binding constants observed in the sub-μM range, which is lower than dNTP concentrations observed in cells (97). After nucleotide binding, the enzyme undergoes a rate-limiting closure of the fingers in order to stabilize the complex and bring all the elements into the correct orientation for the phosphodiester bond to form. The bond formation leaves a DNA chain longer by one nucleotide and a pyrophosphate group as

Fig.1.3 Nucleotide incorporation cycle. The first step before nucleotide incorporation can occur is the binding of the nucleic acid substrate and the correct positioning of the enzyme. Once this occurred, the enzyme can bind the incoming nucleotide. A rate limiting conformational change follows the nucleotide binding (indicated by an asterisk). Based on structural evidence, the closure of the fingers subdomain has been suggested to be this conformational change. The phosphodiester bond is formed between the nucleotide and the 3' end of the primer, forming a DNA chain that is longer by one nucleotide and a pyrophosphate group. In order to start the next cycle, the pyrophosphate group has to be released and the enzyme must translocate to free the nucleotide binding site. The order of the last two steps has not yet been determined.

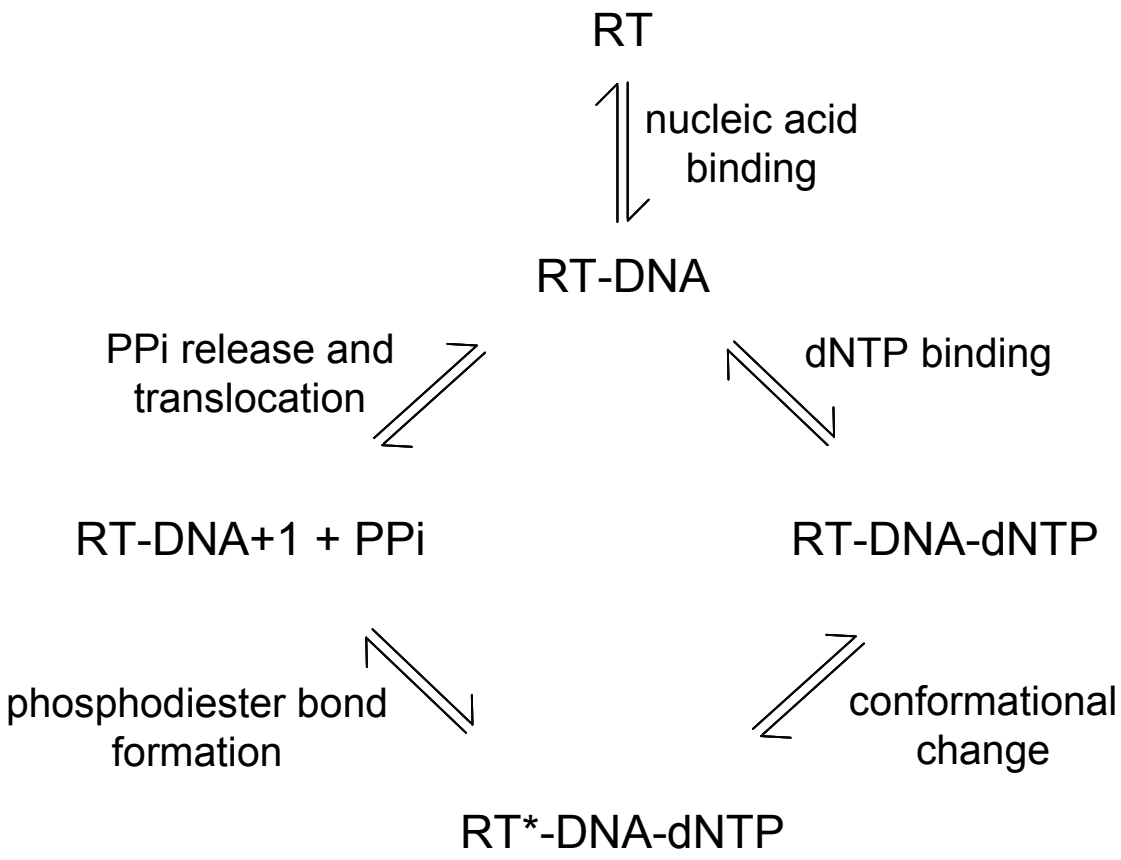
RT
nucleic acid binding
RT-DNA
PPi release and translocation
dNTP binding
RT-DNA+1 + PPi
RT-DNA-dNTP
phosphodiester bond formation
conformational change
RT*-DNA-dNTP

products. At this time, the 3' end of the elongating DNA chain is still located in the nucleotide binding site. In order for the next cycle to begin, pyrophosphate must be released and the nucleotide binding site must be freed. In order to free the nucleotide binding site, the reverse transcriptase could act in two ways; either it dissociates from the nucleic acid substrate and rebinds at the correct site, or it moves along the nucleic acid by one nucleotide and starts the next cycle. The latter mechanism, called processive elongation has been shown to be the one used by the reverse transcriptase (103). The movement by one nucleotide in order to free the nucleotide binding site is referred to as translocation. This step is undetectable in kinetic assays, and a movement of one nucleotide is difficult to identify using current footprinting assays, which explains the little amount of information available in the literature describing translocation.

1.2.1 Mechanisms of translocation

As discussed above, translocation is the movement of the polymerase by one nucleotide in order to free its nucleotide binding site and initiate the next cycle of nucleotide incorporation. Two models of translocation have been proposed; the power stroke model and the Brownian ratchet model. The power stroke model implies that a motor force, most likely triggered by the nucleotide incorporation or the pyrophosphate release, is moving the enzyme along the elongating DNA. The Brownian ratchet model involves an equilibrium between the pre- and post-translocated sites, where the enzyme is free to oscillate between the two conformations. Evidence for each of these models can be found in the literature.

1.2.1.1 The power stroke model

This model requires that a mechanical function of the polymerase pushes the enzyme along the DNA. Energy would be required for this to happen. Crystal structures of the T7 RNA polymerase bring evidence supporting this model. The structure of the T7 RNA polymerase in a transcription bubble with an incoming nucleotide shows the enzyme in the post-translocational state (262). The finger subdomain is in the closed conformation. This structure represents a catalytic complex ready for phosphodiester bond formation. Of interest, the side chain of the amino acid Tyr639 located at the base of the fingers subdomain stacks with the base moiety of the bound NTP. Another crystal structure shows the polymerase after phosphodiester bond formation has occurred (262). The enzyme is shown in the pre-translocational state, and pyrophosphate is still bound to the enzyme. The NMP moiety of the incorporated nucleotide is still in the same position in the nucleotide binding site while the pyrophosphate is slightly displaced, but still contacts the finger subdomain, which is still in the closed conformation, and the Mg^{2+} ions present in the polymerase active site. It is unclear however whether the pyrophosphate was never released from the enzyme or that it was released and rebound in an equilibrium. A third structure of the T7 RNA polymerase shows the enzyme in a transcription bubble without a nucleotide in the active site (261). This structure shows the polymerase in the post-translocational state. The fingers subdomain is in the open conformation in this structure. It can be noticed here that the side chain of amino acid Tyr639 still stacks with the base moiety of the 3' nucleotide. As the finger subdomain opens, amino acid 639 moves toward the active site along with the growing RNA chain. This side chain now occludes the nucleotide binding site in such a way that the next incoming nucleotide cannot stack

with the 3' nucleotide and cannot base-pair with the templated base. It also seems to prevent the 3' end of the RNA chain from moving back to the nucleotide binding site. It is not possible at this time to determine if the side chain of residue 639 actively pushes the RNA, or simply prevents the back movement. It has been proposed by the authors that the fingers movement is powered by the release of the pyrophosphate, and not by the phosphodiester bond formation. This hypothesis is supported by the fact that the enzyme is still in the pre-translocational state before pyrophosphate release, but in the absence of pyrophosphate, it is found in the post-tranlsocational state.

1.2.1.2 The Brownian ratchet model

In this second model, the polymerase is free to oscillate between the pre- and the post-translocational states in a Brownian motion powered by molecular movements in a liquid environment. A mechanism acting as the pawl of a ratchet would block the enzyme in the post-translocational state, allowing the incorporation of a nucleotide. This mechanism is most likely the binding of the incoming nucleotide. Structural, kinetic and energetic evidences are available in the literature supporting this model.

Observation of the energetic distribution in the active site of polymerase brings clues on the mechanism of translocation (68). The structure of various polymerases, including the reverse transcriptase (88) and the T7 RNA polymerase (262) have been obtained in the presence of a nucleic acid substrate as well as an incoming nucleotide. In all these structures, it can be observed that the interactions between the protein and the (d)NTP are mostly located in the pyrophosphate moiety of the nucleotide, while interaction with the

sugar and the base are limited. These observations are supported by inhibition assays of the T7 RNA polymerase carried with pyrophosphate and GMP as competitive inhibitors to GTP (68). In these assays, pyrophosphate is a much better inhibitor than GMP, by approximately 60-fold, meaning that the pyrophosphate moiety bind more tightly to the polymerase than the GMP moiety. This nucleotide binding mode was probably evolved in order to allow the elongating nucleic acid chain to move away from the nucleotide binding site after phosphodiester bond formation and pyrophosphate release without the requirement of high energy input.

The measurement of kinetic constants in the presence of physical blocks to the T7 RNA polymerase also brings evidence of a free sliding mechanism (67). When an obstacle such as a DNA binding protein is present on the template strand, the RNA polymerase will first be slowed down and then completely blocked. If the mechanism of translocation is powered by the release of pyrophosphate, such as suggested by the power stroke mechanism, the obstacle should not affect the affinity of the enzyme for nucleotide, since the enzyme is actively translocated after pyrophosphate release, allowing the next nucleotide to bind. On the other hand, if the enzyme is free to slide between the two conformations and that only nucleotide binding stabilizes the post-translocational state, an enzyme slowed down by an obstacle will not be able to bind nucleotides as well as in the absence of the obstacle. Guajardo *et al.* showed that in the presence of an obstacle, elongation becomes nucleotide dependent, suggesting that this obstacle inhibits translocation, impairing the ability of the polymerase to bind the next incoming nucleotide.

Most experiments conducted to measure translocation were done on stalled complexes. Results on those complexes suggest an equilibrium between the pre- and the post-translocated complexes, consistent with a Brownian ratchet model. In order to evaluate if the enzyme has time to reach an equilibrium during processive elongation, inhibition assays using pyrophosphate were conducted (70). The idea behind these assays was that if an equilibrium is reached during fast elongation, the polymerase should be as sensitive to pyrophosphate than the stalled complex, since in both cases, the enzyme has access to the pre-translocational state, where pyrophosphate is expected to bind. K_i for pyrophosphate on a fast elongating enzyme was calculated to be 2.6±0.79mM, while the K_m for pyrophosphate on a stalled complex was measured at 1.7±0.89mM. The small difference between these two results is within the margin of error for those assays and can be considered insignificant. Similar results suggest a similar access to the pre-translocational state on both a fast elongating enzyme and a stalled complex, pointing to a free sliding mechanism.

Translocation measurements were also conducted with the reverse transcriptase of HIV-1. Through the use of site-specific footprinting assays, it was shown that the reverse transcriptase can occupy both sites in a binary complex containing only the reverse transcriptase and a double-stranded DNA substrate (140-142). This observation is the same when a nucleotide is incorporated before the footprint is executed, showing that the enzyme is in equilibrium between the two states, and that translocation is not linked to nucleotide incorporation or pyrophosphate release (140-142). In depth analysis allowed the identification of factors influencing the translocational equilibrium; the nucleotide sequence (141, 142), the nature of the DNA chain's 3' end (141), the temperature (141),

the presence of nucleotides (141), the presence of drug resistance mutations (141), the presence of mismatches (140), and the presence of pyrophosphate analogues (142) were all shown to affect the translocational equilibrium.

A crystal structure of the reverse transcriptase trapped in the pre-translocational state showed that there is a movement downward of the YMDD motif compared to the unliganded enzyme (211). The authors proposed that this motif could act as a springboard, pushing the DNA to the post-translocational state when released. The spring board would be loaded as the nucleotide is bound to the enzyme and the phosphodiester bond is formed. As mentioned above, temperature has an influence on the translocational equilibrium. Lower temperatures favour the formation of the post-translocated complex, when compared to higher temperatures. In the case of crystal structures, which are formed at low temperatures, it is possible that this lower state of energy makes the active site of the enzyme more rigid, which would not be the case at 37^0C. The effect observed in the structure might not be significant at higher temperatures.

Although evidence is available for both models, the Brownian ratchet model seems to have more definitive support, and is favoured because of the observations mentioned above.

1.3 Fidelity of the reverse transcriptae

Retroviruses have a highly variable genome. This trend has been well documented, most particularly in HIV-1 and the simian immunodeficiency virus (SIV) (19, 72, 100, 174).

The mutation rate of retroviruses measured in cell culture ranged from 10^{-6} to 10^{-4} mutations per nucleotide per cycle (129, 178). Single cycle viral replications assays showed a mutation rate of 3 to 4 x 10^{-5} mutations per nucleotide per cycle (137, 139). This mutation rate is well above the mutation rate of 10^{-11} to 10^{-7} observed in organisms possessing a DNA genome (41). This mutation rate in retroviruses may be due to many factors. The viral RNA genome is copied to DNA by the reverse transcriptase. This proviral DNA is then incorporated to the cellular genome, where it gets copied by cellular DNA polymerases at each cell division. The viral genome is also copied by the cellular RNA polymerases in order to produce new viruses. Although cellular factors cannot be completely ignored, it is believed that the reverse transcriptase is the major factor of viral variation.

Assays to test the error rate of the purified reverse transcriptase were conducted and a rate of 5 x 10^{-4} was observed when the reverse transcriptase is used to copy a long heteropolymeric template (186). Comparisons of kinetic parameters for the correct nucleotide versus the incorrect nucleotide incorporation varied enormously according to the sequence and the type of mismatch. The ratio of incorrect nucleotide incorporation over correct nucleotide incorporation varied from no detectable mismatch formation to 35 x 10^{-4} (200). The lowest rate of misinsertions observed were A:G, G:G and G:C (150), while the most frequent misinsertion was G:T (209, 263). The major determinant in reduced mismatched nucleotide incorporation seems to be at the level of the K_m rather than the k_{cat} (186, 200). This observation is in good agreement with a model based on base pair geometry in order to reject mismatched nucleotides (57).

Another aspect of a polymerase error rate is the elongation of a mismatched primer. The HIV-1 reverse transcriptase was shown to be relatively efficient at elongating primers with a mismatch at the 3' end of the primer; the reverse transcriptase was revealed to be 50 times more efficient than the mammalian DNA polymerase α (182). HIV-1 reverse transcriptase was also shown to be able to elongate primers containing up to 3 mismatched nucleotides at their 3' end (263).

Mutagenesis studies helped in identifying the major residues and sites responsible for the relatively high error rate of the HIV-1 reverse transcriptase. The side chain of Gln151 contacts the incoming nucleotide between the sugar and the base moiety. Its close proximity with the incoming nucleotide makes it a good candidate for correct base pairing control. Substitution of the residue Gln151 to Asn leads to a more accurate enzyme compared to the wild type reverse transcriptase. This trend was observed in elongation assays lacking one of the four nucleotides (251), as well as in kinetic measurements (105).

Lys65 contacts the phosphates of the incoming nucleotide in closed complex. Mutation K65R displayed better fidelity than the wild type enzyme in genetic assays (220). Mutation of the residue Arg72, which also contacts the phosphates of the incoming nucleotide in the closed complex, leads to a more accurate enzyme than wild type reverse transcriptase with the exception of an unusually high level of misincorporation opposite T in a specific sequence (131). This highlights the importance of the sequence in the incorporation of matched and mismatched nucleotides.

Residues that contact the primer and the template strands also play a role in fidelity. Leu74 contacts the templating base and the incoming dNTP. The mutation L74V produces an enzyme that is significantly more error prone than the wild type enzyme (208). Mutation of residues Asp67 and Arg78 also modifies the ability or the reverse transcriptase to incorporate mispaired nucleotides. These two residues interact with the sugar-phosphate backbone of the templating nucleotide. Mutants D67V and R78N have approximately a 9-fold increase in fidelity compared to wild type reverse transcriptase (111, 112). Glu89 is another residue that interacts with the templating strand. Mutating Glu89 to Gly increases significantly misinsertion and mispair extension fidelity (42, 74, 208). In the residues contacting the primer strand, residue 183 and residues of the primer grip, including 227, 229, 230, 231 and 232 were all shown to have an impact on fidelity in mutagenesis experiments (78, 79, 259).

A factor explaining in part the high error rate of the reverse transcriptase is the apparent lack of a proofreading mechanism such as a 3'-5' exonuclease activity. It was hypothesised that the pyrophosphorolysis reaction, the removal of the primer's 3' nucleotide, could act as proofreading mechanism (140). However, on a template with the base T paired with the primer's 3' end, no removal could be observed when the primer contained the base C or T at its 3' end. Although the G:T mismatch could be efficiently removed, the lack of cleavage of the T:T and the C:T mismatches suggest that this mechanism would not be sufficient to serve as a proofreading mechanism.

1.4 Reverse transcriptase inhibitors and resistance

Due to its vital role in the viral life cycle, the reverse transcriptase is one of the main targets for antiretroviral therapy. Many reverse transcriptase inhibitors have been developed, and these inhibitors are divided in two classes; the nucleoside and nucleotide analogue reverse transcriptase inhibitors (N(t)RTIs), and the non-nucleoside analogue reverse transcriptase inhibitors (NNRTIs). Both classes act against the polymerase activity of the reverse transcriptase. Even though they act against the same activity, their mechanisms of action differ significantly.

1.4.1 Nucleoside and nucleotide analogue inhibitors

Nucleoside analogue reverse transcriptase inhibitors all resemble nucleosides; they all have a sugar and a base, although there can be modifications present in each of those moieties. They all lack a 3'-OH group, necessary for phosphodiester bond formation. The 3'-OH group may be either absent or replaced by another chemical group. Nucleoside analogue are administered as unphosphorylated prodrugs, and are phopshorylated to their active triphosphate form by cellular kinases. The only nucleotide analogue used in the clinic to treat HIV-1 infection has an open sugar moiety and a phosphonate group replacing the α-phosphate of natural nucleotides. This nucleotide analogue must be phosphorylated to its diphosphate active form by cellular kinases. The active form of all N(t)RTIs competes with natural nucleotides for incorporation in the growing DNA chain. Once incorporated, they act as chain-terminators due to the lack of the 3'-OH group (58, 164). There are 7 nucleoside analogues and 1 nucleotide analogue

used in the clinic; 3'-azido-2',3'-dideoxythymidine (AZT, zidovudine), 2',3'-dideoxyinosine (ddI, didanosine), 2',3'-dideoxycytidine (ddC, zalcitabine), 2',3'-didehydro-2',3'-dideoxythymidine (d4T, stavudine), (-)-β-L-3'-thia-2',3'-dideoxycytidine (3TC, lamivudine), (1*S*,4*R*)-4-[2-amino-6-(cyclopropyl-amino)-9*H*-purin-9-yl]-2-cyclopentene-1-methanol succinate (ABC, abacavir), (-)-β-L-3'-thia-2',3'-dideoxy-5-fluorocytidine (FTC, emtricitabine), and the nucleotide analogue (*R*)-9-(2-phosphonylmethoxypropyl)adenine (PMPA, tenofovir) (Fig. 1.4). Abacavir and didanosine must undergo extra modifications by cellular enzyme on their base moiety to create the active forms; carbovir-triphosphate and dideoxyadenosine-triphosphate (ddATP) respectively. The incorporation rates of the different analogues differ significantly. While it was shown that AZT-triphosphate (TP) and d4T-TP are barely discriminated when competing with dTTP for incorporation (108), the incorporation of ddCTP is incorporated with less efficiency than dCTP (49). 3TC-TP had a lower level of incorporation than dCTP and ddCTP (49, 116).

Even though N(t)RTIs efficiently terminate DNA elongation once incorporated, the reverse transcriptase is able to remove an incorporated chain-terminator in the presence of pyrophosphate or a pyrophosphate donor such as ATP (2, 156). The removal reaction resembles the inverse of the nucleotide incorporation reaction. The enzyme uses the pyrophosphate or pyrophosphate donor to attack the phosphate junction between the chain-terminator and the penultimate nucleotide and reforms the triphosphate form of the analogue or a dinucleotide tetraphosphate, respectively. The rate of removal also varies significantly between different nucleotide analogues, with AZT-MP being removed at a

Fig.1.4 Chemical structure of the clinically used nucleoside and nucleotide analogue inhibitors.

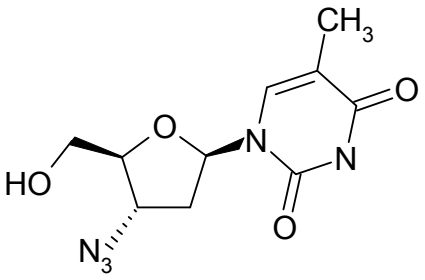

AZT

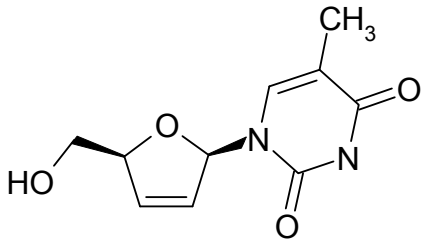

d4T

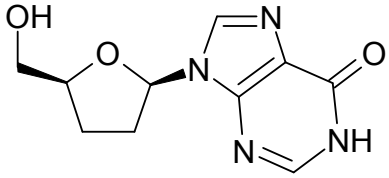

ddI

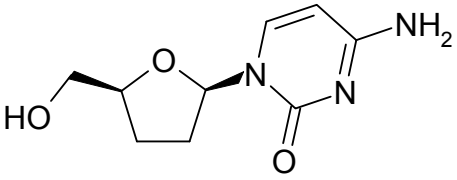

ddC

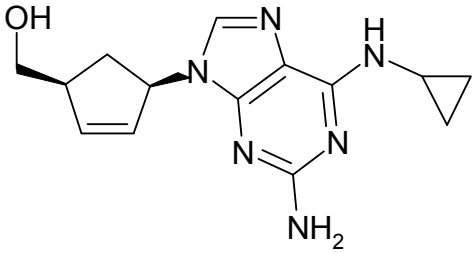

ABC

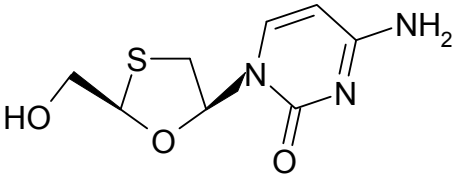

3TC

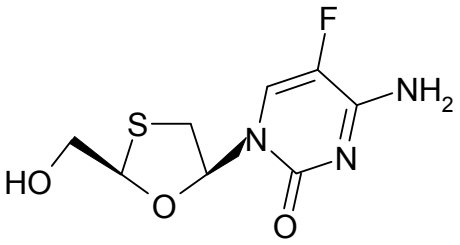

FTC

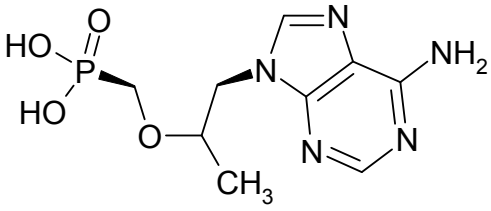

PMPA

relatively fast rate compared to other chain-terminators, and 3TC-MP being cleaved at a very slow rate (92).

Due to the low fidelity of the reverse transcriptase, mutations frequently occur in the various genes of HIV-1, including the *pol* gene, coding for the reverse transcriptase. Under the pressure of inhibitors, drug resistance mutations are selected, which impair the efficiency of the antiviral treatment. Resistance to N(t)RTIs can occur with a single mutation, as is the case with 3TC (241), or may require the accumulation of many mutations.

At least two distinct mechanisms of resistance to N(t)RTIs have been described. In the first one, the mutant enzyme is able to discriminate the nucleoside analogue to the profit of the natural nucleotide. This results in a lower incorporation level of the drug when in competiton with the natural nucleotide. The second mechanism involves the pyrophosphate or pyrophosphate donor dependent removal of the chain-terminator. The mutant enzyme is faster at removing the nucleotide analogue, increasing the possibility of incorporating a natural nucleotide instead.

1.4.1.1 Mechanism of discrimination

The discrimination mechanism was extensively described with the 3TC and FTC resistant enzyme M184I/V reverse transcriptase (116, 187). In steady-state kinetic assays, K_m and V_{max} values for dCTP incorporation were measured using both homo- and heteropolymeric templates for wild-type and M184V reverse transcriptases (187). The

kinetic constants were unchanged by the mutation M184V. K_i values for 3CT-TP incorporation were also measured using the same two enzymes. While dCTP incorporation remained the same with the two enzymes, the incorporation of 3TC-MP against a heteropolymeric template was diminished by 36-fold. The K_i/K_m value, which is an indication of which will be incorporated, the natural dNTP or the chain-terminator, varied from 0.32 for wild-type reverse transcriptase to 11.69 for the M184V mutant, again resulting in a 36-fold decrease in the likelihood of 3TC-TP to be incorporated when competing with dCTP. Pre-steady state studies of the same enzymes demonstrated that the increase in K_i observed earlier is due to an equivalent decrease (22 fold for a DNA template and 35 fold for an RNA template) in k_{pol} rather than a decrease in the affinity for 3TC-TP (116). The M184V enzyme also confers low level of resistance (4 to 8 fold) to ddATP (the active metabolite of ddI) and ddCTP in cell culture (54, 66). A small difference in k_{pol} was observed between the two enzyme for ddATP (1.6 fold) while no significant difference could be seen for ddCTP. This minor change in k_{pol} seems to correlate with the low level of resistance observed *in vivo*. The opposite was observed with FTC, the fluorinated analogue of 3TC. Pre-steady state constants were determined for wild-type and M184 reverse transcriptase. While a difference in k_{pol} was observed between the two enzymes using 3TC, no difference in k_{pol} was observed when FTC was the inhibitor (256). Instead, a difference of 19-fold in the K_d was observed. While the level of resistance to 3TC and FTC differs for the M184V enzyme, the similarity between the two inhibitors would have suggested the same mechanism of resistance.

The crystal structure of the ternary complex of the reverse transcriptase bound to a double-stranded DNA substrate and an incoming dNTP showed that M184 contacts both

the 3' end of the primer and the incoming dNTP (88) (Fig. 1.5A). The crystal structure of the M184I mutant provides important evidence for the resistance mechanism of this mutant (213). When dCTP and 3TC-TP are modeled in this structure, the biggest difference is observed in the positioning of the sugar moiety of the nucleotides. 3TC is an L enantiomer of the nucleotides, which projects its sugar 1.5-2Å toward residue 184. This closer contacts results in steric hindrance between the $C_\gamma 2$ methyl of Ile and the oxathiolane ring of the nucleotide analogue. This observation is supported by the resistant phenotype observed with every β-L enantiomers of nucleotide analogue tested with the M184V mutant (256). It is also supported by the nature of other mutations at residue 184 resulting in resistance to 3TC. In addition to Ile and Val substitutions at residue 184, Thr is the only other mutation conferring resistance to 3TC, meaning that only β-branched amino acids will result in 3TC resistance (4, 109).

The L74V mutation develops during the treatment of HIV-1 infected patient with ddI (227, 258). It confers moderate resistance to ddI (6 to 26 fold) and low level resistance to ddC (approximately 15 fold). L74V in combination with M184V also confers low level resistance to ABC (77, 162). Enzymatic assays using wild-type and L74V reverse transcriptase showed no significant difference in the kinetic constants for dNTP incorporation, but differences of 4.5- and 3.3-fold were observed in the K_i for ddATP and ddCTP respectively, suggesting a discrimination mechanism of resistance (143). The same conclusion can be drawn with pre-steady state incorporation assays of dGTP and ABC by wild-type and L74V reverse transcriptase (190). While no major difference is observed between the two enzymes for the incorporation of dCTP, a decrease in the

Fig.1.5 Position of the residues involved in the discrimination mechanism of resistance to nucleoside analogue inhibitors. The residues are shown relative to the DNA:DNA substrate and the incoming nucleotide. The DNA primer is colored red and the template is shown in yellow. The incoming nucleotide is colored by atoms (carbon; grey, nitrogen; blue, oxygen; red and phosphorus; yellow). The highlighted residues are also colored by atoms using the same color code.

A

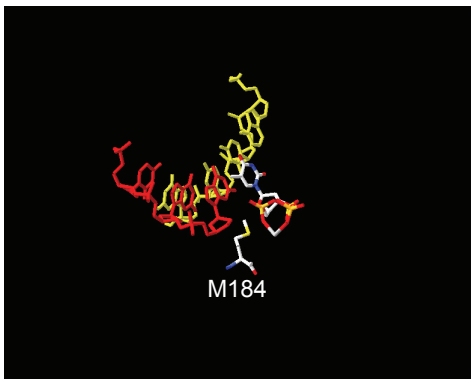

B

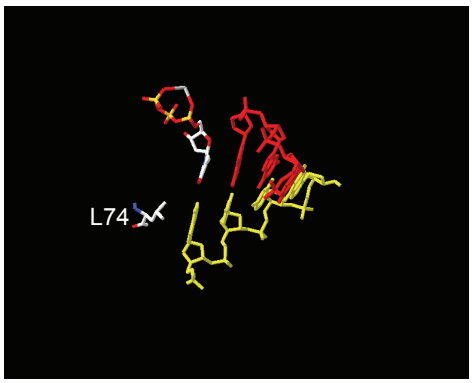

C

D

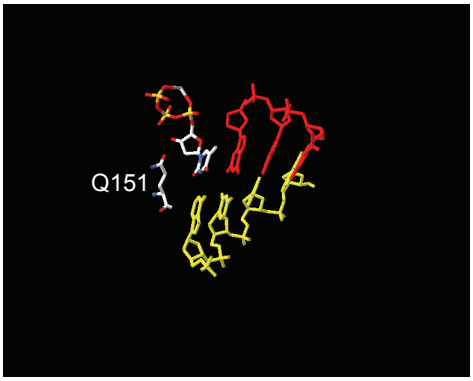

k_{pol}/K_d ratio of 4.2-fold is observed with the L74V mutant compared to the wild-type enzyme.

Leu74 contacts the template base pairing with the incoming nucleotide (88) (Fig. 1.5B). A crystal structure of the unliganded L74V enzyme shows no significant change compared to the wild-type enzyme (196). It has been hypothesised that the diminished incorporation of ddNTPs by the L74V enzyme is due to a repositioning of the template/primer at the active site, which would yield an unfavourable complex for ddNTP incorporation (18).

The K65R mutation in the reverse transcriptase is associated with resistance to ddI, ABC, PMPA, 3TC and ddC (77, 162, 250, 258). The mechanism of resistance conferred by the K65R mutation has been found to be linked to reduced incorporation of the inhibitor in steady state and pre-steady state kinetic studies (36, 255). Although this mutation confers an advantage in the presence of drug pressure, its appearance is not frequently observed in treated patients. It has been observed that this advantage comes at a cost; the mutant enzyme has a decreased replicative capacity compared to the wild-type enzyme, caused by a decreased ability to use natural nucleotides (35, 36).

In the ternary complex of reverse transcriptase, Lys65 forms contact with the γ-phosphate of the incoming nucleotide (88) (Fig. 1.5C). In a ternary structure of the reverse transcriptase with PMPA-diphosphate (PMPA-DP) as an incoming nucleotide, Lys65 is in a position to potentially make contact with the α-phosphate of PMPA-DP (244). Since it has been shown that both Lys65 and the 3'-OH of the incoming nucleotide are

important in the conformation of the ternary complex, the loss of both of these contacts may be behind the poor use of dideoxynucleotides and analogues lacking a 3'-OH group compared to natural deoxynucleotides.

The Q151M mutation confers resistance to a wide variety of NRTIs. This mutation is observed after treatment of infected individuals with thymidine analogues (AZT or d4T) along with ddI or ddC (93, 221). Although the Q151M mutation confers NRTI resistance, it is at the sacrifice of its replicative capacity (136). The appearance of other mutations (A62V, V75I, F77L and F116Y) along with Q151M corrects the replication deficiencies as well as increases the level of resistance (247). An enzyme harbouring all five of these mutations was resistant to ddATP, AZT-TP, d4T-TP, and ddCTP, but was still sensitive to PMEApp (a NtRTI analogous to PMPApp) and 3TC-TP (246).

As with Lys65, Gln151 also forms contacts with the incoming nucleotide (Fig. 1.5D). The loss of this contact is expected to destabilize the ternary complex. Added to the loss of contact with the absent 3'-OH group, this might be sufficient to significantly decrease the incorporation of analogues lacking the 3'-OH.

1.4.1.2 Mechanism of excision

Resistance to the T analogues AZT and d4T occurs with the appearance of a specific set of mutations including M41L, D67N, K70R, L210W, T215Y/F and K219Q (76, 106, 123, 147). These residues are all distant from the bound nucleotide and the nucleic acid substrate (88) (Fig. 1.6). The presence of these mutations does not affect the incorporation

Fig.1.6 Position of the residues involved in the excision mechanism of resistance to nucleoside analogue inhibitors. The residues are shown relative to the DNA:DNA substrate (A) and the incoming nucleotide (B). The DNA primer is colored red and the template is shown in yellow. The incoming nucleotide is colored by atoms (carbon; grey, nitrogen; blue, oxygen; red and phosphorus; yellow). The highlighted residues are also colored by atoms using the same color code.

A

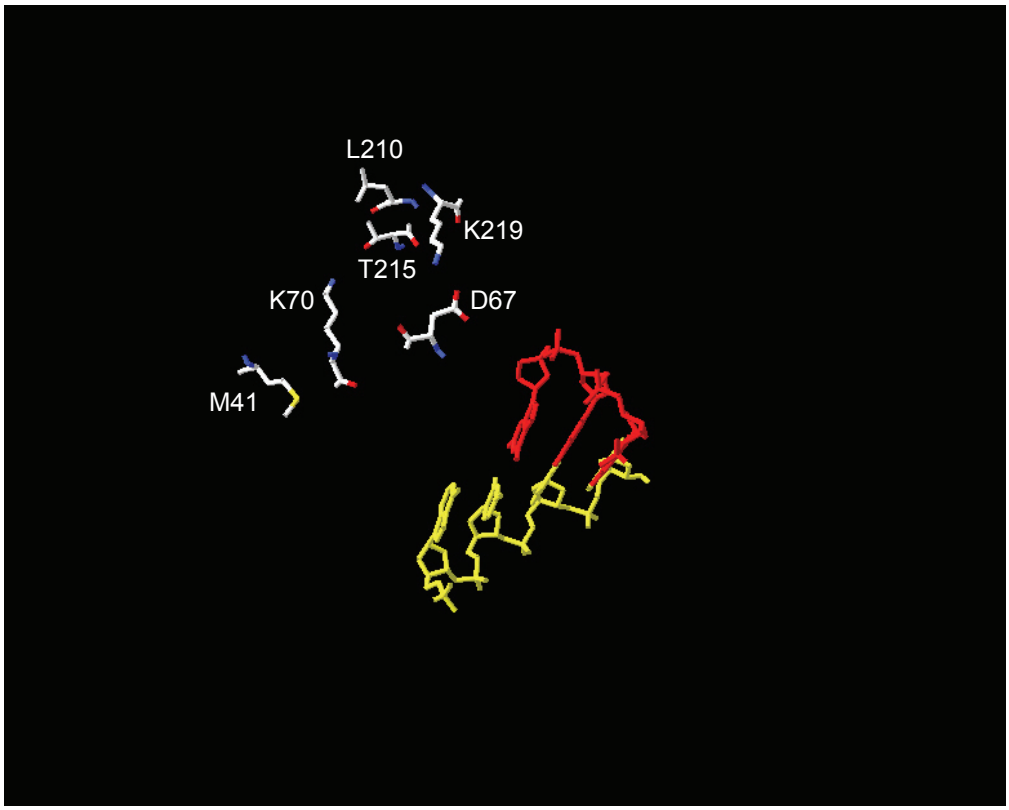

B

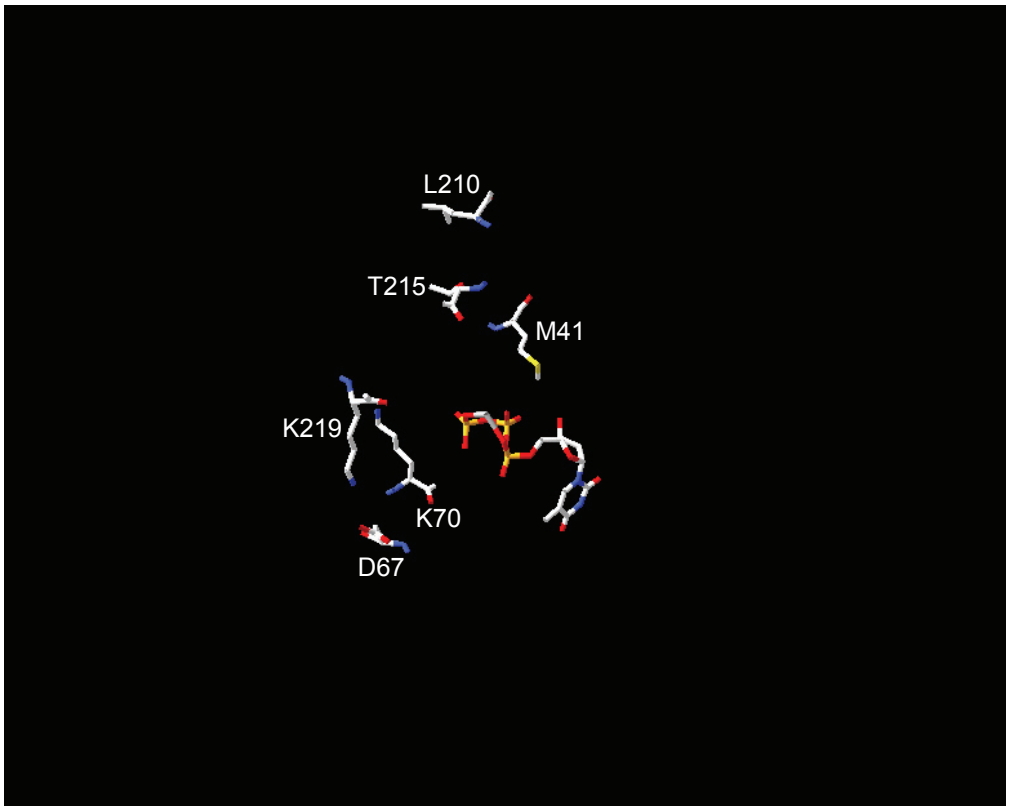

of nucleotide analogues in the elongating DNA chain (120). Instead, they accelerate the ATP-dependent removal of the incorporated NRTI in order to resume the elongation of the formerly terminated DNA strand (154). Detailed kinetic analysis of this reaction showed that the increased rate of chain-terminator removal conferred by the above mentioned set of mutations is due to an increase in the maximum rate of the removal reaction while no significant difference in ATP binding was observed (189). This observation suggests a favourable modification in the orientation of the bound ATP to the catalytic site of the reverse transcriptase. A study of the substrate (nucleotide-triphosphate) showed that an aromatic base enhances the removal reaction, suggesting a π-π interaction between the NTP and the aromatic side chain of one of the residues, most likely 215F/Y (157). This interaction probably favours the correct orientation of the NTP for the removal reaction to occur.

It was hypothesised that the removal reaction can only occur when the chain-terminator sits in the nucleotide binding site, prior to enzyme translocation (17). This hypothesis is supported by the inhibitory effect of the next complementary nucleotide on the removal reaction, which suggests that the chain-terminator is moved to the priming site in order to bind the incoming nucleotide, forming a dead-end complex (156). The hypothesis was later confirmed using site-specific footprinting assays (141) and cross-linking assays (212). It was shown with site-specific footprinting assays that complexes which have a preference for the pre-translocational state are more efficient at removing the 3' nucleotide of the primer than complexes showing a preference for the post-translocational state. With cross-linking assays, the complex was trapped either in the pre- or post-

translocated complex. Using these trapped complexes, it was demonstrated that only the pre-translocated complex is able to conduct the removal reaction.

As mentioned earlier, different chain-terminators are removed at different rates. Another factor that influences the rate of removal is the sensitivity to the next templated nucleotide. An enzyme with mutations D67N, K70R, T215F and K219Q was shown to have increase removal rate for both AZT-MP and ddAMP. Although this enzyme is resistant to AZT *in vivo*, it is still sensitive to ddI, the prodrug of ddATP (122). This discrepancy was reconciled when it was shown that the removal of ddAMP at the 3' end of the primer is much more susceptible to inhibition by the next complementary nucleotide (IC_{50} of 12μM) compared to the removal of AZT (IC_{50} of 230μM) (154). At physiologically relevant concentrations of dNTPs, the reaction with ddAMP is most likely inhibited while the reaction with AZT-MP would not. Dead-end complex formation was also measured using band mobility shift assays. When the reverse transcriptase binds the next templated nucleotide after a chain-terminator was incorporated, a stable closed complex is formed between the enzyme, the nucleic acid substrate and the dNTP. When resolved on a non-denaturing gel, this complex will show a shift in the gel compared to a less stable complex in the absence of dNTP. A ddAMP terminated complex is more easily shifted compared to an AZT-MP terminated complex, suggesting a more efficient binding of the next complementary nucleotide when ddAMP is the chain-terminator (154, 242). It was proposed that this difference is due to the bulky azido group at the 3' end of AZT (17). This is supported by the cross-resistant phenotype to all azido-containing nucleoside analogues (122) and the observation using site-specific footprinting that azido-containing analogues tend to reside in the nucleotide binding site after incorporation at

higher concentration of the next complementary nucleotide when compared to dideoxynuleotides (141). Two complexes of the reverse transcriptase were crystallized with a double-stranded DNA substrate containing and AZT-MP molecule at the 3' end of its primer (211). One of the complexes had the AZT-MP molecule in its nucleotide binding site, prior to translocation (pre-translocated complex), while the other had the AZT-MP in the priming site, after translocation (post-translocated complex). While the structure of the post-translocated complex shows some flexibility of the azido group of AZT-MP, modeling of an incoming nucleotide shows steric hindrance caused by this azido group between the incoming nucleotide and the reverse transcriptase-DNA complex. This strongly suggests that the azido group is responsible to the low sensitivity to the next complementary nucleotide in inhibition of the excision reaction.

AZT resistance mutations are also selected by the NRTI d4T (24, 33, 133, 180), and the presence of these mutations decrease the efficacy of d4T in antiretroviral treatment (94, 104). In addition to d4T, they also cause reduced sensitivity to the nucleotide analogue tenofovir (161). Resistance to these analogues has been related to the excision reaction (14, 155, 253, 254). This high level of excision of PMPA was not expected since a structure of the reverse transcriptase with a double-stranded DNA substrate containing a PMPA molecule at the 3' end of the primer showed a high flexibility of the linear sugar moiety, which suggest a resistance to the excision mechanism (244). The level of resistance observed with d4T and PMPA is lower when compared to AZT, which can be explained by the higher susceptibility to nucleotide concentration for inhibition of the removal reaction (154, 254).

Some mutational patterns appear to be incompatible. For instance, when the mutation M184V is added to the AZT resistance conferring mutations, a resensitization to AZT can be observed (124). Similar phenotypes have been observed with the mutations K65R and L74V (227) as well as the NNRTI resistance mutations L110I and Y181C (20, 121) and the foscarnet resistance mutations W88G and E89K (233). It has been demonstrated that many of these mutations decrease the rate of AZT removal from the 3' end of the primer, hence reducing the resistance level of AZT resistant enzymes (15, 50, 61, 158, 163, 219, 222, 254). In the case of the M184V mutation, it has been proposed that the decrease in the rate of excision may be due to a steric conflict with Val184 which affects the positioning of the reaction's components (213). Unfortunately, the resensitization to AZT conferred by the M184V mutation can be compensated for by the appearance of mutations H208Y, R211K and L214F in addition to the classical AZT resistance mutations (230). These residues are in close proximity to the proposed ATP binding site and may alter the orientation of ATP in a favourable manner for the excision reaction to occur in the presence of the M184V mutation (215).

In addition to the mutations mentioned above, other mutations can be selected during HIV-1 treatment with multiple NRTIs. The mutations M41L, D67N, K70R, L210W, T215Y/F and K219Q confer resistance to AZT via the excision mechanism. The addition of mutation E44D/A confers additional resistance to 3TC (82). It was shown that the 3TC resistance due to mutation E44D/A is associated with the excision mechanism. In the presence of the latter mutation, 3TC is more efficiently cleaved from the 3' end of the primer (56).

Another mutation that appears in the background of AZT resistance is the 69 insertion complex. This complex consists of a mutation at residue 69 from Thr to Ser with the insertion of two or more amino acids (usually SS, SA or SG) between residues 69 and 70 and confers resistance to all clinically used NRTIs (30, 235, 257). A mutant enzyme containing this mutational pattern confers resistance by increasing the rate of chain-terminator removal (16, 144, 153, 253). Site-specific footprinting assays showed that the increase in chain-terminator removal is due to an increased access to the pre-translocational state (141). This observation is also supported by gel mobility shift assays (16).

It was demonstrated that the selection of a mechanism of resistance is based on the initial properties of the inhibitor. For instance, nucleoside analogues that are poorly incorporated, such as 3TC, will favour a discrimination mechanism as opposed to AZT, which is efficiently incorporated, but also easily removed, which will favour the removal mechanism (92).

1.4.2 Non-nucleoside analogue inhibitors

Non-nucleoside analogue reverse transcriptase inhibitors are part of a chemically diverse class of inhibitors. They all bind to the same binding pocket in the polymerase domain to inhibit the nucleotide incorporation activity of the reverse transcriptase. There are three NNRTIs clinically used; the first generation inhibitors nevirapine and delavirdine and the second generation inhibitor efavirenz (Fig. 1.7). Crystal structures showed that all three of these inhibitors bind to the NNRTI binding pocket (NNIBP) which is close but not

Fig.1.7 Chemical structure of clinically used non-nucleoside analogue inhibitors.

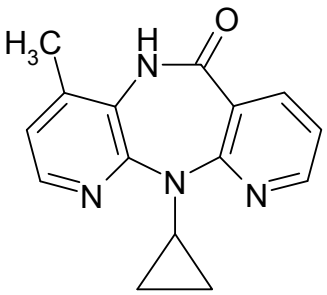

nevirapine

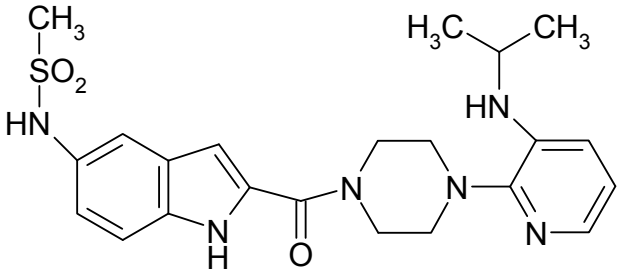

delavirdine

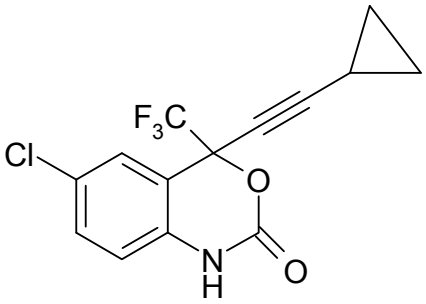

efavirenz

directly at the polymerase active site of the reverse transcriptase (47, 114, 134, 195, 197). The NNIBP is formed of two β-sheets, which include the catalytic Asp (β9-β10) and the primer grip (β12-β13-β14). It is formed by residues Y181, Y188, F227, W229, Y318, P95, L100, V106, V179, L234 and P236. The NNIBP is not present on reverse transcriptase structures in the absence of NNRTI (87, 207). It is only formed when the inhibitor binds to the enzyme.

Kinetic studies allowed a better understanding of the mechanism of action of NNRTIs. NNRTIs do not affect nucleic acid or nucleotide binding. Instead, it inhibits the chemical step of phosphodiester bond formation (205, 225). According to available structures, this decrease in the catalytic rate may be due to structural changes close to the active site as well as a repositioning of the primer grip, which may affect the orientation of the primer and the incoming nucleotide. Unfortunately, no structure is available where the reverse transcriptase is bond to a nucleic acid substrate in the presence of an NNRTI. In the absence of such structure, it is difficult to confirm the specific alignment of all components of the reaction. Looking at the structures that are available, we can see that the thumb is in an open configuration in the absence of a nucleic acid substrate, while the enzyme in the absence of NNRTI is in a closed configuration. Photoaffinity cross-linking experiments also showed that the fingers mobility is reduced in the presence of NNRTIs (179). These observations suggest a more rigid structure of the polymerase domain in the presence of NNRTIs which can yield unfavourable complexes for nucleotide incorporation.

Mutations conferring resistance to NNRTIs are all located in or around the NNIBP. The most frequent mutations observed during NNRTI treatment are Y181C, Y188C/L and K103N (149, 170, 201, 217). Other mutations include L100I, V106A and G190A (183) (Fig. 1.8).

The aromatic rings of Tyr181 and Tyr188 make important contributions in NNRTI binding (114, 195). Mutation to non aromatic residues, usually Y181C and Y188C/L reduces the affinity for NNRTIs due a loss of contacts at these two residues. These residues are less important in efavirenz binding, therefore mutations at 181 or 188 do not confer a high level of resistance to this inhibitor (197).

K103N causes resistance to all NNRTIs (183). Crystal structures showed a hydrogen bond between Y188 and 103N in the absence of NNRTI, which closes the entrance to the NNIBP (134, 197), efficiently reducing its access to NNRTIs. The L100I mutation confers resistance to delavirdine. Crystal structures showed that the presence of an Ile at position 100 causes steric hindrance either with the NNRTI or in the NNIBP (198). The NNIBP is not rigid and can adapt to the conformation of different NNRTIs. NNRTIs can also adapt to different conformation of the NNIBP, but delavirdine cannot easily reposition itself in the presence of L100I rendering it vulnerable to this mutation.

Mutation V106A confers resistance mainly to nevirapine. Crystal structures of wild-type reverse transcriptase and the 106A mutant show little structural differences (198). One difference is the loss of a Van der Waals interaction with the smaller Ala at 106 compared to the wild-type Val. A perturbation of the nevirapine's ring stacking with Y181 and

Fig.1.8 Position of the residues involved in resistance to non-nucleoside analogue inhibitors. The position of the residues is shown relative to the bound inhibitor. Nevirapine is represented in green, while the residues are colored by atoms (carbon; grey, nitrogen; blue and oxygen; red).

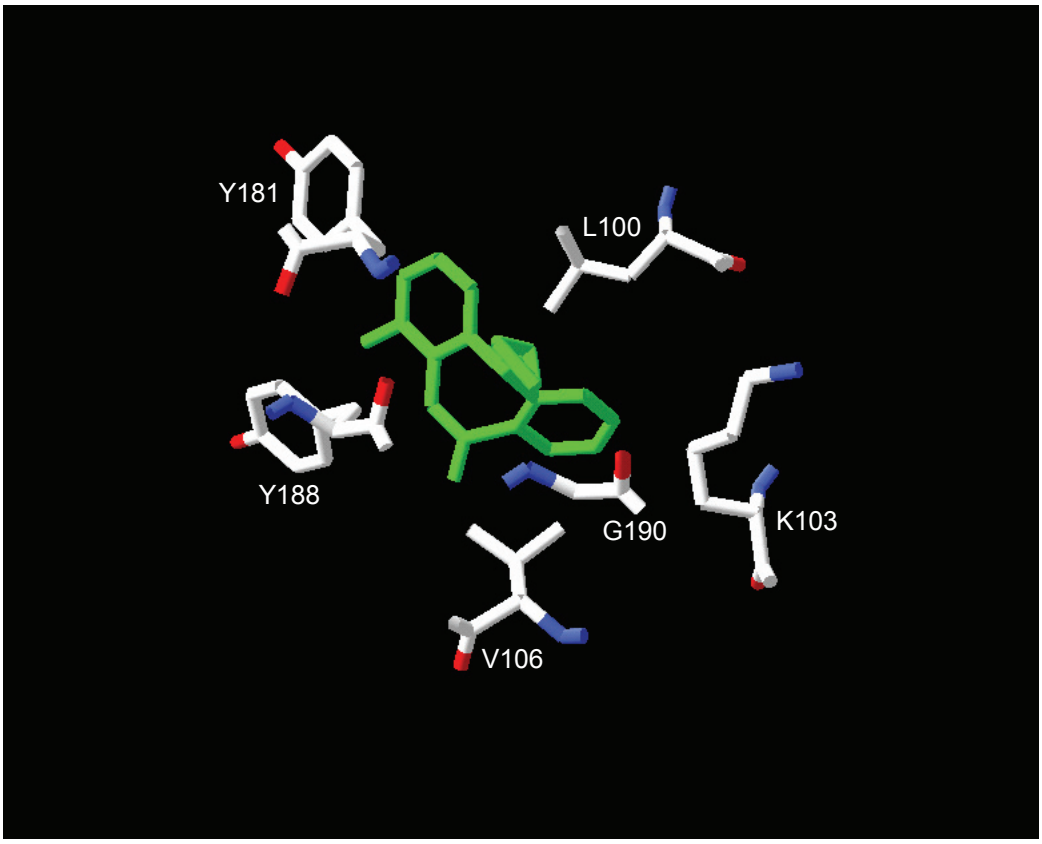
Y181
L100
Y188
G190
K103
V106

Y188 can also be observed. It seems that those small changes are sufficient to decrease the susceptibility of the reverse transcriptase to nevirapine.

The mutation G190A is selected by a NNRTI not used in the clinic, HBY 097, and cause cross-resistance to nevirapine and efavirenz. A crystal structure of the reverse transcriptase with HBY 097 shows a contact between the inhibitor and G190 (86). Modelling of an Ala at position 190 shows that steric hindrance between 190A and the inhibitor would occur. Similar conflicts could be expected with other NNRTIs (215).

1.4.3 Pyrophosphate analogues

Foscarnet (phosphonoformic acid, PFA) is a pyrophosphate analogue (Fig. 1.9) that inhibits a broad spectrum of viral polymerases, including the influenza RNA polymerase (229), the herpes type 1 and type 2 DNA polymerases (81, 199), The cytomegalovirus DNA polymerase (46), as well as the reverse transcriptase of many retroviruses such as the avian myeloblastosis virus (AMV), the bovine leukemia virus, the simian sarcoma virus (231) and HIV-1 (218). Foscarnet is used in the treatment of HIV-1 infection as a last solution when no response is obtained with FDA approved drugs (73, 146).

Kinetic studies have been conducted to elucidate the mechanism of action of foscarnet. Foscarnet inhibits polymerases in a non-competitive manner with respect to nucleotide-triphosphates and uncompetitive with respect to the nucleic acid substrate (34, 46, 173, 237). Foscarnet was found to be competitive with pyrophosphate, suggesting a common binding site on the polymerase (34). Another sign that foscarnet binds near or at the

Fig.1.9 Chemical structure of pyrophosphate and the inhibitor foscarnet.

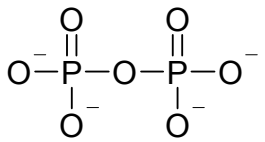

pyrophosphate

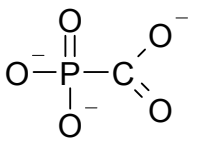

foscarnet

pyrophosphate binding site is the metal ion dependence in foscarnet action (231). As seen earlier, two metal ions interact with the incoming nucleotide and the Asp triad of the reverse transcriptase. One of these metal ions contacts the β- and the γ-phosphates of the incoming nucleotide. These two phosphates are cleaved from the nucleotide during phosphodiester bond formation becoming the leaving pyrophosphate. However, there must be significant differences in the mode of binding of each of these molecules since their inhibitory concentrations differ significantly (low μM for foscarnet versus mM for pyrophosphate) (34) and foscarnet is only a substrate for nucleotide removal at very high concentrations (27).

A detailed enzymatic study of the action of PFA on the reverse transcriptase including kinetic measurement, site-specific footprinting and mobility-shift assays was conducted (142). Site-specific footprints showed that the reverse transcriptase resides preferentially in the pre-translocational state in the presence of foscarnet. This was expected since, as mentioned above, it is believed that foscarnet binds to the same site as pyrophosphate, which binds the pre-translocated enzyme. When monitoring the elongation of a DNA primer in the presence of foscarnet, specific pausing sites could be observed. Site-specific footprints showed that these foscarnet sensitive sites promote the pre-translocated state of the reverse transcriptase. This latter observation allowed the proposition of a mechanism of inhibition for foscarnet; the drug traps the reverse transcriptase in the pre-translocational state, efficiently blocking binding of the next incoming nucleotide. This mechanism would suggest competitive inhibition of foscarnet with regard to nucleotide. Kinetic constants were measured at sites where the enzyme sits preferentially in the pre- or post-translocational states. At sites where the enzyme bind in the pre-translocational

state, where foscarnet can bind to the enzyme, competitive inhibition could be observed, meaning that either foscarnet or the nucleotide can bind, but not both at the same time. At sites where the reverse transcriptase is fount at the post-translocational state, where foscarnet cannot bind the enzyme, a non-competitive inhibition was observed. In order to explain the latter result, mobility shift assays were performed. It was shown that foscarnet binding forms a stable enzyme-DNA-inhibitor complex. In steady state kinetic assays, the DNA substrate is in excess over the enzyme. After single nucleotide incorporation, the enzyme must dissociate and bind to another substrate. Since foscarnet induces a stable complex, it doesn't allow the enzyme to dissociate, resulting in lower incorporation level, which is reflected in the catalytic rate (k_{cat}). These results strongly suggest that the above proposed mechanism of inhibition is the significant one during processive elongation.

Resistance mutations could be identified from clinical isolates and *in vitro* by serial passage of HIV-1 with increasing concentrations of foscarnet. From clinical isolates, mutations W88G, W88S, Q161L and H208Y were identified (148). Mutations W88G, E89K, L92I, S156A, Q161L and H208Y could be recovered from HIV-1 in cell culture (148, 232). The NRTI resistance mutation K65R was also shown to be cross-resistant to foscarnet even though it is not selected during foscarnet treatment (75). Most of these mutations resensitize AZT-resistant enzyme to AZT by decreasing the rate of chain-terminator removal (158, 222).

Residue Lys65 makes two H-bonds with the γ-phosphate of the incoming nucleotide (88). When Arg is modeled at residue 65, one H-bond is lost with the γ-phosphate and one is

gained with the β-phosphate. Although the charge remains the same, the specific interactions of the residue 65 are disturbed. This change in orientation may be sufficient to decrease the affinity of the reverse transcriptase for foscarnet.

The other mutations mentioned above are all away from the nucleotide binding site (88) (Fig. 1.10), which suggest an indirect role in resistance to foscarnet. Most of these mutations are in contact or close to the template strand. It was shown that the mutant enzyme E89K has a reduced affinity for the pre-translocated state (142). At sites where the wild-type reverse transcriptase preferentially binds in the pre-translocated state, the mutant E89K slides away from this site. Since foscarnet binds to a pre-translocated enzyme, this mutation will reduce the chances of the inhibitor to bind to the enzyme, resulting in resistance to foscarnet.

Fig.1.10 Position of the residues involved in resistance to foscarnet. The residues are shown relative to the DNA:DNA substrate and the incoming nucleotide. The DNA primer is colored red and the template is shown in yellow. The incoming nucleotide is colored by atoms (carbon; grey, nitrogen; blue, oxygen; red and phosphorus; yellow). The highlighted residues are also colored by atoms using the same color code.

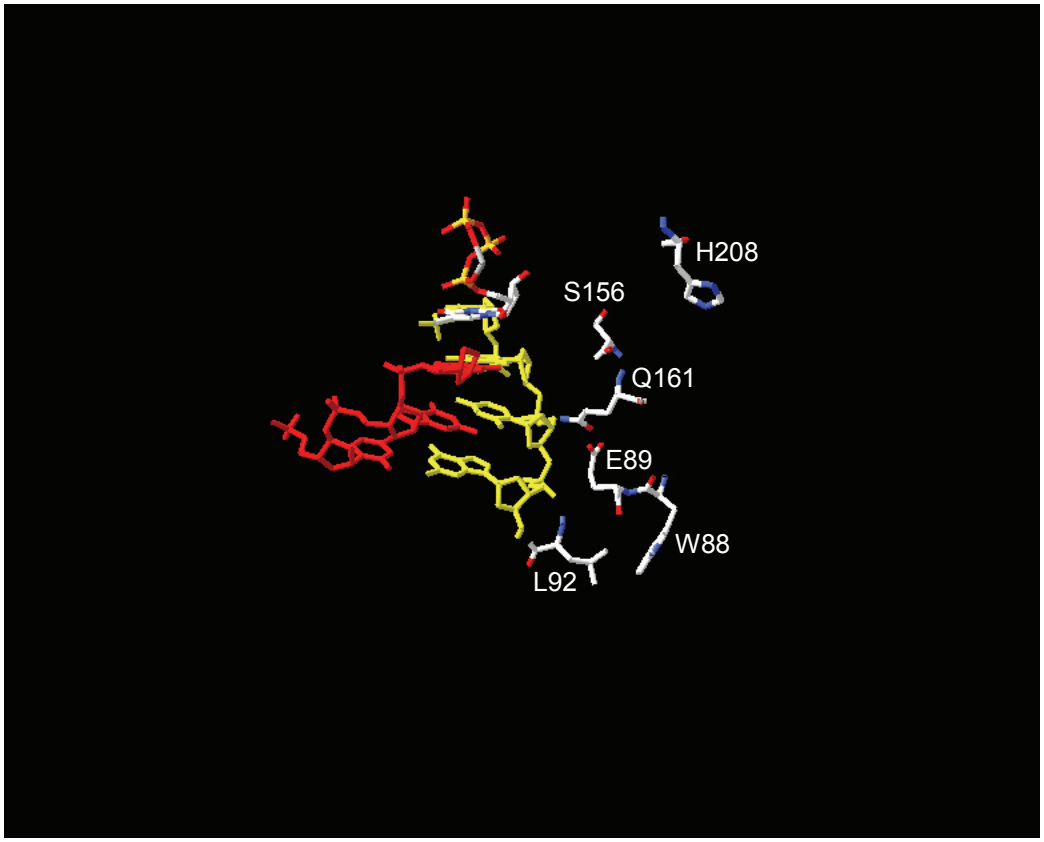
H208
S156
Q161
E89
W88
L92

1.5 Objectives

At the start of this research project, very little was known about translocation, and this step of the nucleotide incorporation cycle had never been studied on the reverse transcriptase. One of the main reasons for this lack of information on translocation was the absence of a sensitive assay to detect this subtle movement. Therefore, our first objective was to develop such an assay. As mentioned earlier, translocation is kinetically invisible, thus we opted for a structural assay allowing us to identify the precise positioning of the reverse transcriptase on its DNA substrate. Our site-specific footprinting assays, with a resolution of a single nucleotide, proved to be specific and precise enough to detect the translocational status of the reverse transcriptase.

The next objective was to use these assays to understand the mechanism of translocation and to study its influence in drug action and drug resistance. By combining the site-specific footprinting assays with kinetic measurements and other enzymatic assays, we could accumulate evidences pointing to a Brownian ratchet mechanism of translocation. We could identify the major factors influencing the translocational equilibrium such as the nucleic acid substrate sequence, the nature of the 3' nucleotide of the elongating chain, the presence of drug resistance mutations, the presence of drugs and the temperature.

We also used these assays to push forward our understanding of drug resistance such as the removal mechanism of chain-terminators. I demonstrated that the reverse transcriptase can only cleave a nucleotide from the primer when this nucleotide is located

in the nucleotide binding site, meaning that the enzyme is positioned in the pre-translocational state. My studies also allowed us to identify a mechanism of action for the drug foscarnet, as well as a mechanism of resistance to that drug. Translocation is the major determinant in foscarnet action since the drug binds to the pre-translocated enzyme to stabilize it in this conformation, blocking nucleotide binding. In the case of drug resistance the mutation E89K was observed to reduce the stability of the pre-translocational state of the reverse transcriptase, reducing the chances of foscarnet binding.

CHAPTER 2

SITE-SPECIFIC FOOTPRINTING REVEALS DIFFERENCES IN THE TRANSLOCATION STATUS OF HIV-1 REVERSE TRANSCRIPTASE: IMPLICATIONS FOR POLYMERASE TRANSLOCATION AND DRUG RESISTANCE

This chapter was adapted from an article authored by B. Marchand and M. Götte that appeared in the ***Journal of Biological Chemistry***, 2003, 278(37):35362-72.

2.1 Abstract

Resistance to nucleoside analogue inhibitors of the reverse transcriptase of the HIV-1 often involves phosphorolytic excision of the incorporated chain terminator. Previous crystallographic and modeling studies suggested that this reaction could only occur when the enzyme resides in a pre-translocational stage. Here we studied mechanisms of polymerase translocation using novel site-specific footprinting techniques. Classical footprinting approaches, based on the detection of protected nucleic acid residues, are not sensitive enough to visualize subtle structural differences at single nucleotide resolution. Thus, we developed chemical footprinting techniques that give rise to hyperreactive cleavage on the template strand mediated through specific contacts with the enzyme. Two specific cuts served as markers that defined the position of the polymerase and RNase H domain, respectively. We show that the presence of the next correct dNTP, following the incorporated chain terminator, caused a shift in the position of the two cuts a single nucleotide further downstream. The footprints point to monotonic sliding motions and provide compelling evidence for the existence of an equilibrium between pre- and post-translocational stages. Our data show that enzyme translocation is reversible and uncoupled from nucleotide incorporation and the release of pyrophosphate. This translocational equilibrium ensures access to the pre-translocational stage after incorporation of the chain terminator. The efficiency of excision correlates with an increase in the population of complexes that exist in the pre-translocational stage, and we show that the latter configuration is preferred with an enzyme that contains mutations associated with resistance to nucleoside analogue inhibitors.

2.2 Introduction

Nucleoside analogue inhibitors of the retroviral reverse transcriptase (NRTIs) represent important components in currently used drug regimens to treat infection with the human immunodeficiency virus, type 1 (HIV-1). 3'-Azido-3'-deoxythymidine (zidovudine or AZT), 2',3'-dideoxyinosine (didanosine), and (-)-β-L-2',3'-dideoxy-3'-thyacytidine (lamivudine) are prominent members of this class of compounds. NRTIs are intracellularly phosphorylated and act as chain terminators. Previous biochemical studies have shown that the incorporated chain terminator can be removed from the primer terminus through phosphorolytic cleavage in the presence of either pyrophosphate (PPi) (2) or in the presence of ribonucleotide triphosphates (NTPs) (156), which were shown to act as pyrophosphate donors. Increasing evidence suggests that the latter reaction pathway provides an important mechanism for HIV resistance to AZT and, to a certain degree, also to other NRTIs (16, 61, 130, 144, 153, 154, 168, 202).

Recombinant RT enzymes that contain mutations associated with resistance to AZT (M41L, D67N, K70R, T215Y/T215F, and K219Q) do not prevent or diminish the incorporation of AZT-MP (116). Based on findings showing enhanced binding of the 3' end of AZT-terminated primer strands to HIV-1 RT, it has later been suggested that pyrophosphorolysis might provide a possible reaction pathway involved in resistance to AZT (21). Excision of AZT-MP occurs with considerable efficiency with wild-type HIV-1 RT, and the rate of pyrophosphorolysis appeared to be increased with resistant RT enzymes (2). The difference in regard to efficiency of the excision reaction between both enzymes is dramatically increased when NTPs act as a pyrophosphate donor (154). In the

light of these findings it is now widely accepted that ATP can act as a physiologically relevant pyrophosphate donor. It appears that excision of AZT-MP is particularly efficient as compared with other NRTIs, even in the context of wild-type HIV-1 RT (92). The rate with which each individual inhibitor is removed from the primer terminus depends critically on the concentration of the dNTP that is complementary to the next template position (92, 145, 154, 168). Phosphorolytic cleavage of incorporated 2',3'-dideoxynucleotides, including ddAMP and ddTMP, is compromised at nucleotide concentrations as low as 1 μM, whereas significantly higher concentrations are required to inhibit the excision of AZT-MP. The formation of a stable ternary dead end complex is diminished with AZT-terminated primer strands, which provides an explanation for the efficient removal of AZT-MP (242).

Based on crystallographic and modeling studies (17, 211, 212), it has been suggested that the excision reaction could only occur when the 3' end of the primer terminus remains in the same position at the polymerase active site, referred to as nucleotide binding site (N-site), where the chain-terminating nucleoside triphosphate was bound prior to its incorporation. This configuration defines a possible pre-translocational stage. Following the chemical step, the extended primer/template duplex translocates by a single base pair into the so-called priming site (P-site), and as a consequence, the next incoming nucleotide gains access to the N-site. The authors hypothesized that AZT-terminated primer strands reside preferentially at the N-site, because the bulky azido group may interfere with a P-site occupation of the primer terminus and/or with dNTP binding to the N-site.

If this model is correct, there must be a mechanism that controls the formation of the pre-translocational stage after the incorporation of the chain terminator. This mechanism is unknown. Earlier studies suggested that translocation may take place during the release of PPi, immediately after incorporation of the last nucleotide (103). Thus, the 3' end of the primer may ultimately move into the P-site, which is a prerequisite for dNTP binding and continuation of DNA synthesis. It has indeed never been demonstrated that the primer terminus has free access to the N-site. Rather, recent studies (211, 212) suggested that the N-site complex is a short-lived, unstable polymerization intermediate that needs to be covalently trapped. The available crystal structure models without an incoming dNTP show the primer terminus exclusively in the P-site (38, 88, 95), unless the enzyme is cross-linked to its nucleic acid substrate immediately after catalysis and before translocation takes place (211). Here we employed site-specific footprinting experiments to characterize the relationship between the precise position of HIV-1 RT on its primer/template substrate and the efficiency with which chain-terminating nucleotides are removed from the primer terminus. Our data provide compelling evidence for the existence of a translocational equilibrium between pre- and post-translocational stages that ensures access of the 3' end of the primer to the N-site after nucleotide incorporation and the release of pyrophosphate.

2.3 Experimental procedures

Enzymes and Nucleic Acids—Wild-type HIV-1 RT (p66/p51) was expressed in Escherichia coli and purified essentially as described previously (127). Mutant enzymes were generated through site-directed mutagenesis using the Stratagene Quick-change kit

according to the manufacturer's protocol. Substrates used in this study were derived from the HIV-1 polypurine tract (PPT) as described in our previous studies (62, 64): 5'-TTAAAAGAAAAGGGGGGA (PPT-1/18D); 5'-TTAAAAGAAAAGGGGGG (PPT-1/17D); and 5'-ACTGGAAGGGCTGATTCA (PPT-2/18D). The model template used in this study provides complementarity to these primers: 5'-CGTTGTCAGTGAATCAGCCCTTCCAGTCCCCCCTTTTCTTTTAAAAAGTGGCA AGA. Oligonucleotides (Invitrogen) were purified on 12% polyacrylamide, 7 M urea gels containing 50 mM Tris borate, pH 8.0, and 1 mM EDTA. Purified nucleic acids were eluted from gel slices in a buffer containing 500 mM ammonium acetate and 0.1% SDS. 5' end-labeling of DNA primers was conducted with [γ-^{32}P]ATP and T4 polynucleotide kinase. 3' end-labeling of the DNA template was performed with [α-^{32}P]ddATP using terminal transferase according to the manufacturer's recommendation (Roche Applied Science). Labeled oligonucleotides were gel-purified as described above.

Rescue of Chain-terminated DNA Synthesis—Rescue of DNA synthesis was studied at a single template position using a similar assay as we described earlier (61). The pre-hybridized duplex (8.5 pmol), composed of the aforementioned template and primer strands, was incubated with 25.5 pmol of HIV-1 RT in a buffer containing 50 mM Tris-HCl, pH 7.8, 50 mM NaCl, and 6 mM $MgCl_2$ followed by the addition 10 μM dCTP and 10 μM AZT-TP (TriLink BioTechnologies) to generate primer strands terminated with AZT-MP. Chain termination with ddTTP and AZA-TP (TriLink BioTechnologies) was performed analogously. Reactions were allowed to proceed for 20 min to ensure complete extension of the primer and its quantitative chain termination with the nucleotide analogue. The excision of the analogue was initiated with ATP (3.5 mM) or, as indicated

in some cases, with PPi (150 μM). Excision and the ensuing rescue of chain-terminated DNA synthesis was monitored in time course experiments. Samples were heat-denatured for 5 min at 95 °C and finally resolved on 8% polyacrylamide, 7 M urea gels.

Site-specific Footprinting—Site-specific footprints with KOONO and Fe^{2+} were monitored on 3' end-labeled DNA templates. Hybridization of the template (2.7 pmol) with the complementary primer (8.1 pmol) was conducted in a buffer containing 20 mM sodium cacodylate, pH 7, and 20 mM NaCl. The duplex was incubated with HIV-1 RT (16.2 pmol) in a buffer containing 120 mM sodium cacodylate, pH 7, 20 mM NaCl, 6 mM $MgCl_2$, and a mixture of nucleotide triphosphates that allow quantitative chain termination as described above. Prior to the treatment with KOONO or Fe^{2+}, complexes were preincubated for 20 min with increasing concentrations of the next nucleotide and at different temperatures as indicated in the figures. Treatment with Fe^{2+} and KOONO, respectively, was performed essentially as described recently (63, 65).

2.4 Results

Site-specific Footprinting—It was our initial aim to develop novel footprinting techniques that would allow us to identify and to distinguish between pre- and post-translocational stages. We have previously applied high resolution footprinting techniques to study the interaction between HIV-1 RT and its DNA/DNA primer/template substrate (63, 152). Two chemically distinct sources of hydroxyl radicals were utilized: the classical method with $[Fe(EDTA)]^{2-}$ that yields hydroxyl radicals via Fenton-like chemistry; and potassium peroxynitrite (KOONO), which is a metal-free source of hydroxyl radicals that are

generated during decomposition of the conjugate acid HOONO. Despite a relatively high resolution of the hydroxyl radical footprints, the boundaries of the protected regions are not as clearly defined as required for the detection of structural differences associated with the translocation of RT. However, the same reactions give rise to hyperreactive cleavage at two distant template positions. Treatment of RT-DNA-DNA complexes with divalent Fe^{2+} ions in the absence of EDTA yields oxidative cleavage at template position -17 and a minor cut at position -18. We showed that Fe^{2+} ions can bind in the vicinity of the RNase H active center, and oxidation of the bound metal ions yields a local source of hydroxyl radicals that cleave the template in site-specific fashion. Treatment with KOONO yielded hyperreactive cleavage at template position -7. Specific binding of the enzyme is a prerequisite for hyperreactivity, and therefore, both of these signals may serve as specific markers to identify the precise position of the enzyme in the presence and absence of an incoming nucleotide.

The KOONO-induced cut is of particular interest in this regard, because the observed hyperreactivity involves a single nucleotide in highly specific fashion. The model of the ternary complex shows Cys-280 of the large subunit of heterodimeric (p66/p51)HIV-1 RT in close proximity to the DNA template. Previous reports (188) have shown that peroxynitrite mediates oxidation of the thiol group of cysteines, which may provide a link to the mechanism involved in the reaction. To test a possible involvement of Cys-280 in the reaction with KOONO, we generated complexes composed of an AZT-terminated primer strand and RT enzymes that contained either cysteine or serine at position 280 (Fig. 2.1*A*). KOONO-induced cleavage is specific for the Cys-280 enzyme, whereas the reaction is undetectable with the Ser-280 mutant (Fig. 2.1*B, lanes 3* and *7*). The efficiency

Fig.2.1 Site-specific footprinting. *A*, experimental strategy for the treatment of RT-DNA-DNA complexes with KOONO. The template was radioactively labeled at the 3' end (*asterisks*) to monitor the reaction. DNA synthesis was chain-terminated with HIV-1 RT in the presence of AZT-TP as described under "Experimental Procedures." *Boldface C* and *Z* point to newly incorporated dCMP and AZT-MP. The dNTP that is complementary to next template position (dGTP, offset) was added to reaction mixture at high concentrations of 1 mM to stabilize the complex. *B*, the footprint experiment was conducted by the addition of a stable alkaline solution of KOONO. *Lane 1* shows the control in the absence of HIV-1 RT. *Lanes 2–5* show reactions with HIV-1 RT containing a cysteine at position 280 in both subunits. Reactions were conducted in the presence of low concentrations of glycerol (0.5%, *lanes 2* and *3*) and at higher concentrations (5%, *lanes 4* and *5*). *Lanes 6* and *7* show reactions with an enzyme that contains a serine at position 280. The *arrow* points to a highly specific KOONO-mediated cut with RT (Cys-280) at low concentrations of glycerol.

A

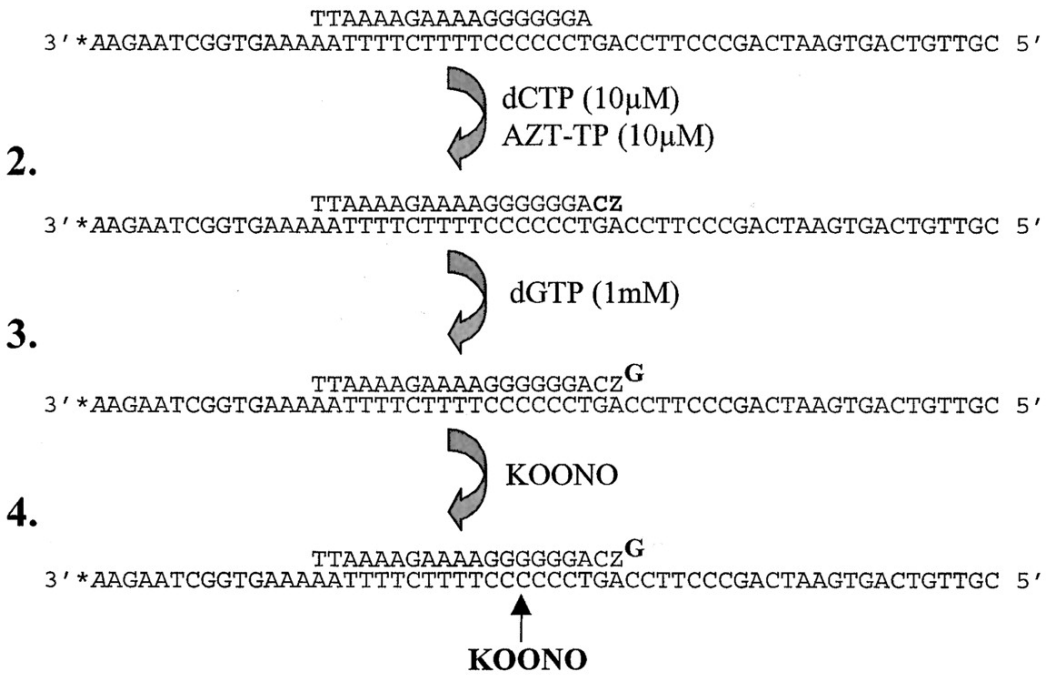
1.
TTAAAAGAAAAGGGGGGA
3'*AAGAATCGGTGAAAAATTTTCTTTTCCCCCCTGACCTTCCCGACTAAGTGACTGTTGC 5'
dCTP (10μM)
AZT-TP (10μM)
2.
TTAAAAGAAAAGGGGGGACZ
3'*AAGAATCGGTGAAAAATTTTCTTTTCCCCCCTGACCTTCCCGACTAAGTGACTGTTGC 5'
dGTP (1mM)
3.
TTAAAAGAAAAGGGGGGACZG
3'*AAGAATCGGTGAAAAATTTTCTTTTCCCCCCTGACCTTCCCGACTAAGTGACTGTTGC 5'
KOONO
4.
TTAAAAGAAAAGGGGGGACZG
3'*AAGAATCGGTGAAAAATTTTCTTTTCCCCCCTGACCTTCCCGACTAAGTGACTGTTGC 5'
KOONO

B

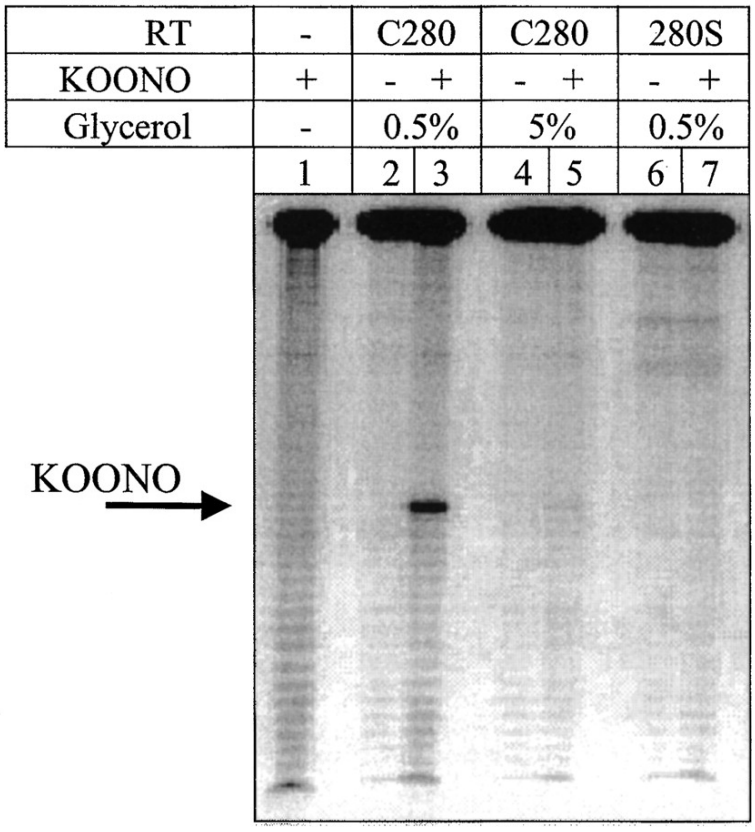
RT - C280 C280 280S
KOONO + - + - + - +
Glycerol - 0.5% 5% 0.5%
1 2 3 4 5 6 7
KOONO

of the reaction is severely compromised in the presence of the radical scavenger glycerol, suggesting the involvement of either hydroxyl radicals and/or thiyl radicals (Fig. 2.1*B*, *lanes 3* and *5*). Regardless of the precise chemical mechanism, the specific signal on the template strand is unambiguously assigned to the interaction between the cleaved nucleotide and Cys-280. We therefore refer to "site-specific footprinting" as opposed to classical footprinting techniques that do not yield information regarding the contribution of individual amino acid residues.

Pre- and Post-translocational Stages—Both techniques were utilized to study possible differences in regard to the position of the enzyme in the presence of the next dNTP (Fig. 2.2, *A* and *B*). RT-DNA-DNA complexes, with an AZT-terminated primer strand, were pre-incubated in the absence or in the presence of the next complementary dNTP. In the absence of dNTPs, we observed Fe^{2+}-mediated cuts at position -18 and less pronounced at position -19 (Fig. 2.2*A*, *lane 3*). These cuts are seen a single position further downstream -17/-18) when the next dNTP was present at high concentrations of 1 mM (Fig. 2.2*A*, *lane 4*). A similar shift is evident when comparing the positions of the KOONO-induced cut. In the absence of the next nucleotide, the cut is seen at position -8, whereas in the presence of the templated dNTP, the cut is seen at position -7 (Fig. 2.2*A*, *lanes 7* and *8*). Thus, it appears that the formation of a ternary dead end complex is associated with enzyme translocation. Our data suggest that the cut at position -8 is indicative for the pre-translocational stage in which the primer terminus occupies the N-site, whereas the cut at position -7 is indicative for the post-translocational stage in which the primer terminus occupies the P-site.

Fig.2.2 Site-specific footprinting in the presence and absence of the templated dNTP (dGTP). *A*, treatment of RT-DNA-DNA complexes containing AZT-terminated primer strands with Fe^{2+} (*lanes 1–4*) and KOONO (*lanes 5* and *6*). *Lane A* shows an "A-ladder," generated by treating the 3' end-labeled DNA template with diethyl pyrocarbonate and piperidine (69). *Lanes 1* and *5* are controls in the absence of treatment. *Lanes 2* and *6* are controls that show treatment with Fe^{2+} or KOONO in the absence of HIV-1 RT. *Lanes 3* and *7* show treatment of complexes in the absence of the templated nucleotide, and *lanes 4* and *8* show reactions in the presence of 1 mM dGTP. Positions of Fe^{2+}- and KOONO-mediated cleavage are indicated by *arrows* on the *left* of the figure. *B*, schematic representation of results shown in *A*. Per definition, position -1 represents the last base pair that contains the chain-terminating nucleotide. *C*, treatment of RT-DNA-DNA complexes with KOONO (*top*) and Fe^{2+} (*bottom*) in the presence of increasing concentrations of the templated dGTP. *Lanes 1–16* show footprints obtained with the following different concentrations of dGTP: 0, 1, 3.125, 6.25, 12.5, 25, 50, 100, 250, 500, and 750 μM and 1, 1.25, 1.5, 1.75, and 2 mM. *D*, graphic representation of the data shown under *C*. The *graph* shows relative populations of complexes in post- and pre-translocational stages (P-site, and N-site, respectively), as measured by the ratios of cuts at positions -7 and -8(KOONO-mediated), or -17/-18 and -18/-19 (Fe^{2+}-mediated). Concentrations of the templated nucleotide required to obtain 50% translocation are indicated below.

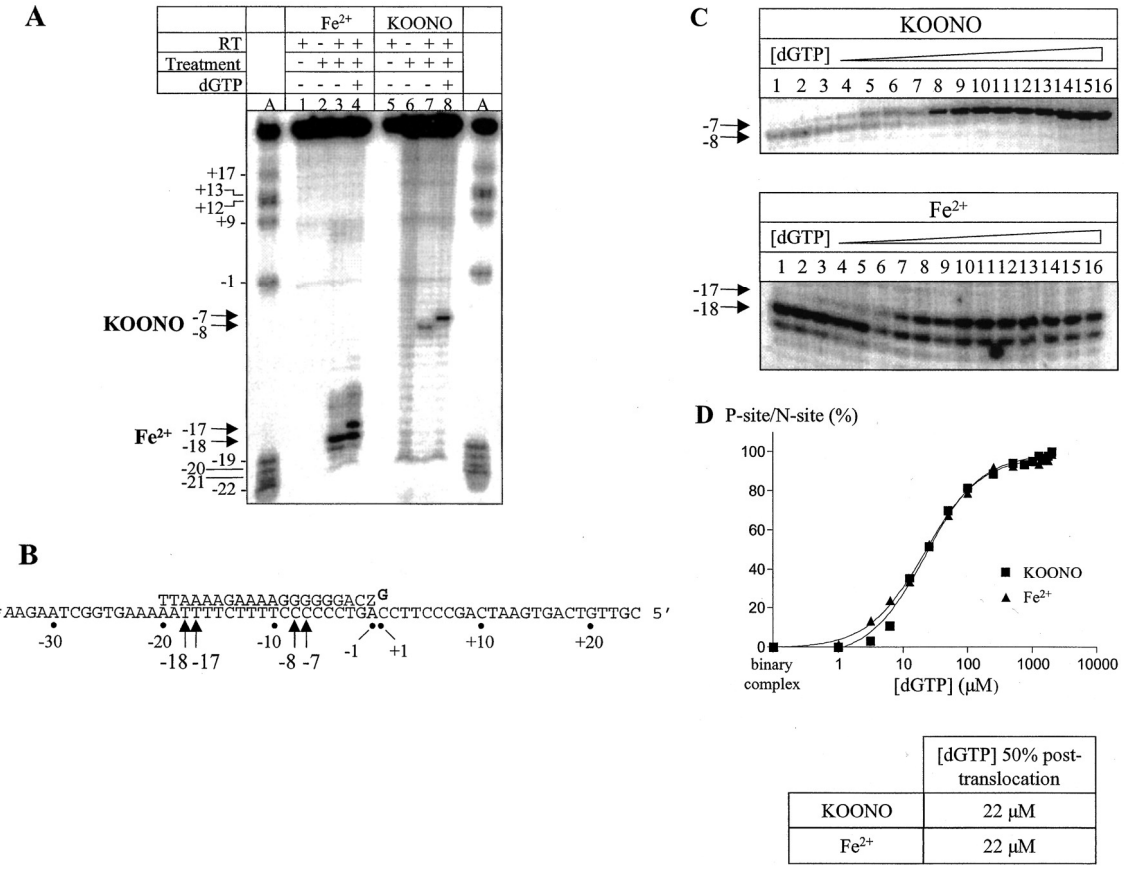

	[dGTP] 50% post-translocation
KOONO	22 μM
Fe^{2+}	22 μM

A comparison of cleavage patterns with KOONO and Fe^{2+}, respectively, shows that the ratio of cuts representing pre- and post-translocational stages is literally identical, for the two methods employed here, at any given dNTP concentration tested (Fig. 2.2*C*). Both methods suggest that dNTP concentrations of ~22 μM are required to obtain 50% of complexes post-translocation (Fig. 2.2*D*). We note that the total amount of radioactivity increased selectively in the KOONO experiment at relatively high concentrations of dNTPs (≥100 μM), when 80% of the complexes exist already in the post-translocational stage. An increase in band intensities is not evident in the Fe^{2+} assay. It remains to be elucidated whether these data point to a local increase in the stability of the ternary complex, in close proximity to the polymerase active site, and/or to differences with respect to the efficiency of the KOONO-mediated reaction as the ternary complex is formed.

Impact of the Temperature—Fig. 2.2 shows unambiguously that low dNTP concentrations facilitate the pre-translocational N-configuration. This result appears to be in conflict with the crystal structure models that show the primer terminus exclusively in the P-site (38, 95). In fact, the structures of the binary and the ternary complex show Cys-280 in close proximity to template position -7. Several factors may account for the apparent discrepancy between our biochemical data in solution and the crystal structure models. We initially evaluated the impact of the temperature. AZT-terminated complexes were pre-incubated in the presence of different dNTP concentrations and were kept at low temperatures on ice, *i.e.* conditions referred to as 0°C, or at 37°C, followed by treatment with KOONO at the same temperatures (Fig. 2.3). Reactions at 37°C show a gradual shift of the KOONO-induced cut from position -8 toward position -7, as the concentration of

Fig.2.3 Temperature dependence of P-site and N-site occupations. RT-DNA-DNA complexes with AZT-terminated primer strands were treated with KOONO at different temperatures with increasing concentrations of the templated dGTP. *Lanes 1–9*, 0, 1, 3.125, 6.25, 12.5, 25, 50, and 100 μM and 1 mM. Reactions were conducted at 37°C (*37°C*, *left*), with a pre-incubation period on ice (*0°C→37°C*, *middle*) or on ice (*0°C*, *right*). Specific cuts at positions -7, and -8 are labeled, and other faint bands represent background cleavage as shown in Fig. 2.1*B* (*lane 6*).

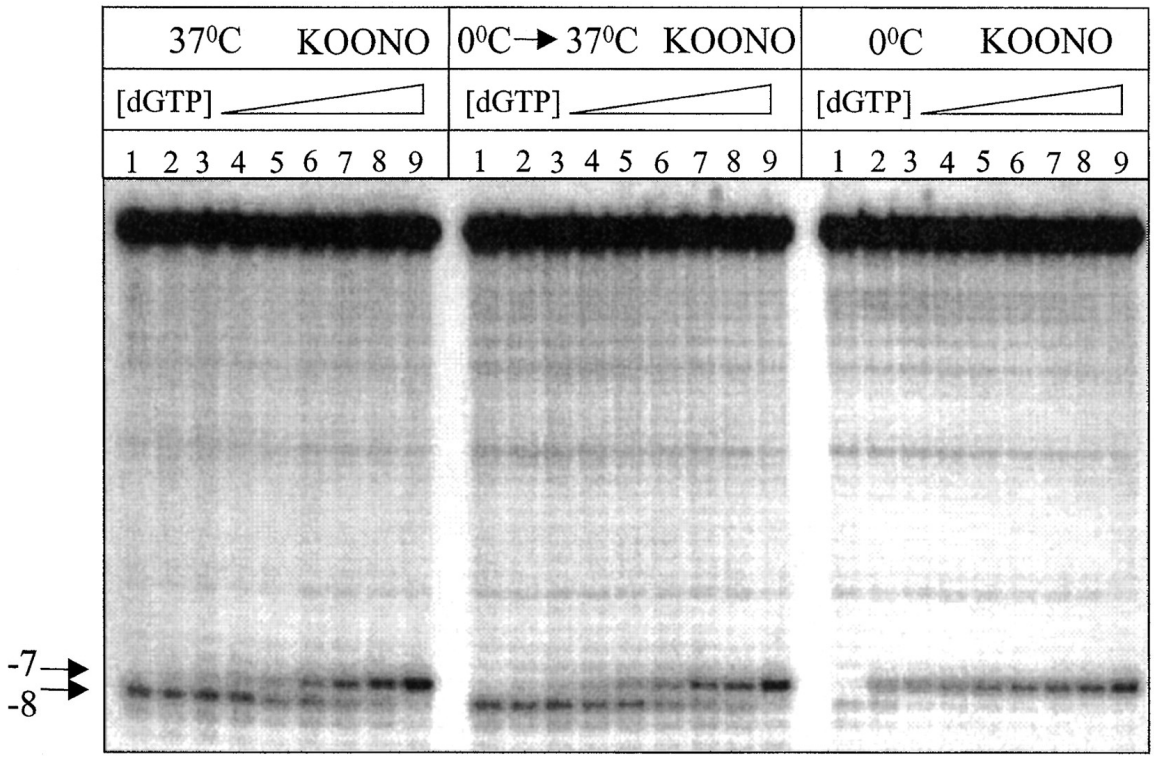
37⁰C KOONO
0⁰C→37⁰C KOONO
0⁰C KOONO
[dGTP]
[dGTP]
[dGTP]
1 2 3 4 5 6 7 8 9
1 2 3 4 5 6 7 8 9
1 2 3 4 5 6 7 8 9
-7
-8

the templated dNTP was increased (Fig. 2.3, *left panel*); however, the non-translocated complex with the primer terminus in the N-site is still detectable in the presence of 100 μM dNTP (Fig. 2.3, *left panel*, *lane 8*). In contrast, at 0°C the binary complex is only seen as a faint band in the pre-translocational stage (Fig. 2.3, *lane 1*, *right panel*), and the dNTP concentrations required to form the post-translocated stage is much lower as compared with the reaction at 37°C (Fig. 2.3, compare *lanes 2–5*, *left* and *right panels*). The temperature-dependent differences in regard to the relative N- and P-site occupations are completely reversible. Reactions conducted at 37°C, with a pre-incubation period of 30 min at low temperatures, gave essentially the same result as seen at 37°C in the absence of pre-incubation on ice (Fig. 2.3, *middle*). These data show that the 3' end of the primer does not ultimately translocate into the P-site to allow binding of the next dNTP. The primer terminus can occlude the N-site, and does this preferentially at physiologically relevant temperatures, *i.e.* at 37°C.

Impact of the Chemical Nature of the Chain Terminator— The aforementioned data form the basis to study the relationship between the precise position of HIV-1 RT on its nucleic acid substrate and the ability of the enzyme to excise the incorporated chain terminator via phosphorolytic cleavage. Excision is here monitored in assays that detect the removal of the chain terminator and the ensuing rescue of DNA synthesis at a single template position as described previously (61) (Fig. 2.4*A*). Our data are in good agreement with published results by others, showing efficient rescue of AZT-terminated DNA synthesis, whereas the excision of ddTMP is almost completely blocked under these conditions (154) (Fig. 2.4*C, top*). To analyze further whether the 3'-azido group may be an important structural feature that facilitates the excision reaction as suggested previously, we tested

Fig.2.4 Efficiency of excision of 3'- azido-containing chain terminators and their 2',3'-dideoxy counterparts. *A* and *B*, schematic description of assays used to monitor the rescue of DNA synthesis through limited extensions of 5' end-labeled primers at a single template position as described under "Experimental Procedures." *C*, time course of the reaction with different chain terminators: AZT-MP and ddTMP (*top*), and AZA-MP and ddAMP (*bottom*). *Lane 1* shows the unextended primer. *Lane 2* the chain-terminated primer. *Lanes 3–12* show different time points after the addition of ATP and the "rescue mixture" (1, 3, 6, 10, 15, 22, 30, 45, 60, and 90 min). *D* and *E*, effect of the different chain terminators on the translocational equilibrium. KOONO footprinting of complexes containing AZT-MP and ddTMP (*D*) was performed and analyzed as described in Fig. 2.2. The footprints with AZA-MP and ddAMP (*E*) were performed in a different range of concentrations of the next nucleotide (dGTP). *Lanes 1–11*, 0.01, 0.025, 0.1, 0.25, 0.5, 1, 3.125, 6.25, 12.5, and 25 μM, and *lane 12* shows the binary complex in the absence of dGTP. *F*, effect of different temperatures on P/N-site occupations with AZA-MP and ddAMP-terminated primer strands. Reactions were performed at 37°C (*left*) and on ice (*right*). *Lane 1* shows a control in the absence of treatment with KOONO. *Lane 2* is a control with KOONO treatment in the absence of RT. *Lanes 3* and *5* show reactions in the absence of the next dNTP, and *lanes 4* and *6* show reactions in the presence of 1 mM of the next dNTP.

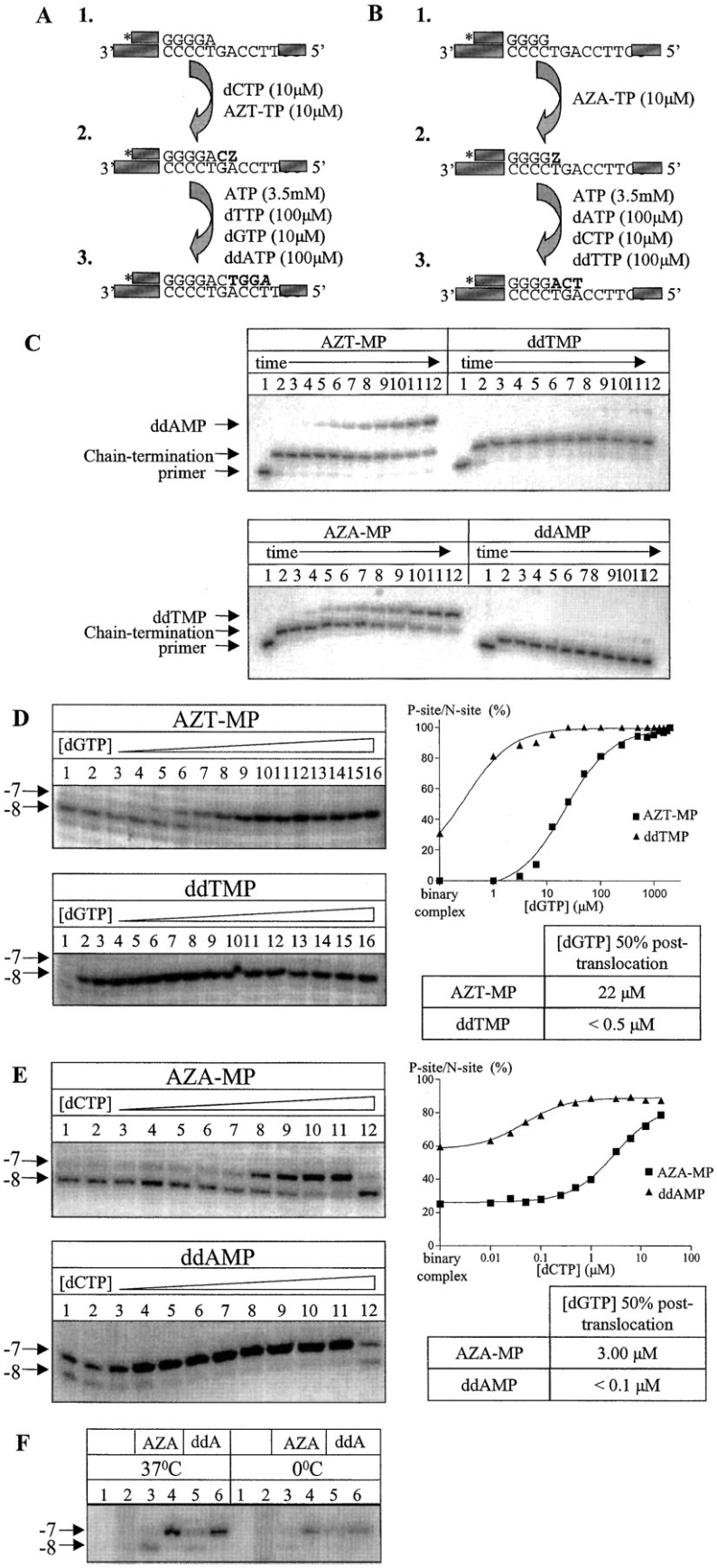

	[dGTP] 50% post-translocation
AZT-MP	22 μM
ddTMP	< 0.5 μM

	[dGTP] 50% post-translocation
AZA-MP	3.00 μM
ddAMP	< 0.1 μM

and compared the efficiency of excision with ddAMP and AZA-MP (Fig. 2.4*B*). Indeed, Fig. 2.4*C* (*bottom*) shows that rescue of AZA-terminated DNA synthesis is significantly increased, as compared with the reaction that involves ddAMP-terminated primers.

The high efficiency with which AZT-MP and AZA-MP are removed from the primer terminus correlates with an increased population of complexes that exist in the N-configuration (Fig. 2.4, *D* and *E*). The site-specific footprints with KOONO revealed that pre-translocational stages with ddTMP or ddAMP-terminated primer strands are only seen at submicromolar concentrations of the templated dNTP or in the absence of dNTPs when the translocational status is not influenced by the formation of a ternary complex. At 37°C, binary complexes with AZA-MP-terminated primer strands are found predominantly in the pre-translocational stage, whereas binary complexes with ddATP-terminated primer strands are characterized by a mixture of complexes in pre- and post-translocational stages (Fig. 2.4*F*, *lanes 3* and *5*, *left panel*). Importantly, at 0°C, binary complexes with ddAMP-terminated primer strands are found exclusively in the post-translocational stage. The fact that the N-configuration is literally undetectable at lower temperatures helps to explain why the crystallographic data show exclusively the P-configuration. This result does not only confirm the temperature dependence of relative occupations of pre- and post-translocational stages, it also demonstrates the existence of an independent equilibrium between both configurations.

Impact of the Sequence—There are also clear differences between the relative occupations of N- and P-sites when comparing AZA-MP and AZT-MP or ddAMP and ddTMP. In order to evaluate a possible impact of the sequence of the template on efficiency of the

Fig2.5 Effects of the sequence on the efficiency of the excision reaction and relative P-site and N-site occupations. *A*, primer/template systems used in this assay. In addition to the primer that has been used throughout this study (PPT-1), we utilized another primer (PPT-2) that allowed the study of rescue of AZT-terminated DNA synthesis at another position. *B*, rescue of AZT-terminated DNA synthesis with PPT-1 (*left*) and PPT-2 (*right*). Reactions were monitored in a time course as described in Fig. 2.4. *Lane 1* shows the unextended primer, *lane 2* shows complete chain-termination with AZT-MP. *Lanes 3–12* show the reaction after 1, 3, 6, 10, 15, 22, 30, 45, 60, and 90 min. *C*, KOONO-footprinting with PPT-1 (*top*) and PPT-2 (*bottom*). *Lanes 1–16* show footprints obtained with the following different concentrations of the templated nucleotide: 0, 1, 3.125, 6.25, 12.5, 25, 50, 100, 250, 500, and 750 μM and 1, 1.25, 1.5, 1.75, and 2 mM.

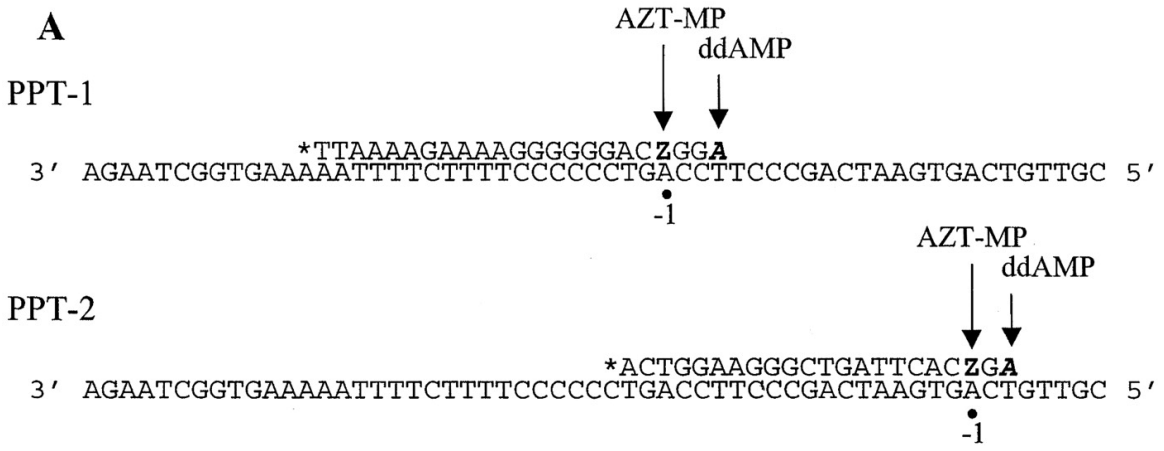
A
AZT-MP
ddAMP
PPT-1
*TTAAAAGAAAAGGGGGGACZGGA
3′ AGAATCGGTGAAAAATTTTCTTTTCCCCCCTGACCTTCCCGACTAAGTGACTGTTGC 5′
-1
AZT-MP
ddAMP
PPT-2
*ACTGGAAGGGCTGATTCACZGA
3′ AGAATCGGTGAAAAATTTTCTTTTCCCCCCTGACCTTCCCGACTAAGTGACTGTTGC 5′
-1

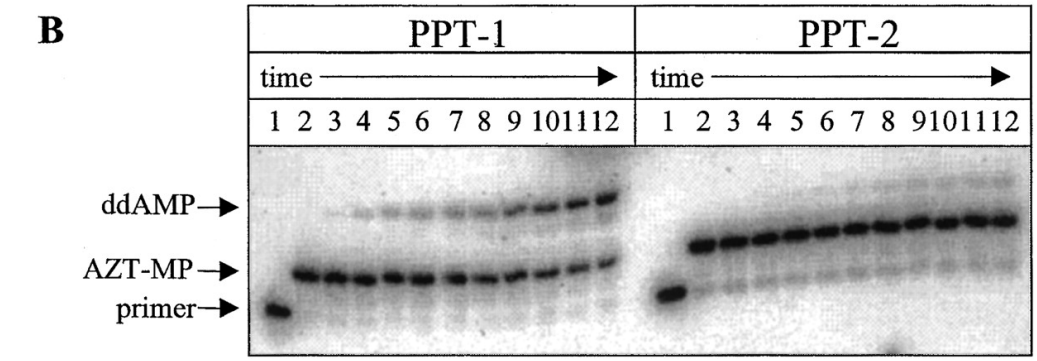
B
PPT-1
PPT-2
time
time
1 2 3 4 5 6 7 8 9 101112
1 2 3 4 5 6 7 8 9101112
ddAMP
AZT-MP
primer

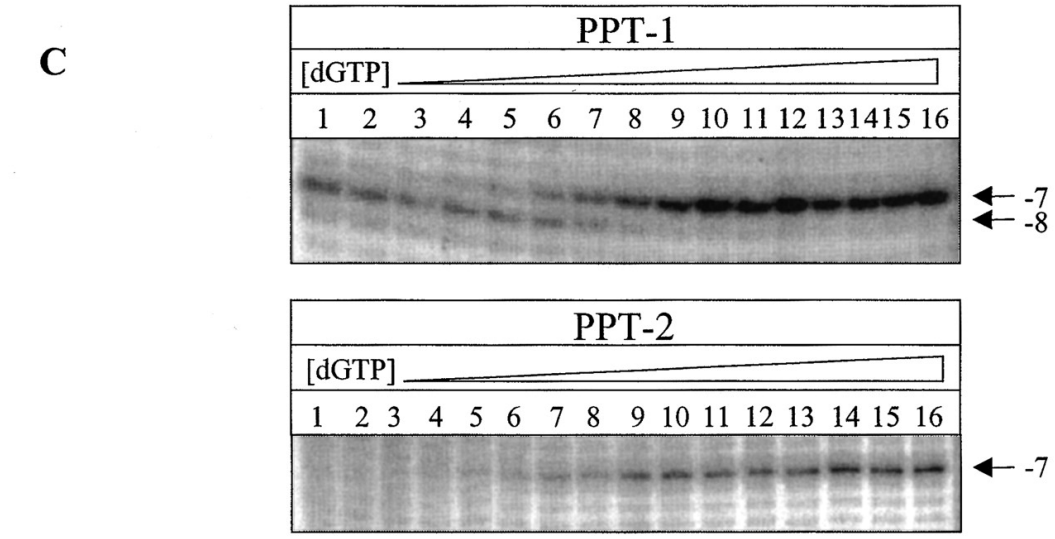
C
PPT-1
[dGTP]
1 2 3 4 5 6 7 8 9 10 11 12 131415 16
-7
-8
PPT-2
[dGTP]
1 2 3 4 5 6 7 8 9 10 11 12 13 14 15 16
-7

excision, we compared reactions with two different primers, termed PPT-1 and PPT-2, that were both terminated with AZT-MP (Fig. 2.5*A*). PPT-1 represents the primer that has been used throughout this study. PPT-2 binds at another location on the same template. In contrast to the high efficiency of rescue of AZT-terminated DNA synthesis with PPT-1, the reaction with PPT-2 is almost completely blocked (Fig. 2.5*B*). The analysis of populations of pre- and post-translocational stages shows that the 3' end of the PPT-2 has no access to the N-site, not even in the absence of the templated dNTP (Fig. 2.5*C*). The formation of the post-translocational stage shows a similar dNTP-dependent appearance as seen with PPT-1, suggesting that the formation of the pre-translocational stage is selectively diminished with PPT-2.

Impact of Drug Resistance Conferring Mutations—Previous biochemical data have shown that RT enzymes with classical AZT resistance conferring mutations 41L and 215Y together with the insertion mutation (41L/215Y/69S-(SS)) are highly efficient with respect to the ATP-dependent unblocking of AZT-terminated primers (16, 130, 144, 145, 153). This mutational pattern is associated with high level resistance to AZT and medium levels of resistance to other NRTIs. Fig. 2.6*A* shows a comparison of rescue of AZT-terminated synthesis with wild-type RT and the mutant enzyme. The results are in good agreement with published reports, showing increased rates of the reaction with the mutant RT. Fig. 2.6*B* shows the analysis with respect to the relative populations of complexes in pre- and post-translocational stages. The insertion-containing mutant enzyme clearly facilitates access of the 3' end of the primer to the N-site. The amount of radioactivity is almost identical in *lanes 4–7* (*top versus bottom*); however, the ratio of cleavage at positions -7/-8 differs significantly. The concentration of the templated dNTP required to

Fig.2.6 Effects of resistance conferring mutations on relative N-site and P-site occupations. *A*, efficiency of excision of AZT-MP with wild-type HIV-1 RT and a mutant enzyme containing AZT resistance conferring mutations M41L, T215Y, and T69S-SS. Rescue of DNA synthesis was monitored in time course experiments as described in Fig. 2.4. *B*, efficiency of translocation with AZT-terminated primers. The *graphs* show the nucleotide-dependent changes of the translocation status with wild-type RT and the mutant enzyme. Experiments were conducted as described in Fig. 2.2*C*. *C*, efficiency of excision of ddTMP with wild-type HIV-1 RT and the mutant enzyme. *D*, efficiency of translocation with ddTMP-terminated primers. The *graphs* show the nucleotide-dependent changes of the translocation status with wild-type RT and the mutant enzyme.

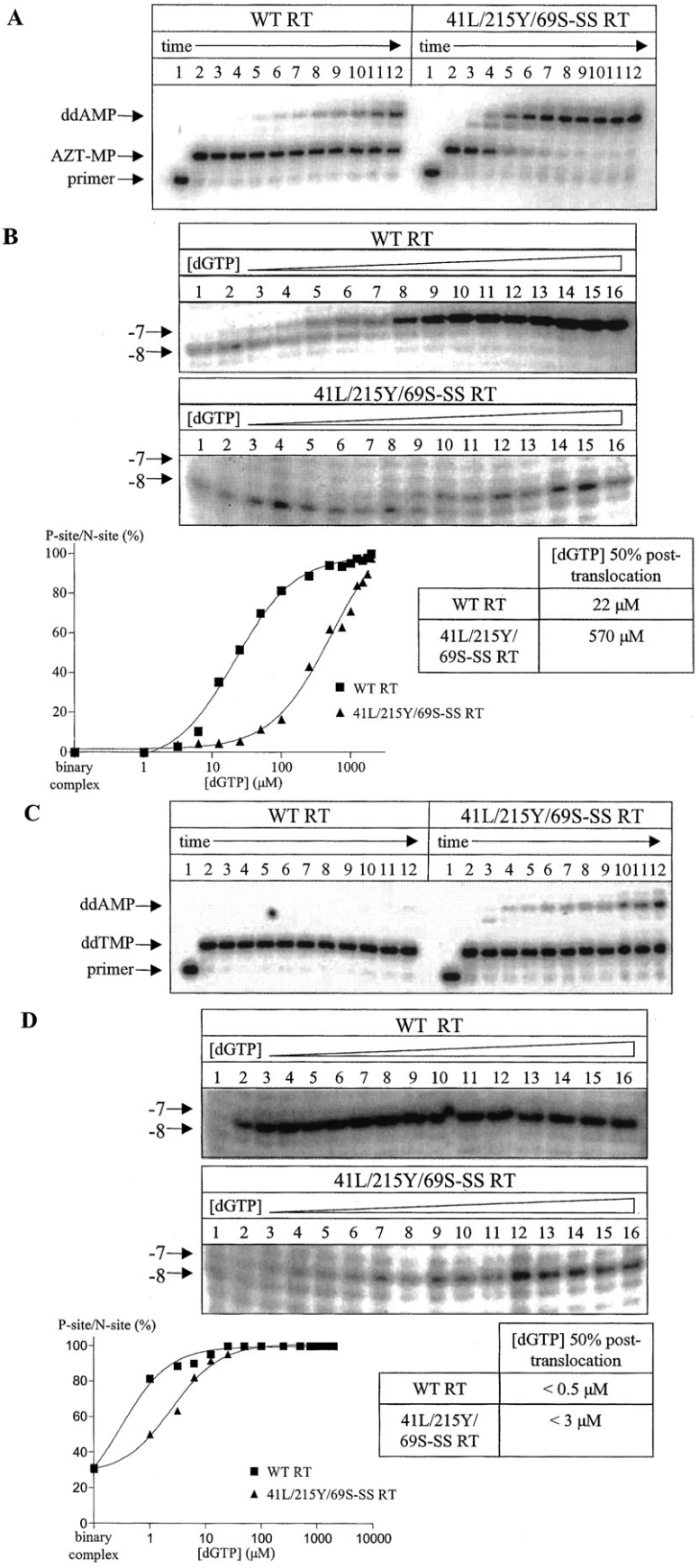
A
WT RT
41L/215Y/69S-SS RT
time
1 2 3 4 5 6 7 8 9 101112
ddAMP
AZT-MP
primer
B
WT RT
[dGTP]
1 2 3 4 5 6 7 8 9 10 11 12 13 14 15 16
-7
-8
41L/215Y/69S-SS RT
P-site/N-site (%)
100
80
60
40
20
0
binary complex
1
10
100
1000
[dGTP] (μM)
WT RT
41L/215Y/69S-SS RT
[dGTP] 50% post-translocation
WT RT
22 μM
41L/215Y/ 69S-SS RT
570 μM
C
WT RT
41L/215Y/69S-SS RT
time
1 2 3 4 5 6 7 8 9 10 11 12
ddAMP
ddTMP
primer
D
WT RT
[dGTP]
1 2 3 4 5 6 7 8 9 10 11 12 13 14 15 16
-7
-8
41L/215Y/69S-SS RT
P-site/N-site (%)
100
80
60
40
20
0
binary complex
1
10
100
1000
10000
[dGTP] (μM)
WT RT
41L/215Y/69S-SS RT
[dGTP] 50% post-translocation
WT RT
< 0.5 μM
41L/215Y/ 69S-SS RT
< 3 μM

obtain 50% of complexes in the post-translocational stages is ~25 times higher as seen with wild-type HIV-1 RT. This value is relatively high as compared with measurements on the basis of functional assays that monitor efficiency of excision. Thus, it is conceivable that not all of the complexes that exist in the pre-translocational stage are competent, and in some cases, the enzyme may dissociate from its nucleic acid substrate before excision can occur. The specific mutational background is likely to be an important factor in this regard (153).

Considering that resistance conferring mutations may also affect the affinity for ATP, we next tested whether the presence of ATP or PPi may further facilitate the formation of the pre-translocational stage. However, the presence of physiologically relevant concentrations of 3 mM ATP and 150 μM PPi did not affect the distribution of the two different configurations, neither in the context of wild-type HIV-1 RT nor in the context of the mutant enzyme (data not shown). Although the same mutant enzyme can also increase rates of rescue of ddTMP-terminated DNA synthesis, this effect is by far not as pronounced as seen with AZT-terminated primers (Fig. 2.6*C*). Similar conclusions can be drawn from the analysis of the translocational stages (Fig. 2.6*D*). The N-site occupation is favored with the mutant enzyme; however, the concentration required to obtain 50% of complexes in the post-translocational stage is still significantly lower as compared with the situation with AZT-terminated primers (2–3 μM *versus* 570 μM). Taken together, our data show consistently a clear correlation between an increase in rates of excision of a chain-terminated nucleotide and an increase in the population of complexes in the pre-translocational stage.

2.5 Discussion

Characterization of Pre- and Post-translocational Stages— Although both the polymerase and RNase H activities of HIV-1 RT have been studied in great detail, our current understanding in regard to mechanisms involved in translocation of this enzyme remains elusive. The study of mechanisms involved in polymerase translocation requires highly sensitive techniques that allow the detection of subtle structural differences at a single nucleotide resolution. We have recently reported that the precise position of the RNase H-mediated Fe^{2+} cut can differ, depending on the structure of the bound nucleic acid. All of these previous experiments were conducted in the presence of high concentrations of dNTPs that facilitate the formation of ternary complexes. Here we show that treatment of binary complexes yielded specific oxidative cleavage at template position -8 (KOONO-mediated) and -18/-19 (Fe^{2+}-mediated), respectively. The specific cuts moved toward position -7 and positions -17/-18 as the concentration of the next correct dNTP was gradually increased. The single nucleotide shift defines the pre- and post-translocational stages (Fig. 2.7).

Our data suggest that the gross conformation of the enzyme and the bound nucleic acid substrate remains unchanged in these two configurations. We measured a constant number of 10 bp between Cys-280 and Glu-478, at any given dNTP concentration. Putative translocational intermediates with 11 or more base pairs between the two markers were not detected, suggesting that both the polymerase and the RNase H domain can translocate simultaneously. Such mode of translocation is not universal. For instance, a recent study with T7 RNA polymerase suggested that the presence of the next NTP

Fig.2.7 Characterization of pre- and post-translocational stages, based on site-specific footprints. The RT-bound nucleic acid substrate is shown schematically. Sugar moieties are *green*; the 3'-terminal residue is shown in *light blue* (the 3'-OH group is represented by a *green circle*, and the 5'-phosphate connections are represented by *brown circles*), and the incoming nucleotide is *dark red.* Base pairs are shown as *dark green bars*; different distances between adjacent bars point to structural differences of the bound nucleic acid. In accordance with previous crystal structure models, the larger distance point to B-like conformations, whereas the narrow association toward the 3' end of the primer points to the more compact A-conformation. *Dark blue* sugar residues illustrate the specific cleavage sites. Cys-280 mediates KOONO cleavage, and Glu-478 mediates Fe^{2+} cuts. In this scheme, the protein moves from the *right* (*top*) to the *left* (*bottom*) relative to the DNA substrates, which remains at a fixed position. In the pre-translocational stage, the 3' end of the primer can occlude the N-site. The displacement of residues Cys-280 and Glu-478 by a single nucleotide, as illustrated by the *pink boxes*, must be accompanied by an equivalent displacement of the polymerase active site (*yellow*). As a result, the primer terminus occludes the P-site in the post-translocational stage and the incoming dNTP gains access to the N-site. The relative distribution of pre- and post-translocational stages depends on several parameters as discussed in the text.

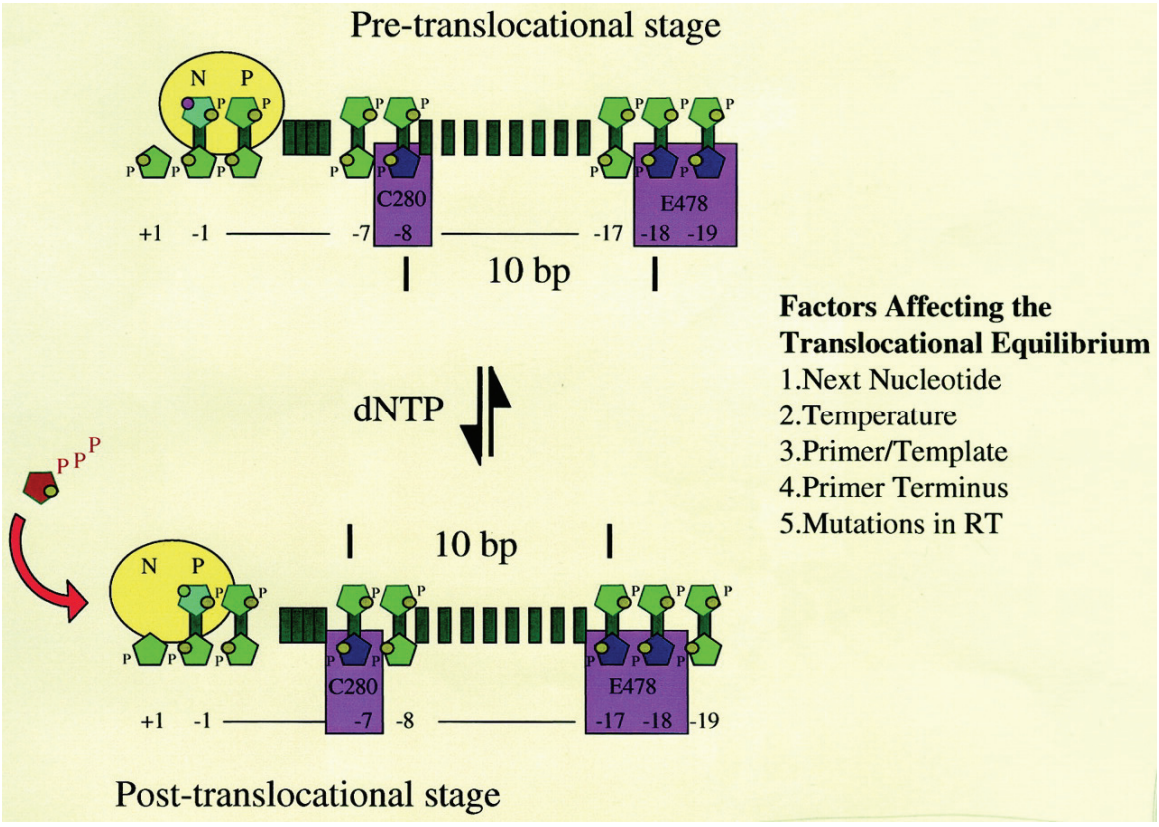

Factors Affecting the Translocational Equilibrium

1. Next Nucleotide
2. Temperature
3. Primer/Template
4. Primer Terminus
5. Mutations in RT

could promote a discontinuous (166), inchworm-like mode of translocation, as described earlier for *E. coli* RNA polymerase (117).

The Translocational Equilibrium Model—Translocation is either coupled with or uncoupled from the catalytic step. Current mechanisms of a single cycle of nucleotide incorporation, which have been developed on the basis of kinetic measurements (29, 85, 103) and crystallographic snapshots (39, 51, 214), do not include the translocation as a distinct step. A widely accepted model involves nucleotide binding to an open RT-primer/ template complex, followed by a rate-limiting conformational change that traps the incoming nucleotide in a closed conformation. The ensuing chemical step is followed by a rapid release of PPi. Enzyme translocation is kinetically invisible (103) and may occur in concert with PPi release. The difficulties to crystallize complexes in the pre-translocational stage may support such type of mechanism. The recent study by Sarafianos *et al.* (211) suggests that HIV-1 RT must be covalently cross-linked to the duplex in order to trap the 3' end of the primer in the N-site before translocation takes place. The authors noted that the N-site configuration is conformationally strained, which may store part of the energy released after bond formation. However, our footprints revealed considerable amounts of N-site complexes at 37°C. Thus, higher temperatures may provide sufficient energy to overcome putative conformational strain. The temperature dependence of the relative populations of N- and P-site complexes makes clear that enzyme translocation is reversible, and the 3' end of the terminus can regain access to the N-site after the incorporation of the chain terminator. The total amount of the N configuration depends also on the chemical nature of the chain terminator (Fig. 2.4*F*). These differences in relative populations of pre- and post-translocational stages,

seen even in the absence of the next dNTP, define the translocation as a distinct step during a single cycle of polymerization (Fig. 2.8).

Our data are consistent with the "translocational equilibrium model," proposed by Sousa and colleagues (67, 68), that is based on a passive mode of polymerase translocation. These authors suggested that a given polymerase could rapidly slide between pre- and post-translocational stages. The pre-translocational stage in which the primer terminus occupies the N-site is favored in the absence of nucleotides, whereas the post-translocational P-site configuration is favored in the presence of nucleotide substrates. This hypothesis is based on the assumption that favored interactions between the polymerase and its substrates are maximized under these circumstances. The model in its general form, as demonstrated by our data, does not make any specific distinctions between processive polymerases and other enzymes, such as HIV-1 RT that dissociate more frequently from their nucleic acid substrates. The site-specific footprints can be seen as snapshots taken within a few seconds that compose the short lifetime of HOONO of ~4 s at neutral pH (113). The relative distribution of the two bands at position -7 and -8 reflect the relative distribution of pre- and post-translocational stages within this time interval. Both passive sliding of the bound RT enzyme as well as rebinding of dissociated molecules in either one of the two configurations are possible scenarios that can contribute to the specific cleavage patterns. The absence of one of the bands indicates that the formation of the corresponding complex is unfavoured under these conditions, and the appearance of two bands points to a mixture of complexes that exist either in the pre-translocational stage or in the post-translocational stage.

Fig.2.8 Scheme of a single cycle of DNA polymerization by HIV-1 RT. The model shows the translocational equilibrium (*yellow box*) as a distinct step in a complete round of nucleotide incorporation. In contrast to previous models, the release of pyrophosphate is uncoupled from translocation. A single cycle of polymerization involves the following sequence: *1*, nucleotide binding; *2*, closure of the "fingers" that traps the incoming dNTP; *3*, phosphodiester bond formation; *4*, release of pyrophosphate that is probably associated with a re-opening of the "fingers" (88); and *5*, translocation of RT relative to the nucleic acid substrate that re-generates the original configuration. The enzyme can also dissociate from the nucleic acid substrate (see "Discussion"). The 3' end of the primer *Dn* or *Dn+1* is shown in *green* or *red*, respectively, to illustrate the different positioning relative to the active site. The primer terminus shown in *green* occludes the P-site (*green box*); the primer terminus shown in red occludes the N-site (*red box*). The incoming dNTP (*red*) must bind to the N-site.

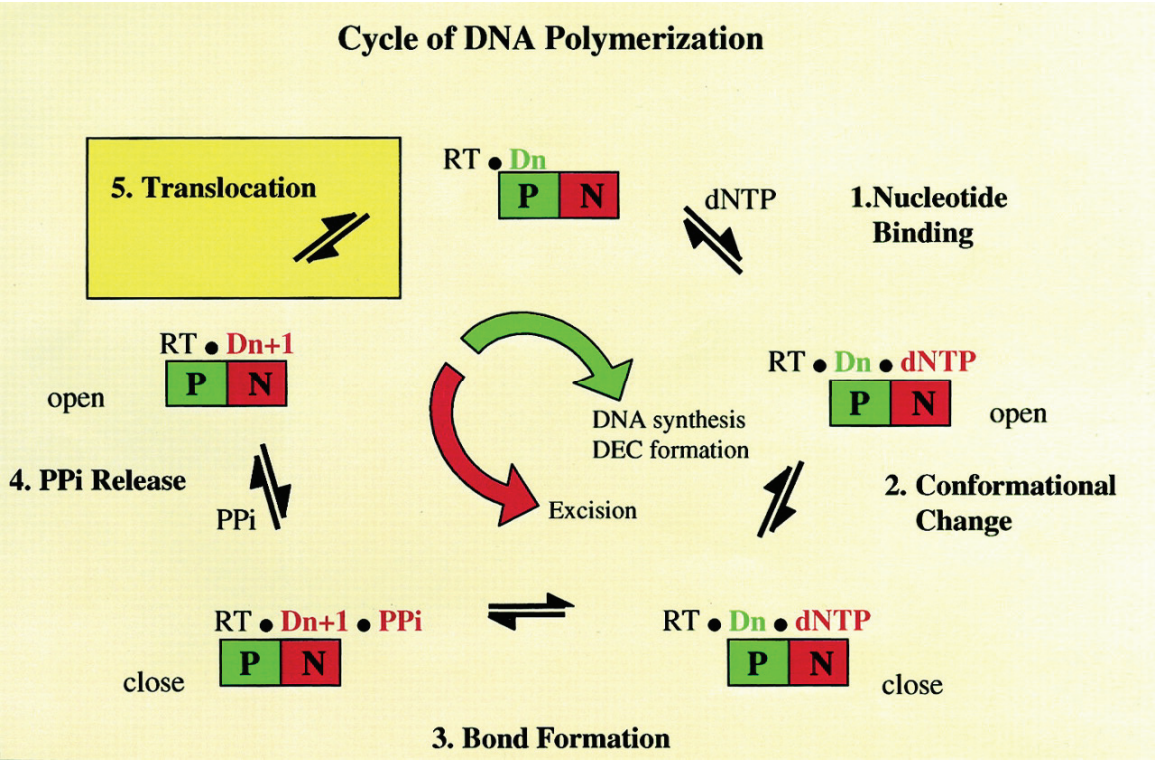
Cycle of DNA Polymerization
5. Translocation
RT • Dn
P N
dNTP
1.Nucleotide Binding
RT • Dn+1
P N
open
RT • Dn • dNTP
P N
open
DNA synthesis
DEC formation
4. PPi Release
PPi
Excision
2. Conformational Change
RT • Dn+1 • PPi
P N
close
RT • Dn • dNTP
P N
close
3. Bond Formation

Effects of Changes of the Relative Distribution of Pre- and Post-translocational Stages— We demonstrate that the relative distribution of both bands depends on several parameters that include the temperature, the sequence of the template, the chemical nature of the primer terminus and the mutational background of the enzyme. Our experiments with primers that were blocked with 2',3'-ddNMPs suggest that the translocational equilibrium cannot be seen as a critical obstacle during the normal polymerization process, because submicromolar concentrations of the templated dNTP are sufficient to pull the overall equilibrium (Fig. 2.8, *steps 5*, *1* and *2*) completely to the ternary complex in the post-translocational stage. However, the translocational equilibrium might play a role in the control of pausing or termination (126) or the extension of misaligned primers.

Here we demonstrate that this equilibrium plays a critical role in regard to the efficiency of excision of AZT-MP. Our data show consistently that increased rates of primer unblocking correlate with an increased population of complexes that exist in the pre-translocational stage. It appears that the drug-resistant enzyme can amplify this effect. This might be the result of a diminished stability of the ternary complex (16). Alternatively, resistance conferring mutation may exert a direct effect on the translocational equilibrium, and binding of the incoming nucleotide might be prevented by the occlusion of the N-site; however, in either case, the increase in the population of complexes in the pre-translocational stage correlates with increased rates of excision. We have also shown that the sequence of the primer/template substrate can affect relative populations of complexes in pre- and post-translocational stages. During the process of reverse transcription, the enzyme is probably in contact with a broad spectrum of different sequences that influence both the excision reaction and the translocational equilibrium to

various degrees. The presence of sites that diminish the ATP-dependent unblocking reactions may well correlate with increased susceptibility to AZT; however, future studies should address whether the nucleotide analogues is also effectively incorporated at these positions.

Conclusions—Taken together, the results of this study demonstrate that translocation of HIV-1 RT is a distinct step during a single cycle of DNA polymerization, which provides the basis for the determination of thermodynamic parameters of this process. The translocational equilibrium model provides a mechanism to ensure free access of the primer terminus to the N-site and also to allow binding of the pyrophosphate donor ATP, after the incorporation of the chain terminator and the release of pyrophosphate. These data validate the translocational equilibrium as a target for the development of novel antiviral agents that may act more effectively against various HIV-1 isolates including viruses that acquired resistance to NRTIs. The site-specific footprinting approach provides a valuable tool in this regard. Previous studies suggested that peroxynitrous acid participates in oxidation of the thiol group of cysteines, giving rise to thiyl radicals at neutral pH (188). Thus, the thiyl radical is presumably the active species that initiates cleavage through abstraction of hydrogens from the sugar moiety of the nearest nucleotide, as described for hydroxyl radical mediated reaction. It is conceivable that substitutions of cysteine residues at other locations implicated in substrate binding may produce similar signals as described in this study with Cys-280. The distance between the thiol group and the nearest nucleic acid residue is certainly an important parameter in this regard. Further studies that address this problem are required to assess the potential and

limitations of KOONO-mediated site-specific footprinting and its application to other systems.

CHAPTER 3

EFFECTS OF THE TRANSLOCATION STATUS OF HIV-1 REVERSE TRANSCRIPTASE ON THE EFFICIENCY OF EXCISION OF TENOFOVIR

This chapter was adapted from an article authored by B. Marchand, K.L. White, J.K. Ly, N.A. Margot, R. Wang, M. McDermott, M.D. Miller and M. Götte recently submitted to the ***Journal of Biological Chemistry***.

3.1 Preface to chapter 3

After using our site-specific footprinting assays to understand the effect of azido-containing chain-terminators on the translocational status of the reverse transcriptase and the relation between this translocational status and the removal of the chain-terminator, it was of interest to study the effects of a chain-terminator with an acyclic sugar and phosphonate moiety replacing the α-phosphate of the natural nucleotide. Therefore, we used the adenine analogue tenofovir, which we compared to the azido-containing analogue AZA-TP and the dideoxy-analogue ddATP. Convincing differences could be observed between these analogues in the translocational state of the reverse transcriptase and the rate of removal of the chain-terminators.

We also studied the effects of drug resistance conferring mutations on the translocational state of the reverse transcriptase and on the rate of removal of the chain-terminators. Mutations M41L, D67N, L210W and T215Y confer resistance to AZT and tenofovir. Although no difference in the translocational status of the enzyme could be observed, significant increase in the rate of removal of AZA and tenofovir were observed.

3.2 Abstract

The ATP-dependent phosphorolytic excision of nucleoside analogue reverse transcriptase inhibitors can diminish their inhibitory effects on human immunodeficiency virus replication. Previous studies have shown that excision can only occur when the reverse transcriptase complex exists in its pre-translocational state. The binding of the next complementary nucleotide causes the formation of a stable dead-end complex in the post-translocational state, which blocks the excision reaction. To provide mechanistic insight into the excision of the acyclic phosphonate nucleotide analog tenofovir, we compared the efficiency of the excision reaction with changes in the translocation status of the enzyme. We found that rates of excision of tenofovir with wild-type reverse transcriptase are as high as seen with 3'-azido-3'-deoxythimidine monophosphate, AZT-MP. Thymidine associated mutations, which confer >100-fold and 3-fold decreased susceptibility to AZT and tenofovir, respectively, caused substantial increases in the efficiency of excision of both inhibitors. However, in contrast to AZT-monophosphate, the removal of tenofovir is highly sensitive to dead-end complex formation. Site-specific footprinting experiments revealed that complexes with AZT-terminated primers exist predominantly pre-translocation. In contrast, complexes with tenofovir-terminated primers are seen in both configurations. Low concentrations of the next nucleotide are sufficient to trap the complex post-translocation despite the flexible, acyclic character of the compound. Thus, the relative high rate of excision of tenofovir is partially neutralized by the facile switch to the post-translocational state and dead-end complex formation, which provides a certain degree of protection from excision in the cellular environment.

3.3 Introduction

Nucleoside and nucleotide analogue reverse transcriptase (RT) inhibitors (N(t)RTIs) remain important components in drug regimens used to treat infection with the human immunodeficiency virus type 1 (HIV-1). Seven different NRTIs and a nucleotide analogue are currently in clinical use: 3' -azido -3' -deoxythymidine (zidovudine or AZT), 2', 3' -didehydro -2', 3' -dideoxythymidine (stavudine or d4T), 2', 3' -dideoxyinosine (didanosine or ddI), 2', 3'dideoxycytidine (zalcitabine or ddC), (-)-β-2', 3' -dideoxy -3' -thiacytidine (lamivudine or 3TC), its fluorinated derivative (-)-β-2′,3′-dideoxy-5-fluoro-3'-thiacytidine (emtricitabine or FTC), (1S,4R)-4-[2-amino-6-(cyclopropyl-amino)-9H-purin-9-yl]-2-cyclopentene-1-methanol succinate (abacavir or ABC), and the acyclic nucleotide 9-[2-(R)-(phosphonomethoxy)propyl]adenine (tenofovir, TFV or PMPA). All NRTIs require phosphorylation to their triphosphate (TP) forms, while metabolic activation of tenofovir requires phosphorylation to its diphosphate (tenofovir-DP) (8, 206). The tenofovir acyclic linker between the adenine base and the phosphonate moiety is another unique feature that is neither shared by NRTIs nor by natural deoxynucleoside triphosphates (dNTPs). Despite such substantial structural differences, tenofovir is efficiently incorporated by HIV-1 RT, and was also shown to act as a chain-terminating nucleotide as a consequence of a missing hydroxyl group in the linker region (9). However, as demonstrated for AZT and other chain-terminators (2, 154, 156), the incorporated tenofovir can be excised in the presence of pyrophosphate (PPi) or a PPi-donor, such as adenosine triphosphate (ATP) (14, 253, 254). The balance between nucleotide excision and excision protection is regulated in a complex manner, and depends critically on the chemical nature of the inhibitor (92, 141, 154). The factors and

mechanisms that determine efficiency of excision of tenofovir and its blockage are poorly understood.

The ATP-dependent excision reaction provides an important mechanism for resistance to NRTIs. Rates of excision of AZT-monophosphate (AZT-MP) are significantly increased with mutant enzymes that contain classical AZT-resistance mutations, including M41L, D67N, K70R, L210W, T215F/Y, and K219Q/E/N (17, 154). Differences between wild-type and mutant enzymes are most pronounced in the presence of ATP, as compared to reaction with PPi, which suggests that some of these mutations facilitate binding of ATP in an orientation that allows excision to occur (17, 191). The aforementioned mutations emerge under the selective pressure of AZT or d4T, and are therefore referred to as thymidine associated mutations (TAMs). However, clinical data have shown that the accumulation of three or more TAMs can also reduce susceptibility to non-thymidine analogues, including tenofovir (161). Biochemical data have shown that HIV-1 RT enzymes containing various combinations of TAMs facilitate the ATP-dependent removal of literally all clinically available chain-terminators, albeit at significantly different rates. For instance, high rates of excision have been reported for AZT-MP, while excision of ddAMP, i.e. the active metabolite of ddI, is sometimes difficult to detect (154).

Progress has been made in relating specific structural features of AZT-MP and deoxynucleoside monophosphates (ddNMPs) to differences seen in the rates of excision. Excision can only occur in the pre-translocation complex, when the 3'-end of the primer occupies the nucleotide binding site (N-site) (17, 140, 211, 212). In contrast, binding of the next complementary nucleotide can only occur when the N-site is freely accessible in

the post-translocation complex. Translocation of RT, relative to its bound primer/template substrate, clears the N-site and brings the 3'end of the primer to the product or priming-site (P-site). This configuration allows binding of the next nucleotide resulting in a dead-end complex (DEC) that blocks excision.

The development of site-specific footprinting techniques has allowed us to distinguish between pre- and post-translocational states (N-complex and P-complex, respectively). It appears that the RT enzyme can rapidly shuttle between both configurations, which defines a translocational equilibrium (59, 60, 141). Increasing concentration of the next nucleotide substrate can trap the complex in the post-translocational state. Both band-shift and site-specific footprinting experiments revealed that the stability of such DEC, and, in turn, blockage of the excision reaction, depends crucially on the chemical nature of the chain-terminator (141, 242). Relatively high concentrations of the next nucleotide are required to form or stabilize a ternary complex with AZT-terminated primer strands, while d4T- or ddA-terminated primers do not appear to diminish the stability of a ternary complex (16, 154, 254).

The factors that govern the ATP-dependent excision of tenofovir in the context of both wild-type and TAM-containing enzymes remain to be characterized. Biochemical data point to relatively high levels of excision of tenofovir (14, 253, 254); however, it is unclear how the acyclic structure and the phosphonate moiety affects the translocational equilibrium and the formation of a DEC. Based on the structure of the RT-DNA complex with a tenofovir-terminated primer (P-complex), it has been suggested that the flexibility of the acyclic nucleotide may provide a certain degree of protection from excision (244).

The stability or catalytic efficiency of the pre-translocation complex could be diminished by multiple conformations of tenofovir, which may disfavor excision. Alternatively, the formation or stability of a ternary DEC in the post-translocational stage could likewise be diminished, which may favor excision.

To provide mechanistic insight, we have studied the three A-analogues ddAMP, tenofovir, and AZA-MP (the adenosine analogue of AZT-MP), and the thymidine analogue AZT-MP (Fig. 3.1), with respect to their influence on the translocational equilibrium in the absence or presence of nucleotides. The data were correlated with kinetic parameters associated with the ATP-dependent excision reaction. Together our results suggest that tenofovir-terminated primers have sufficient access to the N-site in the pre-translocation complex. In the absence of natural nucleotides, excision of tenofovir is relatively high, and the rates are significantly increased with TAM-containing mutant enzymes. The ratio of complexes that exist pre- and post-translocation appears to be unaffected by these mutations. However, slight increases in concentrations of the next templated dNTP shift the translocational equilibrium towards post-translocation, which provides a certain degree of protection from excision.

Fig.3.1 Structures of NRTIs used in this study.

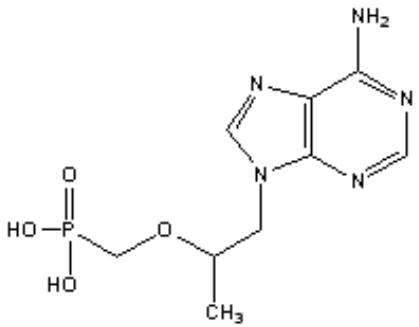

PMPA
(Tenofovir)

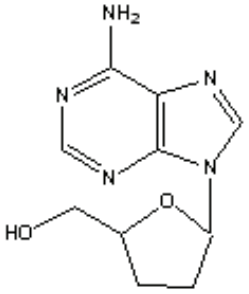

ddA
(Didanosine)

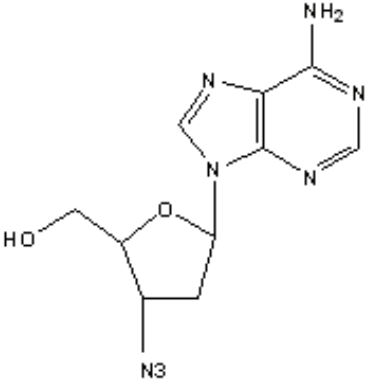

AZA

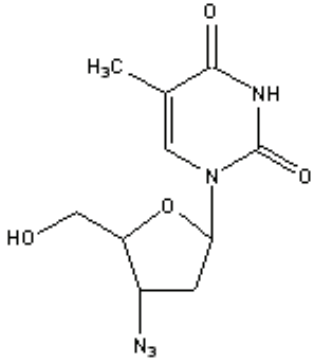

AZT
(Zidovudine)

3.4 Experimental procedures

Recombinant HIV-1 production and antiviral susceptibility assays - PCR fragments corresponding to the first 1000 basepairs (bp) of HIV-1 reverse transcriptase (RT) were amplified from plasmids containing the RT gene of HIV-1 and co-transfected with the RT-deleted HIV-1 proviral molecular clone pHXB2Δ2-261RT (a gift from C. Boucher, Utrecht University, The Netherlands) as previously described (13, 160). The virus 4Y (M41L+D67N+L210W+T215Y) was constructed by oligonucleotide-based site-directed mutagenesis of HXB2D RT and homologous recombination. Replication competent viruses generated by homologous recombination were harvested after 8-18 days when the cultures contained notable syncytia. The genotypes of the recombinant viruses were determined by RT-PCR of viral supernatant followed by sequencing using an ABI Prism 3100 Genetic Analyzer (Applied Biosystems, Foster City, CA).

Susceptibility of the recombinant 4Y virus and the wild-type HIV-1 molecular clone HXB2D to tenofovir, AZT, d4T, ddI (Sigma, St. Louis, MO), abacavir (GlaxoSmithKline, Research Triangle Park, NC), and 3TC was evaluated using an XTT-based viability assay in MT-2 cells as previously described (23). All infections were performed with 1.2×10^6 cells at a multiplicity of infection of approximately 0.001 that resulted in equal levels of cell killing in the absence of drug over the five-day assay period. EC_{50} values were calculated as an average from 8-20 experiments. Statistical significance ($p < 0.05$) was determined using two-tailed Student's t-tests. T-tests were performed on the array of EC_{50} values from all experimental data for each drug against 4Y compared to the wild-type data sets.

Enzymes, nucleic acids, and nucleotides -Heterodimeric p66/p51 wild-type RT and the M41L+D67N+L210W+T215Y (4Y) mutant enzyme were purified as recently described (127, 254). Mutant enzymes were generated through site directed mutagenesis using the Stratagene Quick-change kit according to the manufacturer's protocol. Custom DNA oligonucleotides with the following sequences were purchased from InVitrogen (Carlsbad, CA).

PPT-57T: 5′-CGTTGGGAGTGAATTAGCCCTTCCAG**T**CCCCCCTTTTCTTTTAAAAAGTGGCTAAGA-3′

PPT-57A: 5′-CGTTGGGAGTGAATTAGCCCTTCCAG**A**CCCCCCTTTTCTTTTAAAAAGTGGCTAAGA-3′

Bolded nucleotides highlight the difference among the two oligonucleotides that are used as template strands. PPT-17: 5′-TTAAAAGAAAAGGGGGG-3′ is used as primer that is complementary to the underlined region. The same sequences have previously been utilized to study the relationship between nucleotide excision and the translocation status of RT (141). Chemically synthesized oligonucleotides were purified on 12% polyacrylamide-7M urea gels containing 50 mM Tris-borate (pH 8.0) and 1 mM EDTA. Purified nucleic acids were eluted from gel slices in a buffer containing 500 mM NH_4Ac and 0.1% SDS. 5' end-labeling of oligonucleotides was conducted with [γ-^{32}P]ATP and T4 polynucleotide kinase. Labeled oligonucleotides were gel-purified as described previously(141). ATP, dNTPs and ddNTPs were obtained from Fermentas Life Sciences (Hanover, MD), Roche Diagnostics (Indianapolis, IN), or Sigma-Aldrich Inc. (St. Louis,

MO). AZT-TP and AZA-TP were purchased from TriLink Biotechnologies (Sorrento Mesa, CA). TFV-DP was synthesized at Gilead Sciences, Inc. (Foster City, CA). All dNTPs, dNTP analogues and ATP were treated with inorganic pyrophosphatase in order to eliminate contaminating pyrophosphate. dNTPs were incubated in a buffer containing 1 mM DTT, 50 mM Tris-HCl (pH 8), 50 mM KCl and 6 mM $MgCl_2$ with 0.5 unit of inorganic pyrophosphatase (Roche Diagnostics) in a final volume of 100 µl at 37ºC for 1h. The nucleotides were purified by filtration through a 10 kDa cut-off Microcon filter (Millipore, Billerica, MA).

Nucleotide incorporation - Steady state kinetic constants were determined using activated calf thymus DNA (Amersham Pharmacia Biotech, Piscataway, NJ) and rate determination by linear regression of [^{3}H]dNTP incorporation over a time course using GraphPad Prism, version 3.03 (GraphPad Software, San Diego, CA) followed by K_m and K_i determination using the competitive inhibition equation with simple weighting using the Marquardt-Levenberg algorithm (EnzFitter, version 2.0.16, Biosoft, Stapleford, Cambridge, UK) as described (254). In these experiments, the template was present in excess, and competitive inhibition was observed based on a constant V_{max} when increasing concentrations of NRTIs were assayed. Statistical significance ($p < 0.05$) was determined using two-tailed Student's t-tests.

Excision and rescue of chain-terminated DNA synthesis - Excision and the ensuing rescue of DNA synthesis was studied at a single template position using an assay similar to that described earlier (61). The primer/template duplex was pre-formed in a buffer containing 50 mM Tris-HCl (pH 7.8) and 50 mM NaCl. For this purpose, the 5' end-labeled DNA

primer (8.5 pmol) was hybridized to the complementary DNA template (25.5 pmol) by denaturing at 95ºC for 2 minutes, followed by annealing at 72ºC for 15 minutes and slow cooling to room temperature. The duplex was incubated with 25.5 pmol HIV-1 RT in a buffer containing 50 mM Tris-HCl (pH 7.8), 50 mM NaCl and 6 mM $MgCl_2$ followed by the addition of 10 μM ddATP, TFV-DP, AZA-TP, or AZT-TP. Reactions were allowed to proceed for 20 min to ensure complete incorporation of the nucleotide analogue. Excision and the ensuing rescue of chain-terminated DNA synthesis was monitored in time course experiments after the addition of ATP (3.5 mM) and a dNTP cocktail consisting of 100 μM dATP, 10 μM dCTP, and 100 μM ddTTP for adenosine analogs and 100 μM dTTP, 10 μM dCTP, and 100 μM ddGTP for AZT. Reactions were performed at 37°C and stopped at different times by adding 1 μl aliquots of reaction mixture to 9 μl of 95 % formamide containing 40 mM EDTA. Samples were heat-denatured for 5 min at 95ºC and finally resolved on 8% polyacrylamide-7M urea gels. Kinetic parameters for the combined excision and rescue reaction were determined at different concentrations of the next complementary nucleotide. The results were quantified using ImageQuant 5.2 (Amersham) and analyzed using Prism 4.0 (GraphPad).

Site-specific footprinting – Potassium peroxynitrite (KOONO) was prepared by stirring 10 ml of 1.2 M KNO_2 with 1.4 ml of 30% H_2O_2 on ice. 10 ml of 1.4 M HCl was added to the stirring solution and immediately quenched with 10 ml of 2 M NaOH. Aliquots were stored at -80°C. In preparation of the footprinting reaction, 2.7 pmoles of PPT-57 in combination with trace amount of 3' ^{32}P-labelled PPT-57 were heat annealed with 8 pmoles of PPT-17 (141). The DNA/DNA hybrid was incubated with 16 pmoles of RT and the chain-terminator (10 μM) in a buffer containing cacodylate (pH 7, 120 mM),

NaCl (20 mM), DTT (0.5 mM) and $MgCl_2$ (6 mM) in a final volume of 20 µl for 20 minutes at 37°C in order to form the chain-terminated complex. Different concentrations of the next templated nucleotide were then added to the reaction followed by an incubation of 10 minutes at 37ºC. The complex was finally treated with 1.5 µl of KOONO (100 mM). The samples were analyzed as described above.

Gel mobility shift assay – 1 pmole of the ^{32}P 3'-labelled template PPT-31T (5'CCTTCCAGTCCCCCCTTTTCTTTTAAAAAGT3') or PPT-31A (5'CCTTCCAG**A**CCCCCCTTTTCTTTTAAAAAGT3') was heat annealed to 3 pmoles of PPT-17 primer. The DNA/DNA hybrid (1 pmole) was incubated with 5 pmoles of HIV-1 RT in a buffer containing 50 mM Tris-HCl (pH 7.8), 80 mM NaCl and 6 mM $MgCl_2$ in a final volume of 20 µl. The DNA primer was first chain-terminated with ddATP, TFV-DP, or AZT-TP. The next complementary nucleotide was then added at different concentrations prior to the addition of heparin (1.5 µg/µl). Complexes were incubated for 60 minutes at room temperature before the addition of 20 µl of 50% sucrose and trace amounts of bromophenol blue. The products were resolved on native 6% polyacrylamide Tris-borate gels, and visualized as described above. The results were quantified using the ImageQuant software (Amersham) and fitted to a "One site binding" hyperbola ($Y=B_{max}*X/(K_d+X)$) using GraphPad Prism. K_d values were determined from three independent experiments.

3.5 Results

Cell-based drug susceptibility measurements - TAMs are not selected under pressure of tenofovir; however, the accumulation of three or more of these mutations that include M41L or L210W were shown to reduce susceptibility to the drug *in vitro* and clinically (161, 252). We have generated an HIV-1 variant that contains the M41L + D67N + L210W + T215Y cluster of TAMs, designated 4Y, and determined phenotypic susceptibility to different NRTIs, including tenofovir. The 4Y cluster confers a 3-fold increase in EC_{50} values to tenofovir, as compared to the wild-type (WT) virus (Fig. 3.2). In accordance with published data, susceptibility to AZT was dramatically reduced (>100-fold) in this mutational context, while susceptibility to ddI remained largely unaffected (123, 133). Cell toxicity prevented accurate susceptibility measurements with AZA.

Efficiency of nucleotide incorporation and excision - Steady state kinetic measurements showed no significant differences between WT HIV-1 RT and mutant 4Y when analyzing the efficiency of binding or incorporation of different NRTIs. We found that the ratio of K_i/K_m was only marginally reduced for tenofovir-DP, which is not surprising considering that TAMs are not associated with resistance mechanisms that involve substrate discrimination (108, 116, 248) (Table 3.1). Hence, we have looked at the efficiency of ATP-dependent excision reactions, and the ensuing rescue of DNA synthesis of ddAMP-, and AZA-MP, and tenofovir-terminated primers (Fig. 3.3). In this set-up, ATP was added together with a mixture of dNTP substrates required to produce a longer product upon NRTI excision that is distinguishable from the chain-terminated DNA. The concentration

Fig.3.2 Phenotypic susceptibility of the 4Y variant to different NRTIs compared to WT HIV-1. Drug susceptibility measurements were conducted in MT-2 cells as described under experimental procedures. Fold susceptibility changes for the 4Y mutant compared to WT are indicated above the bars.

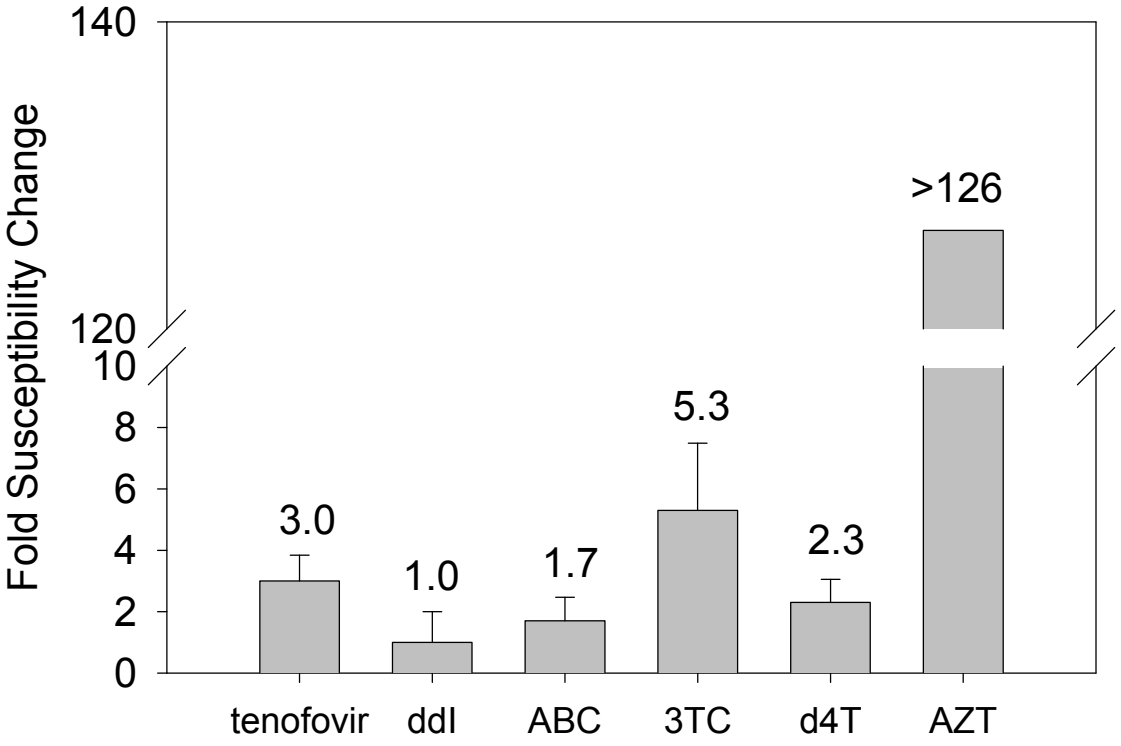
Fold Susceptibility Change
140
120
10
8
6
4
2
0
3.0
1.0
1.7
5.3
2.3
>126
tenofovir
ddI
ABC
3TC
d4T
AZT

TABLE 3.1. K_i and K_i/K_m of wild-type and mutant HIV-1 RT enzymes.

NRTI	WT RT		4Y RT	
	K_i (μM)[a] (fold)[b]	K_i/K_m (μM) (fold)[c]	K_i (μM)[a] (fold)[b]	K_i/K_m (μM) (fold)[c]
Tenofovir-DP	0.21 ± 0.07 (1.0)	0.47 (1.0)	0.11 ± 0.01[d] (0.5)	0.19 (0.4)
ddATP	0.09 ± 0.03 (1.0)	0.20 (1.0)	0.05 ± 0.01 (0.6)	0.09 (0.5)
AZA-TP	0.23 ± 0.07 (1.0)	0.51 (1.0)	0.15 ± 0.04 (0.65)	0.26 (0.5)
AZT-TP	0.041 ± 0.010 (1.0)	0.09 (1.0)	0.047 ± 0.009 (1.2)	0.09 (1.0)

[a] K_i values are averages of at least three experiments ± standard deviation
[b] Fold change in K_i value from that for the wild-type
[c] Fold change in K_i/K_m value from that for the wild-type, however, no statistics were generated for this ratio
[d] $P < 0.01$ compared to the K_m for the wild-type by two-tailed Student's *t* test

Fig.3.3 Excision of chain-terminating nucleotides with WT RT and the 4Y mutant. (A) Combined excision/rescue reactions were monitored in time-course experiments with a radio-labelled primer (lane C). The primer/template sequence and nucleotide mixtures used in this set-up are shown above the gels. The primer was initially chain-terminated with 10 μM ddAMP (left), 10 μM TFV-DP (middle), or 10 μM AZA-MP (right). The reaction was then initiated by the addition ATP (3.5mM) and a mixture of dATP (100 μM), dCTP (10 μM), and ddTTP (100 μM) to generate a defined reaction product, referred to as rescued product, which can be distinguished from the chain-terminated primer. Reactions were stopped at indicated time points and samples were analyzed on denaturing 12% polyacrylamide gels. (B) Graphical representation of data shown under A.

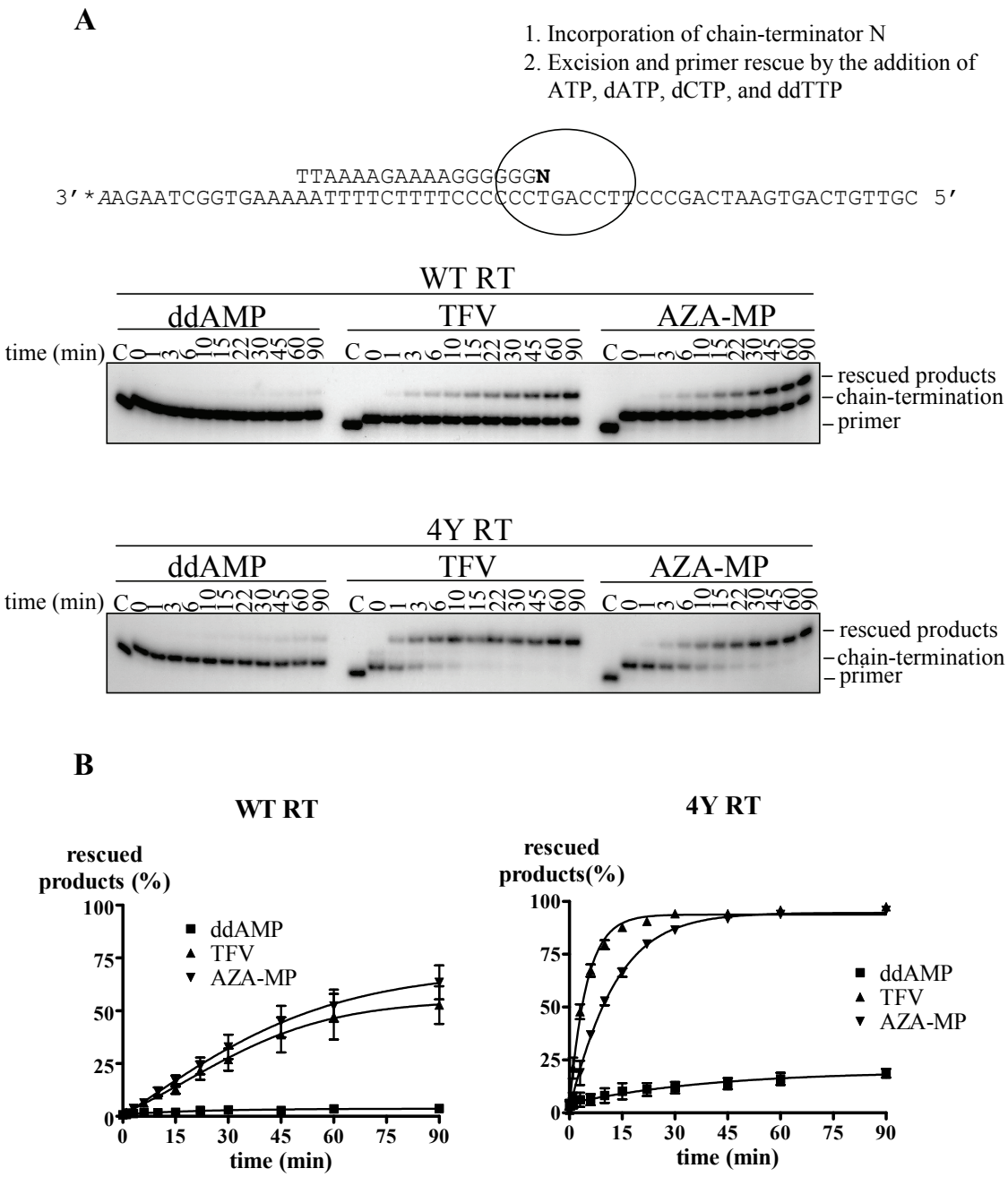
A
1. Incorporation of chain-terminator N
2. Excision and primer rescue by the addition of ATP, dATP, dCTP, and ddTTP
TTAAAAGAAAAGGGGGGN
3′*AAGAATCGGTGAAAAATTTTCTTTTCCCCCCTGACCTTCCCGACTAAGTGACTGTTGC 5′
WT RT
ddAMP
TFV
AZA-MP
time (min) C 0 1 3 6 10 15 22 30 45 60 90
rescued products
chain-termination
primer
4Y RT
ddAMP
TFV
AZA-MP
time (min) C 0 1 3 6 10 15 22 30 45 60 90
rescued products
chain-termination
primer
B
WT RT
rescued products (%)
100
75
50
25
0
ddAMP
TFV
AZA-MP
0 15 30 45 60 75 90
time (min)
4Y RT
rescued products(%)
100
75
50
25
0
ddAMP
TFV
AZA-MP
0 15 30 45 60 75 90
time (min)

of dCTP, i.e. the next complementary nucleotide, was 10 μM, which reasonably mimics physiologically relevant conditions (55, 80, 243).

The rescue of ddAMP-terminated DNA synthesis with WT HIV-1 RT was almost undetectable under these conditions. The 4Y mutant enzyme increased the efficiency of the reaction. In contrast, WT RT is able to rescue tenofovir- and AZA-MP-terminated DNA synthesis, and the efficiency of the reactions was substantially increased with the 4Y mutant RT. These reactions involve the same template position and the same nucleotide base; thus, any differences in rates of the reactions can be assigned to structural differences related to the sugar-phosphate moieties of ddAMP, AZA-MP, or to the acyclic linker and phosphonate moiety of tenofovir. Nucleotide excision can be highly efficient, despite the lack of a 3'azido group, or any other equivalent bulky substituents that could diminish the stability of the post-translocation state. These data suggest that tenofovir-terminated primers have relatively good access to the N-site in the pre-translocation state.

Site-specific footprinting of binary and ternary complexes - To study the influence of the chemical nature of incorporated chain-terminators on the translocational equilibrium of HIV-1 RT, we have determined the relative proportions of complexes that exist either pre- or post-translocation (Fig. 3.4). We utilized site-specific footprinting techniques in the presence of increasing concentrations of the next complementary nucleotide (dCTP) to characterize conditions that promote a shift toward post-translocation (Table 3.2). These quantitative footprinting experiments were conducted with KOONO, which is a metal-free source of hydroxyl radicals that mediates hyperreactive cleavage at template

Fig.3.4 Site-specific footprints of chain-terminated complexes. (A) RT-complexes with radio-labelled template and chain-terminated primers were treated with KOONO, as described under experimental procedures. The next templated nucleotide (dCTP) was added at increasing concentrations prior to the KOONO cleavage. The sequence underneath the gels shows the positions of site-specific cleavages with KOONO treatment. Cleavage at position -8 is indicative for the pre-translocation complex, and cleavage at position -7 is indicative for the post-translocation complex. (B) Graphical representation of data shown in panel A.

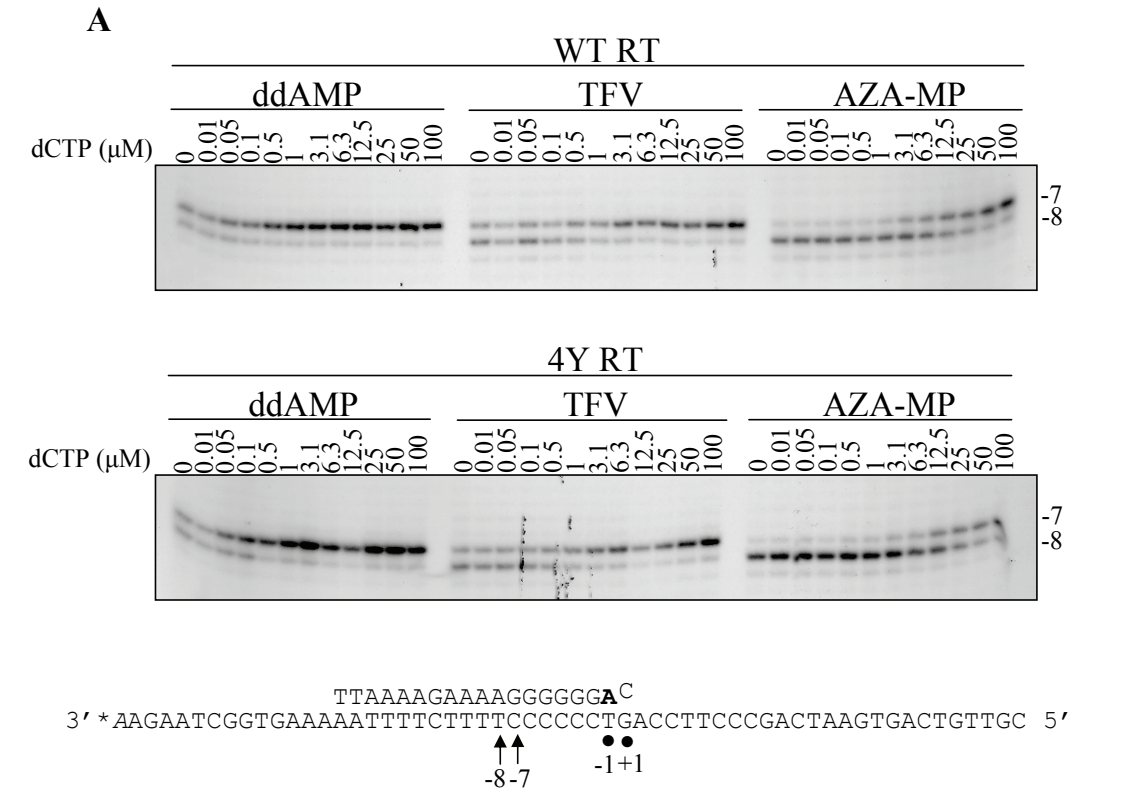
A
WT RT
ddAMP
TFV
AZA-MP
dCTP (μM)
0 0.01 0.05 0.1 0.5 1 3.1 6.3 12.5 25 50 100
-7
-8
4Y RT
ddAMP
TFV
AZA-MP
dCTP (μM)
0 0.01 0.05 0.1 0.5 1 3.1 6.3 12.5 25 50 100
-7
-8
TTAAAAGAAAAGGGGGGAC
3′*AAGAATCGGTGAAAAATTTTCTTTTCCCCCCTGACCTTCCCGACTAAGTGACTGTTGC 5′
-8 -7
-1 +1

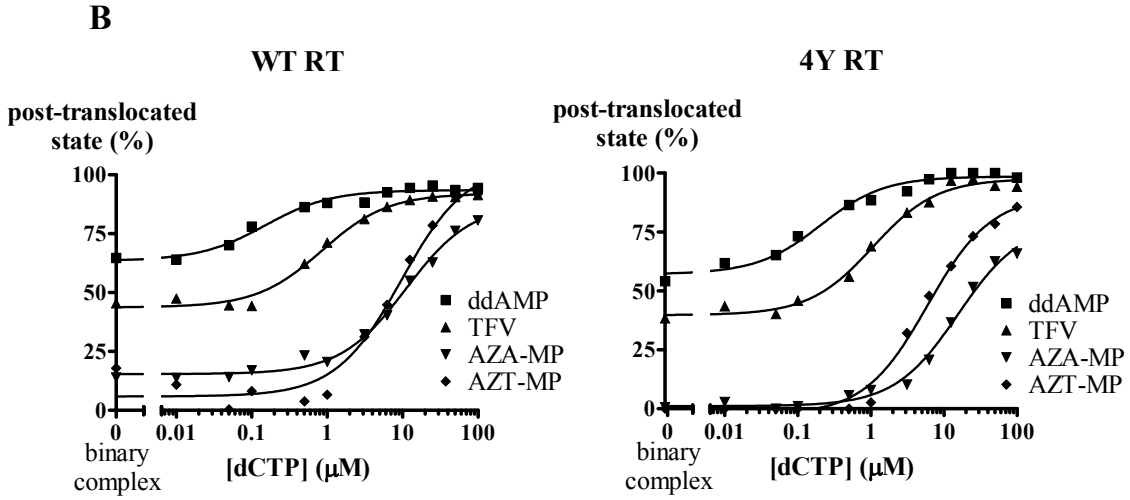
B
WT RT
4Y RT
post-translocated state (%)
100
75
50
25
0
ddAMP
TFV
AZA-MP
AZT-MP
0 0.01 0.1 1 10 100
binary complex
[dCTP] (μM)

Table 3.2. Translocation status of RT

Chain-terminator	Post-translocated state	WT RT	4Y RT
ddAMP	No dCTP[a]	65%	54%
	EC_{50} (dCTP)[b]	ND[c]	ND[c]
	EC_{80} (dCTP)[d]	0.2 μM	0.3 μM
TFV	No dCTP[a]	45%	38%
	EC_{50} (dCTP)[b]	0.1μM	0.3 μM
	EC_{80} (dCTP)[d]	3 μM	2 μM
AZA-MP	No dCTP[a]	14%	1%
	EC_{50} (dCTP)[b]	10 μM	27 μM
	EC_{80} (dCTP)[d]	100 μM	>100 μM
AZT-MP	No dCTP[a]	6%	0%
	EC_{50} (dCTP)[b]	8 μM	8 μM
	EC_{80} (dCTP)[d]	31 μM	50 μM

[a] Percentage of complexes that exist post-translocated in the absence of nucleotide substrate

[b] Nucleotide concentration required to form 50% of the complex population in its post-translocation state

[c] ND = not determined because the post-translocated complex is > 50% in the absence of dCTP

[d] Nucleotide concentration required to form 80% of the complex population in its post-translocation state

positions –7 and –8, depending on the translocational state. A cut at position -7 is indicative of the post-translocation state, while a cut at position -8 is indicative of the pre-translocation state. The relative distribution of the two bands at position –7 and –8 reflects the relative distribution of pre- and post-translocational stages within the time interval of a few seconds. The corresponding acid has a half life at pH 7.4 of 2 seconds (113). Thus, both sliding of the bound RT enzyme as well as rebinding of dissociated molecules in either one of the two configurations are possible scenarios that can contribute to the specific cleavage patterns (141). Cleavage is mediated through C280, which, in the large subunit p66, is located in the vicinity of the template (141).

We found that the binary complex of WT RT with a ddAMP-terminated primer exists predominantly in its post-translocation state (65%) (Fig. 3.4 and Table 3.2). Submicromolar concentrations of the next nucleotide are sufficient to obtain 80% of the complex population in the post-translocational state. This value is referred to as EC_{80}(dNTP). The EC_{50}(dNTP) value (concentration of dCTP required to obtain 50% of the complex population in the post-translocation state) cannot be determined for ddAMP, because the post-translocation complex is already favored in the absence of dNTP substrates.

Translocation appears to be diminished with tenofovir-terminated primers when compared to ddAMP. For tenofovir, 45% of the complex population pre-exist in the post-translocational state in the absence of nucleotides, and EC_{50}(dNTP) and EC_{80}(dNTP) values of 0.1 μM and 3 μM, respectively, were obtained in the presence of the next nucleotide. For comparative purposes, another template was evaluated that allowed us to

monitor RT translocation and excision of the T-analogue AZT-MP at the same position as the A-analogues. In contrast to tenofovir and ddAMP, both AZT-MP and AZA-MP promote formation of the pre-translocational state. In the absence of nucleotides, the complex population exists almost exclusively in its pre-translocational state, and high concentrations of the next templated nucleotide are required to obtain the majority of complexes in the post-translocational state. We measured EC_{80}(dNTP) values of >100 μM (AZA-MP) and 31 μM (AZT-MP), respectively. The difference between the two 3'azido-containing nucleotides may not be significant. Taken together, the footprints show that the concentration of the next nucleotide required to trap the complex post-translocation follows the order: AZA-MP = AZT-MP > tenofovir > ddAMP.

We next analyzed the influence of the chain-terminator on the stability of the ternary complex directly. Previous band shift studies have shown that binary complexes of HIV-1 RT and primer/template are unstable when challenged with a trap, e.g. heparin. However, the presence of the dNTP substrate can stabilize the complex. The concentration of the next nucleotide required to maintain a band shift was significantly higher with AZT-terminated primers as compared to other chain-terminators such as ddATP(242). Here we found that tenofovir-terminated primers behave between the two extremes (Fig. 3.5). Apparent K_d's follow the order AZT-MP > tenofovir > ddAMP (24.9 ± 1.4 μM, 3.2 ± 0.12 μM, and 0.1 ± 0.007 μM, respectively). Relatively high amounts of stable binary complex (≈ 40%) prevented accurate measurements with AZA-terminated primers, while less than 10% binary complex was seen with the other chain-terminators under these conditions. Overall, the data are in good agreement with our footprinting experiments.

Fig.3.5 Formation of ternary complexes. Pre-formed complexes of HIV-1 RT and a DNA/DNA substrate were incubated with increasing concentrations of the templated nucleotide, before the addition of trap. The primers were chain-terminated with ddAMP (left), tenofovir (middle), or AZT-MP (right).

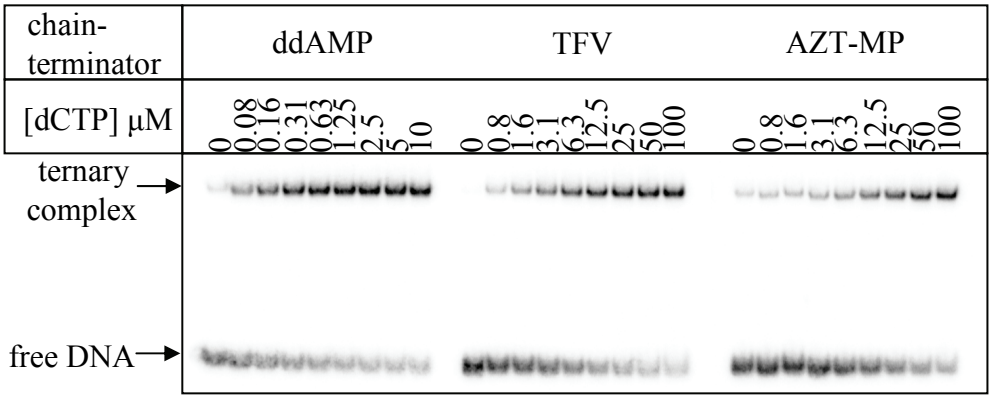
chain-terminator
ddAMP
TFV
AZT-MP
[dCTP] µM
0 0.08 0.16 0.31 0.63 1.25 2.5 5 10
0 0.8 1.6 3.1 6.3 12.5 25 50 100
0 0.8 1.6 3.1 6.3 12.5 25 50 100
ternary complex
free DNA

The K_d for ddAMP is somewhat lower as compared to previous studies, which is probably due to differences in the sequence.

The four TAMs do not appear to largely affect the translocational equilibrium of HIV-1 RT (Fig. 3.4 and Table 3.2). Footprints in the absence of dNTP substrates point to slight increases in the stability of the pre-translocation complex; however, these differences are within a margin of error of approximately 10% translocation. In the presence of the next dNTP, no significant differences between WT RT and the 4Y mutant were observed with ddAMP-terminated primers, which is consistent with the observation that this combination of TAMs does not greatly affect susceptibility to the drug or rates of excision. In contrast, the 4Y cluster facilitates the efficient removal of tenofovir and AZA/T-MP; however, our footprint results show that such increased rates of excision are not due to an increased stability of the pre-translocation complex in the context of TAMs. It is conceivable that differences between wild-type and mutant enzymes may become evident when the footprints are conducted in the presence of the pyrophosphate donor ATP, although it should be noted that these conditions promote excision, which, in turn, affects the positioning of RT enzyme. Protocol modifications such as reducing the efficiency of excision at lower temperatures and/or in the absence of divalent metal ions was also shown to affect the translocational equilibrium. However, ATP binding and the ensuing removal of the nucleotide analogue can be assessed through enzyme kinetic measurements. The rate of the reaction will crucially depend on the concentration of the next templated nucleotide. Thus, to establish meaningful reaction conditions for more detailed kinetic measurements, we have determined the amount of rescued product in the presence of multiple concentrations of the next complementary nucleotide.

Influence of the next dNTP on RT translocation and the efficiency of excision - These experiments were limited to excision reactions with WT RT in the context of tenofovir and AZA-MP terminated primer strands. The lowest nucleotide concentration was 0.5 μM in these experiments. Lower concentrations compromise the forward reaction, following excision of the nucleotide analogue (data not shown). Moreover, following the removal of A-analogues, the absence of the next nucleotide promotes incorporation of ATP and prevents accurate quantification of excision (data not shown). The graphs in Fig. 3.6 A and B show that the efficiency of rescue of AZA-MP and tenofovir-terminated DNA synthesis correlates inversely with the formation of the post-translocation complex, as expected. However, the sensitivity to the dNTP substrate depends crucially on the chemical nature of the chain-terminator. Tenofovir is almost completely removed at submicromolar concentrations of the next templated nucleotide, while the removal of AZA-MP is less efficient under the same conditions. This is surprising, at first glance, because the amount of complex that exists pre-translocation is reduced as compared to AZA-MP. Thus, the data suggest that the N-site is more efficiently used for excision when the primer is terminated with tenofovir under these conditions. However, the presence of the next templated nucleotide, which at low micromolar concentrations mimics the cellular milieu, caused substantial declines in the removal of tenofovir. In contrast, reactions with AZA-MP are less sensitive to changes with respect to concentration of the next nucleotide. The same trend is seen with respect to dNTP-dependence of the translocational equilibrium.

Fig.3.6 Correlation between excision and the translocation status of HIV-1 RT. Combined excision/rescue reactions with (A) TFV- and (B) AZA-MP-terminated primers were performed in the presence of increasing concentrations of the next templated nucleotide (dCTP). The results were graphed together with corresponding footprinting experiments shown in Fig.3.3. The graphs point to inverse correlation between rates of excision (▲) and the shift toward the post-translocation state (■).

A **TFV**

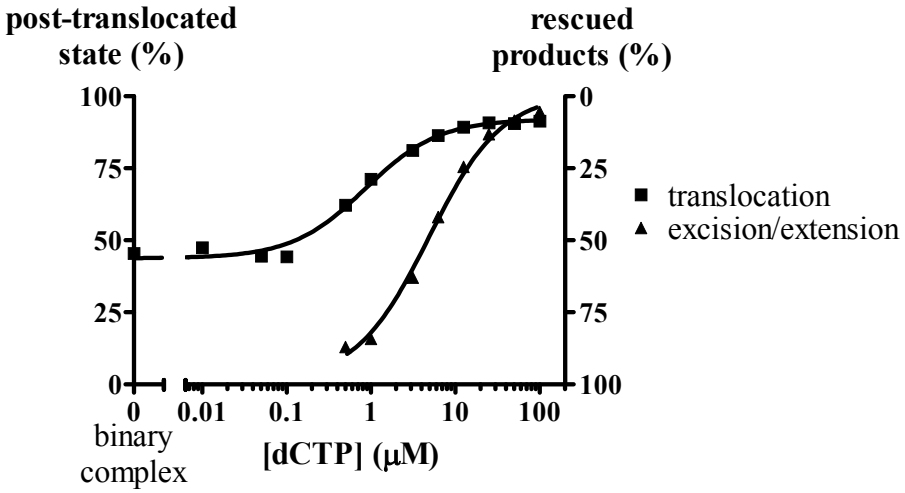
post-translocated state (%)
rescued products (%)
100
75
50
25
0
0
25
50
75
100
translocation
excision/extension
0
0.01
0.1
1
10
100
binary complex
[dCTP] (μM)

B **AZA-MP**

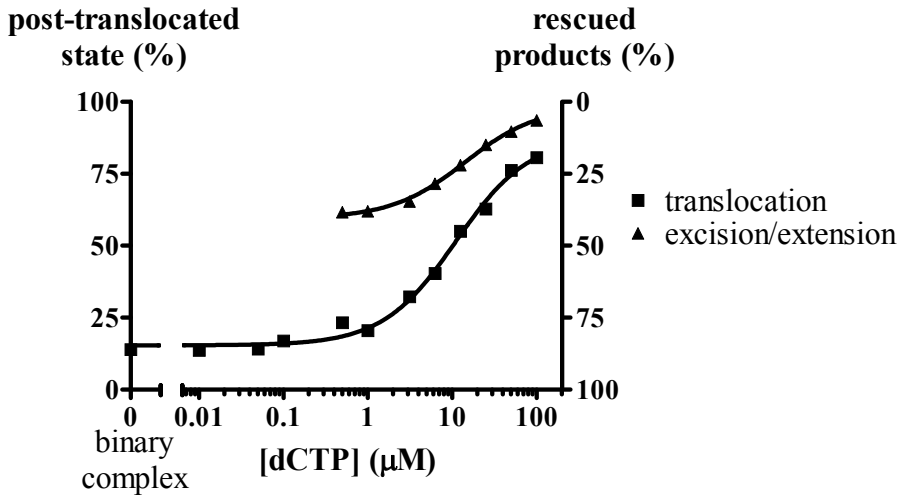
post-translocated state (%)
rescued products (%)
100
75
50
25
0
0
25
50
75
100
translocation
excision/extension
0
0.01
0.1
1
10
100
binary complex
[dCTP] (μM)

Kinetic parameters for ATP-dependent excision of tenofovir - To better understand how the four TAMs in 4Y RT can facilitate the removal of incorporated tenofovir, we measured and compared kinetic parameters for reactions conducted with WT RT and the 4Y mutant in the context of tenofovir, AZA-MP, and AZT-MP. K_m and V_{max} values for ATP were determined in the presence of 0.5 μM and 10 μM of dCTP to assess the sensitivity to inhibition of excision by the next templated nucleotide. 10 μM dCTP may represent a concentration that is well within a physiologically relevant window (55, 80, 243). We found that K_m values do not significantly differ, regardless of the chemical nature of the chain-terminator, the enzyme (WT RT or 4Y), or the nucleotide concentration (Table 3.3). Differences are evident when the maximum rate of excision was examined. The mutant enzyme shows substantially higher values in each case. It is therefore the change in k_{cat} that affects the overall catalytic efficiency of the reaction (k_{cat}/K_m). Excision of tenofovir is 14- to 20-fold increased with the 4Y mutant, while values for the excision of AZA-MP and AZT-MP show 3-fold and 7-fold changes, respectively. Of note, almost identical values were obtained under steady state and under pre-steady state conditions when looking at the excision of these two 3'azido-containing nucleotides (154, 223).

The kinetic measurements indicate that the removal of tenofovir is highly sensitive to inhibition in the presence of the next nucleotide. We calculated a sensitivity index as the ratio of the efficiency of excision measured at 0.5 μM and 10 μM of the next templated nucleotide dCTP. WT RT and the 4Y mutant show relatively high values for tenofovir of 7.3 and 5.7, respectively, while the corresponding values with AZA-MP and AZT-MP are just slightly above 1. These data suggest that intracellular concentrations of dNTP pools,

Table 3.3. Efficiency of the combined ATP-dependent excision/extension reaction

Chain-terminator	Enzyme	dCTP (μM)	K_m (mM)[a]	k_{cat} (min^{-1} X 10^{-3})[a]	k_{cat}/K_m (min^{-1} M^{-1})	Catalytic efficiency[c] (fold-change)	Sensitivity to dNTP inhibition[b]
TFV	WT RT	0.5	1.0 ± 0.11	1.1 ± 0. 04	1.1	----	----
		10	1.9 ± 0.3	0.28 ± 0.02	0.15	----	7.3
	4Y RT	0.5	0.59 ± 0.05	9.7 ± 0.24	16.4	14.9	----
		10	0.96 ± 0.24	2.8 ± 0.24	2.9	19.3	5.7
AZA-MP	WT RT	0.5	1.7 ± 0.21	0.84 ± 0.044	0.49	----	----
		10	1.2 ± 0.21	0.44± 0.03	0.37	----	1.3
	4Y RT	0.5	2.0 ± 0.49	3.2 ± 0.37	1.6	3.3	----
		10	2.0 ± 0.36	2.4 ± 0.22	1.2	3.2	1.3
AZT-MP	WT RT	0.5	1.3 ± 0.34	0.25 ± 0.026	0.19	----	----
		10	1.0 ± 0.25	0.16± 0.014	0.16	----	1.2
	4Y RT	0.5	1.4 ± 0.27	1.8 ± 0.14	1.3	6.8	----
		10	1.2 ± 0.19	1.3 ± 0.076	1.08	6.8	1.2

[a] Values are means of at least three independent experiments ± standard deviation

[b] Sensitivity to dNTP-dependent inhibition is given as ratio of $[k_{cat}/K_m(0.5\ \mu M\ dCTP)]/[k_{cat}/K_m(10\ \mu M\ dCTP)]$

[c] Catalytic efficiency is given as ratio of $[k_{cat}/K_m(4Y\ RT)]/[k_{cat}/K_m(WT\ RT)]$

or variations thereof, may play an important role with respect to differences in HIV-1 susceptibility to AZT and tenofovir. In the case of tenofovir, higher intracellular dNTP concentrations strongly inhibit the excision reaction, which increases the lifetime of chain-termination.

3.6 Discussion

The ATP-dependent excision reaction appears to be influenced by three major parameters. ATP binding, together with the catalytic step and the release of the polynucleotide product, may be treated as a single parameter under steady state conditions. The formation of a DEC in the presence of the next complementary nucleotide is detrimental to excision, which can be seen as a second parameter that influences the efficiency of the reaction. The translocational equilibrium connects the two antagonistic pathways. Binding of the next templated dNTP can only occur in the post-translocational state, while excision can only occur in the pre-translocation state. We have previously shown that the ratio of complexes that exist either pre- or post- translocation depends on the sequence, the temperature, and on the chemical nature of the chain-terminator (141, 159). Thus, the translocational equilibrium may be seen as a third, distinct factor that influences the excision reaction. Here we characterized and quantitatively assessed the impact of the translocational equilibrium on the overall efficiency of excision of tenofovir in comparison to ddAMP, AZA-MP and AZT-MP. Our results are summarized in the model shown in Fig. 3.7.

Fig.3.7 Effects of the translocation status of HIV-1 RT on the ATP-dependent excision of NRTIs. Site-specific footprinting experiments revealed that the RT enzyme can oscillate between pre- and post-translocational states. The ratio of both complexes is given as percentage for wild-type RT and is dependent upon the nature of the chain-terminator present at the 3'end of the primer. Differences in size of the arrows under "translocational equilibrium" represent differences of the translocational equilibrium measured in the absence of dNTPs. The formation of the DEC depends on the dNTP concentration. Differences in the size of the arrows under "dNTP" reflect differences seen in footprints with increasing concentrations of the next templated nucleotide. The efficiency of the excision, seen under steady state conditions, depends upon the chemical nature of the inhibitor, the concentration of ATP, and the presence of resistance conferring mutations (TAMs) in the RT enzyme. Dominant pathways are boxed. The excision of TFV is efficient at low concentrations of dNTPs, while increases to the low micromolar range favour DEC formation and chain-terminator stability.

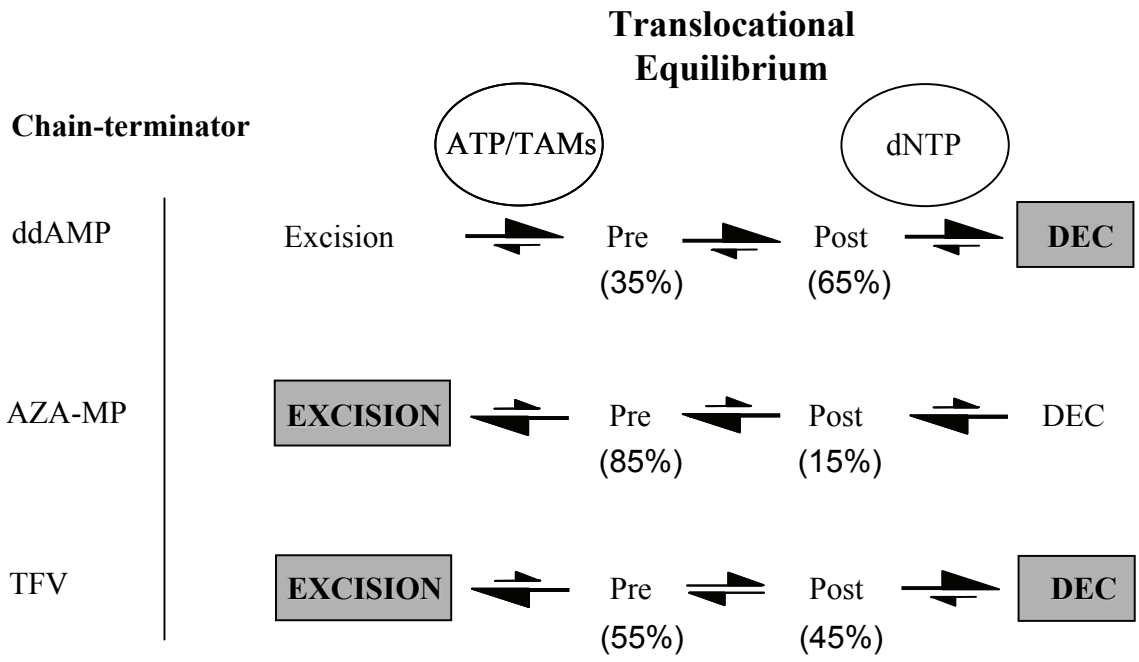
Translocational Equilibrium
Chain-terminator
ATP/TAMs
dNTP
ddAMP
Excision
Pre
(35%)
Post
(65%)
DEC
AZA-MP
EXCISION
Pre
(85%)
Post
(15%)
DEC
TFV
EXCISION
Pre
(55%)
Post
(45%)
DEC

Effects of tenofovir-terminated primers on the translocational equilibrium - Time course experiments and steady state kinetics show that the removal of tenofovir is highly efficient in the presence of limited dNTP pools. Under these conditions, the rates of the combined excision and primer rescue reaction can be even higher than seen with AZT-MP and AZA-MP, while the removal of ddAMP is inefficient. Site-specific footprinting experiments revealed inhibitor-dependent differences of the translocational equilibrium.

In the absence of the next complementary dNTP, complexes with AZT-MP and AZA-MP terminated primers exist predominantly pre-translocation, complexes with tenofovir exist as mixtures of pre- and post-translocational states, while complexes with ddAMP exist predominantly post-translocation. These data provide strong support for the notion that the RT enzyme can oscillate between both configurations, and the chemical nature of the chain-terminator can influence the equilibrium between pre- or post-translocational states. The relatively high rate of excision of tenofovir, despite its more limited access to the N-site as compared to AZA/T-MP, suggests that the nucleophilic attack of the PPi-donor might be more efficient on the phosphonate. The flexibility of the acyclic inhibitor can be seen as an additional parameter in this regard. Comparative experiments with nucleotides containing a phosphonate or a phosphate with identical sugar and base moieties are required to elucidate the contribution of each of the two structural features individually.

Effects of tenofovir on DEC-formation - The ratio of complexes that exist pre- or post-translocation in the absence of the next templated nucleotide appears to be indicative of the efficiency with which a ternary DEC is formed in the presence of nucleotides. The formation of a DEC depends on the post-translocation position of the 3'end of the primer

and follows the order ddAMP > tenofovir > AZA/T-MP. Access to the pre-translocational state follows the inverse order and facilitates nucleotide excision. The diminished ability of RT to form ternary complexes with AZA/T-terminated primer strands is consistent with previous modeling studies and crystallographic data pointing to steric problems between the bulky 3'-azido group and the incoming dNTP substrate (17, 211). In contrast, despite the lack of a sugar moiety, the DEC with a tenofovir-terminated primer strand is remarkably stable, which suggests that base stacking between the bound nucleotide, the incorporated tenofovir, and the penultimate primer base, once formed, may not be largely perturbed. This was unexpected, considering that crystallographic models in the absence of the next nucleotide show multiple conformations of the incorporated acyclic nucleotide (244). The combined biochemical and crystallographic data suggest that the incoming nucleotide may freeze a conformation that allows base stacking with the incoming nucleotide. The differential effects of the next dNTP on the formation of ternary complexes, are in good agreement with steady state kinetics of the combined excision/rescue reaction with different concentrations of the next templated nucleotide. The excision of tenofovir is severely compromised in the presence of 10 μM of the next nucleotide, as compared to reactions conducted in the presence of 0.5 μM nucleotide substrate. In contrast, rates of removal of AZA/T-MP are literally identical under both conditions.

Effects of TAMs on the excision of tenofovir - TAM-containing mutant enzymes can cause significant increases in rates of excision of tenofovir. Here we show that the efficiency of excision, at submicromolar concentrations of the next dNTP, can be even higher than seen with AZA/T-MP. As for the wild-type enzyme, the presence of 10 μM of the next

templated nucleotide caused severe reductions in the combined excision and rescue reaction with tenofovir-terminated primer strands. However, the efficiency of the reaction is still remarkably high, and the mutant confers a clear advantage over the wild type enzyme. The k_{cat}/K_m value for the removal of tenofovir for the TAM mutant is even larger than seen with AZT-MP under the same conditions. In contrast, cell-based susceptibility measurements point to 3-fold and >100-fold increases in IC_{50} values for tenofovir and AZT, respectively, when comparing the TAM-containing virus with wild-type HIV-1. A possible explanation is that the concentration of 10 μM of the next templated nucleotide, as used in our biochemical experiments, may not be high enough to adequately mimic conditions under which drug susceptibility measurements are performed *in vitro*. Values in the range of 10 μM may well represent average concentrations of intracellular dNTP pools; however, dNTP concentrations can fluctuate, depending on the cell cycle, the intracellular compartment, the cell type, and the transformation status of the cell (55, 80, 243).

The threshold for dNTP concentrations required to completely block excision was also shown to depend critically on the primer/template sequence (141, 159). In addition, both site-specific footprinting experiments and binding studies have shown that the translocational equilibrium depends on the sequence (91, 141). Our experiments were performed with a sequence that facilitates the study of RT translocation close to equilibrium. This sequence permits the analysis of changes with respect to the ratio of complexes that exist either pre- or post-translocation. Thus, sequences that promote translocation may have a greater impact on excision protection of tenofovir, because this inhibitor facilitates translocation and the formation of a DEC *per se*. In contrast, AZT-

MP, which compromises translocation and disfavors the formation of a DEC, may still be excised in a particular sequence context that diminishes or even prevents excision of tenofovir. The sequence of the primer/template can also influence the stability of the binary RT-nucleic acid complex. A diminution in the stability of the complex will likewise restrict access to the pre-translocation complex. The chemical footprints are snap-shots of approximately 4 to 5 seconds in which the enzyme may dissociate and associate with its nucleic acid substrate. Thus, these experiments monitor both enzymes that rebind either pre- or post-translocation, and enzymes that slide between the two positions.

Several studies have suggested that TAMs facilitate binding of ATP in a catalytically competent mode, which helps to explain the increased rates of excision of multiple chain-terminators in the presence of these mutations (157, 168, 191). This appears to be the dominant role played by T215F/Y. TAMs do not appear to affect the translocational equilibrium. There are only subtle differences between wild-type RT and the mutant enzyme where the pre-translocation complex could be marginally favored. In contrast, the presence of the T69S-SS finger insertion against a background of TAMs can shift the equilibrium towards pre-translocation, which probably reflects the diminished ability of the enzyme to form a DEC (141, 145, 153, 253).

Taken together, the data shown in this study suggest that the ATP-dependent excision of tenofovir is driven by efficient excision at the N-site in the pre-translocation complex. High rates of excision can be partially neutralized by a facile switch to the post-translocational state and the subsequent formation of a DEC in the presence of relatively

low concentrations of the next templated nucleotide. These results are in agreement with clinical data which have shown decreased virological response in tenofovir DF-treated patients infected with HIV-1 containing multiple TAMs (161). In addition, the results of this study warrant further investigation with regards to the sequence-dependence of the translocational equilibrium and its possible impact on nucleotide excision in the context of both wild-type and mutant RT enzymes. It will be important to screen for and to identify sequences that promote enzyme dissociation and/or formation of the post-translocation state in order to determine lower limits of the concentration of the next templated nucleotide required to render chain-termination irreversible.

CHAPTER 4

THE PYROPHOSPHATE ANALOGUE FOSCARNET TRAPS THE PRE-TRANSLOCATIONAL STATE OF HIV-1 REVERSE TRANSCRIPTASE IN A BROWNIAN RATCHET MODEL OF POLYMERASE TRANSLOCATION

This chapter was adapted from an article authored by B Marchand, E.P. Tchesnokov and M. Götte that was accepted for publication in the ***Journal of Biological Chemistry***.

4.1 Preface to chapter 4

After nucleotide incorporation, a pyrophosphate product is formed and must be released by the reverse transcriptase along with translocation. It has been so far impossible to identify the order of these two steps. In order to clarify this issue, we used our site-specific footprinting assays to observe the translocational state of the reverse transcriptase in the absence and presence of a pyrophosphate analogue. Since the presence of pyrophosphate in our reaction promotes the removal reaction, pyrophosphate could not be used to conduct the footprinting. We used the pyrophosphate analogue foscarnet, which cannot be used as a substrate by the reverse transcriptase for the removal reaction.

Foscarnet is an inhibitor of viral polymerases. Although it has been used to treat infections with HIV-1, its mechanism of action still remains elusive. Our footprinting assays allowed us to identify a mechanism of inhibition by foscarnet. It appears that foscarnet binds and stabilizes the reverse transcriptase in the pre-translocational state, blocking nucleotide binding.

We also identified a novel mechanism of resistance to foscarnet. The E89K reverse transcriptase has a decreased affinity for the pre-translocational state, the conformation to which foscarnet can bind. By doing so, this enzyme is less susceptible to be bound by foscarnet, resulting in a resistant phenotype.

4.2 Abstract

The pyrophosphate (PPi) analogue phosphonoformic acid (PFA or foscarnet) inhibits the reverse transcriptase (RT) of the human immunodeficiency virus type 1 (HIV-1); however, the mechanisms of drug action and resistance remain elusive. Here we studied the effects of the translocational status of HIV-1 RT on drug binding and inhibition of DNA synthesis. We identified "hot spots" for inhibition during active elongation. Site-specific footprinting analyses revealed that the corresponding complexes exist predominantly in the pre-translocational state. The sensitivity to PFA is significantly reduced with sequences that show a bias toward the post-translocational state. Binding studies showed that PFA stabilizes selectively the complex in the pre-translocated configuration. These findings are consistent with a Brownian ratchet model of polymerase translocation. The enzyme can rapidly shuttle between pre- and post-translocated states. The bound inhibitor acts like a pawl of a ratchet and prevents the forward motion of HIV-1 RT, while the bound nucleotide binds to the post-translocated complex and prevents the reverse motion. The proposed mechanisms of RT translocation and drug action are consistent with the PFA resistant phenotypes. We show that certain sequences and the PFA resistant E89K mutant diminishes the stability of the pre-translocated complex. In these cases, the enzyme is seen at multiple positions around the 3' end of the primer, which provides a novel mechanism for resistance. These findings validate the pre-translocated complex as a target for the development of novel, perhaps less toxic and more potent inhibitors that block HIV-1 RT translocation.

4.3 Introduction

Different classes of inhibitors that target the reverse transcriptase (RT) of the human immunodeficiency virus type 1 (HIV-1) have been developed(32). Nucleoside analogue reverse transcriptase inhibitors (NRTIs) are major components in drug regimens that are currently used in the clinic. Two different NRTIs are usually combined with a non-nucleoside analogue RT inhibitor (NNRTI) or a protease inhibitor. The triphosphate forms of NRTIs compete with natural nucleotide pools for incorporation, and, once incorporated, the monophosphate (MP) acts as a chain-terminator. NNRTIs bind to a hydrophobic pocket in the vicinity but not at the active site of HIV-1 RT. Previous studies have suggested that these compounds interfere with the chemical step, while nucleotide binding does not appear to be largely affected (205, 224). Here we studied the mechanism of action of the pyrophosphate (PPi) analogue phosphonoformic acid (PFA or foscarnet), which represents a third class of RT inhibitors.

PFA shows a broad spectrum of antiviral activities against various members of the *Herpesviridae* and *Retroviridae* (171). The inhibitor is used in the clinic to treat infection with herpes simplex virus type 1 and type 2 (HSV-1 and HSV-2), the human cytomegalovirus (HCMV), and other related herpesviruses when first-line agents have failed (31). Toxic side effects and its poor bioavailability limit its clinical utility as a component in drug regimens for HIV treatment. In spite of these problems, PFA is sometimes used in patients infected with multi-drug resistant HIV-1 variants when no other treatment options are available (146). The beneficial effects of this drug have been primarily associated with its resistance profile. With few exceptions, mutations that

confer decreased susceptibility to NRTIs and NNRTIs do not affect susceptibility to PFA (148, 158, 232). Most importantly, mutations associated with PFA resistance were shown to increase susceptibility to the nucleoside analogue 3' -azido -3' -deoxythymidine (zidovudine or AZT) (75, 233). Biochemical data have shown that PFA associated resistance mutations diminish the phosphorolytic excision of incorporated chain-terminators such as AZT-MP (3, 158). Wild type HIV-1 RT is capable of removing AZT-MP in the presence of pyrophosphate (PPi) (203), or a PPi-donor such as ATP (156). Rates of the ATP-dependent excision reaction are significantly increased with RT enzymes containing thymidine associated resistance mutations (TAMs), which provides an important mechanism for resistance to this class of compounds (154).

The mechanisms involved in PFA drug action and drug resistance remain to be elucidated. Steady-state kinetics with retroviral RT enzymes, and DNA polymerases of HSV or CMV suggest a non-competitive mode of inhibition of DNA synthesis with respect to the deoxynucleoside triphosphate (dNTP) substrate (28, 171, 237). In contrast, PFA competitively blocks pyrophosphorolysis and PPi exchange reactions, which points to overlapping binding sites for PFA and PPi (34). HIV-1 RT has been crystallized in various forms in the presence of primer/template without and with a bound dNTP substrate (38, 88); however, structures of ternary complexes with PFA or PPi are not available. In a single cycle of nucleotide incorporation, PPi is generated following the formation of a new phosphodiester bond (29, 85, 103). Binding of the next complementary nucleotide requires the release of PPi from this product complex. The enzyme must translocate a single template position further downstream to clear the nucleotide binding site (N-site). This motion relative to the nucleic acid substrate brings

the 3'end of the primer to the priming or product site (P-site) (211, 262). The latter configuration is referred to as the post-translocational state. Crosslinking and site-specific footprinting experiments revealed that pyrophosphorolysis or the ATP-dependent excision can only occur in the former pre-translocational state (141, 212). To account for the non-competitive mode of inhibition it has been suggested that PFA may likewise bind to the pre-translocated complex (158). High concentrations of PFA appear to excise incorporated AZT-MP, which provides some support for this notion (27). However, it remains to be seen whether the pre-translocational state is accessible during active DNA synthesis. If so, what is the underlying mechanism?

We have recently developed site-specific footprinting techniques that allow the distinction between pre- and post-translocated states (141). Here we demonstrate that the sequence of the nucleic acid substrate affects the ratio of pre- and post-translocational states at a given template position. PFA-mediated inhibition of DNA synthesis is linked to primer/template sequences that facilitate the formation of the pre-translocational state. These findings suggest that pre- and post-translocated complexes equilibrate immediately following each nucleotide incorporation event. The PPi analogue traps the pre-translocated complex, which prevents binding of the next nucleotide. PFA is therefore a competitive inhibitor. The non-competitive mode of inhibition is a consequence of the increased stability of the product complex, which diminishes the turnover. The results of this study validate the pre-translocated complex as a target for drug discovery and development efforts.

4.4 Experimental procedures

Enzymes and nucleic acids. Heterodimeric reverse transcriptase p66/p51 was expressed and purified essentially as described (127). Mutant enzymes were generated through site directed mutagenesis using the Stratagene Quick-change kit according to the manufacturer's protocol. Oligo-deoxynucleotides used in this study were chemically synthesized and purchased from InVitrogen life technologies. The following sequences were used as templates:

PPT57:

CGTTGGGAGTGAATTAGCCCTTCCAGTCCCCCCTTTTCTTTTAAAAAGTGGCT

AAGA,

PPT31: CCATCCAGTCCCCCCTTTTCTTTTAAAAAGT

The following sequences were used a primers:

PPT: TTAAAAGAAAAGGGGGG

PPT+2: TTAAAAGAAAAGGGGGGAC,

PPT+3: TTAAAAGAAAAGGGGGGACT,

PPT+4: TTAAAAGAAAAGGGGGGACTG,

PPT+5: TTAAAAGAAAAGGGGGGACTGG,

PPT+6: TTAAAAGAAAAGGGGGGACTGGA,

PPT+7: TTAAAAGAAAAGGGGGGACTGGAA,

PPT+11: AAAGGGGGGACTGGAAGGGC

PPT+12: AAGGGGGGACTGGAAGGGCT,

PPT+15: GGGGGACTGGAAGGGCTAAT,

PPT+16: GGGGACTGGAAGGGCTAATT.

Deoxynucleotide and dideoxynucleotides were purchased at Fermentas life sciences. AZT-triphosphate was purchased from Trilink Biotechnologies, and phosphonoformic acid was purchased from Sigma.

DNA synthesis. 1 pmole of the 5'-labelled PPT primer was heat annealed with 3 pmoles of the template. The DNA/DNA hybrid was incubated with 3pmoles of HIV-1 RT in a buffer containing 50mM Tris-HCl pH7.8, 50mM NaCl and 6mM $MgCl_2$, in the absence or presence of PFA and 10μM of each of the four dNTPs. The reaction was allowed to proceed at 37^0C for 3 minutes, and stopped by the addition of 100μl of 90% isopropanol, 300mM ammonium-acetate and 10ng/μl bulk *E. coli* tRNA. The DNA was resuspended in 10μl 100% formamide containing traces of bromophenol blue and xylene cyanol. The samples were analyzed on 8% denaturing polyacrylamide gel followed by phosphorimaging.

Site-specific footprinting. KOONO was prepared by stirring 10 ml of 1.2 M KNO_2 with 1.4 ml of 30% H_2O_2 on ice. 10 ml of 1.4 M HCl was added to the stirring solution and immediately quenched with 10 ml of 2 M KOH. Aliquots were stored at -80^0C. In preparation of the footprinting reaction, the 3'end-labelled template was heat annealed with the primer. The DNA/DNA hybrid (1 pmole) was incubated with 6 pmoles of RT in a buffer containing sodium cacodylate pH 7 (120 mM), NaCl (20 mM), DTT (0.5 mM) and $MgCl_2$ (6 mM) in a final volume of 20 μl. Different concentrations of PFA were then added to the reaction followed by an incubation of 10 minutes at 37^0C. The complex was treated with 1.5 μl of KOONO (100 mM).

Gel mobility shift assay. The radiolabelled DNA/DNA hybrid (1pmole) was incubated with 5pmoles of HIV-1 RT in a buffer containing 50mM tris-HCl pH7.8, 50mM NaCl and 6mM $MgCl_2$ in a final volume of 20µl. The DNA primer was first chain-terminated with the appropriate ddNTP to prevent incorporation of the next complementary nucleotide. PFA or the templated nucleotide, respectively, was then added at different concentrations prior to the addition of heparin (1.5µg/µl). The complexes were incubated for 60 minutes at room temperature, and the samples containing 50% sucrose were analyzed on non-denaturing 6% polyacrylamide gels. The results were quantified as the fraction of shifted primer/template for each concentration of substrate used. Apparent K_d was estimated by fitting the quantified results to a hyperbola for one site binding ($Y=B_{max}*X(K_d+X)$) as previously described (242).

Steady-state kinetics. Steady-state kinetic parameters K_m, k_{cat} and K_i for single nucleotide incorporation events in the presence or absence of PFA were determined through gel-based assays (62). We used three different primers (PPT+4, PPT+6, and PPT+16) that allow the study of single nucleotide incorporation events. The incorporation of the nucleotide was monitored at a single time point in the presence of increasing concentrations of the next complementary nucleotide. K_i values were determined in the presence of increasing concentrations of PFA. Reactions were carried out in the presence of 50mM Tris-HCl (pH 7.8), 50mM NaCl, 0.6 pmol primer/template and 0.08 pmol active site RT. Nucleotide incorporation was initiated by the addition of $MgCl_2$ to a final concentration of 6 mM, and reactions were allowed to proceed for 7 min at position +4 and +16, and 3 min at position +6 in order to ensure that the rates of the reactions were

within the linear range. The excess of primer/template (DNA substrate) over the RT and the linear range of product formation ensured and confirmed, respectively, the steady state conditions of single nucleotide incorporation. The samples were analyzed as described above. Single nucleotide incorporation was quantified as the fraction of the DNA substrate (template/primer) converted to product (template/primer+1 nucleotide). The rate of single nucleotide incorporation was plotted versus dNTP concentration. The data were fitted to Michaelis-Menten equation by use of GraphPad Prism (version 4.0) to determine K_m and k_{cat} values. k_{cat} was defined as maximal rate of single nucleotide incorporation. K_m was defined as the concentration of dNTP at which the rate of single nucleotide incorporation was equal to half maximal rate. K_i values were determined by plotting $1/k_{cat}$ and K_m as a function of the concentration of PFA. If increasing concentrations of PFA resulted in increased K_m only (suggesting a competitive mode of inhibition) than K_i values were determined from the x-intercept of K_m versus PFA concentration graphs. If increasing concentrations of PFA resulted in increased K_m and/or decreased k_{cat} (suggesting a non-competitive mode of inhibition) than K_i values were determined from the y-intercept of k_{cat} versus PFA concentration graphs. k_{cat}, K_m and K_i constitute steady state parameters for a single nucleotide incorporation event.

4.5 Results

We conducted experiments that were designed to analyze possible sequence-dependent effects associated with PFA-mediated inhibition of DNA synthesis. The aim of this approach was to isolate and characterize complexes that either increase or decrease the

inhibitory effects of PFA in order to study the possible link between the efficiency of inhibition and the translocation status of HIV-1 RT.

Hot spots for PFA-mediated inhibition of DNA synthesis. We devised a heteropolymeric primer/template substrate and compared the patterns of DNA synthesis in the presence of increasing concentrations of PFA, and PPi, respectively (Fig. 4.1). The substrate was derived from the polypurine tract (PPT) of HIV-1 as previously described (62). Reactions with PFA show distinct bands at positions +2, +3, +7, +8, +12, +14, +16, and +25 (Fig. 4.1A, left). At low concentrations of the inhibitor, i.e. conditions that still permit full-length DNA synthesis, most prominent bands correspond to positions +3 and +16 (Fig. 4.1B, top). At high concentrations of the inhibitor (> 25 μM), less sensitive sites, e.g. position +1, can likewise be affected, which eventually leads to complete inhibition. This data shows that inhibition of DNA synthesis in the presence of PFA is sequence dependent. However, unlike classical chain-terminators that interact with their complementary base, a common sequence-specific feature is not evident.

Reactions with PPi give rise to bands that are frequently offset by a single nucleotide, as compared to the reaction carried out with PFA (Fig. 4.1A, right; Fig. 4.1B, bottom). Major bands that are observed in the presence of PPi are seen at positions +2, +11 and +15, as compared to major sites of inhibition with PFA that appear at +3 and +16 (Fig. 4.1B). The fact that high concentrations of PPi facilitate the reverse reaction can account for this one nucleotide difference. Thus, the shift in the cleavage patterns suggests that PPi and PFA can bind to the same complexes, although the concentrations of PFA required to block DNA synthesis are significantly lower as compared to the inhibitory

Fig.4.1 Effects of the sequence on inhibition of DNA synthesis with PFA and PPi. *A,* DNA synthesis in the presence of increasing concentrations of PFA (left) or PPi (right). Lane C is a control that shows the DNA primer. The asterisk points to the radiolabel at the 5'end of the PPT primer. Arrows point to hot spots for inhibition. Bands associated with PFA inhibition are assigned to the sequence below; positions +3 and +16 show the strongest effect. *B,* Scans of gels shown in *A*. Reactions in the presence of 3 μM of PFA (top) are compared with reactions in the presence of 10 mM PPi (bottom).

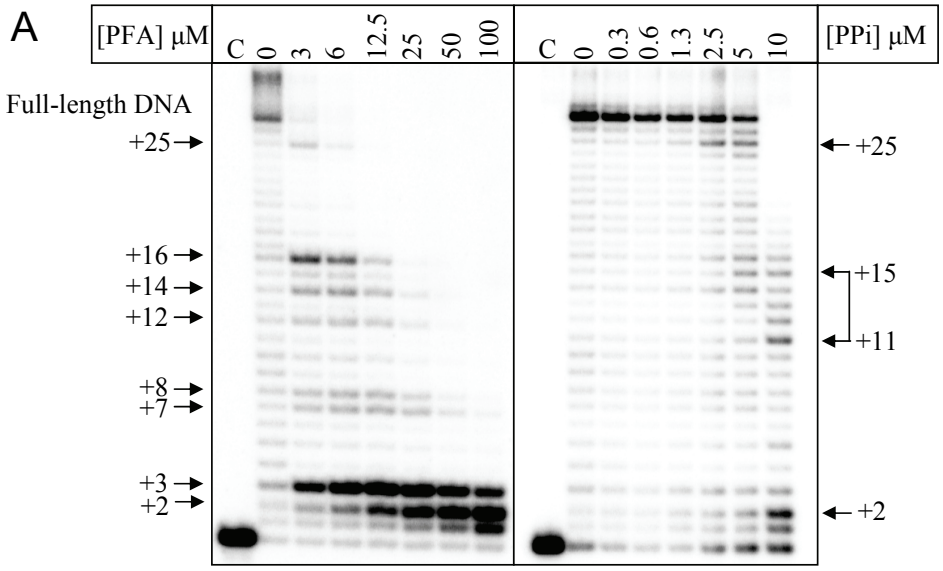
A
[PFA] μM
C 0 3 6 12.5 25 50 100
C 0 0.3 0.6 1.3 2.5 5 10
[PPi] μM
Full-length DNA
+25
+16
+14
+12
+8
+7
+3
+2
+25
+15
+11
+2


5′ *TTAAAAGAAAAGGGGGG
3′ AGAATCGGTGAAAAATTTTCTTTTCCCCCCTGACCTTCCCGATTAAGTGAGGGTTGC 5′
+3
+7 +8
+12 +14 +16

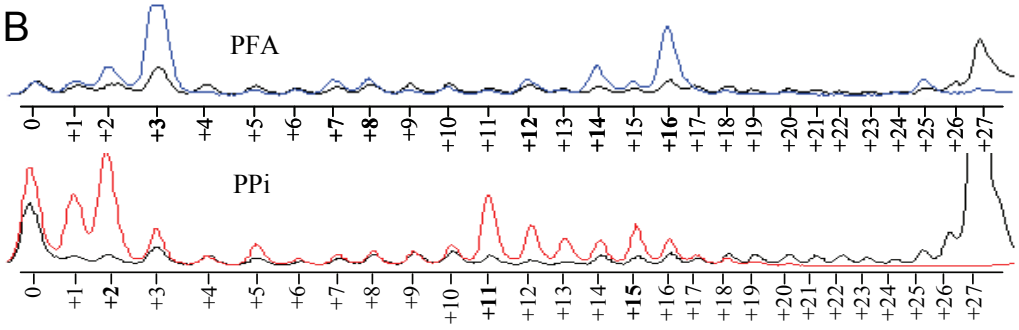
B
PFA
PPi
0 +1 +2 +3 +4 +5 +6 +7 +8 +9 +10 +11 +12 +13 +14 +15 +16 +17 +18 +19 +20 +21 +22 +23 +24 +25 +26 +27

concentrations of PPi (micromolar versus millimolar) (Fig. 4.1A). As pyrophosphorolysis must occur at the N-site in the pre-translocated state, it is conceivable that sequences associated with hot spots for PPi- or PFA binding stabilize the pre-translocated state. To address this problem directly, we employed site-specific footprinting techniques that allow us to determine the position of HIV-1 RT on its primer/template substrates at single nucleotide resolution.

Effects of the translocational state of HIV-1 RT on PFA inhibition. We devised primer/template substrates to generate the complexes that are associated with hot spots of inhibition. These substrates are referred to as PPT+3, PPT+7, PPT+12, and PPT+16. For comparative purpose, we have also included substrates for complexes at adjacent template positions (PPT+2, PPT+6, PPT+11, and PPT+15). With the exception of position +2, the inhibitory effects of PFA are much less pronounced at the latter sequences. Inhibition at position +2 is seen at concentrations > 6μM, which indicates medium levels of inhibition. Treatment of these RT-DNA complexes with the chemical nuclease potassium peroxynitrite (KOONO), which is a metal-free source of hydroxyl radicals, was shown to cleave the template site-specifically at positions –7 and/or –8 (141). Position -1 corresponds to the template nucleotide that is base paired with the 3'-terminal nucleotide of the primer (141). Cleavage at position -7 is indicative for the post-translocated state, while cleavage at position -8 is indicative for the pre-translocation state. The reaction is mediated through C280 in the large subunit p66, which is located in the vicinity of the template. Here, we conducted the footprinting experiments in the absence and in the presence of increasing concentrations of PFA to study whether variations in the sequence

can affect the ratio of complexes that exist pre- or post-translocation, and whether the inhibitor traps one or the other configuration.

The data show that complexes associated with PFA hot spots, e.g. PPT+16, exist predominantly in the pre-translocated state (cleavage at position -8) in the absence of inhibitor. Increasing concentrations of PFA do not cause a shift in the cleavage pattern (Fig. 4.2A, top, right). In contrast, complex PPT+15, which is not a PFA hot spot, exists as a mixture of pre- and post-translocated configurations, with preference toward post-translocation (cleavage at position -7) (Fig. 4.2A, top, left). Increasing concentrations of PFA cause a shift toward pre-translocation, which provides strong evidence that the inhibitor binds to and stabilizes specifically the pre-translocated state. A very similar trend is seen with the other pairs: PPT+3 and PPT+2, PPT+7 and PPT+6, and PPT+12 and PPT+11 (Fig. 4.2B). Both PPT+3 and PPT+16 strongly promote PFA mediated inhibition and these two complexes pre-exist in the pre-translocated state in the absence of inhibitor. The other complexes exist as mixtures. The ratio of pre- and post-translocated states depends on both parameters the sequence context and the concentration of PFA that is required to trap the complex in the pre-translocated configuration. Highest concentrations of PFA are required at positions +6, +11, and +15 that are literally resistant to PFA inhibition. Intermediate concentrations of PFA are required at positions +2, +7 and +12, and these complexes are associated with moderate levels of inhibition with PFA. These findings point to a correlation between the efficiency of inhibition and access to the pre-translocational state, which is further explored.

Fig.4.2 Effects of the translocational state of HIV-1 RT on PFA inhibition. *A,* Site-specific footprinting with KOONO. Primer/template substrates were derived from the results shown in Fig. 4.1. Lane 0 shows the binary RT-DNA complex in the absence of PFA, subsequent lanes show footprints at various concentrations of PFA. Cleavage at position n-7 is indicative for the post-translocated state, while cleavage at position n-8 is indicative for the pre-translocated state, whereby "n" refers to the newly added nucleotides to the PPT primer shown in Fig.4.1. The asterisk points to the radiolabel at the 3'end of the template. *B*, Percentage of the complex population that exists pre-translocation at positions analyzed in this study.

A

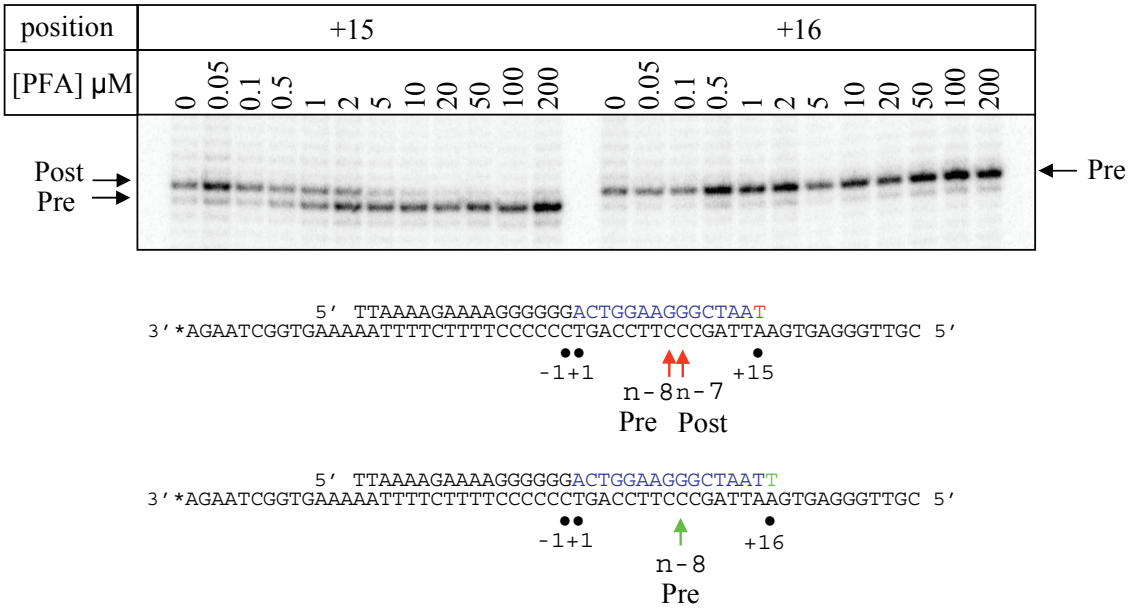
position
+15
+16
[PFA] µM
0 0.05 0.1 0.5 1 2 5 10 20 50 100 200
0 0.05 0.1 0.5 1 2 5 10 20 50 100 200
Post
Pre
Pre
5′ TTAAAAGAAAAGGGGGGACTGGAAGGGCTAAT
3′*AGAATCGGTGAAAAATTTTCTTTTCCCCCCTGACCTTCCCGATTAAGTGAGGGTTGC 5′
-1+1
n-8n-7
+15
Pre Post
5′ TTAAAAGAAAAGGGGGGACTGGAAGGGCTAATT
3′*AGAATCGGTGAAAAATTTTCTTTTCCCCCCTGACCTTCCCGATTAAGTGAGGGTTGC 5′
-1+1
n-8
+16
Pre

B

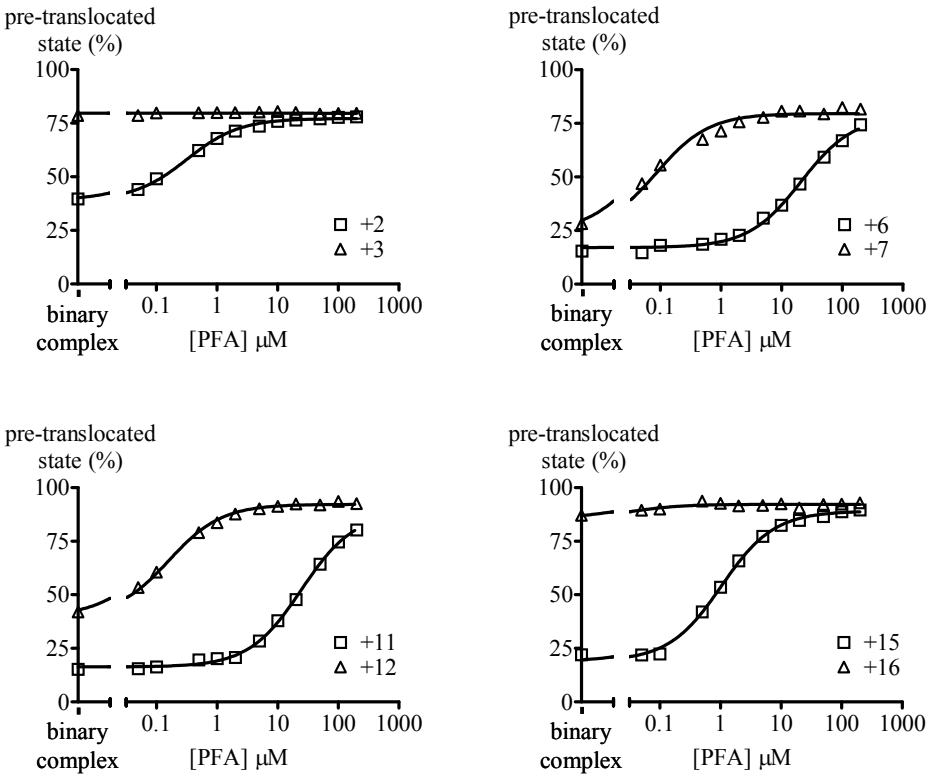
pre-translocated state (%)
100
75
50
25
0
binary complex
0.1 1 10 100 1000
[PFA] µM
+2
+3
+6
+7
+11
+12
+15
+16

Relative stability of ternary complexes with PFA or dNTP substrate. To further study the role of the translocation status of HIV-1 RT with regards to the mechanism of PFA inhibition, we analyzed whether the sequence-dependent increase in access of the pre-translocational state correlates with increased binding of the inhibitor. Band shift experiments have revealed that binary complexes of HIV-1 RT and primer/template are unstable when challenged with a trap, e.g. heparin (242). However, the presence of dNTP substrate can stabilize the complex, which prevents dissociation in the presence of trap. These findings are consistent with site-specific footprinting experiments showing that the nucleotide traps the complex in the post-translocated state (140, 141). Here we used complexes PPT+3, as an example for a pre-translocated complex, and PPT+6, as an example for a post-translocated complex, to look at the stability of ternary complexes with PFA and the next nucleotide, respectively (Fig. 4.3A). We found that PPT+3 is stabilized with increasing concentrations of PFA, while a stable ternary complex is not formed with PPT+6. The extent to which the templated nucleotide stabilizes the two complexes follows the opposite trend. The apparent K_d for dNTP at complex PPT+6 ($K_{d,app}$ = 0.7 μM) is significantly lower as compared to complex PPT+3 ($K_{d,app}$ = 17.7 μM). The data are consistent with our footprints and provide strong evidence to support the notion that PFA and the templated nucleotide bind to pre- and post-translocated states, respectively. Sequence variations that determine whether a given complex exists predominantly in one or the other configuration, play a critical role in this regard.

To study whether PFA binds at or close to the PPi binding site in the pre-translocated state, we performed band shift experiments in the absence and presence of Mg^{2+} ions (Fig. 4.3B). Significantly lower concentrations of PFA are required to stabilize the

Fig.4.3 Binding of PFA and dNTP in dependence of the translocational state of HIV-1 RT. *A,* Gel mobility shift assays with sequences that facilitate formation of the pre-translocated complex (PPT+3) and the post-translocated state (PPT+6), respectively. Pre-formed complexes were incubated with increasing concentrations of PFA or the templated nucleotide, before the addition of trap. The primers were chain-terminated to prevent nucleotide incorporation. *B*, Gel shifts with a range of PFA in the absence or presence of 6 mM $MgCl_2$.

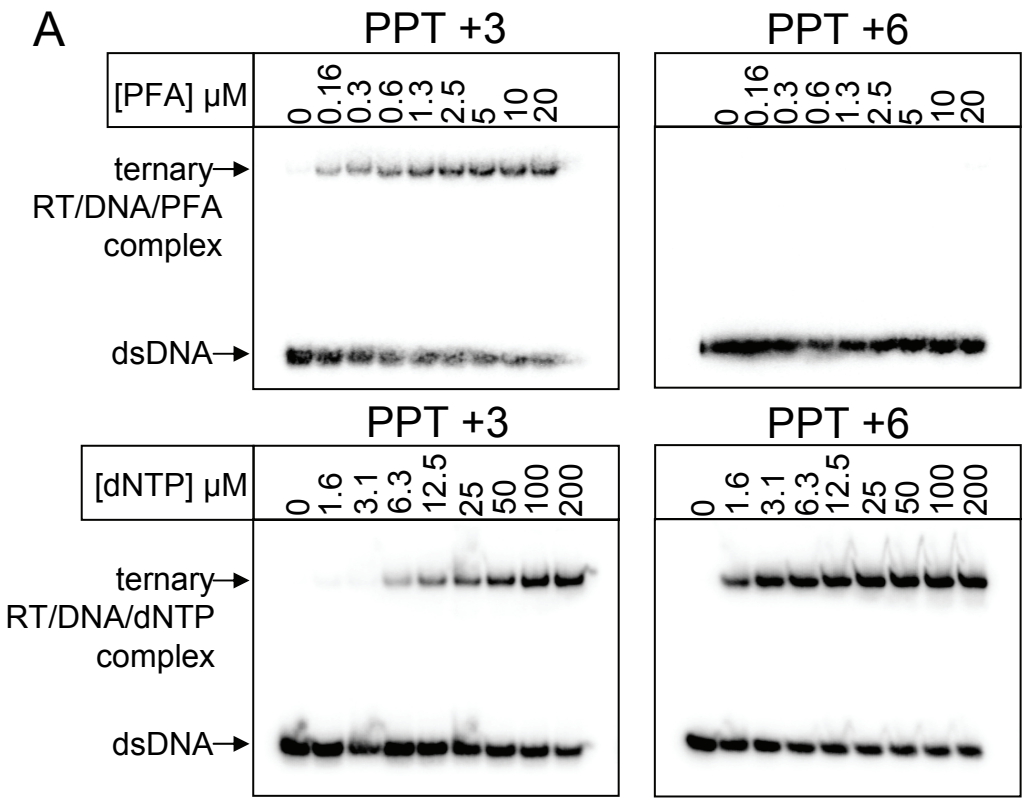
A
PPT +3
PPT +6
[PFA] µM
0 0.16 0.3 0.6 1.3 2.5 5 10 20
ternary RT/DNA/PFA complex
dsDNA
PPT +3
PPT +6
[dNTP] µM
0 1.6 3.1 6.3 12.5 25 50 100 200
ternary RT/DNA/dNTP complex
dsDNA

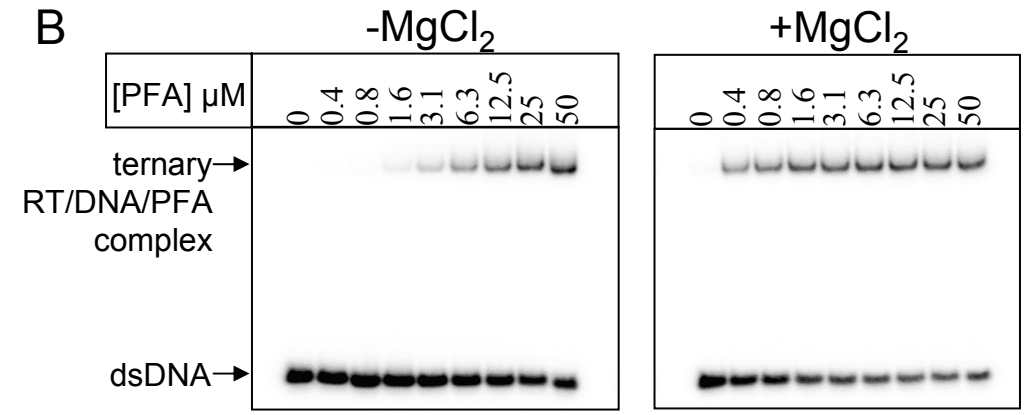
B
-MgCl2
+MgCl2
[PFA] µM
0 0.4 0.8 1.6 3.1 6.3 12.5 25 50
ternary RT/DNA/PFA complex
dsDNA

complex in the presence of 6 mM Mg^{2+}, which is reflected in the estimation of apparent K_d values. The K_d for complex PPT+3 with Mg^{2+} was lower ($K_{d,app}$ = 0.4 μM) when compared to measurements without Mg^{2+} ($K_{d,app}$ = 13.9 μM). This data suggest that PFA binding to the pre-translocated state occurs in close proximity to the metal binding sites at the active site of HIV-1 RT. PPi may bind to a similar location; however, there must be subtle differences in the mode of binding of PPi and PFA if one considers the differences in the inhibitory concentrations and the inability of PFA to act as PPi donor. Together these findings suggest that binding of PFA and the subsequent stabilization of the pre-translocated state could limit access to the post-translocated state. The dNTP substrate cannot bind to the pre-translocated state, because the 3'end of the primer and the bound PFA occlude the nucleotide binding site. This model predicts that the inhibition of DNA synthesis with PFA is competitive in nature.

Kinetic consequences. To study the influence of the translocation status on steady-state kinetic parameters for a single nucleotide incorporation event and its inhibition with PFA, we devised a complex that is highly sensitive to PFA inhibition (PPT+16), and a complex that is less sensitive to PFA inhibition (PPT+6). We have also analyzed complex PPT+4, as another independent example for a template position that is not associated with PFA inhibition (see Fig. 4.1). The three sequences allow us to limit DNA synthesis to single nucleotide incorporation events in standing-start experiments (Fig. 4.4A). The kinetic parameters are shown in Table 4.1 and changes with regards to K_m and k_{cat} values are shown in Fig. 4.4B-D. The efficiency of nucleotide incorporation (k_{cat} / K_m) follows the order PPT+6 > PPT+16. These findings are consistent with the notion that sequences that promote the post-translocated state facilitate nucleotide incorporation (PPT+6), while

Fig.4.4 Effects of the sequence on kinetic parameters. *A*. Sequences used to determine kinetic parameters for single nucleotide incorporations. *B, C, D*. Steady-state kinetic parameters for complexes PPT+4, PPT+6, and PPT+16 (see also Table 4.1).

A

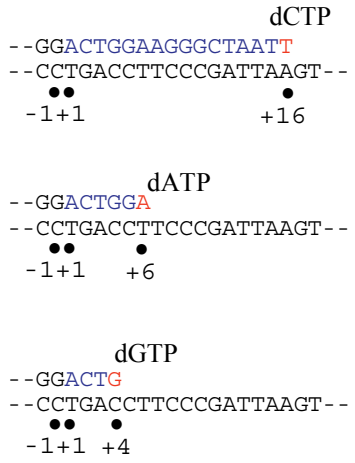
dCTP
--GGACTGGAAGGGCTAATT
--CCTGACCTTCCCGATTAAGT--
-1+1
+16
dATP
--GGACTGGA
--CCTGACCTTCCCGATTAAGT--
-1+1
+6
dGTP
--GGACTG
--CCTGACCTTCCCGATTAAGT--
-1+1
+4

B

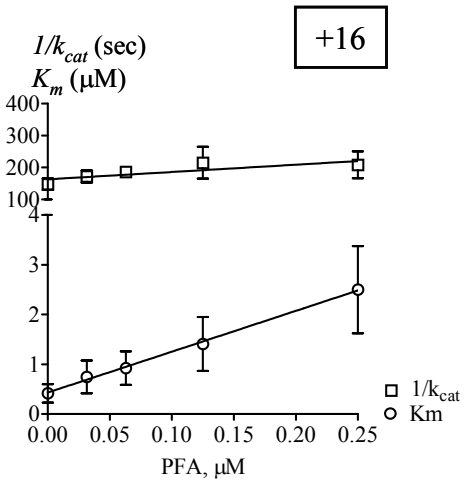
+16
1/k_cat (sec)
K_m (μM)
400
300
200
100
4
3
2
1
0
0.00
0.05
0.10
0.15
0.20
0.25
PFA, μM
1/k_cat
Km

C

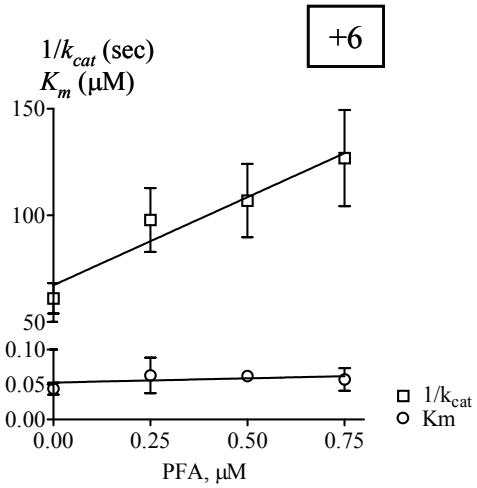
+6
1/k_cat (sec)
K_m (μM)
150
100
50
0.10
0.05
0.00
0.00
0.25
0.50
0.75
PFA, μM
1/k_cat
Km

D

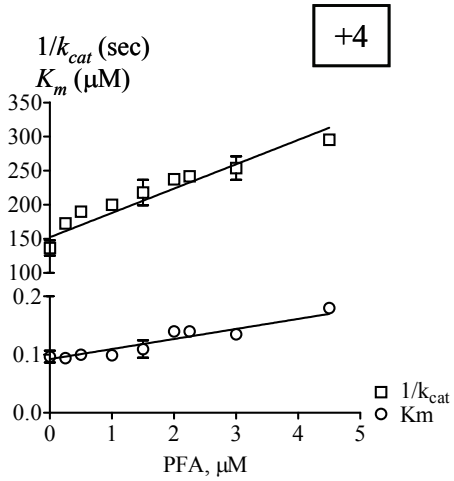
+4
1/k_cat (sec)
K_m (μM)
350
300
250
200
150
100
0.2
0.1
0.0
0
1
2
3
4
5
PFA, μM
1/k_cat
Km

TABLE 4.1

Kinetic constants of single nucleotide incorporation and its inhibition by foscarnet[a]

Enzyme	Position	Substrate nucleotide	k_{cat} (sec^{-1})	K_m (μM)	k_{cat}/K_m (sec^{-1}/μM)	K_i (μM)	K_i/K_m
WT	+4	dGTP	0.0074 ± 0.0004	0.10 ± 0.01	0.074	4.3 ± 0.66	43
	+ 6	dATP	0.022 ± 0.001	0.06 ± 0.01	0.37	0.8 ± 0.04	13
	+ 16	dCTP	0.0068 ± 0.0002	0.38 ± 0.04	0.018	0.053 ± 0.01	0.14
E89K	+ 16	dCTP	0.00031 ± 0.00002	0.053 ± 0.012	0.006	0.42 ± 0.04	7.9

[a] Single nucleotide incorporation reactions were performed at positions +4, +6 and +16 using heat annealed primer/templates PPT+4/PPT54, PPT+6/PPT57 and PPT+16/PPT57, respectively, and analyzed as described in Materials and Methods. Values are means of three determinations ± standard deviations.

sequences that exist predominantly pre-translocation (PPT+16) diminish the efficiency of nucleotide incorporation. The different nature of the incoming nucleotide, i.e. dATP and dCTP, respectively, is an additional factor that can affect the measurements of kinetic parameters. However, the inhibitor is identical in both reactions, and the efficiency of PFA inhibition follows the opposite order: PPT+16 > PPT+6. These findings are consistent with the notion that sequences that promote the pre-translocated state facilitate PFA binding (PPT+16), while sequences that exist predominantly post-translocation (PPT+6) diminish PFA binding.

Inhibition with the PPT+6 complex is associated with decreases in k_{cat} values, while K_m values stay constant (Fig. 4.4C). This pattern points to a non-competitive mode of inhibition, which is also evident when the assay involves multiple incorporation events on either homo- or heteropolymeric substrates (171). In contrast, inhibition of the PPT+16 complex is characterized by increases in K_m values, while k_{cat} values stay constant. This pattern points to a competitive mode of inhibition. Thus, in this sequence context, simultaneous binding of PFA and the nucleotide substrate is mutually exclusive. The footprints and the band shifts experiments are in good agreement with steady-state kinetics, and these data together demonstrate that PFA is a competitive inhibitor that acts most efficiently at sequences that promote the pre-translocated state. The non-competitive mode of inhibition seen with PPT+6 is a result of product inhibition under steady-state conditions. The stabilization of the product complex diminishes enzyme dissociation and its rebinding to the original substrate, which reduces the turnover. PPT+4 is literally resistant to PFA, which suggests that binding of the inhibitor to both the original and the product complex is severely compromised.

Resistance to PFA inhibition. To study mechanisms associated with "natural", mutation independent, resistance to PFA, we performed site-specific footprinting experiments with complexes at position +4 and +5. The footprints suggest that PPT+4 exist predominantly post-translocation, which allows nucleotide binding and prevents binding of PFA (Fig. 4.5A). In contrast, cleavage associated with PPT+5 occurs at multiple sites, which indicates that neither the dNTP substrate nor PFA can efficiently bind in this sequence context. The presence of PFA eventually traps the pre-translocated state at relatively high concentrations. Thus, binding of PFA to both complexes PPT+4 and PPT+5 is severely compromised, which helps to explain the resistance phenotype at these sequences. In this context it is also important to note that template position +5 is associated with intrinsic pausing of RT at limiting dNTP concentrations, which is in keeping with the observation that the stability of the post-translocated complex is likewise diminished.

The selective pressure of PFA can cause the emergence of resistance conferring mutations in the RT gene *in vitro* and *in vivo* (148, 232). With few exceptions, many of these mutations are too far away from the active site to affect the interaction with the dNTP or nucleic acid substrate directly (158). The W88G change is perhaps the most prevalent mutation that is found in clinical isolates (148). Crystallographic data suggest that a change at the adjacent position, i.e. E89K that is likewise selected under pressure of PFA, could affect the interaction with template at position -2 (88). To test the possible consequences with respect to primer/template binding, we conducted band shift experiments and found that the mutant does not diminish the affinity to the primer/template substrate. This result is not surprising in view of the additional positive

Fig.4.5 Effects of the translocational state of HIV-1 RT on PFA resistance. *A*, Site-specific footprinting of complexes at positions +4 and +5 that show natural resistance to PFA inhibition. The footprints were conducted in the presence of increasing concentrations of PFA as described in Fig.4.2. *B*, Footprinting of complexes with WT RT and the resistant E89K mutant at positions +3 and +6 that favour pre- and post-translocational states, respectively.

A

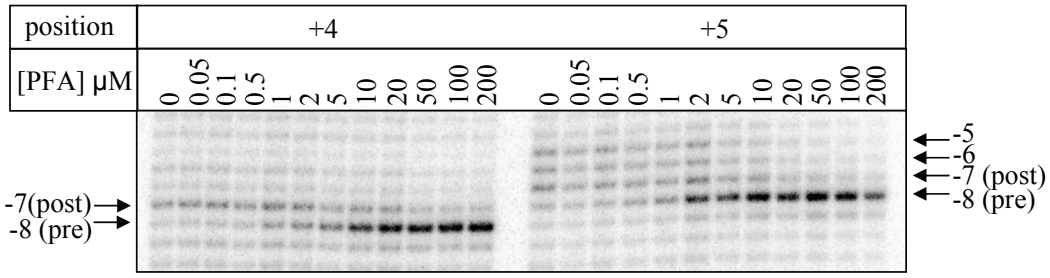
position
+4
+5
[PFA] µM
0 0.05 0.1 0.5 1 2 5 10 20 50 100 200
0 0.05 0.1 0.5 1 2 5 10 20 50 100 200
-7(post)
-8 (pre)
-5
-6
-7 (post)
-8 (pre)

B

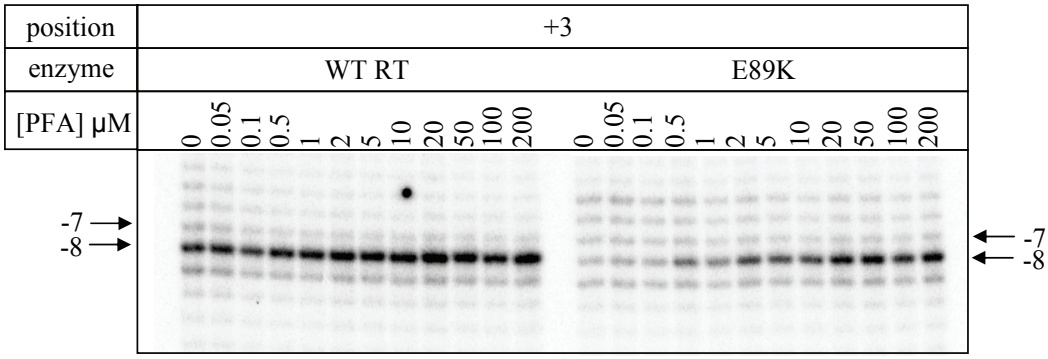
position
+3
enzyme
WT RT
E89K
[PFA] µM
0 0.05 0.1 0.5 1 2 5 10 20 50 100 200
0 0.05 0.1 0.5 1 2 5 10 20 50 100 200
-7
-8
-7
-8

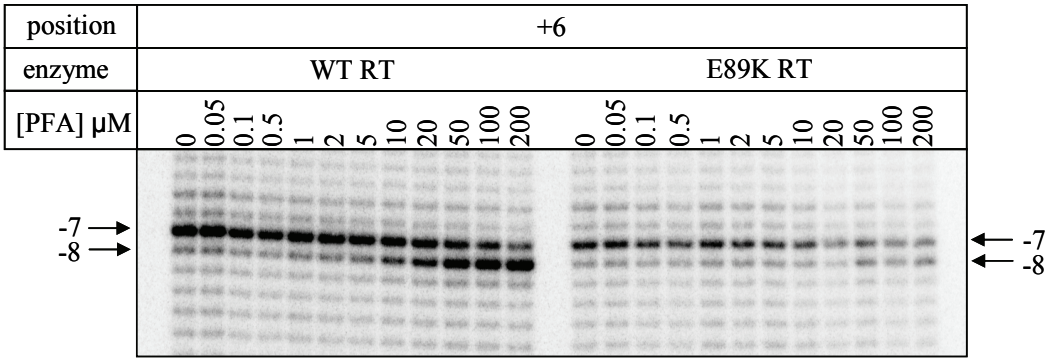
position
+6
enzyme
WT RT
E89K RT
[PFA] µM
0 0.05 0.1 0.5 1 2 5 10 20 50 100 200
0 0.05 0.1 0.5 1 2 5 10 20 50 100 200
-7
-8
-7
-8

charge provided by the lysine. We then conducted footprinting experiments with complexes PPT+3 and PPT+6 to study possible effects of the mutant on the translocation status (Fig. 4.5B). The pattern with PPT+3 that exist predominantly pre-translocation is reminiscent of the data obtained with PPT+5 (Fig. 4.5A). In the absence of PFA, the wild type enzyme produces a single cut at template position -8, while the position of the mutant enzyme is not clearly defined (Fig. 4.5B). There are four bands between -9 and -6 under the same conditions. Increasing concentrations of PFA eventually traps the complex specifically in the pre-translocated state. However, the concentration of PFA that is required to form the pre-translocated complex is higher with the mutant enzyme when compared to wild type RT. Overall, the footprinting results with the mutant enzyme suggest that the E89K change diminishes the access to the pre-translocated state, which provides a plausible mechanism for PFA resistance (Table 4.1). The efficiency of nucleotide incorporation is likewise diminished when compared with WT RT, which is in keeping with our observation that the mutant enzyme can be localized at multiple positions around the active site.

4.6 Discussion

The data presented in this study show that the PPi-analogue PFA traps the pre-translocational state of HIV-1 RT. These findings have important implications for both the mechanism of action of this inhibitor and the mechanism of HIV-1 RT translocation. The proposed mechanisms for drug action and resistance have been developed on the basis of a “Brownian ratchet” model for polymerase translocation.

Mechanism of HIV-1 RT translocation. Previous studies with T7 RNA polymerase described the mechanism of translocation during elongation either as an active process that requires nucleotide hydrolysis, or as a passive process that occurs independently of nucleotide hydrolysis. The former, referred to as "power-stroke" model (262), was developed on the basis of crystallographic snap shots of complexes with and without bound NTP and PPi, respectively. The power stroke model demands that the chemical energy from nucleotide hydrolysis is transformed into conformational changes that drive polymerase translocation following or concomitant with the release of PPi. A similar model that involves nucleotide hydrolysis as crucial requirement for polymerase translocation has been proposed for HIV-1 RT on the basis of crystal structures of the polymerase trapped in pre- and post-translocated states (176, 211). The power stroke model implies that the enzyme ultimately translocates to the next position, which restricts the access to the pre-translocated state during active DNA synthesis. Our findings with HIV-1 RT, showing that PFA traps the pre-translocated under these conditions, are inconsistent with this model.

A second model of polymerase translocation, referred to as "Brownian ratchet" or "translocational equilibrium" model (68) demands that the polymerase can rapidly move between pre- and post-translocated states and thermal energy is sufficient to drive forward and reverse motion. The incoming nucleotide substrate acts like a pawl of a ratchet that traps the complex in its post-translocational state, which prevents the reverse motion. A related, more complex version of this model has also been proposed for multisubunit RNA polymerases (10, 245). Our previous site-specific footprinting experiments with stalled HIV-1 RT complexes revealed that the presence of the templated nucleotide can

stabilize and trap the post-translocated complex (141). The next complementary nucleotide facilitates the formation of a stable ternary complex that blocks pyrophosphorolysis and the ATP-dependent excision of chain-terminating nucleotides (154, 242). Together, these observations are consistent with a Brownian ratchet model for polymerase translocation (59). However, it has never been shown before that the pre-translocated complex can be trapped in the absence of nucleotide substrates. This is essential to demonstrate that the enzyme can shuttle between both configurations. Here we provide direct evidence to show that PFA traps the pre-translocated complex. Thus, the bound PFA can be described as a pawl of a ratchet that prevents the forward motion.

Effects of the sequence on the translocational equilibrium. We identified complexes that exist predominantly pre- or post-translocation, or as mixtures of the two configurations. The presence of only one or two cuts in our footprinting experiments suggests that pre- and post-translocated configurations are likely to be the most stable complexes; however, the sequence dependence points to differences in the relative stability between the two species. This is crucial for the mechanism of PFA drug action. Hot spots for inhibition are seen at primer/template sequences that promote the formation of the pre-translocated state. In the absence of PFA or dNTP substrate, these complexes exist predominantly in the pre-translocated state. Complexes that exist predominantly post-translocation are less sensitive or resistant to PFA inhibition. These results suggest that the translocational equilibrium is rapidly established following the formation of each novel phosphodiester bond and the release of PPi. A similar conclusion was drawn from studies with T7 RNA polymerase showing that stalled and actively elongating complexes are equally sensitive to PPi (70). Enzymatic and chemical footprinting studies with this enzyme have likewise

pointed to single nucleotide shifts of the cleavage patterns when the experiments were conducted in the presence of PPi and NTP, respectively (67, 70, 89). Moreover, single molecule studies with *Escherichia coli* RNA polymerase revealed single base-pair stepping during transcriptional elongation (1). The Brownian ratchet model for polymerase translocation is consistent with all of the aforementioned observations made with *Escherichia coli* RNA polymerase, T7 RNA polymerase, and here with the DNA polymerase HIV-1 RT.

The structural determinants that affect the translocational equilibrium remain to be characterized. The RT enzyme forms numerous contacts with the bound nucleic acid substrate, and each of these interactions could affect polymerase translocation (38). Of note, changes at residues that confer resistance to PFA affect the positioning of the enzyme (see below). However, it will be challenging to define consensus sequences that promote either the pre- or the post-translocational state. The pre-translocated state is often associated with a thymidine at the 3'end of the primer; however, other bases have also been identified in this context, which supports the notion that interactions distant from the active site can also affect polymerase translocation.

Binding of PFA. Binding of PFA to the pre-translocational state suggests that the binding sites for PPi and its analogue may at least partly overlap, which is here supported by showing that the presence of divalent Mg^{2+} ions increase the stability of the ternary complex (Fig. 4.6A). Crystallographic data have shown that dNTP binding is associated with a closure of the fingers subdomain of HIV-1 RT (88). It is probably this conformational change that stabilizes the ternary complex as compared to its binary form

Fig.4.6 Model for PFA binding, mechanism of action and drug resistance. *A*, Binding of PFA to HIV-1 RT. Pre- and post-translocational states are in equilibrium. PFA is shown schematically as grey circles in the pre-translocated complex. The nucleotide occupies the N-site in the post-translocated complex. PFA and the phosphates of the bound nucleotide are shown in close proximity to the divalent metal ions (red). *B*, Mechanism of action. Competitive inhibition is shown on the top, and product inhibition is shown below. The incorporation of a single nucleotide involves the establishment of a translocational equilibrium yellow before and after catalysis (boxed in yellow). Different sizes of arrows point to bias toward pre- or post-translocational states. "Pre" and "Post" represent pre- and post-translocated complexes. "E" represents HIV-1 RT in the open conformation and "E'" points to a closed conformation. "I" stands for PFA. PFA affect solely the translocational equilibrium before and after nucleotide incorporation. PFA does neither affect nucleotide binding, provided that post-translocated complex is available, nor the closure of the fingers subdomain. Complex dissociation can occur from both pre- and post-translocated complexes (91), without bound nucleotide or PFA. *C,* Mechanism of resistance. PFA resistance is seen with complexes that show a bias toward post-translocation, and with complexes that do not allow a clear assignment to pre- and post-translocated states. The latter conditions are here referred to as "sliding".

A PFA Binding

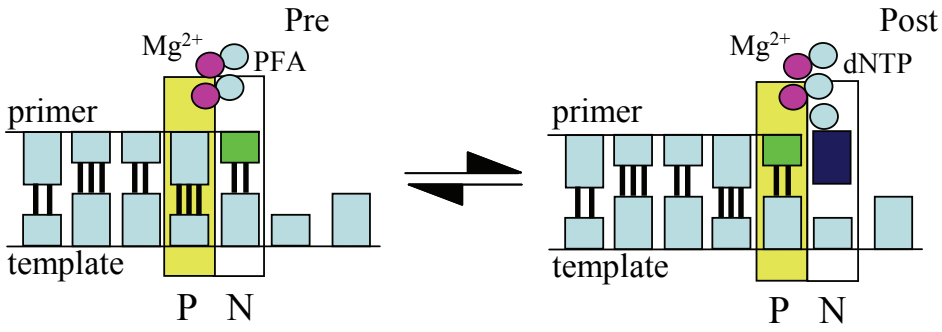

B PFA Inhibition

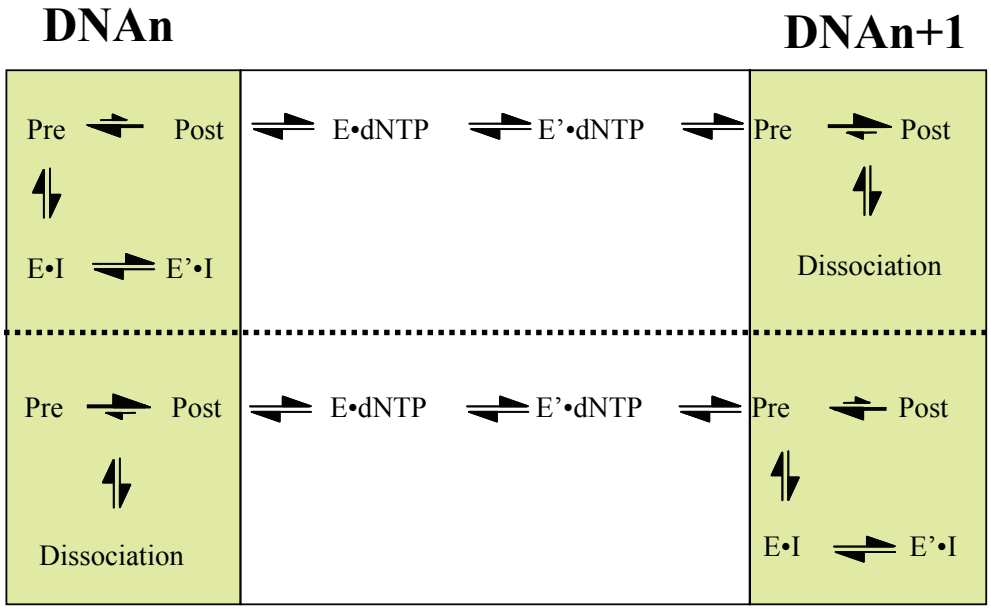

C

Resistance to PFA

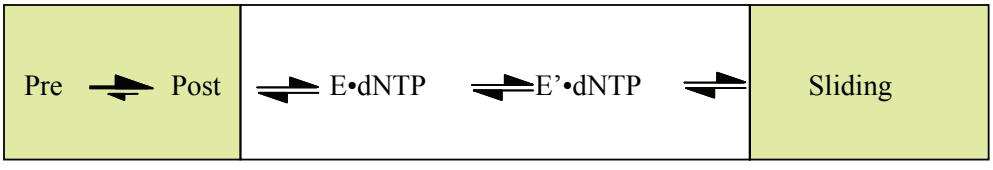

(242). Binding of PFA to the pre-translocated complex may cause a similar structural change. The differences between PPi and PFA and their interactions with HIV-1 RT could be manifested at this state. The concentrations required to inhibit DNA synthesis with PPi are two to three orders of magnitude higher as compared to PFA. This is also reflected in the estimation of apparent K_d values. We measured $K_{d,app}$'s for PFA in the low μM range, while K_d's for PPi are in the range between 5 and 10 mM (85). Thus, PFA may facilitate the closure of the fingers, in contrast to its natural counterpart PPi that needs to be released from the complex. The primer/template combinations that have been identified in this study and exist predominantly pre-translocation may help to crystallize HIV-1 RT in the ternary complex with PPi and/or PFA to address these questions. For T7 RNA polymerase, crystallographic data show that PPi binds to the pre-translocated state to the same location as the β- and γ-phosphate of an incoming nucleotide in the post-translocated configuration (262).

Mechanism of action. We consider two scenarios with regards to the mechanism of drug action of PFA. First, the complex prior to nucleotide binding and incorporation exists predominantly in its pre-translocated state. PFA binds and traps the complex in this configuration (Fig. 4.6B, top scheme), which in turn prevents binding of the nucleotide. These conditions translate in a competitive mode of inhibition. Moreover, binding of the next nucleotide is also diminished in the context of complexes that pre-exist pre-translocation, and limited dNTP pools cause intrinsic pausing of HIV-1 RT at these positions (data not shown). Thus, simultaneous binding of PFA and the dNTP substrate to the same complex in its pre-translocated state is mutually exclusive. This differs from

models of translocation of multisubunit RNA polymerases in which nucleotide binding can occur pre- and post-translocation at distinct sites (1, 169).

We consider a second scenario to explain the apparent non-competitive mode of inhibition described in previous studies (28, 171). Following the release of PFA, the nucleotide is eventually incorporated and a translocational equilibrium is established at the next position (Fig. 4.6B, bottom scheme). A bias toward pre-translocation at this stage facilitates binding of PFA, which stabilizes the complex. Thus, the non-competitive mode of inhibition is a result of a reduced turnover, which explains why measurements under steady-state conditions that include multiple nucleotide incorporation events point to a non-competitive mechanism.

Mechanism of resistance. Resistance to PFA inhibition is seen in the context of sequences that neither promote binding of PFA to the original complex, nor to the product complex after incorporation of a nucleotide (Fig. 4.6C). The two complexes may exist predominantly post-translocation, or the stability of both configurations is diminished and neither configuration can be unambiguously identified. At the same time, these data demonstrate that the enzyme is not always positioned in the pre- or post-translocated states, although the sum of our footprinting experiments suggests that the two configurations provide the highest degree of stability. However, the PFA resistant E89K mutant diminishes the stability of the pre-translocated complex, which provides a novel mechanism for resistance to PFA. The same mechanism helps to explain the diminished rates of the ATP-dependent excision reaction in the context of the E89K mutant. The "fuzzy" definition of pre- and post-translocated states affects also the incorporation of the

next nucleotide. The diminished rates of DNA synthesis appear to translate into diminished viral replication fitness, which is the price for the development of resistance (234).

Conclusions. The data presented in this study provide strong support for a Brownian ratchet model of HIV-1 RT translocation. The rapid establishment of a translocational equilibrium following each nucleotide incorporation event helps to explain how the pre-translocated state can be accessed and trapped during active DNA synthesis. These findings warrant further investigation with regards to the sequence dependence of this equilibrium and how changes in the ratio of pre- and post-translocational states affect nucleotide binding and incorporation, fidelity, mismatch extensions, and interactions with other RT inhibitors. Most importantly, the results of this study validate the pre-translocated complex as a target for the development of novel, more potent and less toxic compounds that block the translocation process. The primer/template substrates identified in this study may facilitate the screening for inhibitors that block polymerase translocation.

CHAPTER 5

IMPACT OF THE TRANSLOCATIONAL EQUILIBRIUM OF HIV-1 REVERSE TRANSCRIPTASE ON THE EFFICIENCY OF MISMATCH EXTENSIONS AND THE EXCISION OF MISPAIRED NUCLEOTIDES

This chapter was adapted from an article authored by B. Marchand and M. Götte that appeared in the ***International Journal of Biochemistry & Cell Biology***, 2004, 36: 1823-35.

5.1 Preface to chapter 5

The reverse transcriptase lacks a 3'→5' exonuclease activity, which results in a relatively high error rate during transcription. We studied the effects of mismatch formation on the translocational status of the enzyme. We found that the presence of a C:T or a T:T mismatch promotes the formation of a post-translocated complex, compared to a mixture of pre- and post-translocated enzymes in the presence of a G:T mismatch of the correct A:T match.

We also analysed wheter the pyrophosphorolysis reaction could serve as a proofreading mechanism. We found that the reverse transcriptase could efficiently cleave the correct A:T match and a G:T mismatch, but could not cleave a C:T or a T:T mismatch. This correlates well with the translocational status of the reverse transcriptase in these 4 situations, where the enzyme has to be in the pre-translocated state in order to cleave the nucleotide at the 3' end of the primer.

Even though the reverse transcriptase is able to remove a G:T mismatch, we concluded that this reaction could not constitute a proffreading mechanism due to incapacity of the enzyme to remove a C:T or a T:T mismatch.

5.2 Abstract

The reverse transcriptase of the human immunodeficiency virus type 1 (HIV-1 RT) does not possess an exonucleolytic proofreading activity; however, previous studies have shown that this enzyme can excise incorporated chain-terminators in the presence of pyrophosphate or ATP. This type of reaction provides a plausible mechanism for HIV-1 resistance to several nucleoside analogue inhibitors. Here we studied the efficiency of pyrophosphorolysis in the context of mismatched nucleotides, and found that the removal of dCMP and dTMP opposite T is literally blocked. Thus, pyrophosphorolysis may not provide an alternative, universal proofreading mechanism, although excision of dGMP and the correct dAMP opposite T can occur with considerable efficiency. Site-specific footprinting experiments revealed that the 3' end of C:T- and T:T-mispaired primer strands is predominantly found in a post-translocational configuration, which prevents the removal of terminal nucleotides. In contrast, complexes containing G:T and A:T base pairs can exist in both post- and pre-translocational stages. Excision can only occur in the latter, which helps to explain the observed selectivity of the reaction. The efficiency of mismatch extensions does not appear to depend on pre-existing changes of the translocational equilibrium. However, footprints of complexes containing 3' penultimate mismatches suggest that the incorporation of the first nucleotide following the mispair can force the enzyme to slide backwards, which can inhibit ensuing polymerization events. The fact that misincorporated nucleotides can affect the precise positioning of RT provides a rational for the development of novel nucleoside analogue inhibitors that contain modifications in the base moiety.

5.3 Introduction

The reverse transcriptase (RT) of the human immunodeficiency virus type 1 (HIV-1) is an error prone enzyme, which creates approximately one or two mutations per round of replication. Retroviral reverse transcriptase enzymes convert the single-stranded RNA genome into double-stranded DNA that is later integrated into the host chromosome. The low fidelity of HIV-1 RT is an important factor that contributes to the enormous genetic variability of the virus. RT enzymes possess DNA polymerase activities on both DNA and RNA templates, and a ribonuclease H (RNase H) activity that degrades RNA/DNA replication intermediates; however, they lack a 3' → 5' exonuclease activity that could excise misincorporated nucleotides. Thus, the incorporation of mispaired nucleotides and the ensuing extension of mismatches can establish mutations in the proviral DNA (for recent reviews see (119, 151)). The continuous generation of mutant variants is closely related to the problem of HIV drug resistance (for a recent review see (138)). Despite the availability of potent anti-retroviral drugs, the emergence of resistant mutant viruses cannot be prevented, which remains a major cause for treatment failure.

Nucleoside analogue RT inhibitors (NRTIs) are important components in currently used drug regimens to treat infection with HIV-1. 3'-Azido-3'- deoxythymidine (zidovudine or AZT), and (-)-β-L- 2', 3'-dideoxy-3'-thyacytidine (lamivudine or 3TC) are prominent members of this class of compounds. The triphosphate form of these drugs compete with natural dNTP pools for incorporation. Once incorporated into the growing DNA chain, they act as chain-terminators due to the lack of a 3' hydroxyl group in the sugar moiety that is required for continuation of DNA synthesis. However, previous biochemical

studies have shown that this step is not irreversible (2, 156). The incorporated chain-terminator can be removed from the primer terminus through phosphorolytic cleavage in the presence of either pyrophosphate (PPi) or ATP, which can act as a pyrophosphate donor. Excision of AZT-MP in the presence of PPi occurs with considerable efficiency, although the rates of pyrophosphorolysis are approximately two orders of magnitude lower as compared to rates of nucleotide incorporation (2, 203). The rates of ATP-dependent excision are further diminished; however, the efficiency is significantly increased with AZT-resistant mutant enzymes, suggesting that this reaction provides a possible mechanism for HIV resistance to AZT (154).

The efficiency of both PPi- and ATP-dependent cleavage also depends critically on the chemical nature of the inhibitor. Unlike AZT-MP, ddTMP is poorly excised (141). Modelling studies (17), crystallographic data (211), and biochemical studies have shown that the excision reaction can only occur when the 3' end of the primer terminus remains in the nucleotide binding site or N-site (141, 212). Binding of the next nucleotide requires that the extended 3' end of the primer translocates by a single position into the priming site or P site, which is equivalent to a post-translocational configuration. Using site-specific footprinting techniques, we have demonstrated that access to the N-site is controlled by a translocational equilibrium between the pre- and post-translocational stages (141). The relative occupation of N- and P-sites depends on several parameters that include the temperature, the concentration of the next complementary nucleotide, the chemical nature of the chain-terminator, the sequence of the template, and the mutational background of the enzyme. We have shown that AZT-terminated primer strands reside preferentially in the N-site, while ddTMP-terminated primers reside preferentially in the

P-site. Relatively high concentrations of the next complementary nucleotide are required to force translocation of RT, and this concentration is significantly increased with an AZT-resistant enzyme. Together these data demonstrate that changes of the translocational equilibrium can control access to the pre-translocational stage and, in turn, efficiency of excision.

Here, we studied the role of the translocational equilibrium on both the efficiency of mismatch extensions and the pyrophosphorolytic excision of mispaired nucleotides. Mismatched primers are sometimes extended with considerable efficiency, but appear to resist PPi-mediated cleavage (264). This suggests that pyrophosphorolysis may not provide an alternative proofreading mechanism. The apparent poor efficiency of the back reaction is difficult to explain in the absence of available crystal structures that contain a mispaired primer. In this study, we utilized our site-specific footprinting approach to address this problem, and found that the translocational equilibrium represents an important checkpoint that can influence both extension and excision of mismatched primers.

5.4 Experimental procedures

Enzymes and nucleic acids. Heterodimeric wild-type HIV-1 RT (p66/p51) was expressed in *Escherichia coli* and purified essentially as previously described (127). The DNA primer/template substrates used in this study were derived from sequences used in our previous studies (62, 64): 5'-TTAAAAGAAAAGGGGGGA, 5'-TTAAAAGAAAAGGGGGGC, 5'-TTAAAAGAAAAGGGGGGG, and 5'-

TTAAAAGAAAAGGGGGGT served as primer strands, and 5'-CGTTGGGAGTGAATTAGCCCTTCCAGTCCCCCCTTTTCTTTTAAAAAGTGGCT AAGA served as template strand. Chemically synthesized oligonucleotides were purified on 12% polyacrylamide-7M urea gels containing 50mM Tris-borate (pH 8.0) and 1mM EDTA. The purified nucleic acids were eluted from gel slices in a buffer containing 500mM NH_4Ac and 0.05% SDS. 5' end-labeling of DNA primers was conducted with [γ-^{32}P]ATP and T4 polynucleotide kinase, followed by gel-purification as describe above.

Pyrophosphorolysis and primer extension. The primer/template duplex was pre-formed in a buffer containing 50mM Tris–HCl (pH 7.8) and 50mM NaCl. For this purpose, the 5' end-labeled DNA primer (0.85 pmol) was hybridized to the complementary DNA template (2.55 pmol) by denaturing at 95 ^{0}C for 3 min, followed by annealing at 72 ^{0}C for 15 min and slow cooling to room temperature. The duplex was incubated with 2.55 pmol HIV-1 RT in a buffer containing 50mM Tris–HCl, pH 7.8, 50mM NaCl, 6mM $MgCl_2$. The excision of nucleotides was initiated with the addition of PPi (150 μM). Primer extension and nucleotide excision were monitored in time course experiments. Reactions were performed at 37 ^{0}C and stopped at different times by adding 1μl aliquots of reaction mixture to 9μl of 95% formamide containing 40mM EDTA. Samples were heat-denatured for 5 min at 95 ^{0}C and finally resolved on 8% polyacrylamide-7M urea gels. Steady-state kinetic parameters were determined essentially as we have recently described (62). These measurements were performed in excess of primer/template (8.5 pmol) over RT (1.2 pmol).

Site-specific footprinting. Site-specific footprints with Fe^{2+} were monitored on 5' end-labeled DNA templates. Hybridization of the template (2.7 pmol) with the complementary primer (8.1 pmol) was conducted in a buffer containing 20mM sodium cacodylate (pH 7) and 20mM NaCl. The duplex was incubated with HIV-1 RT (16.2 pmol) in a buffer containing 120mM sodium cacodylate (pH 7), 20mM NaCl, 6mM $MgCl_2$, and a cocktail of nucleotide triphosphates as described in the legends to the figures. The Fe^{2+}-treatment was conducted as recently described (63). Briefly, pre-formed complexes in a volume of 20µl were incubated with a mixture of 2µl $Fe(NH_4)_2{\cdot}SO_4{\cdot}6H_2O$ (50 mM) and 2µl DTT (50 mM). Reactions were allowed to proceed for 5 min and stopped with 100µl of a solution containing 0.3M NH_4Ac, 1µg bulk tRNA and 90% isopropanol. Samples were precipitated and loaded on a 8% polyacrylamide-urea gel.

5.5 Results

Experimental strategy. We have recently developed novel footprinting techniques that allowed us to determine the precise positioning of HIV-1 RT on its primer/template substrate (63, 64, 141). We have demonstrated that treatment of complexes with potassium peroxynitrite (KOONO) or Fe^{2+} can cause site-specific cleavage on the template strand. KOONO is a metal-free source of hydroxyl radicals that cleaves the template at positions -7 or -8. Although the chemistry of the reaction remains to be studied, it is clear that such hyperreactive cleavage is mediated through cysteine 280, which is located in close proximity to the template strand. Treatment with Fe^{2+} can cause site-specific cleavage at positions -17 or -18 (Fig. 5.1). We presented strong evidence to show that Fe^{2+} can bind at or close to the metal binding site(s) of the RT-associated

Fig.5.1 Fe-mediated site-specific footprinting. Structure of HIV-1 RT (A). The two subunits of HIV-1 reverse transcriptase p66 and p51 are shown in cyan and purple, respectively. The bound DNA/DNA primer/template (red/violet) substrate, and a trapped nucleotide (dTTP) are highlighted. Subdomains fingers and thumb that play important roles in nucleotide and nucleic acid binding, as well as the RT-associated RNase H are labeled. The divalent metal binding site of the RNase H active center is represented by the green spheres. Residue E478 (highlighted) is implicated in metal binding. Biochemical data suggest that 17–19 base pairs fit between both active sites, depending on the structure of the nucleic acid substrate (63, 64), and the translocational status of the complex (141). (B) Generation of hydroxyl radicals through Fenton-like reactions. Divalent iron ions can bind at or close to the active site of the RNase H activity. Continuous oxidation and reduction produces a high local concentration of hydroxyl radicals that cleave the template site-specifically.

A

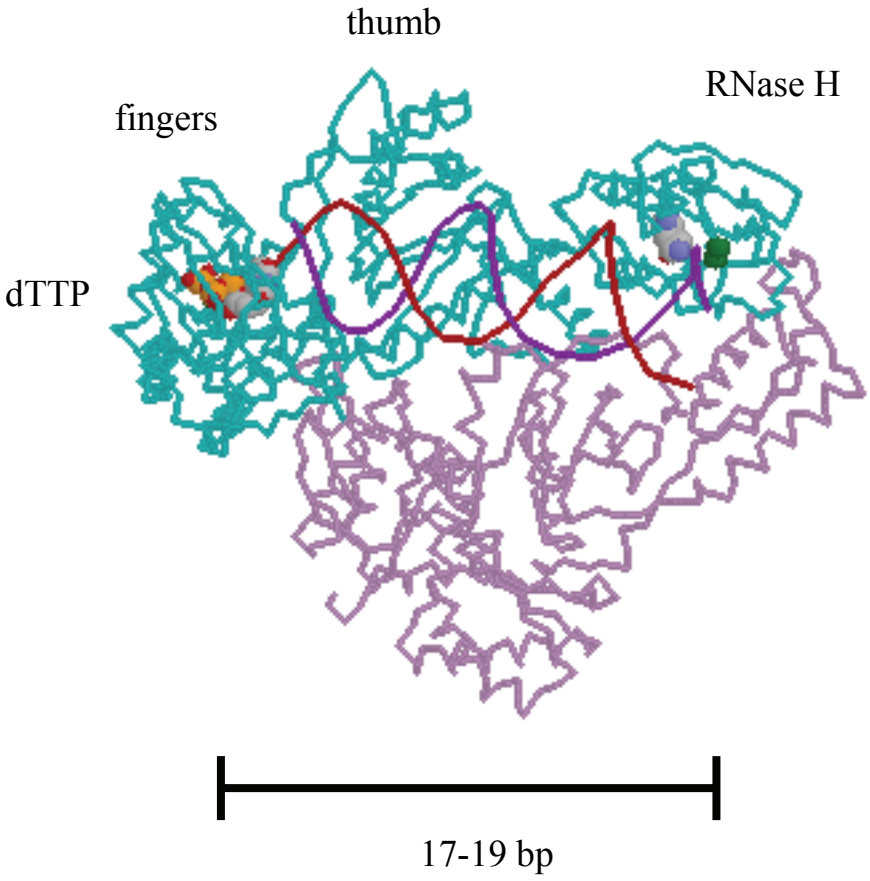

B

$$Fe^{2+} + H_2O_2 \rightleftharpoons Fe^{3+} + OH\bullet + OH^-$$

DTT

RNase H domain, which generates high local concentrations of hydroxyl radicals that cleave the most proximal residues of the template. In our previous studies, we utilized primer strands that contained a chain-terminator at the 3' end. We showed that cleavage at positions -8 or -18 represent the pre-translocational configuration (N-site complex), while cleavage at positions -7 and -17 are indicative for the post-translocational stage (P-site complex). In view of these recent findings, showing that the relative populations of N- and P-site complexes depend on the chemical nature of the terminal nucleotide, it is tempting to hypothesize that mismatched nucleotides may affect the translocational equilibrium likewise. Here we used the iron-assay to study the precise positioning of HIV-1 RT in the context of complexes that contain mispaired primers.

Positioning of HIV-1 RT on mispaired primer strands in the absence of dNTPs. It was the major goal of this study to characterize the relation between the translocational status of the enzyme and its ability to extend or to excise mispaired nucleotides. As shown in Fig. 5.2, we generated complexes composed of HIV-1 RT and DNA/DNA substrates that contained the four different bases at the 3' end of the primer. These four complexes were treated with Fe^{2+} to study the impact of the different primer termini on the precise positioning of HIV-1 RT in the absence of added nucleotides. Treatment of the complex with the correct A:T base pair caused cleavage at positions -17 and -18 at the template (Fig. 5.2, lane 1). Both cuts are equally distributed, which suggests the existence of a mixture of N- and P-site complexes. The same pattern is obtained with ddAMP-terminated primer strands (141). Thus, it appears that the absence or presence of the 3'-OH group may not affect the translocational equilibrium.

Fig.5.2 Site-specific footprinting of complexes containing mispaired primer strands. (A) Lanes 1–4 show the footprints with A:T, C:T, G:T, and T:T mispairs, respectively. Cleavage in the vicinity of the end-labeled DNA (asterisk) might be attributable to unspecific binding effects at the 3' end of the substrate. Minor cuts at positions -16 and -19 may result from diffusion of hydroxyl radicals (63), and are thus not further considered. (B) Graphic representation of data shown in A. The cleavage assignment is shown underneath (N: A, C, G, or T).

A

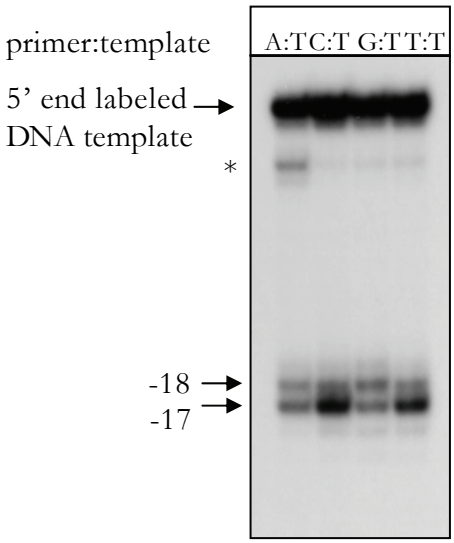

B

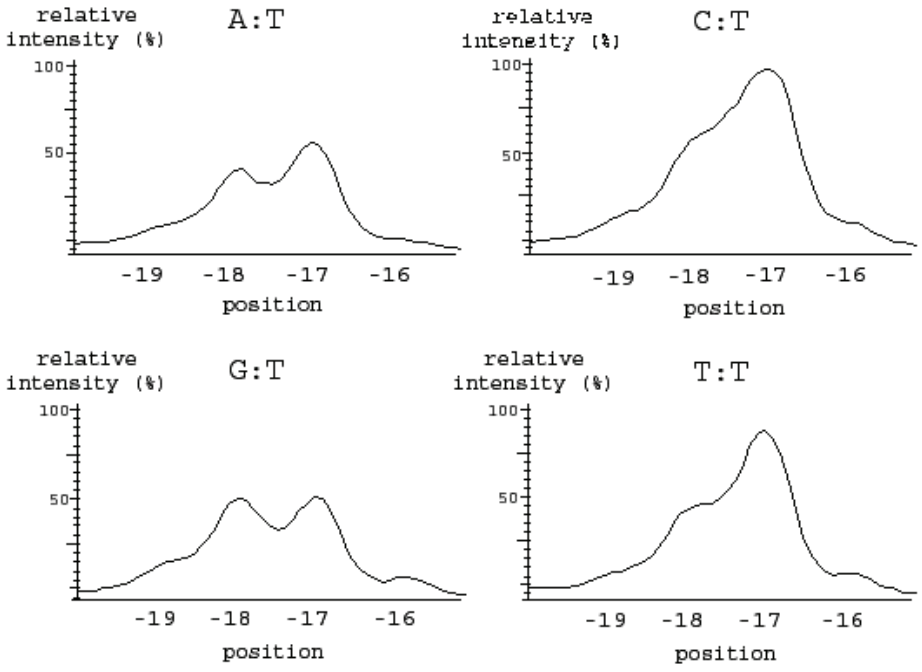

TTAAAAGAAAAGGGGGG**N**

3′AGAATCGGTGAAAAATTTTCTTTTCCCCCCTGACCTTCCCGATTAAGTGAGGGTTGC* 5′

-18 -17 -1

Differences in the distribution of the two cuts are seen with C:T and T:T mispairs (Fig. 5.2, lanes 2 and 4). The -17 cut is clearly dominant in these cases, which suggest that these complexes exist predominantly in the post-translocational stage. In contrast, the G:T mispair caused a similar band distribution as seen with the correct A:T base pair (lane 3). The data suggest that the N-site may not be able to efficiently accommodate C:T and T:T mismatches, while the G:T base-pair appears to be tolerated. The appearance of an intense band at position -17, in association with complexes containing C:T and T:T mispairs, suggest that the primer terminus resides in the P-site, and the N-site is likely to be accessible for the next complementary nucleotide. However, it remains to be seen how or whether differences in the distribution of N- and P-site complexes may affect pyrophosphorolysis and mismatch extensions, respectively.

Excision of mispaired nucleotides. We initially studied the effects of the different primer termini on the efficiency of pyrophosphorolysis. The four complexes were incubated in the presence of physiologically relevant concentrations of 150μM PPi, and the extent of excision was monitored in a time course experiment. The data show that the correct A:T and the incorrect G:T mispairs are efficient substrates in this regard, while C:T and T:T mispairs are literally resistant to pyrophosphorolysis. Thus, the data shown in Figs. 5.2 and 5.3 are in good agreement with our earlier study (141), and show that an increase in populations of complexes that exist in the P-configuration can diminish excision of the terminal nucleotide.

Positioning of HIV-1 RT in the presence of dNTPs. The use of chain-terminated primer strands in our previous studies allowed us to study the effects of the presence of the next

Fig.5.3 Efficiency of pyrophosphorolysis on mispaired primer strands. (A) The experiment shows a time course of pyrophosphorolytic excision of 3' ultimate A, C, G, and T residues opposite template T. Lanes 1–8 show reactions after 0, 1, 5, 15, 30, 45, 60 and 90 min. (B) Graphic representation of data shown in A.

A

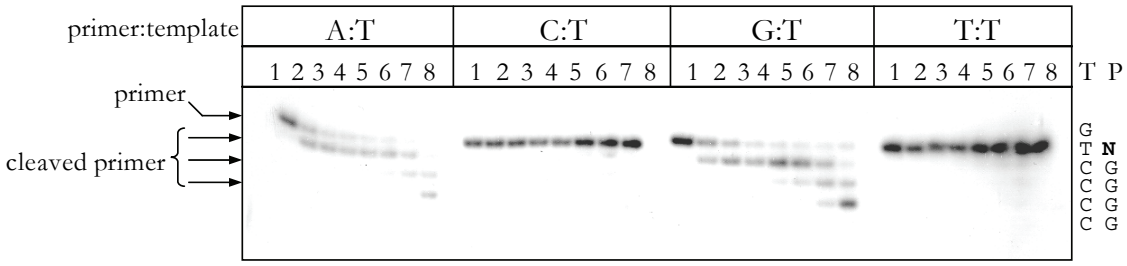
primer:template
A:T
C:T
G:T
T:T
1 2 3 4 5 6 7 8
T P
primer
cleaved primer
G
T
C
C
C
C
N
G
G
G
G

B

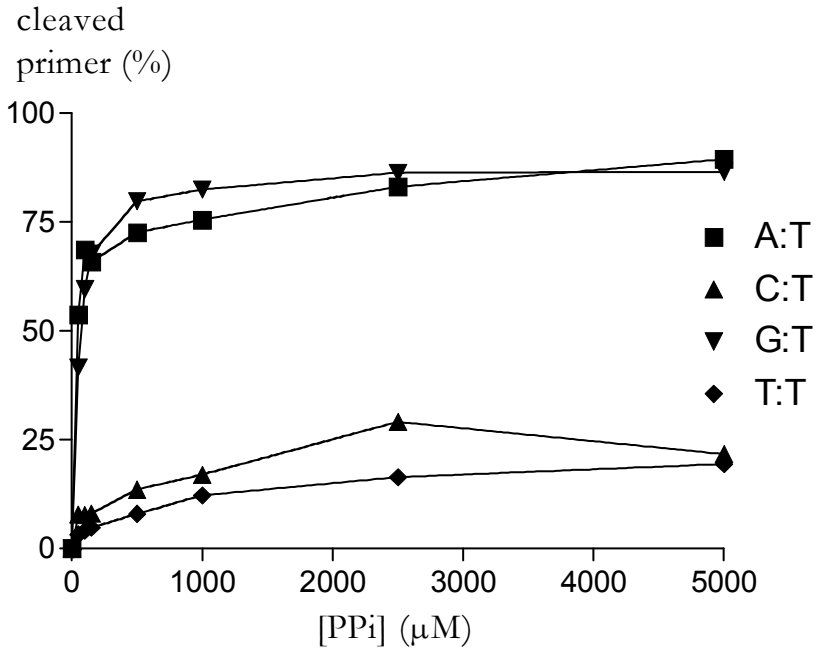
cleaved
primer (%)
100
75
50
25
0
0
1000
2000
3000
4000
5000
[PPi] (μM)
A:T
C:T
G:T
T:T

complementary dNTP on the translocational equilibrium in the absence of primer extension. Here, we studied the effects of different concentration of the templated nucleotide on the efficiency of primer extension and on the precise positioning of the enzyme in two separate experiments (Figs. 5.4 and 5.5, respectively). The preformed RT-primer/template complexes were incubated with increasing concentration of ddCTP. The stop-nucleotide is complementary to the next template position and limits DNA synthesis to a single incorporation event. We found that the extension of A:T and G:T mispairs is highly efficient, while T:T and C:T mispairs compromise ensuing polymerization events (Fig. 5.4A). These data are in agreement with steady-state kinetic studies showing that the extension of G:T base pairs is less efficient than the extension of a correctly paired primer, but more efficient than extensions of other mismatches (Fig. 5.4B). However, the comparison with Fig. 5.2 does not point to an obvious correlation between the efficiency of primer extension and the ratio of complexes that pre-exist in the P-site configuration. Complexes containing C:T or T:T mismatches are found predominantly in the post-translocational conformation, but the efficiency of nucleotide incorporation is clearly diminished. Conversely, complexes containing the correct A:T base-pair or the G:T mispair pre-exist in a mixture of N- and P-site complexes, but the efficiency of nucleotide incorporation is relatively high despite the partial occupation of the nucleotide binding site. Thus, it appears that productive binding of the nucleotide, that includes the proper alignment of the 3'-OH group of the primer with the incoming nucleotide, is more important in this regard.

Fig. 5.5 shows that the footprint patterns of complexes containing A:T and G:T base pairs in the presence of increasing concentrations of the next nucleotide correlate well with the

Fig.5.4 Extension of mismatched primer strands. (A) The experiment shows the efficiency of incorporation of ddCMP at increasing concentrations after a 20 min reaction. Lanes 1–8, show reactions in the presence of 0, 1, 5, 10, 50, 100, 200μM and 1mM ddCTP. (B) Steady-state kinetic parameters. [(a)] "nd" not determined, because the extension of T:T and C:T mispairs required concentrations >1 mM.

A

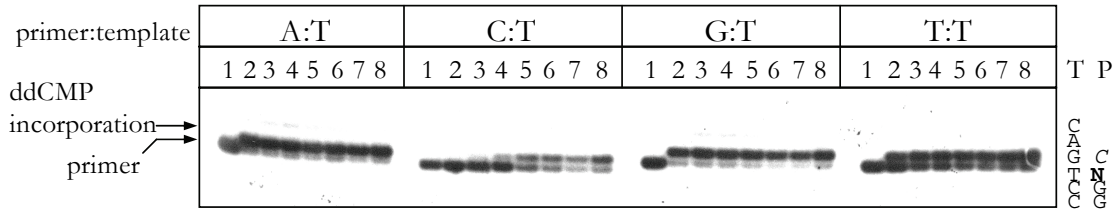

B

Base pair at 3'end	k_{cat} (min^{-1})	K_m (μM)	k_{cat} / K_m (μM^{-1} min^{-1})
A:T	2.00	0.05	40.0
G:T	1.16	0.95	1.22
C:T			nd[a]
T:T			nd

Fig.5.5 Site-specific footprints on differentially extended primer strands. (A) Footprints were conducted in the presence of 0, 1, 5, 10, 50, 100, 200μM and 1mM ddCTP (lanes 1–8) as described in Fig.5.4. (B) Schematic representation of results shown in A. Light characters label the differences at the beginning of the reaction at the 3' end of the primer/template. Underlined characters represent Fe-mediated cleavage; bold characters label the major cut. Offset characters are nucleotides that are bound to RT, but remain unincorporated due to the presence of the chain-terminating nucleotide. Position -1 refers to template position opposite the 3' end of the primer.

A

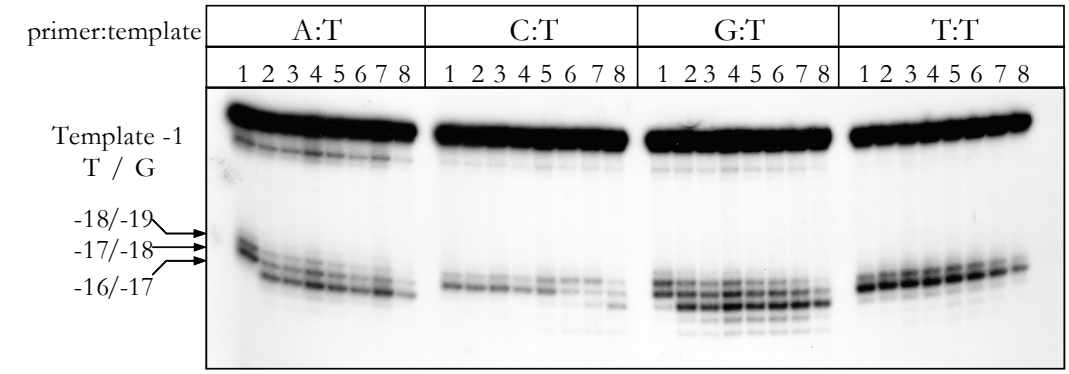

B A:T and G:T

[ddCTP] 0μM

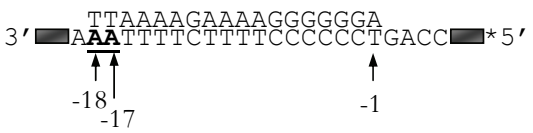

[ddCTP] 1μM-1mM

C:T

[ddCTP] 0-10μM

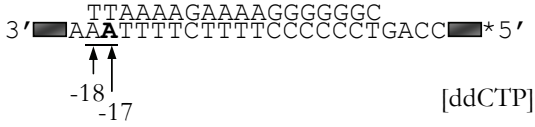

[ddCTP] 50-200μM

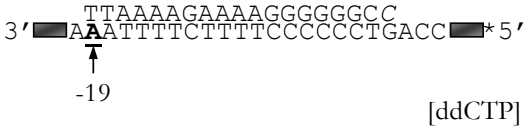

[ddCTP] 1mM or higher

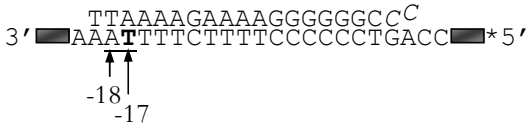

T:T

[ddCTP] 0μM

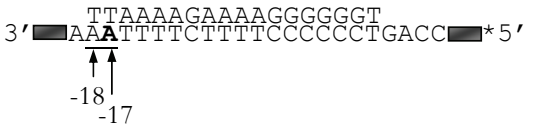

[ddCTP] 1μM-1mM

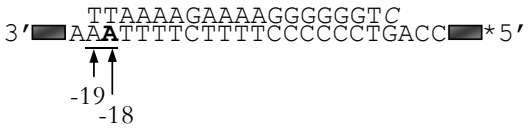

corresponding extension pattern shown in Fig. 5.4. Concentrations of ddCTP as low as 1μM are sufficient to cause almost complete extension (Fig. 5.4), and complete translocation (Fig. 5.5), respectively. However, the footprint patterns with complexes containing the T:T mispair do not change over the entire range of concentrations of ddCTP, and C:T-containing complexes show unusual fluctuations in the cleavage pattern. Concentrations of 10μM of ddCTP are not sufficient to cause significant primer extension (Fig.5.4, lanes 1–4), and the corresponding footprinting patterns are literally identical (Fig.5.5, lanes 1–4). The major cut is always seen at position -17. Concentrations of ddCTP as high as 50μM facilitate the extension of the primer (Fig. 5.4, lane 5); however, this is not reflected by the corresponding footprint (Fig. 5.5, lane 5). We do not observe the appearance of shorter fragments that would indicate translocation of RT, as seen with the A:T and G:T base-pairs. Instead, footprints conducted in the presence of 50–200μM ddCTP show intense cleavage at position -19, despite the partial extension of the primer. High concentrations of 1mM of ddCTP are required to obtain the expected cut at position -17 (Fig. 5.5, lane 8). A major cut at this position suggest that the primer is effectively extended, and the 3' end of the primer resides in the P-site.

Translocation of complexes with mispairs at the 3' penultimate position. At first glance, it is difficult to explain the footprint patterns obtained at median concentrations of the next nucleotide. It appears that the incorporation of ddCMP can force the enzyme to translocate backwards, and only the presence of high concentrations of this nucleotide can force translocation in the correct direction. Thus, high concentrations of ddCTP may facilitate the formation of a ternary complex with the nucleotide bound to the N-site. However, this would create a C:A mismatch, which may help to explain the requirements

Fig.5.6 Effect of 3' penultimate mismatch on the positioning of RT. (A) Fe-mediated cleavage of complexes containing the correct A:T base pair, and the C:T mismatch following incubation with 200μM ddCTP (lane 1, left and right). Lanes 2–12 show the footprints at different concentrations of the second correct nucleotide, i.e. dTTP: 1, 3.125, 6.25, 12.5, 25, 50, 100, 250, 500, 750μM and 1 mM. (B) Schematic representation of results shown in A, as introduced in Fig.5.5.

A

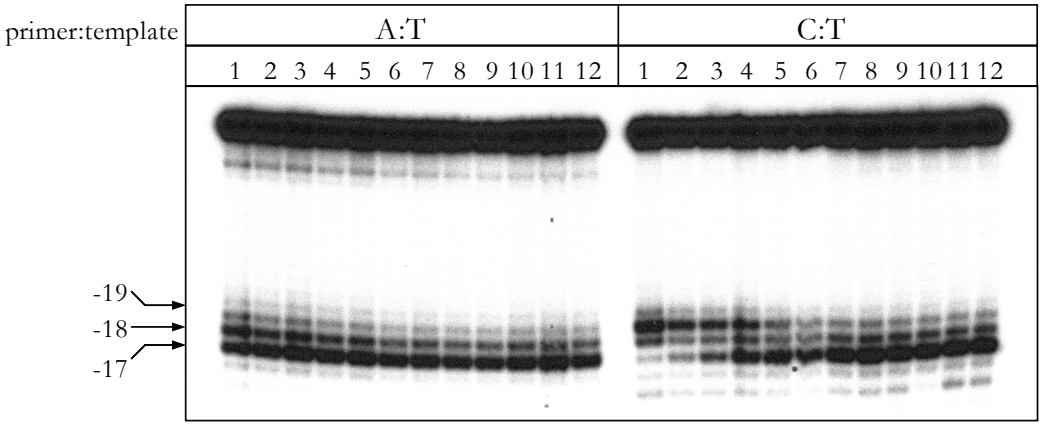

B

A:T

[dTTP] 0μM

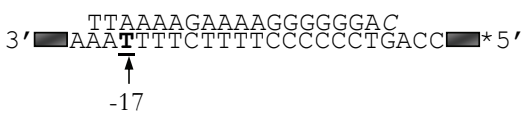

[dTTP] 1μM-1mM

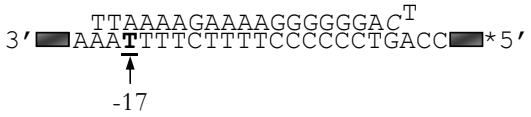

C:T

[dTTP] 0-6.25μM

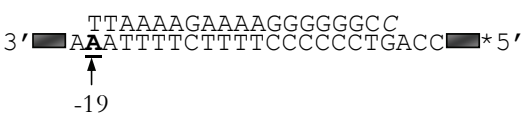

[dTTP] 12.5μM-1mM

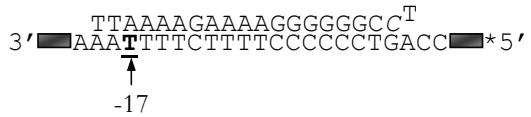

for such high concentrations to force translocation. To address this issue, we generated complexes in the presence of 200μM ddCTP to facilitate the extension of the primer, and to force the enzyme to slide backwards. These complexes were then incubated in the presence of increasing concentrations of dTTP to facilitate the formation of a complex that contains the correct nucleotide in the N-site. The results show that approximately 10μM of this nucleotide is sufficient to cause a shift of the major cut from position -19 (Fig. 5.6, lanes 1–3) to position -17 (Fig. 5.6, lanes 4–12). These data show that the mismatch at the 3' penultimate position can also significantly affect the positioning of the enzyme.

5.6 Discussion

In this study, we asked whether changes in the translocational equilibrium of HIV-1 RT can influence mismatch extensions and the phosphorolytic excision of mispaired nucleotides. Our data show that misincorporated nucleotides can induce changes in the translocational equilibrium, and these changes can affect the efficiency of excision; however, the impact on mismatch extension is complex and depends critically on subsequent nucleotide binding and incorporation events.

Translocation and excision of mismatched nucleotides. Pyrophosphorolysis can only occur in the pre-translocational stage when the 3' end of the primer resides in the N-site (17, 141, 211, 212) (Fig. 5.7A). We found that complexes with the correct A:T base pair and the G:T base-pair can exist in both the pre- and the post-translocational configuration. Thus, these primer termini may have access to the N-site, which helps to explain the

Fig.5.7 Simplified models describing the effects of mismatches on the precise positioning of RT and consequences regarding the efficiency of excision and mismatch extension. The proposed models describe events that take place directly at the active site of the enzyme. (A) Pyrophosphorolysis of a dGMP opposite template T. The mispaired 3' end of the primer (dark blue dGTP) is located in the N-site of the RT, and PPi occupies the binding site for the β- and the γ-phosphates of the incoming nucleotide. Specific binding sites for divalent metal ions (pink circles) are shown in close proximity to the phosphates according to the two-metal ion mechanism proposed by Steitz (228). The red arrow indicates the attack on the ultimate phosphodiester bond. (B) Translocation and mismatch extension. Following the incorporation of the mismatched nucleotide, the 3' end of the primer must leave the N-site to allow binding of the next nucleotide (yellow), which is a chain-terminator in this case. The translocation of the nucleic acid relative to the enzyme brings the mismatched nucleotide to the P-site. Nucleotide incorporation and the release of PPi is indicated by the arrow. (C) Incorporation of the second correct nucleotide. Binding of the second correct nucleotide requires again translocation, which brings the mismatch in close proximity to RT's primer grip. (D) Displacement of RT in the context of the 3' penultimate mismatch. Our footprints suggest that RT tends to slide backwards under these circumstances, and in the absence of adequate concentrations of the second correct nucleotide.

A. Pyrophosphorolysis

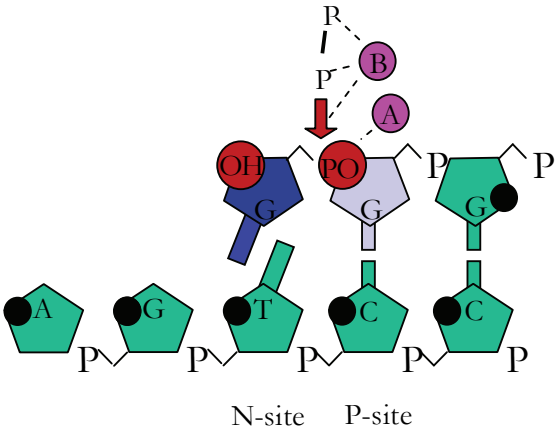

B. Translocation and Mismatch Extension

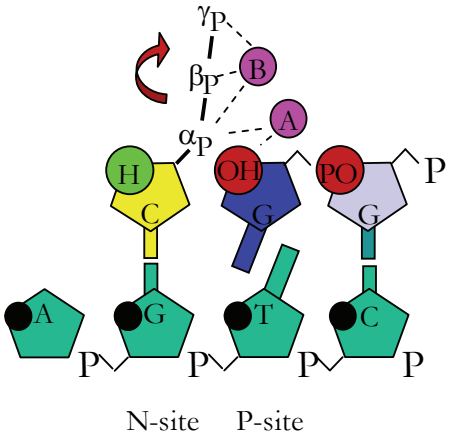

Primer grip

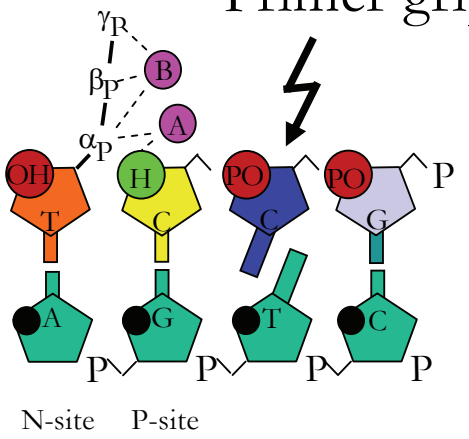

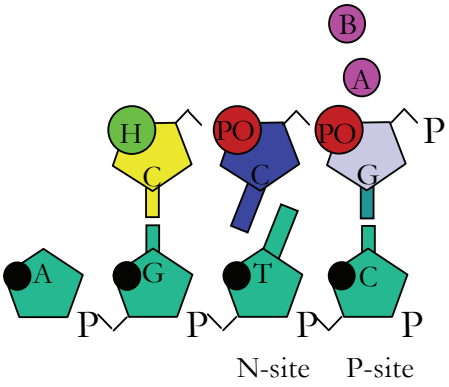

C. Translocation of the 3'Penultimate Mismatch

D. Back Translocation

efficient removal of dAMP and dGMP opposite template T. In contrast, complexes containing C:T and T:T mismatches appear to exist predominantly in the post-translocational stage, which helps to explain why these mispairs are poor substrates regarding the back reaction. Thus, it appears that the N-site tends to repel C:T, and T:T base pairs, while the G:T mispair is tolerated to a certain degree. These data are consistent with the relatively high rates of incorporation of dGMP opposite T, since the N-site must accommodate the G:T base pair in both cases. However, proper access to the N-site can only be seen as a necessary, but not as a sufficient requirement for the excision of incorporated nucleotide monophosphates. The precise geometry of the phosphate between the last two nucleotides of the primer and the attacking PPi is certainly another important parameter that cannot be assessed on the basis of our footprints.

Translocation and mismatch extension: incorporation of the first nucleotide. The efficiency of mismatch extensions (Fig. 5.7B), i.e. the incorporation of the first correct nucleotide following the mismatch, does not appear to depend on the aforementioned changes of the translocational equilibrium. Although the N-site is not occluded by the primer terminus of C:T and T:T mispairs, the efficiency of nucleotide incorporation is severely compromised when compared with complexes containing G:T and A:T base pairs. Thus, the proper alignment between the 3' OH group of the primer terminus and the α-phosphate of the incoming nucleotide is likely to be significantly disturbed in complexes containing C:T and T:T mispairs. In contrast, G:T and A:T mismatches are efficiently extended, although the corresponding binary complexes can partially exist in the pre-translocational configuration that blocks the N-site. In this context, it is important to note that our footprints are snapshots that show the relative populations of complexes

within a range of seconds; however, the translocational equilibrium is kinetically invisible, which suggests rapid changes between pre- and post-translocational stages, presumably in a range below milliseconds (68, 85, 103). In this model, the next complementary nucleotide may rapidly bind to available open N-site complexes, which pulls the overall equilibrium to the post-translocational stage and DNA synthesis can proceed (141), provided that the primer terminus is properly aligned with the incoming nucleotide.

Translocation and mismatch extension: binding of the second correct nucleotide. Consistent with the efficient extension of the primer, the iron-mediated cuts of complexes containing the newly incorporated nucleotide as a chain-terminator following A:T or G:T mispairs are shifted by a single position further downstream. Thus, the RT enzyme has advanced to the next position, and established a novel translocational equilibrium. In this case, the majority of the complexes are found in the post-translocational stage, presumably because the chain-terminator, which is still present in the reaction mixture, can bind to the N-site. In contrast, the footprints obtained with primer/templates containing the chain-terminator following C:T or T:T mismatches point to a complex relation between primer extension and RT translocation (Fig. 5.7C and D). Conditions that allow the incorporation of the chain-terminator are not sufficient to facilitate translocation of the enzyme. The footprints with T:T mismatches are literally identical over the entire range of concentrations of the next nucleotide. This indicates that the enzyme resides at the same position prior and post-nucleotide incorporation. The footprints associated with the 3' penultimate C:T mismatch are even more complex. It appears that the incorporation of the chain-terminator forces the enzyme to slide a single

position backwards. Relatively high concentrations of the second correct nucleotide are required to force downstream translocation. Thus, these data indicate that efficient mismatch extension requires the incorporation of more than a single correct nucleotide.

Previous data have shown the 3' penultimate mismatches can also result in severe reductions in rates of pyrophosphorolysis (264). These results are in good agreement with our footprints obtained with the C:T mismatch, showing that the primer terminus is not properly positioned to be cleaved (Fig. 5.7D). We suggest that the displacement of the RT enzyme is attributable to unfavorable interaction between the distorted terminus of the duplex and the primer grip motif in the vicinity of the active site of HIV-1 RT. Mutations in the primer grip (96) can have profound effects on the fidelity of the enzyme (71, 96, 185). Moreover, certain mutations in this region can affect RNase H activity (175), which is consistent with our footprints that actually show an altered position of the RNase H active site on the template strand. It will now be of interest to study the effects of mismatches on the relative positioning of RT, as the enzyme continues to incorporate nucleotides. It is conceivable that the unfavorable interaction with residues that belong to the 'minor groove binding track' (12) may affect the translocation of the enzyme in similar fashion. Mutations at these positions can alter the interaction with the first 3–7 nucleotides, and were shown to affect numerous properties of the enzyme including the fidelity of DNA synthesis and processivity (12, 184).

Interface between accuracy of DNA synthesis and the development of antiretroviral drugs. The excision data described in this study are reminiscent of our previous results obtained with chain-terminating nucleotides. An increase in the population of complexes

that can exist in the pre-translocational stage correlated with increased rates of excision of the 3' ultimate nucleotide. These data help to explain why AZT-MP is more effectively cleaved as compared to incorporated dAMP; and these data help to explain why the mispaired G opposite T can undergo phosphorolytic cleaved, while C:T and T:T mismatches resist excision. Thus, pyrophosphorolysis may not provide an alternative proofreading mechanism in vivo. The G:T base pair might be an exception in this regard; however, G:T mispairs are also the easiest to form, which likely provides an important mechanism for frequently occurring G → A changes in the HIV genome. Our findings suggests that nucleoside analogues that combine the properties of a chain-terminator together with modifications in the base moiety that force translocation of RT, in similar fashion as shown for C:T and T:T mispairs, may create a novel class of potent RT inhibitors that could resist excision. Nucleoside analogues with changes in the base moiety may be incorporated opposite both 'correct' and 'incorrect' template positions, as previously shown for ribavirin (25, 26), which is a clinically used nucleoside analogue that inhibits the activity of viral RNA-dependent RNA polymerases. This compound does not act as a classical chain-terminator (135); however, the continuation of RNA synthesis following the incorporated monophosphate appears to be diminished. In the light of our data it is tempting to conjecture that ribavirin and related compounds may affect the precise positioning of the polymerase on its nucleic acid substrate in similar fashion as described here in regard to effects of 3' ultimate and 3' penultimate mismatches on the position of HIV-1 RT. It is now of interest to study the potency of novel nucleotide analogue inhibitors that contain base modifications together with structural alterations at the 3' position of the sugar moiety.

CHAPTER 6

CONCLUSION

With this research project, I made significant findings contributing to the understanding of the reverse transcriptase and polymerases in general. By developing the site-specific footprinting assays, I contributed the first assay with a high enough sensitivity to detect the position of the reverse transcriptase at a single nucleotide resolution. Before the development of this assay, only indirect methods were used to detect polymerase translocation such as kinetic measurements in the presence of obstacles along the templating strand (67), or the observation of immobilized enzymes in crystal structures (38, 88, 95, 211, 216, 261, 262). The site-specific footprinting assays function by cleaving the DNA template at the nucleotide that contacts a specific amino acid residue or metal binding site on the reverse transcriptase. By developing two assays that show the positions of distant domains on the enzyme, one in the polymerase domain and the other in the RNase H domain, one can evaluate the movement of these two domains independently.

The potassium peroxinitrate footprinting assay gives a cut at the template nucleotide in contact to amino acid Cys280. The thiyl group of Cys280 is approximately 4Å from the template base -7 in the structure of the reverse transcriptase with a double-stranded DNA substrate and an incoming nucleotide (88). The chemical probably reacts with the Cys residue to produce local high concentration of hydroxyl or thiyl radicals, which attack the sugar moiety of the DNA chain (5). Although attempts to transpose this technique to other sites of the reverse transcriptase or other proteins have been unsuccessful so far, this technique could theoretically be used on any nucleic acid binding proteins. In order to do so, a Cys residue needs to be solvent exposed and in close contact with the nucleic acid.

The Fe^{2+} footprinting technique functions by binding divalent iron to the RNase H active site. With the oxidation of the iron ions, hydroxyl radicals are created, which will cleave the DNA template in close proximity to the RNase H active site. This technique works very well with the reverse transcriptase, but it would be difficult to transfer it to other enzymes. Most polymerases bind divalent metals in their active site, but since this site is located at the 3' end of the primer, no information on the location of the enzyme on the template can be obtained. Only enzymes with a second active site, like the reverse transcriptase, could yield a footprint with divalent iron.

With the help of these two techniques, in combination with other enzymatic assays, I studied the translocation mechanism of the reverse transcriptase. We found that the reverse transcriptase moves from one position to another with a Brownian motion, reaching an equilibrium between the pre- and the post-translocational states. During processive elongation, the binding of a nucleotide stabilizes the post-translocational state and the reaction is allowed to take place. Once the reaction has occurred, the pyrophosphate product must be released in order for the enzyme to translocate and reach an equilibrium at the next position.

I identified factors that affect the translocational equilibrium. The sequence of the nucleic acid template is an important factor influencing the translocational state. I identified sequences where the reverse transcriptase is located almost completely in the pre- or the post-translocational state and other sequences were the enzyme is distributed between the two sites. It is not clear so far how the sequence affects the equilibrium. The 3' nucleotide may play a role in the equilibrium, but according to our results, the presence of

A or T at the template nucleotide paired to the 3' end of the primer does not change the translocational distribution. However, we did not determine if a G:C base pair instead of a A:T base pair affects the equilibrium. Meyer *et al.* conducted a study of the rate of ATP-dependent nucleotide removal in the context of the template sequence (159), which we have shown earlier to correlate with the translocational state of the reverse transcriptase (141). They first identified two sequences, one where the removal was efficient, and one were little removal could be observed. By using hybrids of these two sequences, they found that the single-stranded portion of the template downstream from the 3' end of the primer, and the double-stranded portion upstream of the 3' end of the primer by more than 22 nucleotide have little effect on the rate of removal. The first 11 nucleotide upstream of the 3' end of the primer had the highest influence, followed by the section including nucleotides 12-21 upstream of the primer's 3' nucleotide. This means that the nucleotide in contact with the polymerase domain have more influence on the rate of removal than the nucleotide contacting the RNase H domain. Further analysis showed that nucleotides -2 to -7 had the greatest impact on the removal rate. Unfortunately, the influence of the template base paired with the primer's 3' nucleotide was not analysed in this study. Further studies are necessary to understand the specific role of each nucleotide position in the translocational equilibrium. Structural studies could show the direct impact of the different template positions.

The nature of the 3' nucleotide of the primer is affecting the translocational equilibrium. We showed that nucleoside analogues containing an azido group at the 3' position of the sugar moiety favours the formation of pre-translocated complexes (141). This is important with regard to drug action and drug resistance. Azido containing nucleotides

are cleaved with a relatively high rate by the reverse transcriptase (92), which is explained by their tendency to reside in the nucleotide binding site after incorporation. I also compared the positioning of the nucleotide analogue tenofovir to other analogues such as azido containing nucleotide and 2',3'-dideoxynucleotides. At a template sequence where the reverse transcriptase is evenly distributed between the pre- and post-translocational states when the 3' end of the primer is a natural nucleotide, we showed that the dideoxy analogue does not affect the positioning of the enzyme, while the azido analogue shifted the enzyme almost completely to the pre-translocational state. The acyclic sugar analogue (tenofovir) also shifted the reverse transcriptase to the pre-translocational state, but not as much as the azido analogue did. We also showed a direct correlation between the translocational state of the reverse transcriptase and the rate of removal of the different analogues, where both tenofovir and the azido analogue were removed faster than the dideoxy analogue. The correlation was not perfectly respected since tenofovir and the azido analogue were cleaved at similar rates even though the azido analogue is found more pre-translocated than tenofovir. Other factors must influence the rate of chain-terminator removal.

Additionally to the template sequence and the nature of the primer's 3' nucleotide, the presence of mismatches in the double-stranded substrate also affects the translocational equilibrium. With a template sequence where we observe a mixture of the two complexes, I analysed the effect of the different base pairs across a template T on translocation (140). The correct A:T match and the mismatch G:T both showed similar results, where the enzyme is almost evenly distributed between the two complexes. The mismatches C:T and T:T shifted the equilibrium towards the post-translocational state.

This correlated with the rate of removal of the primer's 3' nucleotide. The A:T and G:T base pairs where efficiently cleaved from the primer, while the C:T and T:T mismatches where literally uncleaved. It did not however correlate with the rate of extension of the differently paired primer's 3' ends. While it would be expected that the complexes in the post-translocational state are the most efficient at nucleotide incorporation, the A:T and G:T base pairs where the most efficiently elongated. A C:T or a T:T mismatch probably causes a misalignment in the reverse transcriptase active site which reduces the rate of incorporation of these complexes. The presence of a mismatch at the penultimate nucleotide also changes the translocational distribution of the reverse transcriptase. The presence of a C:T mismatch at this position even forces a movement backward of the enzyme, moving the 3' end of the primer out of the active site. It would be interesting to study other positions, in order to understand the specific interactions between the reverse transcriptase and its nucleic acid substrate.

As mentioned above, the presence of nucleotides favours the post-translocational state. Binding of a nucleotide induce the closure of the fingers subdomain, which stabilizes the complex. It is this stabilization mechanism that allows the reaction components to be properly aligned so that the reaction can occur. At sequences where the reverse transcriptase is preferentially in the post-translocational state, nucleotides can bind more easily, due to the accessibility of the nucleotide binding site. This is reflected in the affinity (K_m) of the enzyme for nucleotide. Lower K_m are observed at these sites compared to sites where the enzyme is in the pre-translocational state or at intermediate states (142).

Pyrophosphate is produced as a result of nucleotide incorporation, and is released by the enzyme. Whether pyrophosphate is released before, after or simultaneously with translocation was still not defined. Although it was not possible to study the influence of pyrophosphate on translocation, the pyrophosphate analogue foscarnet could be used. I showed that the enzyme must reside in the pre-translocational state in order to bind foscarnet (142). I also showed that foscarnet binding induced a stable complex, similar to the complex obtained with nucleotide binding. These observations provide clues in the order of event after the phosphodiester bond formation. The fact that a stable complex is obtained after foscarnet binding suggest that the fingers subdomain is in the closed conformation. This shows that pyrophosphate release occurs with the fingers opening, which then allows the enzyme to translocate to the next position and establish an equilibrium between the pre- and the post-translocational states. It has been confirmed with the crystal structure of the T7 RNA polymerase that pyrophosphate binds to a closed pre-translocated complex (262).

Drug resistance mutations were shown to affect the rate of chain-terminator removal. I showed that in the case of some of these mutations, the rate of removal is affected by a shift in the translocational equilibrium. An enzyme containing mutation T69S with an insertion of two Ser between residues 69 and 70 as well as mutation M41L and T215Y confers resistance to all nucleoside analogues by increasing the rate of chain-terminator removal. I showed that this mutant enzyme tends to reside more in the pre-translocational state when compared to the wild-type reverse transcriptase (141). This tendency explains the increased rate of chain-terminator removal since the pre-translocatioanl state is required in order for pyrophosphate or a pyrophosphate donor to bind and carry the

removal reaction. Another mutant, the E89K reverse transcriptase, decreases the rate of chain-terminator removal. We can see with the site-specific footprintings that this enzyme has a decreased tendency to reside in the pre-translocational state. Instead, the enzyme slides either forward or backward from this site, impairing the ability of the enzyme to conduct the removal reaction (142).

Crystal structures of the reverse transcriptase bound to a nucleic acid substrate all show the enzyme in the post-translocational state (38, 95), while our footprintings show that the enzyme can occupy both the pre- and the post-translocational states. In order to reconcile these data, I performed our site-specific footprintings at 4^0C (141), which resembles more the conditions at which crystals are produced. We observed that temperature has an effect on the translocational equilibrium. At low temperature, the enzyme moves to the post-translocational state, which explains why this complex is the one seen in crystal structures, unless the enzyme is cross-linked to the nucleic acid substrate in the pre-translocational state (211).

My findings also have repercussions in the field of drug action and drug resistance. Although it is known that chain-terminating nucleotides can be cleaved from a DNA chain, it had not been demonstrated what complex is able to carry out this reaction. With our site-specific footprintings, I showed a clear relationship between complexes in the pre-translocational state and the ability of such complexes to remove chain-terminators from the DNA chain (141). There are implications of this both in drug discovery and drug resistance. In order to develop more potent chain-terminators, efforts should be put on molecules that would favour the post-translocational state once incorporated in the

elongating DNA chain. Bulky groups such as the azido group in AZT should be avoided to create nucleoside analogues that are efficiently incorporated and not cleaved from the DNA primer.

Using an enzyme with mutation T69S and an insertion of two Ser between residues 69 and 70 as well as mutations M41L and T215Y, we found that drug resistance mutations can affect the translocational equilibrium. When compared to the wild-type reverse transcriptase, this enzyme tends to reside more in the pre-translocational state (141). This enzyme is resistant to all nucleoside analogues by increasing the rate of chain-terminator removal. As mentioned above, chain-terminators promoting the post-translocational state would be better inhibitors of such resistant enzymes.

My work also allowed the identification of a mechanism of action for the pyrophosphate analogue foscarnet. With site-specific footprints, I showed that foscarnet binds to the pre-translocated complex. During primer elongation, I identified the sites that are more sensitive to foscarnet. I demonstrated that these sites pre-exist in the pre-translocational state, or are very easily brought to that state in the presence of foscarnet. Since foscarnet bind to pre-translocated complex, the sites where the enzyme is already present in this state will allow foscarnet to bind more easily. This mechanism suggest that nucleotide and foscarnet cannot bind to the same enzyme since they bind to different complexes; post- and pre-translocated respectively. However, previous kinetic studies with foscarnet concluded in a non-competitive mechanism of inhibition with regard to nucleotide (34, 46, 173, 237). In order to explain this discrepancy, a kinetic study of inhibition of the reverse transcriptase with foscarnet using different template sequences promoting the pre-

or the post-translocational state was conducted (142). In steady-state kinetic assays in the presence of foscarnet, we observed a difference in the catalytic rate (k_{cat}), but not in the affinity for nucleotide (K_m) at a site where the reverse transcriptase is naturally post-translocated, suggesting a non-competitve inhibition mechanism. When the assay was repeated using a template sequence that promotes the pre-translocational state, a difference in the K_m was observed, but not in the k_{cat}, suggesting a competitive mechanism of inhibition. The latter correlates with our observation that foscarnet binds to the pre-translocated complex. In order to explain the former result, we conducted mobility shift assays, and found that foscarnet binding induces a stable complex. This stable complex, in steady-state conditions, will reduce the rate of nucleotide incorporation. Since only one nucleotide is present in the reaction, the enzyme must dissociate in order to bind another substrate and incorporate a nucleotide. Due to the stabilization of the enzyme, it cannot dissociate. This nucleotide incorporation reduction will be observed in the k_{cat}, and not in the K_m. Our results demonstrate the mechanism of inhibition of foscarnet during processive elongation, and form a rational to develop inhibitors that block polymerase translocation.

As mentioned above, drug resistance mutations can affect the translocational equilibrium. The mutant E89K is resistant to foscarnet and hypersusceptible to AZT. Residue E89 contacts the template strand in the reverse transcriptase-nucleic acid complex. My site-specific footprints showed that this mutant enzyme has a reduced affinity for the pre-translocational state. This shows that the enzyme-nucleic acid interface could constitute a target for inhibitors affecting the positioning of the reverse transcriptase on its substrate.

Such molecules could be used in combination with chain-terminator to force the enzyme to leave the pre-translocational state after the chain-terminator incorporation.

In conclusion, my work contributed to the understanding of polymerase mechanisms in general as well as inhibition of the reverse transcriptase. More work on the subject should be undertaken in order to fully understand the interaction of the reverse transcriptase with its substrates. This would allow the development of novel inhibitors enabling us to manipulate the positioning of the enzyme in order to improve the efficiency of existing as well as novel drugs. Inhibitors affecting the translocational status of the reverse transcriptase are currently under development. Molecules stabilizing the pre- (45) and the the post-translocated (98) states are being investigated.

REFERENCES

1. **Abbondanzieri, E. A., W. J. Greenleaf, J. W. Shaevitz, R. Landick, and S. M. Block.** 2005. Direct observation of base-pair stepping by RNA polymerase. Nature **438:**460-5.
2. **Arion, D., N. Kaushik, S. McCormick, G. Borkow, and M. A. Parniak.** 1998. Phenotypic mechanism of HIV-1 resistance to 3'-azido-3'-deoxythymidine (AZT): increased polymerization processivity and enhanced sensitivity to pyrophosphate of the mutant viral reverse transcriptase. Biochemistry **37:**15908-17.
3. **Arion, D., N. Sluis-Cremer, and M. A. Parniak.** 2000. Mechanism by which phosphonoformic acid resistance mutations restore 3'-azido-3'-deoxythymidine (AZT) sensitivity to AZT-resistant HIV-1 reverse transcriptase. J Biol Chem **275:**9251-5.
4. **Back, N. K., M. Nijhuis, W. Keulen, C. A. Boucher, B. O. Oude Essink, A. B. van Kuilenburg, A. H. van Gennip, and B. Berkhout.** 1996. Reduced replication of 3TC-resistant HIV-1 variants in primary cells due to a processivity defect of the reverse transcriptase enzyme. Embo J **15:**4040-9.
5. **Balasubramanian, B., W. K. Pogozelski, and T. D. Tullius.** 1998. DNA strand breaking by the hydroxyl radical is governed by the accessible surface areas of the hydrogen atoms of the DNA backbone. Proc Natl Acad Sci U S A **95:**9738-43.
6. **Baltimore, D.** 1970. RNA-dependent DNA polymerase in virions of RNA tumour viruses. Nature **226:**1209-11.
7. **Baltimore, D., and D. F. Smoler.** 1972. Association of an endoribonuclease with the avian myeloblastosis virus deoxyribonucleic acid polymerase. J Biol Chem **247:**7282-7.
8. **Balzarini, J., and E. De Clercq.** 1991. 5-Phosphoribosyl 1-pyrophosphate synthetase converts the acyclic nucleoside phosphonates 9-(3-hydroxy-2-phosphonylmethoxypropyl)adenine and 9-(2-phosphonylmethoxyethyl)adenine directly to their antivirally active diphosphate derivatives. J Biol Chem **266:**8686-9.
9. **Balzarini, J., Z. Hao, P. Herdewijn, D. G. Johns, and E. De Clercq.** 1991. Intracellular metabolism and mechanism of anti-retrovirus action of 9-(2-phosphonylmethoxyethyl)adenine, a potent anti-human immunodeficiency virus compound. Proc Natl Acad Sci U S A **88:**1499-503.
10. **Bar-Nahum, G., V. Epshtein, A. E. Ruckenstein, R. Rafikov, A. Mustaev, and E. Nudler.** 2005. A ratchet mechanism of transcription elongation and its control. Cell **120:**183-93.
11. **Barre-Sinoussi, F., J. C. Chermann, F. Rey, M. T. Nugeyre, S. Chamaret, J. Gruest, C. Dauguet, C. Axler-Blin, F. Vezinet-Brun, C. Rouzioux, W. Rozenbaum, and L. Montagnier.** 1983. Isolation of a T-lymphotropic retrovirus from a patient at risk for acquired immune deficiency syndrome (AIDS). Science **220:**868-71.
12. **Bebenek, K., W. A. Beard, T. A. Darden, L. Li, R. Prasad, B. A. Luton, D. G. Gorenstein, S. H. Wilson, and T. A. Kunkel.** 1997. A minor groove binding track in reverse transcriptase. Nat Struct Biol **4:**194-7.

13. **Boucher, C. A., W. Keulen, T. van Bommel, M. Nijhuis, D. de Jong, M. D. de Jong, P. Schipper, and N. K. Back.** 1996. Human immunodeficiency virus type 1 drug susceptibility determination by using recombinant viruses generated from patient sera tested in a cell-killing assay. Antimicrob Agents Chemother **40:**2404-9.
14. **Boyer, P. L., T. Imamichi, S. G. Sarafianos, E. Arnold, and S. H. Hughes.** 2004. Effects of the Delta67 complex of mutations in human immunodeficiency virus type 1 reverse transcriptase on nucleoside analog excision. J Virol **78:**9987-97.
15. **Boyer, P. L., S. G. Sarafianos, E. Arnold, and S. H. Hughes.** 2002. The M184V mutation reduces the selective excision of zidovudine 5'-monophosphate (AZTMP) by the reverse transcriptase of human immunodeficiency virus type 1. J Virol **76:**3248-56.
16. **Boyer, P. L., S. G. Sarafianos, E. Arnold, and S. H. Hughes.** 2002. Nucleoside analog resistance caused by insertions in the fingers of human immunodeficiency virus type 1 reverse transcriptase involves ATP-mediated excision. J Virol **76:**9143-51.
17. **Boyer, P. L., S. G. Sarafianos, E. Arnold, and S. H. Hughes.** 2001. Selective excision of AZTMP by drug-resistant human immunodeficiency virus reverse transcriptase. J Virol **75:**4832-42.
18. **Boyer, P. L., C. Tantillo, A. Jacobo-Molina, R. G. Nanni, J. Ding, E. Arnold, and S. H. Hughes.** 1994. Sensitivity of wild-type human immunodeficiency virus type 1 reverse transcriptase to dideoxynucleotides depends on template length; the sensitivity of drug-resistant mutants does not. Proc Natl Acad Sci U S A **91:**4882-6.
19. **Burns, D. P., and R. C. Desrosiers.** 1991. Selection of genetic variants of simian immunodeficiency virus in persistently infected rhesus monkeys. J Virol **65:**1843-54.
20. **Byrnes, V. W., E. A. Emini, W. A. Schleif, J. H. Condra, C. L. Schneider, W. J. Long, J. A. Wolfgang, D. J. Graham, L. Gotlib, A. J. Schlabach, and et al.** 1994. Susceptibilities of human immunodeficiency virus type 1 enzyme and viral variants expressing multiple resistance-engendering amino acid substitutions to reserve transcriptase inhibitors. Antimicrob Agents Chemother **38:**1404-7.
21. **Canard, B., S. R. Sarfati, and C. C. Richardson.** 1998. Enhanced binding of azidothymidine-resistant human immunodeficiency virus 1 reverse transcriptase to the 3'-azido-3'-deoxythymidine 5'-monophosphate-terminated primer. J Biol Chem **273:**14596-604.
22. **Cases-Gonzalez, C. E., M. Gutierrez-Rivas, and L. Menendez-Arias.** 2000. Coupling ribose selection to fidelity of DNA synthesis. The role of Tyr-115 of human immunodeficiency virus type 1 reverse transcriptase. J Biol Chem **275:**19759-67.
23. **Cherrington, J. M., M. D. Fuller, A. S. Mulato, S. J. Allen, S. C. Kunder, M. A. Ussery, Z. Lesnikowski, R. F. Schinazi, J. P. Sommadossi, and M. S. Chen.** 1996. Comparative kinetic analyses of interaction of inhibitors with Rauscher murine leukemia virus and human immunodeficiency virus reverse transcriptases. Antimicrob Agents Chemother **40:**1270-3.

24. **Coakley, E. P., J. M. Gillis, and S. M. Hammer.** 2000. Phenotypic and genotypic resistance patterns of HIV-1 isolates derived from individuals treated with didanosine and stavudine. Aids **14:**F9-15.
25. **Crotty, S., C. E. Cameron, and R. Andino.** 2001. RNA virus error catastrophe: direct molecular test by using ribavirin. Proc Natl Acad Sci U S A **98:**6895-900.
26. **Crotty, S., D. Maag, J. J. Arnold, W. Zhong, J. Y. Lau, Z. Hong, R. Andino, and C. E. Cameron.** 2000. The broad-spectrum antiviral ribonucleoside ribavirin is an RNA virus mutagen. Nat Med **6:**1375-9.
27. **Cruchaga, C., E. Anso, A. Rouzaut, and J. J. Martinez-Irujo.** 2006. Selective excision of chain-terminating nucleotides by HIV-1 reverse transcriptase with phosphonoformate as substrate. J Biol Chem **281:**27744-52.
28. **Crumpacker, C. S.** 1992. Mechanism of action of foscarnet against viral polymerases. Am J Med **92:**3S-7S.
29. **Dahlberg, M. E., and S. J. Benkovic.** 1991. Kinetic mechanism of DNA polymerase I (Klenow fragment): identification of a second conformational change and evaluation of the internal equilibrium constant. Biochemistry **30:**4835-43.
30. **De Antoni, A., A. Foli, J. Lisziewicz, and F. Lori.** 1997. Mutations in the pol gene of human immunodeficiency virus type 1 in infected patients receiving didanosine and hydroxyurea combination therapy. J Infect Dis **176:**899-903.
31. **De Clercq, E.** 2004. Antiviral drugs in current clinical use. J Clin Virol **30:**115-33.
32. **De Clercq, E.** 2005. Emerging anti-HIV drugs. Expert Opin Emerg Drugs **10:**241-73.
33. **de Mendoza, C., V. Soriano, C. Briones, O. Gallego, P. Barreiro, A. Alvarez, and J. Gonzalez-Lahoz.** 2000. Emergence of zidovudine resistance in HIV-infected patients receiving stavudine. J Acquir Immune Defic Syndr **23:**279-81.
34. **Derse, D., K. F. Bastow, and Y. Cheng.** 1982. Characterization of the DNA polymerases induced by a group of herpes simplex virus type I variants selected for growth in the presence of phosphonoformic acid. J Biol Chem **257:**10251-60.
35. **Deval, J., J. M. Navarro, B. Selmi, J. Courcambeck, J. Boretto, P. Halfon, S. Garrido-Urbani, J. Sire, and B. Canard.** 2004. A loss of viral replicative capacity correlates with altered DNA polymerization kinetics by the human immunodeficiency virus reverse transcriptase bearing the K65R and L74V dideoxynucleoside resistance substitutions. J Biol Chem **279:**25489-96.
36. **Deval, J., K. L. White, M. D. Miller, N. T. Parkin, J. Courcambeck, P. Halfon, B. Selmi, J. Boretto, and B. Canard.** 2004. Mechanistic basis for reduced viral and enzymatic fitness of HIV-1 reverse transcriptase containing both K65R and M184V mutations. J Biol Chem **279:**509-16.
37. **di Marzo Veronese, F., T. D. Copeland, A. L. DeVico, R. Rahman, S. Oroszlan, R. C. Gallo, and M. G. Sarngadharan.** 1986. Characterization of highly immunogenic p66/p51 as the reverse transcriptase of HTLV-III/LAV. Science **231:**1289-91.
38. **Ding, J., K. Das, Y. Hsiou, S. G. Sarafianos, A. D. Clark, Jr., A. Jacobo-Molina, C. Tantillo, S. H. Hughes, and E. Arnold.** 1998. Structure and functional implications of the polymerase active site region in a complex of HIV-1

RT with a double-stranded DNA template-primer and an antibody Fab fragment at 2.8 A resolution. J Mol Biol **284:**1095-111.

39. **Doublie, S., M. R. Sawaya, and T. Ellenberger.** 1999. An open and closed case for all polymerases. Structure **7:**R31-5.
40. **Doublie, S., S. Tabor, A. M. Long, C. C. Richardson, and T. Ellenberger.** 1998. Crystal structure of a bacteriophage T7 DNA replication complex at 2.2 A resolution. Nature **391:**251-8.
41. **Drake, J. W.** 1991. A constant rate of spontaneous mutation in DNA-based microbes. Proc Natl Acad Sci U S A **88:**7160-4.
42. **Drosopoulos, W. C., and V. R. Prasad.** 1996. Increased polymerase fidelity of E89G, a nucleoside analog-resistant variant of human immunodeficiency virus type 1 reverse transcriptase. J Virol **70:**4834-8.
43. **Duesberg, P., K. V. Helm, and E. Canaani.** 1971. Comparative properties of RNA and DNA templates for the DNA polymerase of Rous sarcoma virus. Proc Natl Acad Sci U S A **68:**2505-9.
44. **Duesberg, P., K. V. Helm, and E. Canaani.** 1971. Properties of a soluble DNA polymerase isolated from Rous sarcoma virus. Proc Natl Acad Sci U S A **68:**747-51.
45. **El Safadi, Y., V. Vivet-Boudou, and R. Marquet.** 2007. HIV-1 reverse transcriptase inhibitors. Appl Microbiol Biotechnol.
46. **Eriksson, B., B. Oberg, and B. Wahren.** 1982. Pyrophosphate analogues as inhibitors of DNA polymerases of cytomegalovirus, herpes simplex virus and cellular origin. Biochim Biophys Acta **696:**115-23.
47. **Esnouf, R. M., J. Ren, A. L. Hopkins, C. K. Ross, E. Y. Jones, D. K. Stammers, and D. I. Stuart.** 1997. Unique features in the structure of the complex between HIV-1 reverse transcriptase and the bis(heteroaryl)piperazine (BHAP) U-90152 explain resistance mutations for this nonnucleoside inhibitor. Proc Natl Acad Sci U S A **94:**3984-9.
48. **Farmerie, W. G., D. D. Loeb, N. C. Casavant, C. A. Hutchison, 3rd, M. H. Edgell, and R. Swanstrom.** 1987. Expression and processing of the AIDS virus reverse transcriptase in Escherichia coli. Science **236:**305-8.
49. **Feng, J. Y., and K. S. Anderson.** 1999. Mechanistic studies comparing the incorporation of (+) and (-) isomers of 3TCTP by HIV-1 reverse transcriptase. Biochemistry **38:**55-63.
50. **Frankel, F. A., B. Marchand, D. Turner, M. Gotte, and M. A. Wainberg.** 2005. Impaired rescue of chain-terminated DNA synthesis associated with the L74V mutation in human immunodeficiency virus type 1 reverse transcriptase. Antimicrob Agents Chemother **49:**2657-64.
51. **Franklin, M. C., J. Wang, and T. A. Steitz.** 2001. Structure of the replicating complex of a pol alpha family DNA polymerase. Cell **105:**657-67.
52. **Fujinaga, K., J. T. Parsons, J. W. Beard, D. Beard, and M. Green.** 1970. Mechanism of carcinogenesis by RNA tumor viruses. 3. Formation of RNA, DNA complex and duplex DNA molecules by the DNA polymerase (s) of avian myeloblastosis virus. Proc Natl Acad Sci U S A **67:**1432-9.
53. **Gallo, R. C., S. Z. Salahuddin, M. Popovic, G. M. Shearer, M. Kaplan, B. F. Haynes, T. J. Palker, R. Redfield, J. Oleske, B. Safai, and et al.** 1984. Frequent

detection and isolation of cytopathic retroviruses (HTLV-III) from patients with AIDS and at risk for AIDS. Science **224:**500-3.

54. **Gao, Q., Z. Gu, M. A. Parniak, J. Cameron, N. Cammack, C. Boucher, and M. A. Wainberg.** 1993. The same mutation that encodes low-level human immunodeficiency virus type 1 resistance to 2',3'-dideoxyinosine and 2',3'-dideoxycytidine confers high-level resistance to the (-) enantiomer of 2',3'-dideoxy-3'-thiacytidine. Antimicrob Agents Chemother **37:**1390-2.
55. **Gao, W. Y., A. Cara, R. C. Gallo, and F. Lori.** 1993. Low levels of deoxynucleotides in peripheral blood lymphocytes: a strategy to inhibit human immunodeficiency virus type 1 replication. Proc Natl Acad Sci U S A **90:**8925-8.
56. **Girouard, M., K. Diallo, B. Marchand, S. McCormick, and M. Gotte.** 2003. Mutations E44D and V118I in the reverse transcriptase of HIV-1 play distinct mechanistic roles in dual resistance to AZT and 3TC. J Biol Chem **278:**34403-10.
57. **Goodman, M. F.** 1997. Hydrogen bonding revisited: geometric selection as a principal determinant of DNA replication fidelity. Proc Natl Acad Sci U S A **94:**10493-5.
58. **Goody, R. S., B. Muller, and T. Restle.** 1991. Factors contributing to the inhibition of HIV reverse transcriptase by chain-terminating nucleotides in vitro and in vivo. FEBS Lett **291:**1-5.
59. **Gotte, M.** 2006. Effects of nucleotides and nucleotide analogue inhibitors of HIV-1 reverse transcriptase in a ratchet model of polymerase translocation. Curr Pharm Des **12:**1867-77.
60. **Gotte, M.** 2004. Inhibition of HIV-1 reverse transcription: basic principles of drug action and resistance. Expert Rev Anti Infect Ther **2:**707-16.
61. **Gotte, M., D. Arion, M. A. Parniak, and M. A. Wainberg.** 2000. The M184V mutation in the reverse transcriptase of human immunodeficiency virus type 1 impairs rescue of chain-terminated DNA synthesis. J Virol **74:**3579-85.
62. **Gotte, M., M. Kameoka, N. McLellan, L. Cellai, and M. A. Wainberg.** 2001. Analysis of efficiency and fidelity of HIV-1 (+)-strand DNA synthesis reveals a novel rate-limiting step during retroviral reverse transcription. J Biol Chem **276:**6711-9.
63. **Gotte, M., G. Maier, H. J. Gross, and H. Heumann.** 1998. Localization of the active site of HIV-1 reverse transcriptase-associated RNase H domain on a DNA template using site-specific generated hydroxyl radicals. J Biol Chem **273:**10139-46.
64. **Gotte, M., G. Maier, A. M. Onori, L. Cellai, M. A. Wainberg, and H. Heumann.** 1999. Temporal coordination between initiation of HIV (+)-strand DNA synthesis and primer removal. J Biol Chem **274:**11159-69.
65. **Gotte, M., R. Marquet, C. Isel, V. E. Anderson, G. Keith, H. J. Gross, C. Ehresmann, B. Ehresmann, and H. Heumann.** 1996. Probing the higher order structure of RNA with peroxonitrous acid. FEBS Lett **390:**226-8.
66. **Gu, Z., Q. Gao, X. Li, M. A. Parniak, and M. A. Wainberg.** 1992. Novel mutation in the human immunodeficiency virus type 1 reverse transcriptase gene that encodes cross-resistance to 2',3'-dideoxyinosine and 2',3'-dideoxycytidine. J Virol **66:**7128-35.
67. **Guajardo, R., P. Lopez, M. Dreyfus, and R. Sousa.** 1998. NTP concentration effects on initial transcription by T7 RNAP indicate that translocation occurs

through passive sliding and reveal that divergent promoters have distinct NTP concentration requirements for productive initiation. J Mol Biol **281:**777-92.

68. **Guajardo, R., and R. Sousa.** 1997. A model for the mechanism of polymerase translocation. J Mol Biol **265:**8-19.
69. **Guo, Q., M. Lu, M. Shahrestanifar, R. D. Sheardy, and N. R. Kallenbach.** 1991. Drug binding to a DNA BZ molecule: analysis by chemical footprinting. Biochemistry **30:**11735-41.
70. **Guo, Q., and R. Sousa.** 2006. Translocation by T7 RNA polymerase: a sensitively poised Brownian ratchet. J Mol Biol **358:**241-54.
71. **Gutierrez-Rivas, M., and L. Menendez-Arias.** 2001. A mutation in the primer grip region of HIV-1 reverse transcriptase that confers reduced fidelity of DNA synthesis. Nucleic Acids Res **29:**4963-72.
72. **Hahn, B. H., G. M. Shaw, M. E. Taylor, R. R. Redfield, P. D. Markham, S. Z. Salahuddin, F. Wong-Staal, R. C. Gallo, E. S. Parks, and W. P. Parks.** 1986. Genetic variation in HTLV-III/LAV over time in patients with AIDS or at risk for AIDS. Science **232:**1548-53.
73. **Hainaut, M., M. Gerard, C. A. Peltier, H. Souayah, F. Mascart, G. Zissis, and J. Levy.** 2003. Effectiveness of rescue antiretroviral therapy including intravenously administered zidovudine and foscarnet in a child with HIV-1 enteropathy. Eur J Pediatr **162:**528-9.
74. **Hamburgh, M. E., W. C. Drosopoulos, and V. R. Prasad.** 1998. The influence of 3TC-resistance mutations E89G and M184V in the human immunodeficiency virus reverse transcriptase on mispair extension efficiency. Nucleic Acids Res **26:**4389-94.
75. **Hammond, J. L., D. L. Koontz, H. Z. Bazmi, J. R. Beadle, S. E. Hostetler, G. D. Kini, K. A. Aldern, D. D. Richman, K. Y. Hostetler, and J. W. Mellors.** 2001. Alkylglycerol prodrugs of phosphonoformate are potent in vitro inhibitors of nucleoside-resistant human immunodeficiency virus type 1 and select for resistance mutations that suppress zidovudine resistance. Antimicrob Agents Chemother **45:**1621-8.
76. **Harrigan, P. R., I. Kinghorn, S. Bloor, S. D. Kemp, I. Najera, A. Kohli, and B. A. Larder.** 1996. Significance of amino acid variation at human immunodeficiency virus type 1 reverse transcriptase residue 210 for zidovudine susceptibility. J Virol **70:**5930-4.
77. **Harrigan, P. R., C. Stone, P. Griffin, I. Najera, S. Bloor, S. Kemp, M. Tisdale, and B. Larder.** 2000. Resistance profile of the human immunodeficiency virus type 1 reverse transcriptase inhibitor abacavir (1592U89) after monotherapy and combination therapy. CNA2001 Investigative Group. J Infect Dis **181:**912-20.
78. **Harris, D., N. Kaushik, P. K. Pandey, P. N. Yadav, and V. N. Pandey.** 1998. Functional analysis of amino acid residues constituting the dNTP binding pocket of HIV-1 reverse transcriptase. J Biol Chem **273:**33624-34.
79. **Harris, D., P. N. Yadav, and V. N. Pandey.** 1998. Loss of polymerase activity due to Tyr to Phe substitution in the YMDD motif of human immunodeficiency virus type-1 reverse transcriptase is compensated by Met to Val substitution within the same motif. Biochemistry **37:**9630-40.
80. **Hauschka, P. V.** 1973. Analysis of nucleotide pools in animal cells. Methods Cell Biol **7:**361-462.

81. **Helgstrand, E., B. Eriksson, N. G. Johansson, B. Lannero, A. Larsson, A. Misiorny, J. O. Noren, B. Sjoberg, K. Stenberg, G. Stening, S. Stridh, and B. Oberg.** 1978. Trisodium phosphonoformate, a new antiviral compound. Science **201:**819-21.
82. **Hertogs, K., S. Bloor, V. De Vroey, C. van Den Eynde, P. Dehertogh, A. van Cauwenberge, M. Sturmer, T. Alcorn, S. Wegner, M. van Houtte, V. Miller, and B. A. Larder.** 2000. A novel human immunodeficiency virus type 1 reverse transcriptase mutational pattern confers phenotypic lamivudine resistance in the absence of mutation 184V. Antimicrob Agents Chemother **44:**568-73.
83. **Hoffman, A. D., B. Banapour, and J. A. Levy.** 1985. Characterization of the AIDS-associated retrovirus reverse transcriptase and optimal conditions for its detection in virions. Virology **147:**326-35.
84. **Hostomsky, Z., Z. Hostomska, T. B. Fu, and J. Taylor.** 1992. Reverse transcriptase of human immunodeficiency virus type 1: functionality of subunits of the heterodimer in DNA synthesis. J Virol **66:**3179-82.
85. **Hsieh, J. C., S. Zinnen, and P. Modrich.** 1993. Kinetic mechanism of the DNA-dependent DNA polymerase activity of human immunodeficiency virus reverse transcriptase. J Biol Chem **268:**24607-13.
86. **Hsiou, Y., K. Das, J. Ding, A. D. Clark, Jr., J. P. Kleim, M. Rosner, I. Winkler, G. Riess, S. H. Hughes, and E. Arnold.** 1998. Structures of Tyr188Leu mutant and wild-type HIV-1 reverse transcriptase complexed with the non-nucleoside inhibitor HBY 097: inhibitor flexibility is a useful design feature for reducing drug resistance. J Mol Biol **284:**313-23.
87. **Hsiou, Y., J. Ding, K. Das, A. D. Clark, Jr., S. H. Hughes, and E. Arnold.** 1996. Structure of unliganded HIV-1 reverse transcriptase at 2.7 A resolution: implications of conformational changes for polymerization and inhibition mechanisms. Structure **4:**853-60.
88. **Huang, H., R. Chopra, G. L. Verdine, and S. C. Harrison.** 1998. Structure of a covalently trapped catalytic complex of HIV-1 reverse transcriptase: implications for drug resistance. Science **282:**1669-75.
89. **Huang, J., and R. Sousa.** 2000. T7 RNA polymerase elongation complex structure and movement. J Mol Biol **303:**347-58.
90. **Huber, H. E., J. M. McCoy, J. S. Seehra, and C. C. Richardson.** 1989. Human immunodeficiency virus 1 reverse transcriptase. Template binding, processivity, strand displacement synthesis, and template switching. J Biol Chem **264:**4669-78.
91. **Ignatov, M. E., A. J. Berdis, S. F. Le Grice, and M. D. Barkley.** 2005. Attenuation of DNA replication by HIV-1 reverse transcriptase near the central termination sequence. Biochemistry **44:**5346-56.
92. **Isel, C., C. Ehresmann, P. Walter, B. Ehresmann, and R. Marquet.** 2001. The emergence of different resistance mechanisms toward nucleoside inhibitors is explained by the properties of the wild type HIV-1 reverse transcriptase. J Biol Chem **276:**48725-32.
93. **Iversen, A. K., R. W. Shafer, K. Wehrly, M. A. Winters, J. I. Mullins, B. Chesebro, and T. C. Merigan.** 1996. Multidrug-resistant human immunodeficiency virus type 1 strains resulting from combination antiretroviral therapy. J Virol **70:**1086-90.

94. **Izopet, J., A. Bicart-See, C. Pasquier, K. Sandres, E. Bonnet, B. Marchou, J. Puel, and P. Massip.** 1999. Mutations conferring resistance to zidovudine diminish the antiviral effect of stavudine plus didanosine. J Med Virol **59:**507-11.
95. **Jacobo-Molina, A., J. Ding, R. G. Nanni, A. D. Clark, Jr., X. Lu, C. Tantillo, R. L. Williams, G. Kamer, A. L. Ferris, P. Clark, and et al.** 1993. Crystal structure of human immunodeficiency virus type 1 reverse transcriptase complexed with double-stranded DNA at 3.0 A resolution shows bent DNA. Proc Natl Acad Sci U S A **90:**6320-4.
96. **Jacques, P. S., B. M. Wohrl, M. Ottmann, J. L. Darlix, and S. F. Le Grice.** 1994. Mutating the "primer grip" of p66 HIV-1 reverse transcriptase implicates tryptophan-229 in template-primer utilization. J Biol Chem **269:**26472-8.
97. **Jamburuthugoda, V. K., P. Chugh, and B. Kim.** 2006. Modification of human immunodeficiency virus type 1 reverse transcriptase to target cells with elevated cellular dNTP concentrations. J Biol Chem **281:**13388-95.
98. **Jochmans, D., J. Deval, B. Kesteleyn, H. Van Marck, E. Bettens, I. De Baere, P. Dehertogh, T. Ivens, M. Van Ginderen, B. Van Schoubroeck, M. Ehteshami, P. Wigerinck, M. Gotte, and K. Hertogs.** 2006. Indolopyridones inhibit human immunodeficiency virus reverse transcriptase with a novel mechanism of action. J Virol **80:**12283-92.
99. **Johnson, M. S., M. A. McClure, D. F. Feng, J. Gray, and R. F. Doolittle.** 1986. Computer analysis of retroviral pol genes: assignment of enzymatic functions to specific sequences and homologies with nonviral enzymes. Proc Natl Acad Sci U S A **83:**7648-52.
100. **Johnson, P. R., T. E. Hamm, S. Goldstein, S. Kitov, and V. M. Hirsch.** 1991. The genetic fate of molecularly cloned simian immunodeficiency virus in experimentally infected macaques. Virology **185:**217-28.
101. **Kacian, D. L., K. F. Watson, A. Burny, and S. Spiegelman.** 1971. Purification of the DNA polymerase of avian myeloblastosis virus. Biochim Biophys Acta **246:**365-83.
102. **Kamer, G., and P. Argos.** 1984. Primary structural comparison of RNA-dependent polymerases from plant, animal and bacterial viruses. Nucleic Acids Res **12:**7269-82.
103. **Kati, W. M., K. A. Johnson, L. F. Jerva, and K. S. Anderson.** 1992. Mechanism and fidelity of HIV reverse transcriptase. J Biol Chem **267:**25988-97.
104. **Katlama, C., M. A. Valantin, S. Matheron, A. Coutellier, V. Calvez, D. Descamps, C. Longuet, M. Bonmarchand, R. Tubiana, M. De Sa, R. Lancar, H. Agut, F. Brun-Vezinet, and D. Costagliola.** 1998. Efficacy and tolerability of stavudine plus lamivudine in treatment-naive and treatment-experienced patients with HIV-1 infection. Ann Intern Med **129:**525-31.
105. **Kaushik, N., T. T. Talele, P. K. Pandey, D. Harris, P. N. Yadav, and V. N. Pandey.** 2000. Role of glutamine 151 of human immunodeficiency virus type-1 reverse transcriptase in substrate selection as assessed by site-directed mutagenesis. Biochemistry **39:**2912-20.
106. **Kellam, P., C. A. Boucher, and B. A. Larder.** 1992. Fifth mutation in human immunodeficiency virus type 1 reverse transcriptase contributes to the development of high-level resistance to zidovudine. Proc Natl Acad Sci U S A **89:**1934-8.

107. **Keller, W., and R. Crouch.** 1972. Degradation of DNA RNA hybrids by ribonuclease H and DNA polymerases of cellular and viral origin. Proc Natl Acad Sci U S A **69:**3360-4.
108. **Kerr, S. G., and K. S. Anderson.** 1997. Pre-steady-state kinetic characterization of wild type and 3'-azido-3'-deoxythymidine (AZT) resistant human immunodeficiency virus type 1 reverse transcriptase: implication of RNA directed DNA polymerization in the mechanism of AZT resistance. Biochemistry **36:**14064-70.
109. **Keulen, W., N. K. Back, A. van Wijk, C. A. Boucher, and B. Berkhout.** 1997. Initial appearance of the 184Ile variant in lamivudine-treated patients is caused by the mutational bias of human immunodeficiency virus type 1 reverse transcriptase. J Virol **71:**3346-50.
110. **Kiefer, J. R., C. Mao, J. C. Braman, and L. S. Beese.** 1998. Visualizing DNA replication in a catalytically active Bacillus DNA polymerase crystal. Nature **391:**304-7.
111. **Kim, B., J. C. Ayran, S. G. Sagar, E. T. Adman, S. M. Fuller, N. H. Tran, and J. Horrigan.** 1999. New human immunodeficiency virus, type 1 reverse transcriptase (HIV-1 RT) mutants with increased fidelity of DNA synthesis. Accuracy, template binding, and processivity. J Biol Chem **274:**27666-73.
112. **Kim, B., T. R. Hathaway, and L. A. Loeb.** 1998. Fidelity of mutant HIV-1 reverse transcriptases: interaction with the single-stranded template influences the accuracy of DNA synthesis. Biochemistry **37:**5831-9.
113. **King, P. A., E. Jamison, D. Strahs, V. E. Anderson, and M. Brenowitz.** 1993. 'Footprinting' proteins on DNA with peroxonitrous acid. Nucleic Acids Res **21:**2473-8.
114. **Kohlstaedt, L. A., J. Wang, J. M. Friedman, P. A. Rice, and T. A. Steitz.** 1992. Crystal structure at 3.5 A resolution of HIV-1 reverse transcriptase complexed with an inhibitor. Science **256:**1783-90.
115. **Kopp, E. B., J. J. Miglietta, A. G. Shrutkowski, C. K. Shih, P. M. Grob, and M. T. Skoog.** 1991. Steady state kinetics and inhibition of HIV-1 reverse transcriptase by a non-nucleoside dipyridodiazepinone, BI-RG-587, using a heteropolymeric template. Nucleic Acids Res **19:**3035-9.
116. **Krebs, R., U. Immendorfer, S. H. Thrall, B. M. Wohrl, and R. S. Goody.** 1997. Single-step kinetics of HIV-1 reverse transcriptase mutants responsible for virus resistance to nucleoside inhibitors zidovudine and 3-TC. Biochemistry **36:**10292-300.
117. **Krummel, B., and M. J. Chamberlin.** 1992. Structural analysis of ternary complexes of Escherichia coli RNA polymerase. Deoxyribonuclease I footprinting of defined complexes. J Mol Biol **225:**239-50.
118. **Kuchta, R. D., V. Mizrahi, P. A. Benkovic, K. A. Johnson, and S. J. Benkovic.** 1987. Kinetic mechanism of DNA polymerase I (Klenow). Biochemistry **26:**8410-7.
119. **Kunkel, T. A., and K. Bebenek.** 2000. DNA replication fidelity. Annu Rev Biochem **69:**497-529.
120. **Lacey, S. F., J. E. Reardon, E. S. Furfine, T. A. Kunkel, K. Bebenek, K. A. Eckert, S. D. Kemp, and B. A. Larder.** 1992. Biochemical studies on the reverse

transcriptase and RNase H activities from human immunodeficiency virus strains resistant to 3'-azido-3'-deoxythymidine. J Biol Chem **267:**15789-94.

121. **Larder, B. A.** 1992. 3'-Azido-3'-deoxythymidine resistance suppressed by a mutation conferring human immunodeficiency virus type 1 resistance to nonnucleoside reverse transcriptase inhibitors. Antimicrob Agents Chemother **36:**2664-9.
122. **Larder, B. A., B. Chesebro, and D. D. Richman.** 1990. Susceptibilities of zidovudine-susceptible and -resistant human immunodeficiency virus isolates to antiviral agents determined by using a quantitative plaque reduction assay. Antimicrob Agents Chemother **34:**436-41.
123. **Larder, B. A., and S. D. Kemp.** 1989. Multiple mutations in HIV-1 reverse transcriptase confer high-level resistance to zidovudine (AZT). Science **246:**1155-8.
124. **Larder, B. A., S. D. Kemp, and P. R. Harrigan.** 1995. Potential mechanism for sustained antiretroviral efficacy of AZT-3TC combination therapy. Science **269:**696-9.
125. **Larder, B. A., D. J. Purifoy, K. L. Powell, and G. Darby.** 1987. Site-specific mutagenesis of AIDS virus reverse transcriptase. Nature **327:**716-7.
126. **Lavigne, M., L. Polomack, and H. Buc.** 2001. Structures of complexes formed by HIV-1 reverse transcriptase at a termination site of DNA synthesis. J Biol Chem **276:**31439-48.
127. **Le Grice, S. F., and F. Gruninger-Leitch.** 1990. Rapid purification of homodimer and heterodimer HIV-1 reverse transcriptase by metal chelate affinity chromatography. Eur J Biochem **187:**307-14.
128. **Le Grice, S. F., T. Naas, B. Wohlgensinger, and O. Schatz.** 1991. Subunit-selective mutagenesis indicates minimal polymerase activity in heterodimer-associated p51 HIV-1 reverse transcriptase. Embo J **10:**3905-11.
129. **Leider, J. M., P. Palese, and F. I. Smith.** 1988. Determination of the mutation rate of a retrovirus. J Virol **62:**3084-91.
130. **Lennerstrand, J., K. Hertogs, D. K. Stammers, and B. A. Larder.** 2001. Correlation between viral resistance to zidovudine and resistance at the reverse transcriptase level for a panel of human immunodeficiency virus type 1 mutants. J Virol **75:**7202-5.
131. **Lewis, D. A., K. Bebenek, W. A. Beard, S. H. Wilson, and T. A. Kunkel.** 1999. Uniquely altered DNA replication fidelity conferred by an amino acid change in the nucleotide binding pocket of human immunodeficiency virus type 1 reverse transcriptase. J Biol Chem **274:**32924-30.
132. **Lightfoote, M. M., J. E. Coligan, T. M. Folks, A. S. Fauci, M. A. Martin, and S. Venkatesan.** 1986. Structural characterization of reverse transcriptase and endonuclease polypeptides of the acquired immunodeficiency syndrome retrovirus. J Virol **60:**771-5.
133. **Lin, P. F., H. Samanta, R. E. Rose, A. K. Patick, J. Trimble, C. M. Bechtold, D. R. Revie, N. C. Khan, M. E. Federici, H. Li, and et al.** 1994. Genotypic and phenotypic analysis of human immunodeficiency virus type 1 isolates from patients on prolonged stavudine therapy. J Infect Dis **170:**1157-64.
134. **Lindberg, J., S. Sigurdsson, S. Lowgren, H. O. Andersson, C. Sahlberg, R. Noreen, K. Fridborg, H. Zhang, and T. Unge.** 2002. Structural basis for the

inhibitory efficacy of efavirenz (DMP-266), MSC194 and PNU142721 towards the HIV-1 RT K103N mutant. Eur J Biochem **269:**1670-7.

135. **Maag, D., C. Castro, Z. Hong, and C. E. Cameron.** 2001. Hepatitis C virus RNA-dependent RNA polymerase (NS5B) as a mediator of the antiviral activity of ribavirin. J Biol Chem **276:**46094-8.
136. **Maeda, Y., D. J. Venzon, and H. Mitsuya.** 1998. Altered drug sensitivity, fitness, and evolution of human immunodeficiency virus type 1 with pol gene mutations conferring multi-dideoxynucleoside resistance. J Infect Dis **177:**1207-13.
137. **Mansky, L. M.** 1996. Forward mutation rate of human immunodeficiency virus type 1 in a T lymphoid cell line. AIDS Res Hum Retroviruses **12:**307-14.
138. **Mansky, L. M.** 2002. HIV mutagenesis and the evolution of antiretroviral drug resistance. Drug Resist Updat **5:**219-23.
139. **Mansky, L. M., and H. M. Temin.** 1995. Lower in vivo mutation rate of human immunodeficiency virus type 1 than that predicted from the fidelity of purified reverse transcriptase. J Virol **69:**5087-94.
140. **Marchand, B., and M. Gotte.** 2004. Impact of the translocational equilibrium of HIV-1 reverse transcriptase on the efficiency of mismatch extensions and the excision of mispaired nucleotides. Int J Biochem Cell Biol **36:**1823-35.
141. **Marchand, B., and M. Gotte.** 2003. Site-specific footprinting reveals differences in the translocation status of HIV-1 reverse transcriptase. Implications for polymerase translocation and drug resistance. J Biol Chem **278:**35362-72.
142. **Marchand, B., E. P. Tchesnokov, and M. Gotte.** 2006. The pyrophosphate analogue foscarnet traps the pretranslocational state of HIV-1 reverse transcriptase in a Brownian ratchet model of polymerase translocation. J Biol Chem **in press**.
143. **Martin, J. L., J. E. Wilson, R. L. Haynes, and P. A. Furman.** 1993. Mechanism of resistance of human immunodeficiency virus type 1 to 2',3'-dideoxyinosine. Proc Natl Acad Sci U S A **90:**6135-9.
144. **Mas, A., M. Parera, C. Briones, V. Soriano, M. A. Martinez, E. Domingo, and L. Menendez-Arias.** 2000. Role of a dipeptide insertion between codons 69 and 70 of HIV-1 reverse transcriptase in the mechanism of AZT resistance. Embo J **19:**5752-61.
145. **Mas, A., B. M. Vazquez-Alvarez, E. Domingo, and L. Menendez-Arias.** 2002. Multidrug-resistant HIV-1 reverse transcriptase: involvement of ribonucleotide-dependent phosphorolysis in cross-resistance to nucleoside analogue inhibitors. J Mol Biol **323:**181-97.
146. **Mathiesen, S., B. T. Roge, N. Weis, J. D. Lundgren, N. Obel, and J. Gerstoft.** 2004. Foscarnet used in salvage therapy of HIV-1 patients harbouring multiple nucleotide excision mutations. Aids **18:**1076-8.
147. **Mayers, D. L., F. E. McCutchan, E. E. Sanders-Buell, L. I. Merritt, S. Dilworth, A. K. Fowler, C. A. Marks, N. M. Ruiz, D. D. Richman, C. R. Roberts, and et al.** 1992. Characterization of HIV isolates arising after prolonged zidovudine therapy. J Acquir Immune Defic Syndr **5:**749-59.
148. **Mellors, J. W., H. Z. Bazmi, R. F. Schinazi, B. M. Roy, Y. Hsiou, E. Arnold, J. Weir, and D. L. Mayers.** 1995. Novel mutations in reverse transcriptase of human immunodeficiency virus type 1 reduce susceptibility to foscarnet in laboratory and clinical isolates. Antimicrob Agents Chemother **39:**1087-92.

149. **Mellors, J. W., G. E. Dutschman, G. J. Im, E. Tramontano, S. R. Winkler, and Y. C. Cheng.** 1992. In vitro selection and molecular characterization of human immunodeficiency virus-1 resistant to non-nucleoside inhibitors of reverse transcriptase. Mol Pharmacol **41:**446-51.
150. **Mendelman, L. V., M. S. Boosalis, J. Petruska, and M. F. Goodman.** 1989. Nearest neighbor influences on DNA polymerase insertion fidelity. J Biol Chem **264:**14415-23.
151. **Menendez-Arias, L.** 2002. Molecular basis of fidelity of DNA synthesis and nucleotide specificity of retroviral reverse transcriptases. Prog Nucleic Acid Res Mol Biol **71:**91-147.
152. **Metzger, W., T. Hermann, O. Schatz, S. F. Le Grice, and H. Heumann.** 1993. Hydroxyl radical footprint analysis of human immunodeficiency virus reverse transcriptase-template.primer complexes. Proc Natl Acad Sci U S A **90:**5909-13.
153. **Meyer, P. R., J. Lennerstrand, S. E. Matsuura, B. A. Larder, and W. A. Scott.** 2003. Effects of dipeptide insertions between codons 69 and 70 of human immunodeficiency virus type 1 reverse transcriptase on primer unblocking, deoxynucleoside triphosphate inhibition, and DNA chain elongation. J Virol **77:**3871-7.
154. **Meyer, P. R., S. E. Matsuura, A. M. Mian, A. G. So, and W. A. Scott.** 1999. A mechanism of AZT resistance: an increase in nucleotide-dependent primer unblocking by mutant HIV-1 reverse transcriptase. Mol Cell **4:**35-43.
155. **Meyer, P. R., S. E. Matsuura, R. F. Schinazi, A. G. So, and W. A. Scott.** 2000. Differential removal of thymidine nucleotide analogues from blocked DNA chains by human immunodeficiency virus reverse transcriptase in the presence of physiological concentrations of 2'-deoxynucleoside triphosphates. Antimicrob Agents Chemother **44:**3465-72.
156. **Meyer, P. R., S. E. Matsuura, A. G. So, and W. A. Scott.** 1998. Unblocking of chain-terminated primer by HIV-1 reverse transcriptase through a nucleotide-dependent mechanism. Proc Natl Acad Sci U S A **95:**13471-6.
157. **Meyer, P. R., S. E. Matsuura, A. A. Tolun, I. Pfeifer, A. G. So, J. W. Mellors, and W. A. Scott.** 2002. Effects of specific zidovudine resistance mutations and substrate structure on nucleotide-dependent primer unblocking by human immunodeficiency virus type 1 reverse transcriptase. Antimicrob Agents Chemother **46:**1540-5.
158. **Meyer, P. R., S. E. Matsuura, D. Zonarich, R. R. Chopra, E. Pendarvis, H. Z. Bazmi, J. W. Mellors, and W. A. Scott.** 2003. Relationship between 3'-azido-3'-deoxythymidine resistance and primer unblocking activity in foscarnet-resistant mutants of human immunodeficiency virus type 1 reverse transcriptase. J Virol **77:**6127-37.
159. **Meyer, P. R., A. J. Smith, S. E. Matsuura, and W. A. Scott.** 2004. Effects of primer-template sequence on ATP-dependent removal of chain-terminating nucleotide analogues by HIV-1 reverse transcriptase. J Biol Chem **279:**45389-98.
160. **Miller, M. D., K. E. Anton, A. S. Mulato, P. D. Lamy, and J. M. Cherrington.** 1999. Human immunodeficiency virus type 1 expressing the lamivudine-associated M184V mutation in reverse transcriptase shows increased susceptibility to adefovir and decreased replication capability in vitro. J Infect Dis **179:**92-100.

161. **Miller, M. D., N. Margot, B. Lu, L. Zhong, S. S. Chen, A. Cheng, and M. Wulfsohn.** 2004. Genotypic and phenotypic predictors of the magnitude of response to tenofovir disoproxil fumarate treatment in antiretroviral-experienced patients. J Infect Dis **189:**837-46.
162. **Miller, V., M. Ait-Khaled, C. Stone, P. Griffin, D. Mesogiti, A. Cutrell, R. Harrigan, S. Staszewski, C. Katlama, G. Pearce, and M. Tisdale.** 2000. HIV-1 reverse transcriptase (RT) genotype and susceptibility to RT inhibitors during abacavir monotherapy and combination therapy. Aids **14:**163-71.
163. **Miranda, L. R., M. Gotte, F. Liang, and D. R. Kuritzkes.** 2005. The L74V mutation in human immunodeficiency virus type 1 reverse transcriptase counteracts enhanced excision of zidovudine monophosphate associated with thymidine analog resistance mutations. Antimicrob Agents Chemother **49:**2648-56.
164. **Mitsuya, H., R. F. Jarrett, M. Matsukura, F. Di Marzo Veronese, A. L. DeVico, M. G. Sarngadharan, D. G. Johns, M. S. Reitz, and S. Broder.** 1987. Long-term inhibition of human T-lymphotropic virus type III/lymphadenopathy-associated virus (human immunodeficiency virus) DNA synthesis and RNA expression in T cells protected by 2',3'-dideoxynucleosides in vitro. Proc Natl Acad Sci U S A **84:**2033-7.
165. **Molling, K., D. P. Bolognesi, H. Bauer, W. Busen, H. W. Plassmann, and P. Hausen.** 1971. Association of viral reverse transcriptase with an enzyme degrading the RNA moiety of RNA-DNA hybrids. Nat New Biol **234:**240-3.
166. **Mukherjee, S., L. G. Brieba, and R. Sousa.** 2002. Structural transitions mediating transcription initiation by T7 RNA polymerase. Cell **110:**81-91.
167. **Muller, B., T. Restle, S. Weiss, M. Gautel, G. Sczakiel, and R. S. Goody.** 1989. Co-expression of the subunits of the heterodimer of HIV-1 reverse transcriptase in Escherichia coli. J Biol Chem **264:**13975-8.
168. **Naeger, L. K., N. A. Margot, and M. D. Miller.** 2002. ATP-dependent removal of nucleoside reverse transcriptase inhibitors by human immunodeficiency virus type 1 reverse transcriptase. Antimicrob Agents Chemother **46:**2179-84.
169. **Nedialkov, Y. A., X. Q. Gong, S. L. Hovde, Y. Yamaguchi, H. Handa, J. H. Geiger, H. Yan, and Z. F. Burton.** 2003. NTP-driven translocation by human RNA polymerase II. J Biol Chem **278:**18303-12.
170. **Nunberg, J. H., W. A. Schleif, E. J. Boots, J. A. O'Brien, J. C. Quintero, J. M. Hoffman, E. A. Emini, and M. E. Goldman.** 1991. Viral resistance to human immunodeficiency virus type 1-specific pyridinone reverse transcriptase inhibitors. J Virol **65:**4887-92.
171. **Oberg, B.** 1982. Antiviral effects of phosphonoformate (PFA, foscarnet sodium). Pharmacol Ther **19:**387-415.
172. **Ollis, D. L., P. Brick, R. Hamlin, N. G. Xuong, and T. A. Steitz.** 1985. Structure of large fragment of Escherichia coli DNA polymerase I complexed with dTMP. Nature **313:**762-6.
173. **Ostrander, M., and Y. C. Cheng.** 1980. Properties of herpes simplex virus type 1 and type 2 DNA polymerase. Biochim Biophys Acta **609:**232-45.
174. **Overbaugh, J., L. M. Rudensey, M. D. Papenhausen, R. E. Benveniste, and W. R. Morton.** 1991. Variation in simian immunodeficiency virus env is confined to V1 and V4 during progression to simian AIDS. J Virol **65:**7025-31.

175. **Palaniappan, C., M. Wisniewski, P. S. Jacques, S. F. Le Grice, P. J. Fay, and R. A. Bambara.** 1997. Mutations within the primer grip region of HIV-1 reverse transcriptase result in loss of RNase H function. J Biol Chem **272:**11157-64.
176. **Patel, P. H., A. Jacobo-Molina, J. Ding, C. Tantillo, A. D. Clark, Jr., R. Raag, R. G. Nanni, S. H. Hughes, and E. Arnold.** 1995. Insights into DNA polymerization mechanisms from structure and function analysis of HIV-1 reverse transcriptase. Biochemistry **34:**5351-63.
177. **Patel, S. S., I. Wong, and K. A. Johnson.** 1991. Pre-steady-state kinetic analysis of processive DNA replication including complete characterization of an exonuclease-deficient mutant. Biochemistry **30:**511-25.
178. **Pathak, V. K., and H. M. Temin.** 1990. Broad spectrum of in vivo forward mutations, hypermutations, and mutational hotspots in a retroviral shuttle vector after a single replication cycle: deletions and deletions with insertions. Proc Natl Acad Sci U S A **87:**6024-8.
179. **Peletskaya, E. N., A. A. Kogon, S. Tuske, E. Arnold, and S. H. Hughes.** 2004. Nonnucleoside inhibitor binding affects the interactions of the fingers subdomain of human immunodeficiency virus type 1 reverse transcriptase with DNA. J Virol **78:**3387-97.
180. **Pellegrin, I., J. Izopet, J. Reynes, M. Denayrolles, B. Montes, J. L. Pellegrin, P. Massip, J. Puel, H. Fleury, and M. Segondy.** 1999. Emergence of zidovudine and multidrug-resistance mutations in the HIV-1 reverse transcriptase gene in therapy-naive patients receiving stavudine plus didanosine combination therapy. STADI Group. Aids **13:**1705-9.
181. **Pelletier, H., M. R. Sawaya, A. Kumar, S. H. Wilson, and J. Kraut.** 1994. Structures of ternary complexes of rat DNA polymerase beta, a DNA template-primer, and ddCTP. Science **264:**1891-903.
182. **Perrino, F. W., B. D. Preston, L. L. Sandell, and L. A. Loeb.** 1989. Extension of mismatched 3' termini of DNA is a major determinant of the infidelity of human immunodeficiency virus type 1 reverse transcriptase. Proc Natl Acad Sci U S A **86:**8343-7.
183. **Petropoulos, C. J., N. T. Parkin, K. L. Limoli, Y. S. Lie, T. Wrin, W. Huang, H. Tian, D. Smith, G. A. Winslow, D. J. Capon, and J. M. Whitcomb.** 2000. A novel phenotypic drug susceptibility assay for human immunodeficiency virus type 1. Antimicrob Agents Chemother **44:**920-8.
184. **Powell, M. D., W. A. Beard, K. Bebenek, K. J. Howard, S. F. Le Grice, T. A. Darden, T. A. Kunkel, S. H. Wilson, and J. G. Levin.** 1999. Residues in the alphaH and alphaI helices of the HIV-1 reverse transcriptase thumb subdomain required for the specificity of RNase H-catalyzed removal of the polypurine tract primer. J Biol Chem **274:**19885-93.
185. **Powell, M. D., M. Ghosh, P. S. Jacques, K. J. Howard, S. F. Le Grice, and J. G. Levin.** 1997. Alanine-scanning mutations in the "primer grip" of p66 HIV-1 reverse transcriptase result in selective loss of RNA priming activity. J Biol Chem **272:**13262-9.
186. **Preston, B. D., B. J. Poiesz, and L. A. Loeb.** 1988. Fidelity of HIV-1 reverse transcriptase. Science **242:**1168-71.
187. **Quan, Y., Z. Gu, X. Li, Z. Li, C. D. Morrow, and M. A. Wainberg.** 1996. Endogenous reverse transcription assays reveal high-level resistance to the

triphosphate of (-)2'-dideoxy-3'-thiacytidine by mutated M184V human immunodeficiency virus type 1. J Virol **70:**5642-5.

188. **Quijano, C., B. Alvarez, R. M. Gatti, O. Augusto, and R. Radi.** 1997. Pathways of peroxynitrite oxidation of thiol groups. Biochem J **322 (Pt 1):**167-73.
189. **Ratner, L., W. Haseltine, R. Patarca, K. J. Livak, B. Starcich, S. F. Josephs, E. R. Doran, J. A. Rafalski, E. A. Whitehorn, K. Baumeister, and et al.** 1985. Complete nucleotide sequence of the AIDS virus, HTLV-III. Nature **313:**277-84.
190. **Ray, A. S., A. Basavapathruni, and K. S. Anderson.** 2002. Mechanistic studies to understand the progressive development of resistance in human immunodeficiency virus type 1 reverse transcriptase to abacavir. J Biol Chem **277:**40479-90.
191. **Ray, A. S., E. Murakami, A. Basavapathruni, J. A. Vaccaro, D. Ulrich, C. K. Chu, R. F. Schinazi, and K. S. Anderson.** 2003. Probing the molecular mechanisms of AZT drug resistance mediated by HIV-1 reverse transcriptase using a transient kinetic analysis. Biochemistry **42:**8831-41.
192. **Reardon, J. E.** 1992. Human immunodeficiency virus reverse transcriptase: steady-state and pre-steady-state kinetics of nucleotide incorporation. Biochemistry **31:**4473-9.
193. **Reardon, J. E., E. S. Furfine, and N. Cheng.** 1991. Human immunodeficiency virus reverse transcriptase. Effect of primer length on template-primer binding. J Biol Chem **266:**14128-34.
194. **Reardon, J. E., and W. H. Miller.** 1990. Human immunodeficiency virus reverse transcriptase. Substrate and inhibitor kinetics with thymidine 5'-triphosphate and 3'-azido-3'-deoxythymidine 5'-triphosphate. J Biol Chem **265:**20302-7.
195. **Ren, J., R. Esnouf, E. Garman, D. Somers, C. Ross, I. Kirby, J. Keeling, G. Darby, Y. Jones, D. Stuart, and et al.** 1995. High resolution structures of HIV-1 RT from four RT-inhibitor complexes. Nat Struct Biol **2:**293-302.
196. **Ren, J., R. M. Esnouf, A. L. Hopkins, E. Y. Jones, I. Kirby, J. Keeling, C. K. Ross, B. A. Larder, D. I. Stuart, and D. K. Stammers.** 1998. 3'-Azido-3'-deoxythymidine drug resistance mutations in HIV-1 reverse transcriptase can induce long range conformational changes. Proc Natl Acad Sci U S A **95:**9518-23.
197. **Ren, J., J. Milton, K. L. Weaver, S. A. Short, D. I. Stuart, and D. K. Stammers.** 2000. Structural basis for the resilience of efavirenz (DMP-266) to drug resistance mutations in HIV-1 reverse transcriptase. Structure **8:**1089-94.
198. **Ren, J., C. E. Nichols, P. P. Chamberlain, K. L. Weaver, S. A. Short, and D. K. Stammers.** 2004. Crystal structures of HIV-1 reverse transcriptases mutated at codons 100, 106 and 108 and mechanisms of resistance to non-nucleoside inhibitors. J Mol Biol **336:**569-78.
199. **Reno, J. M., L. F. Lee, and J. A. Boezi.** 1978. Inhibition of herpesvirus replication and herpesvirus-induced deoxyribonucleic acid polymerase by phosphonoformate. Antimicrob Agents Chemother **13:**188-92.
200. **Ricchetti, M., and H. Buc.** 1990. Reverse transcriptases and genomic variability: the accuracy of DNA replication is enzyme specific and sequence dependent. Embo J **9:**1583-93.
201. **Richman, D., C. K. Shih, I. Lowy, J. Rose, P. Prodanovich, S. Goff, and J. Griffin.** 1991. Human immunodeficiency virus type 1 mutants resistant to

nonnucleoside inhibitors of reverse transcriptase arise in tissue culture. Proc Natl Acad Sci U S A **88:**11241-5.

202. **Rigourd, M., C. Ehresmann, M. A. Parniak, B. Ehresmann, and R. Marquet.** 2002. Primer unblocking and rescue of DNA synthesis by azidothymidine (AZT)-resistant HIV-1 reverse transcriptase: comparison between initiation and elongation of reverse transcription and between (-) and (+) strand DNA synthesis. J Biol Chem **277:**18611-8.
203. **Rigourd, M., J. M. Lanchy, S. F. Le Grice, B. Ehresmann, C. Ehresmann, and R. Marquet.** 2000. Inhibition of the initiation of HIV-1 reverse transcription by 3'-azido-3'-deoxythymidine. Comparison with elongation. J Biol Chem **275:**26944-51.
204. **Riman, J., and G. S. Beaudreau.** 1970. Viral DNA-dependent DNA polymerase and the properties of thymidine labelled material in virions of an oncogenic RNA virus. Nature **228:**427-30.
205. **Rittinger, K., G. Divita, and R. S. Goody.** 1995. Human immunodeficiency virus reverse transcriptase substrate-induced conformational changes and the mechanism of inhibition by nonnucleoside inhibitors. Proc Natl Acad Sci U S A **92:**8046-9.
206. **Robbins, B. L., J. Greenhaw, M. C. Connelly, and A. Fridland.** 1995. Metabolic pathways for activation of the antiviral agent 9-(2-phosphonylmethoxyethyl)adenine in human lymphoid cells. Antimicrob Agents Chemother **39:**2304-8.
207. **Rodgers, D. W., S. J. Gamblin, B. A. Harris, S. Ray, J. S. Culp, B. Hellmig, D. J. Woolf, C. Debouck, and S. C. Harrison.** 1995. The structure of unliganded reverse transcriptase from the human immunodeficiency virus type 1. Proc Natl Acad Sci U S A **92:**1222-6.
208. **Rubinek, T., M. Bakhanashvili, R. Taube, O. Avidan, and A. Hizi.** 1997. The fidelity of 3' misinsertion and mispair extension during DNA synthesis exhibited by two drug-resistant mutants of the reverse transcriptase of human immunodeficiency virus type 1 with Leu74-->Val and Glu89-->Gly. Eur J Biochem **247:**238-47.
209. **Sala, M., S. Wain-Hobson, and F. Schaeffer.** 1995. Human immunodeficiency virus type 1 reverse transcriptase tG:T mispair formation on RNA and DNA templates with mismatched primers: a kinetic and thermodynamic study. Embo J **14:**4622-7.
210. **Sanchez-Pescador, R., M. D. Power, P. J. Barr, K. S. Steimer, M. M. Stempien, S. L. Brown-Shimer, W. W. Gee, A. Renard, A. Randolph, J. A. Levy, and et al.** 1985. Nucleotide sequence and expression of an AIDS-associated retrovirus (ARV-2). Science **227:**484-92.
211. **Sarafianos, S. G., A. D. Clark, Jr., K. Das, S. Tuske, J. J. Birktoft, P. Ilankumaran, A. R. Ramesha, J. M. Sayer, D. M. Jerina, P. L. Boyer, S. H. Hughes, and E. Arnold.** 2002. Structures of HIV-1 reverse transcriptase with pre- and post-translocation AZTMP-terminated DNA. Embo J **21:**6614-24.
212. **Sarafianos, S. G., A. D. Clark, Jr., S. Tuske, C. J. Squire, K. Das, D. Sheng, P. Ilankumaran, A. R. Ramesha, H. Kroth, J. M. Sayer, D. M. Jerina, P. L. Boyer, S. H. Hughes, and E. Arnold.** 2003. Trapping HIV-1 reverse transcriptase before and after translocation on DNA. J Biol Chem **278:**16280-8.

213. **Sarafianos, S. G., K. Das, A. D. Clark, Jr., J. Ding, P. L. Boyer, S. H. Hughes, and E. Arnold.** 1999. Lamivudine (3TC) resistance in HIV-1 reverse transcriptase involves steric hindrance with beta-branched amino acids. Proc Natl Acad Sci U S A **96:**10027-32.
214. **Sarafianos, S. G., K. Das, J. Ding, P. L. Boyer, S. H. Hughes, and E. Arnold.** 1999. Touching the heart of HIV-1 drug resistance: the fingers close down on the dNTP at the polymerase active site. Chem Biol **6:**R137-46.
215. **Sarafianos, S. G., K. Das, S. H. Hughes, and E. Arnold.** 2004. Taking aim at a moving target: designing drugs to inhibit drug-resistant HIV-1 reverse transcriptases. Curr Opin Struct Biol **14:**716-30.
216. **Sarafianos, S. G., K. Das, C. Tantillo, A. D. Clark, Jr., J. Ding, J. M. Whitcomb, P. L. Boyer, S. H. Hughes, and E. Arnold.** 2001. Crystal structure of HIV-1 reverse transcriptase in complex with a polypurine tract RNA:DNA. Embo J **20:**1449-61.
217. **Sardana, V. V., E. A. Emini, L. Gotlib, D. J. Graham, D. W. Lineberger, W. J. Long, A. J. Schlabach, J. A. Wolfgang, and J. H. Condra.** 1992. Functional analysis of HIV-1 reverse transcriptase amino acids involved in resistance to multiple nonnucleoside inhibitors. J Biol Chem **267:**17526-30.
218. **Sarin, P. S., Y. Taguchi, D. Sun, A. Thornton, R. C. Gallo, and B. Oberg.** 1985. Inhibition of HTLV-III/LAV replication by foscarnet. Biochem Pharmacol **34:**4075-9.
219. **Selmi, B., J. Deval, K. Alvarez, J. Boretto, S. Sarfati, C. Guerreiro, and B. Canard.** 2003. The Y181C substitution in 3'-azido-3'-deoxythymidine-resistant human immunodeficiency virus, type 1, reverse transcriptase suppresses the ATP-mediated repair of the 3'-azido-3'-deoxythymidine 5'-monophosphate-terminated primer. J Biol Chem **278:**40464-72.
220. **Shah, F. S., K. A. Curr, M. E. Hamburgh, M. Parniak, H. Mitsuya, J. G. Arnez, and V. R. Prasad.** 2000. Differential influence of nucleoside analog-resistance mutations K65R and L74V on the overall mutation rate and error specificity of human immunodeficiency virus type 1 reverse transcriptase. J Biol Chem **275:**27037-44.
221. **Shirasaka, T., M. F. Kavlick, T. Ueno, W. Y. Gao, E. Kojima, M. L. Alcaide, S. Chokekijchai, B. M. Roy, E. Arnold, R. Yarchoan, and et al.** 1995. Emergence of human immunodeficiency virus type 1 variants with resistance to multiple dideoxynucleosides in patients receiving therapy with dideoxynucleosides. Proc Natl Acad Sci U S A **92:**2398-402.
222. **Sluis-Cremer, N., D. Arion, N. Kaushik, H. Lim, and M. A. Parniak.** 2000. Mutational analysis of Lys65 of HIV-1 reverse transcriptase. Biochem J **348 Pt 1:**77-82.
223. **Sluis-Cremer, N., D. Arion, U. Parikh, D. Koontz, R. F. Schinazi, J. W. Mellors, and M. A. Parniak.** 2005. The 3'-azido group is not the primary determinant of 3'-azido-3'-deoxythymidine (AZT) responsible for the excision phenotype of AZT-resistant HIV-1. J Biol Chem **280:**29047-52.
224. **Spence, R. A., K. S. Anderson, and K. A. Johnson.** 1996. HIV-1 reverse transcriptase resistance to nonnucleoside inhibitors. Biochemistry **35:**1054-63.

225. **Spence, R. A., W. M. Kati, K. S. Anderson, and K. A. Johnson.** 1995. Mechanism of inhibition of HIV-1 reverse transcriptase by nonnucleoside inhibitors. Science **267:**988-93.
226. **Spiegelman, S., A. Burny, M. R. Das, J. Keydar, J. Schlom, M. Travnicek, and K. Watson.** 1970. DNA-directed DNA polymerase activity in oncogenic RNA viruses. Nature **227:**1029-31.
227. **St Clair, M. H., J. L. Martin, G. Tudor-Williams, M. C. Bach, C. L. Vavro, D. M. King, P. Kellam, S. D. Kemp, and B. A. Larder.** 1991. Resistance to ddI and sensitivity to AZT induced by a mutation in HIV-1 reverse transcriptase. Science **253:**1557-9.
228. **Steitz, T. A.** 1998. A mechanism for all polymerases. Nature **391:**231-2.
229. **Stridh, S., E. Helgstrand, B. Lannero, A. Misiorny, G. Stening, and B. Oberg.** 1979. The effect of pyrophosphate analogues on influenza virus RNA polymerase and influenza virus multiplication. Arch Virol **61:**245-50.
230. **Sturmer, M., S. Staszewski, H. W. Doerr, B. Larder, S. Bloor, and K. Hertogs.** 2003. Correlation of phenotypic zidovudine resistance with mutational patterns in the reverse transcriptase of human immunodeficiency virus type 1: interpretation of established mutations and characterization of new polymorphisms at codons 208, 211, and 214. Antimicrob Agents Chemother **47:**54-61.
231. **Sundquist, B., and B. Oberg.** 1979. Phosphonoformate inhibits reverse transcriptase. J Gen Virol **45:**273-81.
232. **Tachedjian, G., D. J. Hooker, A. D. Gurusinghe, H. Bazmi, N. J. Deacon, J. Mellors, C. Birch, and J. Mills.** 1995. Characterisation of foscarnet-resistant strains of human immunodeficiency virus type 1. Virology **212:**58-68.
233. **Tachedjian, G., J. Mellors, H. Bazmi, C. Birch, and J. Mills.** 1996. Zidovudine resistance is suppressed by mutations conferring resistance of human immunodeficiency virus type 1 to foscarnet. J Virol **70:**7171-81.
234. **Tachedjian, G., J. W. Mellors, H. Bazmi, and J. Mills.** 1998. Impaired fitness of foscarnet-resistant strains of human immunodeficiency virus type 1. AIDS Res Hum Retroviruses **14:**1059-64.
235. **Tamalet, C., J. Izopet, N. Koch, J. Fantini, and N. Yahi.** 1998. Stable rearrangements of the beta3-beta4 hairpin loop of HIV-1 reverse transcriptase in plasma viruses from patients receiving combination therapy. Aids **12:**F161-6.
236. **Tanese, N., and S. P. Goff.** 1988. Domain structure of the Moloney murine leukemia virus reverse transcriptase: mutational analysis and separate expression of the DNA polymerase and RNase H activities. Proc Natl Acad Sci U S A **85:**1777-81.
237. **Tchesnokov, E. P., C. Gilbert, G. Boivin, and M. Gotte.** 2006. Role of helix P of the human cytomegalovirus DNA polymerase in resistance and hypersusceptibility to the antiviral drug foscarnet. J Virol **80:**1440-50.
238. **Temin, H. M.** 1964. Homology between Rna from Rous Sarcoma Virous and DNA from Rous Sarcoma Virus-Infected Cells. Proc Natl Acad Sci U S A **52:**323-9.
239. **Temin, H. M.** 1964. The Participation of DNA in Rous Sarcoma Virus Production. Virology **23:**486-94.

240. **Temin, H. M., and S. Mizutani.** 1970. RNA-dependent DNA polymerase in virions of Rous sarcoma virus. Nature **226:**1211-3.
241. **Tisdale, M., S. D. Kemp, N. R. Parry, and B. A. Larder.** 1993. Rapid in vitro selection of human immunodeficiency virus type 1 resistant to 3'-thiacytidine inhibitors due to a mutation in the YMDD region of reverse transcriptase. Proc Natl Acad Sci U S A **90:**5653-6.
242. **Tong, W., C. D. Lu, S. K. Sharma, S. Matsuura, A. G. So, and W. A. Scott.** 1997. Nucleotide-induced stable complex formation by HIV-1 reverse transcriptase. Biochemistry **36:**5749-57.
243. **Traut, T. W.** 1994. Physiological concentrations of purines and pyrimidines. Mol Cell Biochem **140:**1-22.
244. **Tuske, S., S. G. Sarafianos, A. D. Clark, Jr., J. Ding, L. K. Naeger, K. L. White, M. D. Miller, C. S. Gibbs, P. L. Boyer, P. Clark, G. Wang, B. L. Gaffney, R. A. Jones, D. M. Jerina, S. H. Hughes, and E. Arnold.** 2004. Structures of HIV-1 RT-DNA complexes before and after incorporation of the anti-AIDS drug tenofovir. Nat Struct Mol Biol **11:**469-74.
245. **Tuske, S., S. G. Sarafianos, X. Wang, B. Hudson, E. Sineva, J. Mukhopadhyay, J. J. Birktoft, O. Leroy, S. Ismail, A. D. Clark, Jr., C. Dharia, A. Napoli, O. Laptenko, J. Lee, S. Borukhov, R. H. Ebright, and E. Arnold.** 2005. Inhibition of bacterial RNA polymerase by streptolydigin: stabilization of a straight-bridge-helix active-center conformation. Cell **122:**541-52.
246. **Ueno, T., and H. Mitsuya.** 1997. Comparative enzymatic study of HIV-1 reverse transcriptase resistant to 2',3'-dideoxynucleotide analogs using the single-nucleotide incorporation assay. Biochemistry **36:**1092-9.
247. **Ueno, T., T. Shirasaka, and H. Mitsuya.** 1995. Enzymatic characterization of human immunodeficiency virus type 1 reverse transcriptase resistant to multiple 2',3'-dideoxynucleoside 5'-triphosphates. J Biol Chem **270:**23605-11.
248. **Vaccaro, J. A., and K. S. Anderson.** 1998. Implication of the tRNA initiation step for human immunodeficiency virus type 1 reverse transcriptase in the mechanism of 3'-azido-3'-deoxythymidine (AZT) resistance. Biochemistry **37:**14189-94.
249. **Wain-Hobson, S., P. Sonigo, O. Danos, S. Cole, and M. Alizon.** 1985. Nucleotide sequence of the AIDS virus, LAV. Cell **40:**9-17.
250. **Wainberg, M. A., M. D. Miller, Y. Quan, H. Salomon, A. S. Mulato, P. D. Lamy, N. A. Margot, K. E. Anton, and J. M. Cherrington.** 1999. In vitro selection and characterization of HIV-1 with reduced susceptibility to PMPA. Antivir Ther **4:**87-94.
251. **Weiss, K. K., S. J. Isaacs, N. H. Tran, E. T. Adman, and B. Kim.** 2000. Molecular architecture of the mutagenic active site of human immunodeficiency virus type 1 reverse transcriptase: roles of the beta 8-alpha E loop in fidelity, processivity, and substrate interactions. Biochemistry **39:**10684-94.
252. **White, K. L., J. M. Chen, J. Y. Feng, N. A. Margot, J. K. Ly, A. S. Ray, H. L. Macarthur, M. J. McDermott, S. Swaminathan, and M. D. Miller.** 2006. The K65R reverse transcriptase mutation in HIV-1 reverses the excision phenotype of zidovudine resistance mutations. Antivir Ther **11:**155-63.

253. **White, K. L., J. M. Chen, N. A. Margot, T. Wrin, C. J. Petropoulos, L. K. Naeger, S. Swaminathan, and M. D. Miller.** 2004. Molecular mechanisms of tenofovir resistance conferred by human immunodeficiency virus type 1 reverse transcriptase containing a diserine insertion after residue 69 and multiple thymidine analog-associated mutations. Antimicrob Agents Chemother **48:**992-1003.
254. **White, K. L., N. A. Margot, J. K. Ly, J. M. Chen, A. S. Ray, M. Pavelko, R. Wang, M. McDermott, S. Swaminathan, and M. D. Miller.** 2005. A combination of decreased NRTI incorporation and decreased excision determines the resistance profile of HIV-1 K65R RT. Aids **19:**1751-60.
255. **White, K. L., N. A. Margot, T. Wrin, C. J. Petropoulos, M. D. Miller, and L. K. Naeger.** 2002. Molecular mechanisms of resistance to human immunodeficiency virus type 1 with reverse transcriptase mutations K65R and K65R+M184V and their effects on enzyme function and viral replication capacity. Antimicrob Agents Chemother **46:**3437-46.
256. **Wilson, J. E., A. Aulabaugh, B. Caligan, S. McPherson, J. K. Wakefield, S. Jablonski, C. D. Morrow, J. E. Reardon, and P. A. Furman.** 1996. Human immunodeficiency virus type-1 reverse transcriptase. Contribution of Met-184 to binding of nucleoside 5'-triphosphate. J Biol Chem **271:**13656-62.
257. **Winters, M. A., K. L. Coolley, Y. A. Girard, D. J. Levee, H. Hamdan, R. W. Shafer, D. A. Katzenstein, and T. C. Merigan.** 1998. A 6-basepair insert in the reverse transcriptase gene of human immunodeficiency virus type 1 confers resistance to multiple nucleoside inhibitors. J Clin Invest **102:**1769-75.
258. **Winters, M. A., R. W. Shafer, R. A. Jellinger, G. Mamtora, T. Gingeras, and T. C. Merigan.** 1997. Human immunodeficiency virus type 1 reverse transcriptase genotype and drug susceptibility changes in infected individuals receiving dideoxyinosine monotherapy for 1 to 2 years. Antimicrob Agents Chemother **41:**757-62.
259. **Wisniewski, M., C. Palaniappan, Z. Fu, S. F. Le Grice, P. Fay, and R. A. Bambara.** 1999. Mutations in the primer grip region of HIV reverse transcriptase can increase replication fidelity. J Biol Chem **274:**28175-84.
260. **Wong, I., S. S. Patel, and K. A. Johnson.** 1991. An induced-fit kinetic mechanism for DNA replication fidelity: direct measurement by single-turnover kinetics. Biochemistry **30:**526-37.
261. **Yin, Y. W., and T. A. Steitz.** 2002. Structural basis for the transition from initiation to elongation transcription in T7 RNA polymerase. Science **298:**1387-95.
262. **Yin, Y. W., and T. A. Steitz.** 2004. The structural mechanism of translocation and helicase activity in T7 RNA polymerase. Cell **116:**393-404.
263. **Yu, H., and M. F. Goodman.** 1992. Comparison of HIV-1 and avian myeloblastosis virus reverse transcriptase fidelity on RNA and DNA templates. J Biol Chem **267:**10888-96.
264. **Zinnen, S., J. C. Hsieh, and P. Modrich.** 1994. Misincorporation and mispaired primer extension by human immunodeficiency virus reverse transcriptase. J Biol Chem **269:**24195-202.